Improving Intraperitoneal Adenovirus Virotherapy for Ovarian Cancer

Clemens Matthias Manuel Thoma

St. Peter's College

University of Oxford

A thesis submitted for the degree of Doctor of Philosophy

to the Faculty of Clinical Medicine, University of Oxford

Trinity Term 2011

Supervisors: Dr J. Morrison and Prof. L.W. Seymour

Improving Intraperitoneal Adenovirus Virotherapy for Ovarian Cancer

Clemens Matthias Manuel Thoma

St. Peter's College, University of Oxford

A thesis submitted for the degree of Doctor of Philosophy to the Faculty of Clinical Medicine
University of Oxford, Trinity Term 2011

Abstract

The use of intraperitoneal (i.p.) adenovirus virotherapy of ovarian cancer is currently limited by insufficient efficacy and high toxicity. Both factors are associated with adenovirus serotype 5 (Ad5) in this setting and may be serotype-specific. Low levels of uptake receptors (CAR and α_V integrins) on ovarian tumour cells and widespread immunity against Ad5 among patients appear to restrict efficacy and intraperitoneal inflammatory responses against Ad5 were among the reasons for the termination of a phase II/III clinical trial in ovarian cancer. This thesis sought to overcome these obstacles by investigating the alternative adenovirus serotypes Ad3 and Ad11. For these viruses lower pre-existing antiviral immunity and utilisation of different uptake receptors have been reported. Furthermore, virus cloaking with novel polymers which could impart enhanced protection from neutralisation was examined.

In vitro, wild-type Ad3, Ad5 and Ad11 displayed differential oncolytic activity in a panel of ovarian cancer cell lines which partly correlated to uptake receptor expression and virus internalisation. However, some cell lines displayed lysis resistance in a serotype-specific manner. While the inflammatory response six hours after i.p. administration of Ad11 in CD46-transgenic mice did not differ from Ad5, in long-term studies of repeated administration Ad5 induced significantly more severe pathologic effects in the form of adhesions and liver toxicity than Ad11 or mock-treatment. Oncolysis inhibition assays using malignant exudate samples demonstrated greater neutralisation of Ad3 and Ad5 in comparison to Ad11 at low concentrations of samples. Notably, 10-fold less Ad11 than Ad5 was required for oncolytic efficacy at a sample concentration of 10%. In an *ex vivo* model of ascites from ovarian cancer patients Ad5 modified with novel polymer formulations achieved at least 50% cell kill in six of eight samples, in contrast to two of eight samples for non-modified Ad5.

These data suggest that virotherapy using Ad11 might be advantageous over Ad3 or Ad5. The lack of strong inflammation and the possibility to decrease treatment doses due to less neutralisation of Ad11 might result in considerably improved patient safety. Chemical modification of Ad with novel polymers presents an exciting advancement in overcoming treatment neutralisation in adenovirus virotherapy.

Declaration of Authentication

All the work presented in this thesis was performed entirely by me and in no way forms part of any other thesis in this or any other university. Where contributions have been made by others, this is acknowledged. The work was performed under the supervision of Dr Joanne Morrison, Nuffield Department of Obstetrics and Gynaecology, Division of Medical Sciences, University of Oxford and Professor Leonard W. Seymour, Department of Oncology, Division of Medical Sciences, University of Oxford.

Clemens Matthias Manuel Thoma

Oxford, September 2011

Dedication

Für meine Eltern

Acknowledgments

Foremost, I would like to thank my supervisors Dr Joanne Morrison and Professor Leonard Seymour. I am deeply grateful to Dr Morrison for giving me the opportunity to work with her and trusting me to pursue this DPhil project. Her expert advice and support were invaluable throughout. I wish to thank Professor Seymour for his experienced guidance and, not least, for providing the research environment, without which this thesis would not have been possible.

I am indebted to many past and present members of the lab for their professional and personal support, in particular, Drs Robert Carlisle, Kerry Fisher, Patricia Seaton, Carolin Fella and Miriam Bazan-Peregrino for their insightful advice, thoughtful debate, inspirational ideas and scientific support. I am also thankful to all other lab colleagues who made my time in Oxford worthwhile and enjoyable.

I am ever grateful to my godmother Dorothea Brosi for her love and support. She made Oxford a second home for me. Particular thanks also to my dear friend and housemate Panos Zalmas for his support and patience during the process of writing this thesis.

I would like to thank all individuals who helped in accomplishing this project through provision of materials, instrumentation and advice on scientific techniques. These include Drs Linda Klavinskis and Veronique Bachy of King's College London for access to transgenic mice and assistance with animal work and at the University of Oxford: Professor Sean Kehoe and the late Professor Robert Davies and their colleagues for provision of patient samples and Professor David Greaves and his team for provision of murine macrophages and scientific advice. For access to and advice on Bio-Plex® I wish to thank Dr Janet Ferneyhough and the team at Systems Biology Laboratory as well as Dr Amin Moghaddam at the University of Oxford. Also, many thanks to Georgina Berridge and Rod Chalk of the Structural Genomics Consortium, University of Oxford for LC-MS/MS and support with data analysis.

Finally, I am grateful to Wellbeing of Women and the Oxfordshire Health Services Research Committee for providing my salary and funding laboratory consumables which gave me the opportunity to perform this research project.

Table of Contents

ABSTRACT ..... **I**

DECLARATION OF AUTHENTICATION ..... **II**

DEDICATION ..... **III**

ACKNOWLEDGMENTS ..... **IV**

TABLE OF CONTENTS ..... **V**

LIST OF FIGURES ..... **XI**

LIST OF TABLES ..... **XIV**

LIST OF ABBREVIATIONS ..... **XV**

1 INTRODUCTION **1**

1.1 Ovarian cancer **2**

1.1.1 Current standard of care 2

1.1.2 Obstacles to increased efficacy and new directions 3

1.2 Cancer gene therapy **7**

1.2.1 The use of viruses in cancer treatment 7

1.2.1.1 Viral vectors in cancer gene therapy 7

1.2.1.2 Oncolytic virotherapy 11

1.3 Adenovirus treatments in ovarian cancer **13**

1.3.1 Adenovirus biology 14

1.3.1.1 Adenovirus proteins 14

1.3.1.2 Adenovirus life-cycle 17
1.3.2 Strategies in the use of adenovirus in ovarian cancer treatment 21
1.3.2.1 Selected early clinical trials of i.p. adenovirus therapy 21
1.3.2.2 Emerging impediments to i.p. adenovirus in ovarian cancer 22
1.3.2.3 New strategies for i.p. adenovirus 24

1.4 Aims and scope of this thesis 27
1.4.1 Hypothesis 30
1.4.2 Aims 30

2 MATERIALS AND METHODS 31

2.1 General laboratory methods 32
2.1.1 Cell lines and cell culture techniques 32
2.1.1.1 Cell Passage 32
2.1.1.2 Storage of cell lines 33
2.1.1.3 Cell plating 34
2.1.2 Adenoviruses 34

2.2 Methods of Chapter 3 35
2.2.1 Photon Correlation Spectroscopy 35
2.2.2 PicoGreen® assay 36
2.2.3 Plaque assay 36
2.2.4 $TCID_{50}$ assay 38
2.2.5 MTS assay 39
2.2.6 Analysis of cell receptor status by flow cytometry 40
2.2.7 Real time Q-PCR for measurement of virus particle uptake 41

2.3 Methods of Chapter 4 44
2.3.1 Generation and treatment of elicited murine peritoneal macrophages 44
2.3.2 ELISA for quantification of murine RANTES 44
2.3.3 Cytokine analysis using a multiplex suspension array (BioPlex®) 45
2.3.4 Animal studies 45

2.3.4.1 Housing conditions and diet 46
2.3.4.2 Short-term i.p. infection and sample collection 46
2.3.4.3 Long-term i.p. infection, sample collection and adhesion scoring 46
2.3.5 Assessment of neutrophil and macrophage infiltration 47

2.4 Methods of Chapter 5 49
2.4.1 Collection of primary pleural effusions 49
2.4.2 Protein Assay 49
2.4.3 Anti-adenovirus antibody ELISA 50
2.4.4 Adenovirus neutralisation capacity of patient samples 51
2.4.5 SDS-PAGE and Western blot 53
2.4.6 Mass-Spectrometry 55

2.5 Methods of Chapter 6 56
2.5.1 Polymer coating virus 56
2.5.2 Adenovirus capsid protection ELISA 58
2.5.3 Luciferase assay 58
2.5.4 Uptake and cytotoxicity study of polymer-coated Ad5 59
2.5.5 Primary ascites culture 59

2.6 Data processing and statistical analysis 60

3 ONCOLYTIC ACTIVITY OF AD3, AD5 AND AD11 IN HUMAN TUMOUR CELL LINES 61

3.1 Introduction 62

3.2 Characterisation of the oncolytic activity of Ad3, Ad5 and Ad11 63
3.2.1 Physical and biological characterisation of virus preparations 63
3.2.1.1 Assessment of particle size distribution 63
3.2.1.2 Determination of virus particle concentration 64
3.2.1.3 Biological activity of adenovirus preparations 66
3.2.2 Assessment of oncolytic potency through cytotoxicity measurements 71

3.2.2.1 Time-course of oncolytic effect and virus production 71
3.2.2.2 Assessment of oncolytic activity of Ad3, Ad5 and Ad11 with MTS-assays 75
3.2.3 Replication dependence of cytotoxicity 79
3.2.4 Confirmation of findings with other adenovirus batches 83

3.3 Factors influencing oncolytic activity in tumour cell lines 85
3.3.1 Receptor expression of human tumour cell lines 85
3.3.2 Quantification of adenovirus uptake into cells 89
3.3.2.1 Development of probe and primers for real time Q-PCR 89
3.3.2.2 Measurement of virus particle uptake into cells 90
3.3.3 Correlation of virus particles uptake to receptor expression levels on cell lines 93
3.3.4 Correlation of virus particle uptake to IC_{50} values 97

3.4 Conclusion 99

4 THE INFLAMMATORY RESPONSE TOWARDS AD3, AD5 AND AD11 103

4.1 Introduction 104

4.2 Cytokine responses of ex vivo murine macrophages towards adenovirus 106
4.2.1 Selection of markers to assess inflammatory signalling 106
4.2.2 *Ex vivo* cytokine response towards different adenovirus serotypes 109

4.3 Immune responses towards Ad5 and Ad11 in murine models of intraperitoneal administration 112
4.3.1 Short-term *in vivo* inflammatory responses to i.p. adenovirus 113
4.3.2 Long-term *in vivo* inflammatory responses to i.p. adenovirus 119

4.4 Discussion 124

5 NEUTRALISATION OF AD3, AD5 AND AD11 BY MALIGNANT EXUDATES 128

5.1 Introduction 129

5.2 Total antibody content against different adenovirus serotypes of patient samples 131

5.2.1 ELISA development ... 131

5.2.1.1 Adenovirus antigen solutions ... 132

5.2.1.2 Whole purified adenovirus ... 133

5.2.2 Sample screen ... 137

5.2.3 Discussion ... 139

5.3 Neutralisation capacity of patient samples 141

5.3.1 Assay development ... 141

5.3.2 Sample screen ... 144

5.3.3 Overcoming neutralisation by increased virus doses ... 148

5.3.4 Discussion ... 151

5.4 Antigen specificity of anti-Ad antibodies 152

5.4.1 Method development and optimisation ... 153

5.4.1.1 Gel electrophoresis migration patterns and protein identification ... 153

5.4.1.2 Protein transfer and western blotting ... 154

5.4.2 Sample screen ... 160

5.5 Conclusion 165

6 IMPROVED POLYMER COATING TO OVERCOME BARRIERS TO *IN VIVO* ADENOVIRUS EFFICACY ... 168

6.1 Introduction 169

6.2 Assessment of different polymer formulations 171

6.2.1 Coating efficiency and virus activity ... 172

6.2.1.1 Ad5 capsid shielding ... 172

6.2.1.2 Biological activity of polymer-coated Ad5luc ... 175

6.2.1.3 Effect of different polymers on the oncolytic activity of Ad5 ... 178

6.2.2 Polymer-coated Ad5 in neutralising environments ... 181

6.3 Discussion 185

7 CONCLUSION 189

7.1 Preface 190

7.2 Principal findings 191

7.2.1 Oncolytic activity of Ad3, Ad5 and Ad11 in human tumour cell lines 191

7.2.2 The inflammatory response towards Ad3, Ad5 and Ad11 191

7.2.3 Neutralisation of Ad3, Ad5 and Ad11 by malignant exudates 192

7.2.4 Improved polymer coating to overcome barriers to *in vivo* adenovirus efficacy 193

7.3 General Discussion 195

7.3.1 The use of Ad11 195

7.3.2 New ways of enhancing efficacy 197

7.3.3 Protecting adenovirus from neutralisation 199

7.3.4 Future directions 202

7.4 Final conclusion 205

REFERENCES 206

List of Figures

Figure 1-1 The structure of adenovirus....16
Figure 1-2 The adenovirus life-cycle....20

Figure 2-1 Conversion of the MTS reagent by viable cells....39
Figure 2-2 Schematic of ELISA to quantify total anti-Ad antibody content....52
Figure 2-3 Method to determine the neutralising capacity of patient samples....52
Figure 2-4 The chemical structure of a positively charged polymer (EC236)....57

Figure 3-1 Size distribution of virus particles....65
Figure 3-2 Determination of virus particle number....67
Figure 3-3 Virus activity determined by plaque assay....67
Figure 3-4 Virus activity determined by the $TCID_{50}$ method....70
Figure 3-5 Time-course of oncolytic effect determined by viability assays (MTS)....73
Figure 3-6 Time-course of oncolytic effect and virus replication in SKOV3 cells....74
Figure 3-7 Virus activity determined by viability assays (MTS)....77
Figure 3-8 Comparison of serotype activity expressed as IC_{50} values....78
Figure 3-9 Cytotoxicity of replicating and non-replicating Ad5....81
Figure 3-10 Progeny genome number of replicating and non-replicating Ad5....82
Figure 3-11 Confirmation of differential activity of Ad5 and Ad11....84
Figure 3-12 Adenovirus receptor expression profiles of investigated cell lines....87
Figure 3-13 Levels of adenovirus receptor expression of investigated cell lines....88
Figure 3-14 Performance of real time Q-PCR setup....91
Figure 3-15 Uptake of Ad3, Ad5 and Ad11 into investigated cell lines....92
Figure 3-16 Correlation of virus uptake to receptor expression....96
Figure 3-17 Correlation of IC_{50} values (oncolytic activity) to virus uptake....98

Figure 4-1 Time-course of cytokine expression of peritoneal murine macrophages following *ex vivo* incubation with Ad5 108
Figure 4-2 RANTES expression following *ex vivo* incubation of peritoneal murine macrophages with Ad3, Ad5 or Ad11 111
Figure 4-3 Short-term *in vivo* cytokine response to i.p. adenovirus 117
Figure 4-4 Short-term cellular *in vivo* response to i.p. adenovirus 118
Figure 4-5 Long-term *in vivo* pathologic effects after i.p. adenovirus 122
Figure 4-6 Long-term *in vivo* cytokine response to i.p. adenovirus 123
Figure 4-7 Long-term cellular *in vivo* response to i.p. adenovirus 123

Figure 5-1 Determination of optimal concentrations of capture antigen, sample and detection antibody 135
Figure 5-2 Dynamic range of ELISA system 135
Figure 5-3 Determination of optimal adenovirus concentration for well coating 136
Figure 5-4 Well coating efficiency of Ad3, Ad5 and Ad11 136
Figure 5-5 Antibody content of malignant exudates against Ad3, Ad5 and Ad11 138
Figure 5-6 Effects of anticoagulants on cell viability 143
Figure 5-7 Viability of cells incubated with Ad3, Ad5 or Ad11 in the presence of malignant exudates 146
Figure 5-8 Neutralisation capacity of malignant exudates 146
Figure 5-9 Neutralisation capacity at low concentrations of exudates 147
Figure 5-10 Effect of increasing virus doses on neutralisation by pooled serum 150
Figure 5-11 Overcoming neutralisation of 10% exudate by increasing virus doses 150
Figure 5-12 Silver stain 157
Figure 5-13 Coomassie stain 157
Figure 5-14 Identity of protein bands on Coomassie-stained adenovirus gels 157
Figure 5-15 Western blot of separated adenovirus proteins detected by exudates 158
Figure 5-16 Purity of Ad5 preparation 158
Figure 5-17 Equalisation of protein amount per lane 159
Figure 5-18 Determination of analyte dilution 159

Figure 5-19 Western blot example of the sample screen 163

Figure 5-20 Comparison of antibody amounts against proteins of Ad3, Ad5 and Ad11 164

Figure 6-1 Determination of optimal polymer concentration for virus coating 174

Figure 6-2 Activity of coated virus and efficiency of hexon shielding 177

Figure 6-3 Evaluation of shielding, uptake and activity of polymer-coated Ad5 180

Figure 6-4 Transduction efficacy and neutralisation resistance of EC265Ad5luc 183

Figure 6-5 Oncolytic activity and neutralisation resistance of EC265Ad5 in *ex vivo* human malignant ascites 184

List of Tables

Table 1-1 Main classes of viruses used for vector constructs in cancer gene therapy 8

Table 1-2 Selected gene therapy trials with non-replicating viral vectors in ovarian cancer 10

Table 1-3 Oncolytic virotherapy trials in ovarian cancer or malignant ascites 13

Table 2-1 Details of established cell lines 33

Table 2-2 Antibodies used for flow cytometry.....41

Table 2-3 KT-primer sequences for Ad5 42

Table 2-4 Universal and individual primer sequences for Ad3, Ad5 and Ad11 43

Table 2-5 Scoring of inflammation and symptoms of adhesion formation 47

Table 2-6 Panel of investigated polymers 56

Table 5-1 Molecular weights and immunoblot locations of penton base and fibre proteins 162

Table 6-1 Panel of investigated polymers 171

List of Abbreviations

/	per
3’ and 5’	3 prime and 5 prime ends of a DNA molecule
µ	micro
Ad	adenovirus
Ad3	human adenovirus serotype 3
Ad5	human adenovirus serotype 5
Ad11	human adenovirus serotype 11
Ad5luc	E1/E3-deleted Ad5, expressing firefly luciferase under CMV promoter control
ADP	Adenovirus Death Protein
BRCA1 / 2	breast cancer 1 / 2, early onset gene
BSA	bovine serum albumine
c	centi
CA125	cancer antigen 125
CAR	Coxsackie virus and adenovirus receptor
CD	cluster of differentiation
cDNA	copy DNA
CEACAM6	carcinoembryonic antigen–related cell adhesion molecule 6
CMV	cytomegalovirus
CPE	cytopathic effect
CR	complete response
CRAd	conditionally replicating adenovirus
CRUK	Cancer Research UK
d	dilution factor
D	Dalton
DC	dendritic cell
DLS	Dynamic Light Scattering
DMEM	Dulbecco’s modified Eagle’s Medium

DMSO	dimethyl sulphoxide
DNA	deoxyribonucleic acid
DPX	p-Xylene-bis-N-pyridinium bromide
ds	double-stranded
EDTA	ethylenediamine tetra-acetic acid
EGFR	epithelial growth factor receptor
ELISA	enzyme linked immunosorbent assay
FCS	fetal calf serum
FIGO	Fédération Internationale de Gynécologie et d'Obstétrique
FX	coagulation factor X
g	gram or gravitational force
GFP	green fluorescent protein from Aequorea Victoria
GMCSF	human granulocyte-macrophage colony-stimulating factor
HEPES	4-(2-hydroxyethyl)-1-piperazineethanesulfonic acid
HRP	horseradish peroxidase
HSPG	Heparan sulphate proteoglycan
HSV	Herpes simplex virus
i.p.	intraperitoneal
i.t.	intratumoural
i.v.	intravenous
IC_{50}	half maximal inhibitory concentration
IFNγ	interferon gamma
IL	interleukin
k	kilo
KC	Kupffer cell
KT	knob turn
l	litre
LC - MS / MS	liquid chromatography – tandem mass spectrometry
LPS	lipopolysaccharide
m	metre or milli

min	minute(s)
MLP	major late promoter
mRNA	messenger RNA
MTOC	microtubule organising centre
MTS	tetrazolium compound for analysis of cell viability
n	nano or number of
NPC	nuclear pore complex
NR	no response
nt	nucleotide
OD	optical density
OOR	out of range
p	pico or p-value in statistical significance testing
P/I	particle to infectious unit ratio
p21	cyclin dependent kinase inhibitor 1
p53	tumour protein 53
PAGE	polyacrylamide gel electrophoresis
PARP	poly (ADP-ribose) polymerase
PBS	phosphate-buffered saline
PCS	Photon Correlation Spectroscopy
PD	progressive disease
PEG	polyethylene glycol
pfu	plaque-forming units
pHPMA	poly(N-[2-hydroxypropyl]methacrylamide)
PR	partial response
pRb	retinoblastoma protein
QA	quaternary amine
Q-PCR	real time quantitative polymerase chain reaction
R-PE	R-Phycoerythrin
R^2	coefficient of determination

RANTES	Regulated upon Activation, Normal T-cell Expressed, and Secreted (also CCL5)
RGD	Arg-Gly-Asp motif
RLU	relative light units
RNA	ribonucleic acid
rpm	revolutions per minute
RPMI	Roswell Park Memorial Institute medium
RT	room temperature
SD	stable disease
SDS	Sodium dodecyl sulfate
sec	second(s)
ss	single-stranded
T/E	trypsin-EDTA
$TCID_{50}$	50% Tissue Culture Infective Dose
TE	Tris-EDTA-buffer
TK	thymidine kinase
TMB	tetramethylbenzidine
TRIS	Tris(hydroxymethyl)aminomethane
TP53	tumour protein 53 gene
TT	thiazolidine-2-thione
V	volume
v/v	volume per volume
VEGF-A	vascular endothelial growth factor A
vp	virus particles
vs	versus, in comparison to
vsb	virus storage buffer
w	weight
w/v	weight per volume
x	multiplied by

1 Introduction

1.1 Ovarian cancer

Despite the introduction of new chemotherapeutic agents and improved treatment regimens and drug combinations over the last 30 years, ovarian cancer remains the leading killer among all gynaecological cancers. Although the overall 5-year survival rate of patients has risen from 30% to 40% over the last 20 years, this is predominantly due to improved survival of patients presenting at FIGO (**F**édération **I**nternationale de **G**ynécologie et d'**O**bstétrique) stages I and II (25% and 10%, respectively). In contrast, current treatment possibilities for the late stage disease (FIGO III and IV) have yet to significantly improve patient prognosis (CRUK, accessed 6 June 2011). This is of particular importance as the majority of women with ovarian cancer are diagnosed with advanced disease due to its relatively silent onset and progression, which leaves patients unaware of the developing malignancy.

Early stage symptoms of ovarian cancer are predominantly non-specific and often misinterpreted as other common bowel-related ailments. Most frequently women may experience abdominal pain and bloating in early stage ovarian cancer, followed by swelling of the abdomen, intensified pain, constipation or incontinence caused by dissemination of the tumour cells (Hennessy *et al.*, 2009). It is mostly at this later stage that patients are diagnosed through histology, measurement of serum CA125 levels and ultrasonography.

1.1.1 Current standard of care

Surgery is often the first step of intervention for the majority of ovarian cancer patients, although there is increasing evidence for chemotherapy prior to debulking surgery (Vergote *et al.*, 2010). The aim of surgery is to remove all macroscopic disease; this most commonly includes oophorectomy, hysterectomy, lymph node sampling and omentectomy, although it can involve extensive, so-called, ultra-radical surgery with extensive upper abdominal surgery and stripping of peritoneal surfaces. At this point the disease is staged according to FIGO and subsequent histology confirms the diagnosis and staging. In patients with early disease (FIGO Ia) surgery can be curative, but adjuvant chemotherapy is recommended for all those with greater than

stage Ia disease, even if macroscopically cleared, to minimise the risk of recurrence (Hennessy *et al.*, 2009).

The current standard treatment regimen consists of intravenous (i.v.) administration of the alkylating-like platinum agent carboplatin either as a single agent or in combination with the mitosis inhibitor paclitaxel. Carboplatin is a cisplatin-derivative, which can cross-link DNA bases (predominantly guanine and adenine), effectively interfering with mitosis and inducing frustrated DNA-repair mechanisms, which activates apoptotic signalling. Carboplatin is the preferred agent for the treatment of ovarian cancer due to equivalent efficacy to cisplatin in this cancer type and markedly reduced side-effects (Go and Adjei, 1999). Paclitaxel is recommended in combination with carboplatin for first-line treatment (Sandercock *et al.*, 2002; ICON and AGO, 2003), although it has activity as a single agent and can be given alone for recurrent platinum-resistant disease (Kumar *et al.*, 2010). Paclitaxel binds tubulin molecules and promotes polymerisation into disassembly-resistant microtubules, effectively inhibiting mitosis and ultimately stimulating apoptotic signalling (Eisenhauer and Vermorken, 1998). Hence, both drugs used in the current standard care of ovarian cancer rely on the induction of apoptosis, a mechanism, which, in many cancer cells, develops defects during progression to a malignant phenotype.

1.1.2 Obstacles to increased efficacy and new directions

Despite improvements in surgical procedures and refined chemotherapy regimens, the increase in overall patient five-year survival rates over the last 20 years remains low. This is predominantly caused by a failure to improve the survival rate of patients presenting with late stage disease, who constitute the majority of newly diagnosed cases. While many do initially experience tumour regression and disease-free intervals, recurrence is common and, due to incomplete cytoreduction after first-line treatment and the high mutation rate of tumour cells, the development of chemoresistance is a hallmark of relapsed disease.

In an endeavour to altogether avoid the difficulties encountered in late stage patients, efforts are made to enable early diagnosis of ovarian cancer when patient prognosis is significantly better. At present there is no screening programme for ovarian cancer, in contrast to the very effective cervical cancer screening programme, established in the UK more than twenty years ago. However, with the UK Collaborative Trial of Ovarian Cancer Screening (UKCTOCS), a multi-centre randomised controlled trial, an effort is made to evaluate, if an approach of regular screens can improve mortality rates in ovarian cancer. The study compares a combination of annual testing of the serum level of the ovarian tumour marker CA125 and transvaginal ultrasound scans, when measured CA125 indicates elevated cancer risk, or annual transvaginal ultrasound alone. While it has recently been reported that both methods lead to effective detection of early stage disease (Menon *et al.*, 2009), it is not yet clear, if an actual decrease in mortality rates can be achieved as data from the non-examined control group have not yet been published. The costs of establishing nation-wide screening facilities and providing training in gynaecological ultrasound are difficult to estimate. Furthermore, the risk to patients through unnecessary operations on benign tumour masses needs to be considered (Vergote *et al.*, 2009). Until final results will be presented in 2014 it is difficult to estimate, if the benefits of this project outweigh the risks for patients and costs for the health system

One way to improve prognosis is to increase the efficacy of current treatments in order to achieve total elimination of malignant cells after first-line treatment. In patients with disease localised to the peritoneal cavity intraperitoneal (i.p.) administration of chemotherapy may increase efficacy and reduce toxicity, due to higher local and lower systemic drug concentrations. While evidence from a range of clinical trials was, overall, inconclusive, some studies did, indeed, demonstrate a significant increase in overall survival of i.p. treated patients (Metzger-Filho *et al.*, 2010). However, as chemotherapy dosage in the i.p. and i.v. arms were not always equivalent, it remains unclear if the beneficial effect of i.p. administration was only due to increased doses in the i.p. arm. In addition, i.p. treatment adds complicating factors to chemotherapy administration. It requires greater attention from medical personnel than i.v. administration and problems with inflammation and local infection due to catheter placement

have been observed during trials. Hence, due to a lack of evidence, the use of this treatment modality is not part of current standard care.

A second strategy to improve efficacy emerged with the development of novel targeted treatments for other kinds of solid tumours such as breast cancer and colorectal cancer (trastuzumab and bevacizumab, respectively). This has provoked considerable efforts to investigate these and similar agents in ovarian cancer and several drugs are undergoing clinical trials, particularly in patients with relapsed, platinum-resistant disease (Mantia-Smaldone *et al.*, 2010). These treatments are targeted towards signalling pathways, which are frequently aberrant in cancer cells, hence providing higher tumour selectivity than conventional chemotherapy. For instance, the antiangiogenic, VEGF-A (vascular endothelial growth factor A) -binding antibody, bevacizumab, has shown activity in monotherapy in phase II trials in multi-drug-resistant ovarian cancer (Burger, 2011). Recently, two phase III trials (ICON7 and OCEANS) evaluating clinical efficacy of bevacizumab in combination with carboplatin / paclitaxel or carboplatin / gemcitabine, respectively, demonstrated significantly enhanced progression-free survival in the bevacizumab treatment arms (Aghajanian, 2011; Kristensen, 2011). Other targets include growth-stimulatory tyrosine kinase-mediated signalling by members of the epithelial growth factor receptor (EGFR) family. Direct tyrosine kinase inhibitors include gefitinib and erlotinib. Trastuzumab, cetuximab and panitumumab are monoclonal antibodies which bind the extracellular domain of EGFR and inhibit down-stream signalling. Many of these treatments are currently undergoing clinical testing and it is anticipated that some might improve the prognosis of patients, particularly in combination with current chemotherapeutic agents.

The targeted treatments discussed above were developed after gaining new insights into tumour etiology and biology. Similarly, the discovery that mutations in the tumour-suppressor genes BRCA1 / 2, which are involved in the repair of double-strand breaks after DNA damage, increase women's risk of developing breast and ovarian cancer led to the investigation of PARP-inhibitors such as iniparib and olaparib. BRCA dysfunction causes genome instability in the form of accumulation of DNA mutations, which can result in malignant transformation and

tumourigenesis. It has been found that in patients with germline or somatic BRCA mutations (which often occur in non-hereditary ovarian cancer) the inhibition of PARP, a base excision repair enzyme, leads to “synthetic lethality” in BRCA-mutated cells and several clinical trials are underway to investigate efficacy of this treatment (Mantia-Smaldone *et al.*, 2010).

1.2 Cancer gene therapy

As mentioned above (section 1.1.1), efficacy of most classic cancer treatments relies on the induction of apoptosis. Currently approved chemotherapeutic drugs for ovarian cancer interfere with DNA function, DNA replication or mitosis with the aim of provoking cell-cycle arrest which, in the case of irreparable damage, leads to apoptotic cell death. However, increased knowledge of tumour-biology revealed that many of the proteins involved in cell-cycle control and apoptotic signalling are mutated during malignant transformation of cells resulting in down-regulation of apoptotic pathways. This is thought to severely impact on the efficacy of classic chemotherapeutic agents and has inspired the search for novel kinds of therapies, whose efficacy does not rely on functional apoptotic pathways.

1.2.1 The use of viruses in cancer treatment

Viruses are obligate intracellular parasites and have evolved to efficiently enter host cells, deliver their genome to the site of replication (the nucleus or cytoplasm) and exploit the cell's replication machinery for genome amplification and protein expression. These intrinsic abilities make viruses very interesting for two closely related areas in current cancer-therapeutics research: gene therapy and oncolytic virotherapy.

1.2.1.1 Viral vectors in cancer gene therapy

With the advent of genetic engineering the need for potent vectors for gene therapy arose. From the very beginning the great potential in the use of viruses in this approach had been recognised. Successful cancer gene therapy relies on the efficient delivery and functional expression of the therapeutic genes it is attempting to supplement, in very much the same way viruses have done for millennia. Hence, much research is concerned with the investigation of different viruses in terms of their suitability as gene therapy vectors. Ideally, in addition to efficiency in gene delivery and expression, a viral vector used in cancer treatment should be able to selectively infect both dividing and non-dividing tumour cells, safely introduce an intact

transgene, express high levels of the therapeutic gene long-term and avoid deleterious host responses. Furthermore, ease of manufacturing of large quantities of vectors and large transgene capacity are essential for its suitability as a therapeutic agent. The most commonly investigated viruses are summarised and their individual advantages and drawbacks detailed in Table 1-1.

Table 1-1 Main classes of viruses used for vector constructs in cancer gene therapy

Vector	Genome	Trans-gene capacity	Tropism	Immune reponse	Main advantages	Main disadvantages
vector genome form: episomal						
Adenovirus	ds DNA	large	broad	strong	very efficient transduction, low pathogenicity, producible to high titres, good storage stability	strong inflammatory response, wide tropism
Herpes simplex virus I	ds DNA	very large	broad, strong for neurons	strong	very large transgene capacity	persistent transduction only in neurons
vector genome form: episomal / integrated						
Adeno-associated virus	ss DNA	small	broad	weak	non-inflammatory, non-pathogenic	small packaging capacity
vector genome form: integrated						
Lentivirus	RNA	large	broad	weak	persistent gene transfer	oncogenic potential
Retrovirus	RNA	large	dividing cells only	weak	persistent gene transfer	transduces only dividing cells, oncogenic potential

ds = double-stranded; ss = single-stranded

adapted from (Thomas *et al.*, 2003)

Classic gene therapy strategies were using viruses solely to deliver the genes of interest. Hence, in these studies viruses were rendered replication-defective through deletion of virus genes essential for replication. Only a small number of gene therapy clinical trials employing these vectors have been performed in ovarian cancer (summarised in Table 1-2) and two main strategies have been explored: supplementation of lost or mutant tumour suppressor genes or introduction of new therapeutic genes.

Tumour suppressor replacement

As described above (section 1.1.2), BRCA1 is involved in repair of DNA double-strand breaks, thus maintaining genome stability. As over-expression of this gene in animal xenograft models of ovarian cancer had demonstrated inhibition of tumour growth, clinical trials in patients with recurrent or persistent ovarian cancer were performed with a non-replicating retrovirus construct (Tait *et al.*, 1999) (see Table 1-2 for results). Similarly, the TP53 gene product p53 is the main regulator of the G1-S checkpoint and controls the expression of many genes involved in cell-cycle arrest, DNA-repair and apoptosis. TP53 had been found to be frequently mutated in a variety of cancers and, in particular, up to 70% of advanced tumours in ovarian cancer (Buller *et al.*, 2002a). In addition, it had been shown that mutations in TP53 are associated with chemotherapy resistance and more aggressive tumours in advanced ovarian cancer (Buttitta *et al.*, 1997). Hence, it was hypothesised that replacement of TP53 would render ovarian cancer cells both apoptosis- and chemotherapy-sensitive and replication-deficient adenovirus constructs were used to re-introduce the TP53 gene in ovarian tumour cells (Buller *et al.*, 2002a; Wolf *et al.*, 2004) (see Table 1-2 for results of clinical trials).

Introduction of therapeutic genes

This approach, which has been termed “Suicide gene therapy” or “Virus directed enzyme-prodrug therapy”, introduces an enzyme-encoding gene into tumour cells, which can convert a non-toxic prodrug into an active chemotherapeutic agent. A combination of the delivery of a thymidine kinase (TK) encoding gene, derived from the Herpes simplex virus (HSV) employing a

replication-deficient adenoviral vector, and administration of Ganciclovir has been investigated in two clinical trials (Alvarez *et al.*, 2000; Hasenburg *et al.*, 2000; Hasenburg *et al.*, 2001).

Overall, it was found that clinical anti-tumour efficacy of these treatments was low (see Table 1-2). However, some valuable insights into the complications associated with virus application to the peritoneal cavity emerged and helped in the development of more sophisticated virus-derived treatments (discussed in section 1.3.2.2).

Table 1-2 Selected gene therapy trials with non-replicating viral vectors in ovarian cancer

Construct	Grade 3 / 4 toxicity	Response rate, *n/n*			Study
		SD	PR	CR	
Tumour suppressor replacement					
Retroviral LXSN*BRCA1sv*	3/12	8/12	3/12	0/12	(Tait *et al.*, 1999)
SCH58500 (*p53*)	11/36	4/36	0/36	0/36	(Buller *et al.*, 2002a)
Ad *p53*	6/15	6/11	0/11	0/11	(Wolf *et al.*, 2004)
Introduction of therapeutic genes					
Ad *HSV-TK*	0/14	5/13	0/13	0/13	(Alvarez *et al.*, 2000)
Ad *HSV-TK*	4/10	3/10	0/10	0/10	(Hasenburg *et al.*, 2000; Hasenburg *et al.*, 2001)
SD = stable disease; PR = partial response; CR = complete response adapted from (Kimball *et al.*, 2006)					

1.2.1.2 Oncolytic virotherapy

Since early clinical trials using replication-deficient viral vectors demonstrated a lack of efficacy, the use of replicating viruses, in order to increase cytotoxicity of treatments, attracted increasing attention. The concept of oncolytic virotherapy describes treatment strategies where replication-competent viruses selectively kill tumour cells directly during a lytic replication cycle, releasing new virions, which spread through the tumour.

Knowledge of the possibility of treating tumours with replicating wild-type viruses has existed for nearly a century. Beneficial responses of haematological cancers to natural virus infections were first reported at the turn of the 19th century and in the 1950s and 1960s a series of studies examined the use of viruses as antineoplastic agents against a variety of malignant diseases (Newman and Southam, 1954; Smith *et al.*, 1956; Cassel and Garrett, 1965; Kelly and Russell, 2007). Due to limited clinical success and the advent of combination chemotherapy the interest in this treatment modality diminished temporarily and only isolated studies were performed until the 1990s. However, a better understanding of cell and tumour biology and advances in virology and genetic engineering during the second half of the 20th century led to the current revival of interest in the use of replication-competent viruses as therapeutics in cancer treatment.

The focus of this field of research lies on viruses that undergo a lytic replication cycle such as adenovirus, measles, vaccinia, vesicular stomatitis and Newcastle disease virus. Central to this strategy was the discovery that some viruses appeared to possess a degree of inherent selectivity for the replication in, and lysis of, tumour cells (Roberts *et al.*, 2006). Naturally, a virus needs to subvert the host cell's replication machinery in order to propagate; many viruses do encode genes whose products interrupt cellular mechanisms of cell-cycle control and DNA damage sensing. Notably, it was found that many of these virus proteins act on the same pathways which are mutated in malignant cells (for example p53), revealing intriguing possibilities for the use of these viruses in cancer treatment (Parato *et al.*, 2005). Hence, while gene therapy with non-replicating viruses seeks to replace mutant proteins or insert new proteins into malignant cells, oncolytic virotherapy exploits the absence of functional tumour

suppressors. Furthermore, the release of replication-competent progeny after the initial replication cycle of the input dose makes this treatment unique, as it is capable of amplification of its active agent, in the patient, after administration. As a whole, this makes oncolytic virotherapy a very attractive treatment option for advanced, chemotherapy-resistant, aggressive and potentially even disseminated types of cancer.

1.3 Adenovirus treatments in ovarian cancer

A wide range of oncolytic viruses has been evaluated for their potential as oncolytic agents in a variety of tumours of different origin and many clinical trials have been conducted or are currently under way. For the treatment of ovarian cancer, reovirus, vaccinia virus, measles vaccine strain viruses and adenovirus are being explored and several are undergoing testing in phase I or II trials (Table 1-3) (Hartkopf *et al.*, 2011). Adenovirus has been an immensely popular research subject since the very beginning of the development of gene therapy due to its specific advantages as detailed in Table 1-1. In addition, the approval of an adenovirus-derived virotherapy agent, the first licensed virotherapeutic in general, for the treatment of head and neck cancer in China (Garber, 2006) confirmed its efficacy in approaches of local administration and the validity of the use of adenoviruses as oncolytic agents in general.

Table 1-3 Oncolytic virotherapy trials in ovarian cancer or malignant ascites

Virus / construct name	Trial description	Safety	Responses *n/n*	Study
Adenovirus (serotype 5)				
Onyx-015	phase I i.p. administration patients with recurrent disease	well tolerated no severe AE	no clear evidence of response	(Vasey *et al.*, 2002)
H101	phase I i.p. administration patients with malignant ascites (non-ovarian cancer origin)	well tolerated no severe AE	NR: 4 / 9 PR: 2 / 9 CR: 3 / 9	(Liu and Chen, 2009)
Ad5-Δ24-RGD	phase I i.p. administration patients with recurrent disease	well tolerated	PD: 5/19 SD: 14/19	(Kimball *et al.*, 2010)
Measles Virus (Edmonston vaccine strain)				
MeV-CEA	phase I i.p. administration patients with recurrent disease	well tolerated	SD: 14/21 (dose dependent, median duration 92.5 days)	(Galanis *et al.*, 2010)

PD = progressive disease; SD = stable disease;
NR = no response; PR = partial response; CR = complete response
adapted from (Hartkopf *et al.*, 2011)

1.3.1 Adenovirus biology

Adenoviruses have been isolated from a wide range of vertebrates including fish, birds and mammals. The genus *Mastadenovirus* includes all human adenoviruses and 51 serotypes have been distinguished by their resistance to neutralisation by antisera specific for other human serotypes. These have been further classified into six species / groups (A – F) according to their haemagglutination capacity in human, rat and monkey blood. Adenoviruses are comprised of a non-enveloped, icosahedral protein capsid with protruding fibres at its vertices containing a linear double-stranded DNA genome (Figure 1-1).

1.3.1.1 Adenovirus proteins

The most studied serotype is the species C adenovirus 5 (Ad5). Its capsid is composed of three major and ten minor proteins and its major structural proteins are protein II (hexon, 240 copies), protein III (penton base, 12 copies) and protein IV (fibre, 12 copies). Penton base and fibre form the covalently linked penton protein, of which one copy is situated at each of the virus' twelve vertices. While structural proteins of other virus serotypes differ in amino acid sequence their functions in the formation of the virus capsid and the adenovirus life-cycle are similar.

Hexon

The 240 copies of protein II cover the largest part of the capsid surface and have been shown to play roles in immune responses, dismantling after cell infection and cellular uptake of virions. Nine hypervariable regions in the hexon protein form the basis for differential neutralisation of adenovirus serotypes (Russell, 2009). Hence, the hexon protein appears to be the main immunogenic component of the virus capsid. Furthermore, hexon may have a physiological role in cell entry via binding of the coagulation factor X (Waddington *et al.*, 2008).

Penton base

12 copies of protein III are distributed at the vertices of the adenovirus capsid and play a major role in capsid stability through interaction with adjacent capsomeres. The penton base contains an Arg-Gly-Asp (RGD) motif (termed "RGD loop"), which is conserved among adenovirus

groups A, B, C and E (Rux and Burnett, 2004) and is essential for the adenovirus internalisation process through integrins (Wickham *et al.*, 1993). It has also been shown to help in the release of the virus from endosomes after internalisation (Shayakhmetov *et al.*, 2005).

Fibre

The 12 copies of protein IV are covalently linked to the penton base proteins so that they project from the vertices of the virus capsid. The fibre protein can be divided into the tail and shaft (making up the rod) and the knob region. The length of fibres can vary markedly between serotypes and is dependent on the number of pseudo-repeats of a short amino acid sequence in the shaft. Hinge regions in the shaft allow flexibility of the fibre, which is necessary for interaction with uptake receptors. The knob domain holds a number of variable loop sequences, which are responsible for the varying haemagglutination capacity on which the distinction of the six adenovirus species is based. In addition, these loops convey the specificity in uptake receptor usage observed for the different species (reviewed in (Russell, 2009)).

All three major structural proteins (hexon, penton base and fibre) have been shown to have roles in adenovirus neutralisation by antibodies. For example, it has been demonstrated that a monoclonal antibody directed against hexon could block microtubular transport to the nucleus (Smith *et al.*, 2008). Antibodies directed against the penton base protein have been demonstrated to neutralise infection by blocking virus uptake or release from the endosome (Wohlfart, 1988). Furthermore, antibodies directed against epitopes on the fibre protein have been identified in human sera (Bauer *et al.*, 2005).

The roles of other structural proteins in the virus capsid remain mostly undefined. However, functions in capsid stabilisation (protein IX) and release from endosomes after cellular uptake (protein VI) have been demonstrated. Similarly, a wide range of functions has been discussed for the adenovirus core proteins. For instance, both proteins V and VII have been shown to interact with the virus DNA. Furthermore, protein VII was demonstrated to participate in nuclear trafficking and DNA import (reviewed in (Russell, 2009)).

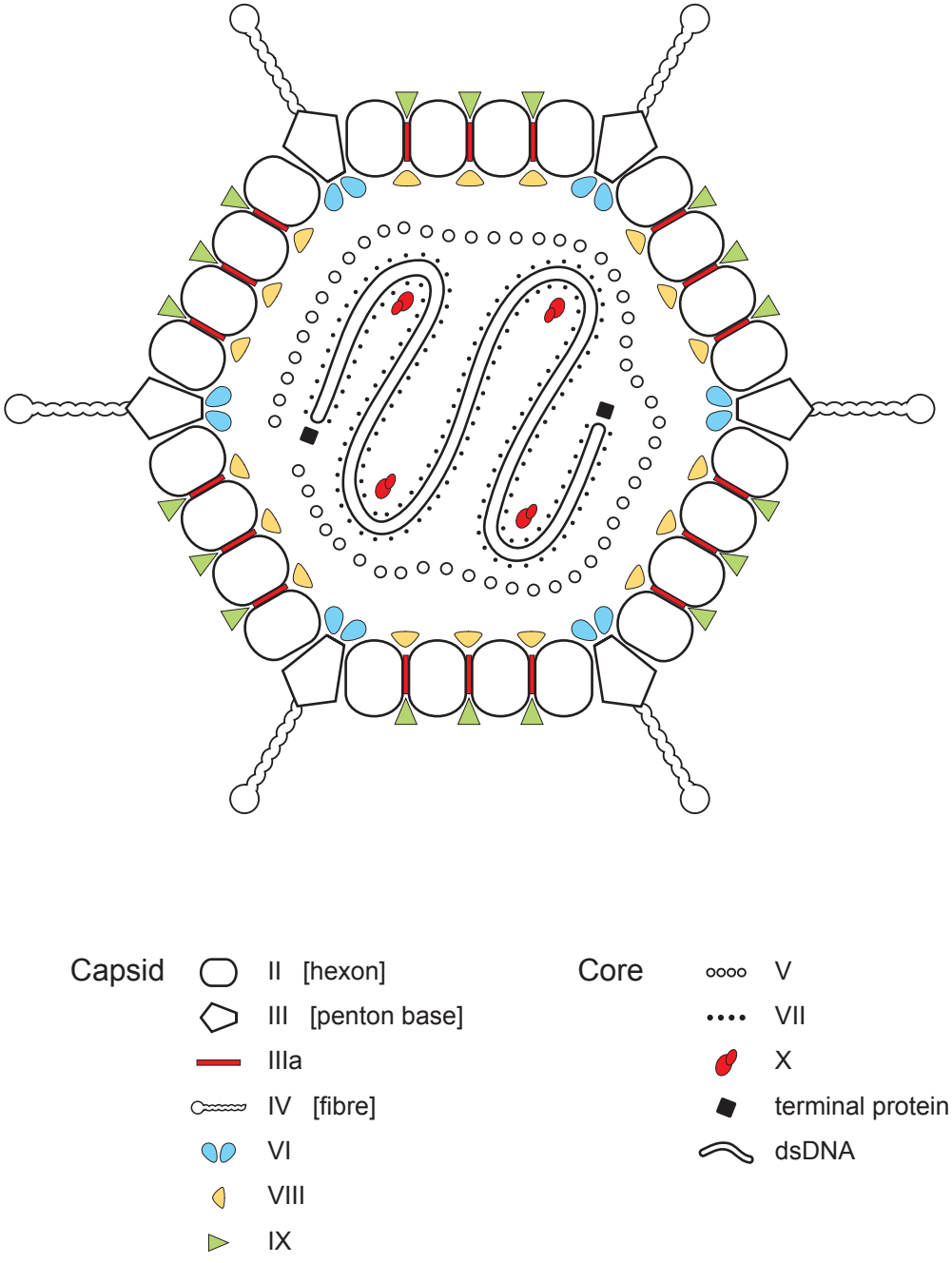


Figure 1 - 1 The structure of adenovirus

A stylised, schematic depiction of a cross-section of adenovirus based on cryo-electron microscopy and crystallography predominantly based on Ad2 and Ad5. The picture indicates the relative position of proteins; components are not to scale. Adenoviruses are comprised of a non-enveloped, icosahedral protein capsid with protruding fibres at its vertices containing a linear double-stranded DNA genome. The capsid is composed of 3 major and 10 minor proteins. Its major structural proteins are protein II (hexon, 240 copies), protein III (penton base, 12 copies) and protein IV (fibre, 12 copies). Penton base and fibre form the covalently linked penton protein, of which one copy is situated at each of the virus' 12 vertices. While structural proteins of other virus serotypes differ in amino acid sequence their functions in the formation of the virus capsid and the adenovirus life-cycle are similar. Figure adapted from Russell, 2009 and Rux and Burnett, 2004.

1.3.1.2 Adenovirus life-cycle

The adenovirus life-cycle consists of host cell infection, nuclear trafficking and virus DNA import followed by genome and virion replication and virus release through lytic host cell death (Figure 1-2).

Cell attachment and entry

The first step of the adenovirus life-cycle consists of infection of cells via binding to cell-surface receptors and receptor-mediated uptake. As mentioned above (section 1.3.1.1, Fibre), different species employ different receptors due to varying knob domain sequences. The most widely studied adenovirus, group C Ad5, uses the Coxsackie virus and adenovirus receptor (CAR) for virion attachment via the fibre knob to the cell surface (Bergelson *et al.*, 1997). It has been observed that even in the absence of intracellular and trans-membrane domains of CAR, virus uptake is possible, demonstrating that the extracellular domain appears to act as an anchor for virions only (Wang and Bergelson, 1999). Virion attachment is followed by binding of integrins $a_V\beta_3$ and $a_V\beta_5$ through the RGD loop of the penton base (Wickham *et al.*, 1993). This has been shown to induce conformational changes in the integrins and to stimulate down-stream signalling events leading to clathrin-mediated endocytosis. Recently, it has been demonstrated that Ad5 can also achieve access to cells after interaction of the coagulation factor X with hypervariable regions of the hexon protein (Waddington *et al.*, 2008). In addition, macropinocytotic uptake of adenovirus has been demonstrated (Meier and Greber, 2004).

It has long been reported that group B adenoviruses such as serotypes 3 (Ad3) and 11 (Ad11), in contrast to members of all other adenovirus groups, employ the complement receptor CD46 for cellular uptake (Segerman *et al.*, 2003; Sirena *et al.*, 2004). However, early reports also highlighted low binding affinity of Ad3 to certain CD46 isoforms, divergent from other group B adenoviruses (Gaggar *et al.*, 2003). Heparan sulphate proteoglycans (HSPGs), CD80 and CD86 have since been proposed as alternative receptors for members of this species (Tuve *et al.*, 2006; Tuve *et al.*, 2008; Hall *et al.*, 2009) and recently, Ad3 and Ad11 attachment to Desmoglein 2, a transmembrane protein of the cadherin family, on epithelial cells has been demonstrated (Wang *et al.*, 2011). Furthermore, it has been suggested that integrins could also

play a role in cell entry of group B adenoviruses, as the penton base RGD motif was found to be conserved throughout adenovirus groups, with the exception of group F (Arnberg, 2009). Indeed, uptake of Ad5 by integrin $a_V\beta_5$ in the absence of CAR has been demonstrated (Lyle and McCormick, 2010) corroborating a potential role of these receptors also in group B uptake. Hence, it appears that several receptors can play a role in the attachment and uptake process of group B adenoviruses and further studies are required to fully characterise their functions in the cell infection process.

Endosomal escape, translocation and nuclear uptake

Following endosomal uptake Ad5 particles rapidly (3-15 minutes) escape to the cytosol (Leopold and Crystal, 2007). This has been shown to be mediated by protein VI, which, alongside protein IIIa, penton and peripentonal hexons, is initially dissociated from the capsid through the increasing acidification of the endosome (Greber *et al.*, 1993). Separation of protein VI triggers conformational changes in this protein followed by its association with, and ultimately disruption of, the endosomal membrane (Wiethoff *et al.*, 2005). Once in the cytosol, the partially dismantled capsid moves towards the microtubule organising centre (MTOC) close to the nucleus through interaction with microtubules via dynein motors (Leopold and Pfister, 2006). It has been shown that the nucleus itself is required to allow subsequent detachment from the MTOC (Bailey *et al.*, 2003) before association of particles with the nuclear pore complex (NPC), the major gateway for macromolecules through the double-layered nuclear membrane. It has been demonstrated that attachment to the NPC is required for final disassembly of the remaining capsid components and release of DNA (Greber *et al.*, 1997). While a role of histone H1, nuclear export protein CRM1 and HSC70, a molecular chaperone, in capsid attachment to the NPC and nuclear import of DNA have been demonstrated, the exact mechanisms and further proteins involved in these mechanisms remain unknown so far (Leopold and Crystal, 2007). Furthermore, group C serotypes 2 and 5 have predominantly been used to investigate this “classic” pathway of intracellular adenovirus trafficking and some studies examining these processes employing group B adenoviruses found variations to these concepts in terms of duration of trafficking, attachment to the nucleus and nuclear import of virus DNA (Leopold and Crystal, 2007).

Replication

The Ad5 double-stranded DNA genome consists of five early (E1A, E1B, E2, E3 and E4), two delayed (IX and Iva2) and five late transcription regions (L1 – L5). Virus replication after nuclear entry begins with the expression of E1A followed by E1B, which directly and indirectly interact with the cell-cycle control proteins pRb and p53, respectively, to induce entry into cell-cycle S phase and DNA replication. These mechanisms are also responsible for the transactivation of E2, which encodes proteins required for virus genome replication. Proteins expressed from E3 inhibit host immune responses and apoptosis mechanisms and E4 is essential for late gene expression. The late genome regions L1 – L5 encode the structural proteins of the adenovirus capsid and regulate its production and assembly. Their expression is regulated by the major late promoter (MLP), which is highly upregulated at later stages of virus replication. Eventually, progeny virions are assembled and released during the lytic death of the host cell.

Not all mechanisms involved in adenovirus replication have been elucidated to date and for many the exact interactions that lead to the subversion of the host cell machinery required for adenovirus replication, packaging and release of progeny and induction of cell lysis remain unknown. Importantly, while the overall organisation into early and late regions and their respective functions appear to be similar across adenovirus serotypes, different serotypes do carry some specific sequences, which have not been detected in others. This might be of great importance in the choice of serotype for a specific therapeutic approach. For instance, while the E3 regions of Ad5 and Ad3 encode sequences for the Adenovirus Death Protein (ADP), which has been demonstrated to facilitate cell lysis and progeny virion release after replication (Tollefson *et al.*, 1996) through an unknown process, a corresponding sequence could not be detected in Ad11 (Mei *et al.*, 2003).

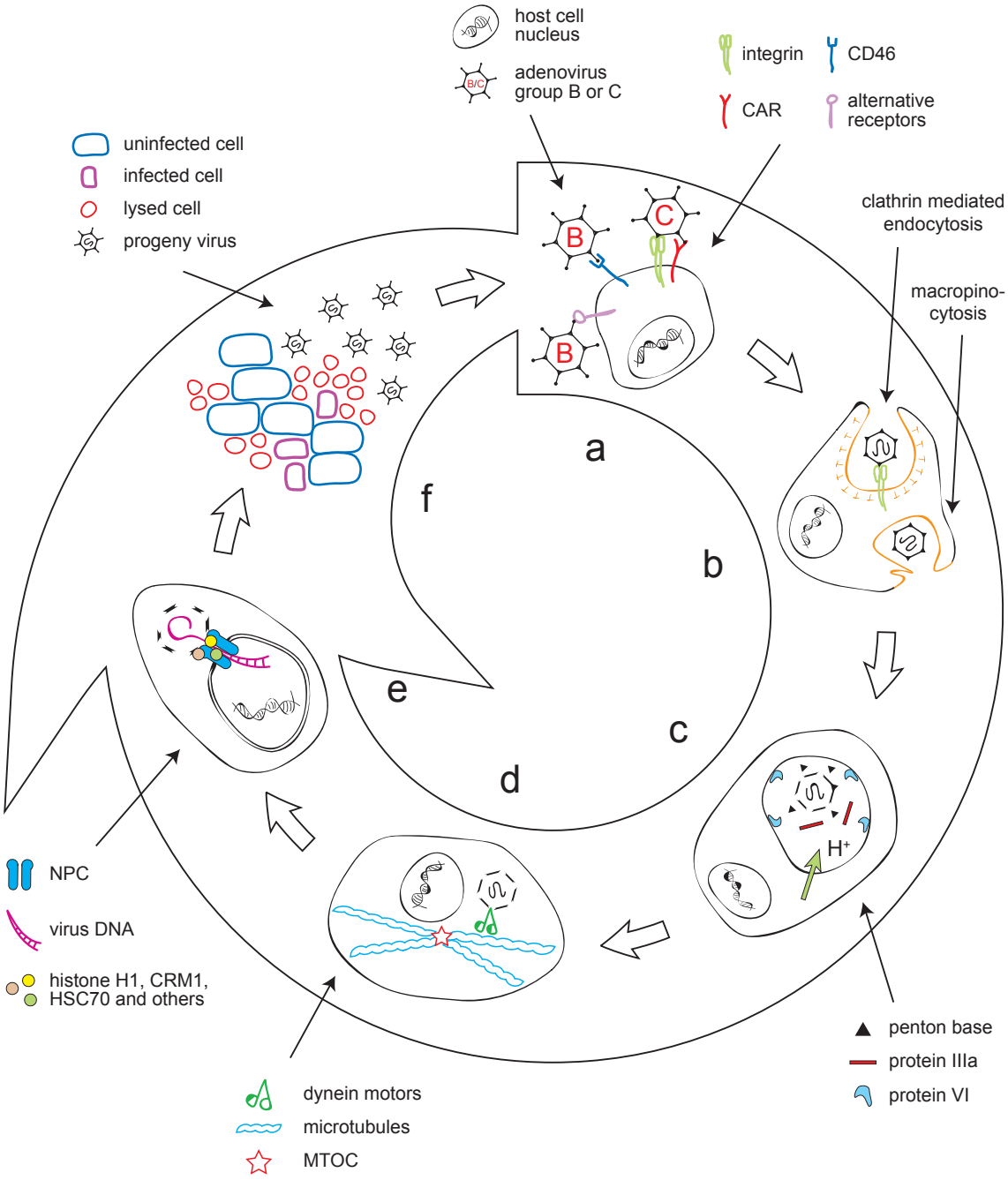


Figure 1 - 2 The adenovirus life-cycle

A stylised. schematic depiction of the adenovirus life-cycle. Adenovirus binds cell-surface receptors (e.g. group C: CAR and $a_V\beta_{3/5}$; group B: CD46 or alternative receptors such as Desmoglein 2) (a) and is internalised through clathrin mediated endocytosis or macropinocytosis (b). The early endosome becomes acidified through proton pumps triggering partial capsid disassembly with loss of penton base and proteins IIIa and VI. After conformational changes protein VI associates with the endosomal membrane and aids its disruption (c). Once in the cytosol the partially dismantled capsid moves towards the microtubule organising centre (MTOC), close to the nucleus, through interaction with microtubules via dynein motors (d). Attachment to the nucleus at nuclear pore complexes (NPC), further capsid disassembly and DNA import is mediated via cellular proteins such as histone H1, CRM1 and HSC70 (e). Expression of early genes then triggers virus replication followed by progeny virus assembly ultimately resulting in virion release via the lytic death of the infected cells (f). Variations from this basic schematic in e.g. cellular attachment and trafficking have been demonstrated for different Ad serotypes. Figure adapted from Meier and Greber, 2004.

1.3.2 Strategies in the use of adenovirus in ovarian cancer treatment

1.3.2.1 Selected early clinical trials of i.p. adenovirus therapy

Early strategies in adenovirus-based i.p. treatments for ovarian cancer employed replication-deficient Ad5 as a gene-delivery vehicle only. The most prominent clinical trial was using an Ad5-derived vector to re-introduce the TP53 gene in ovarian tumour cells as described above (section 1.2.1.1) (Buller *et al.*, 2002a). Replacement of TP53 was thought to restore both apoptosis- and chemotherapy-sensitivity in ovarian tumour cells making it a very attractive candidate for a gene replacement strategy with or without combination with traditional chemotherapeutic agents. The non-replicating recombinant Ad5 vector (termed SCH58500) was constructed by deletion of E1A, E1B and pIX genes and insertion of human wild-type TP53 under the control of a cytomegalovirus (CMV) promoter (Wills *et al.*, 1994) and its anti-tumour activity validated in xenograft models (Nielsen *et al.*, 1998; Gurnani *et al.*, 1999). A phase I clinical trial evaluating the toxicity and safety of SCH58500 after intraperitoneal delivery demonstrated that, while adverse events such as fever, abdominal complaints, nausea or hypotension were frequent, this vector was well tolerated in humans and no dose-limiting toxicities were observed (Buller *et al.*, 2002a). In addition, long-term follow-up of patients suggested increased survival in the gene therapy arm of this study (Buller *et al.*, 2002b). However, this promising data was not reproducible in a subsequent phase II / III multicentre trial. Due to a lack of therapeutic effect and increased morbidity in the patient group receiving SCH58500, the study was halted at interim analysis. Although results have never been published, a number of reasons were hypothesised to be responsible for the failure of this gene therapy approach (Zeimet and Marth, 2003). Overall, while it appeared that the choice of TP53 for gene replacement in itself might have been the critical factor, decreased efficiency was certainly also due to complications caused by the adenoviral vector.

Conditionally replicating adenoviruses (CRAds) were developed to improve tumour-selectivity and anti-tumour activity of treatments by preserving adenovirus' ability of lytic replication while restricting it to tumour cells. Onyx-015 (Ad dl1520) is an Ad2 / Ad5 mutant which has a deletion

in the E1B gene resulting in the absence of expression of the E1B 55k protein (Bischoff *et al.*, 1996). E1B 55k interacts with p53 targeting it for proteasomal degradation as well as turning it into a repressor of p53 target genes. In adenovirus-infected normal cells with functional p53 this mechanism is essential to allow G1 – S phase transition and virus genome replication, while inhibiting apoptosis to allow progeny production. It was thought that deletion of E1B 55k would inhibit replication in non-transformed cells and restrict it to tumour cells, as it had previously been shown that many advanced tumours have mutant p53 or are p53-deficient (Buller *et al.*, 2002a). Notably, as Onyx-015 retained E1A and other genes essential for replication, it retained its oncolytic features. It was soon found that while tumour cell-selectivity was achieved, this was not due to p53 status *in vitro*. However, data from *in vivo* experiments in p53-mutant xenografts of ovarian tumours using i.p. Onyx-015 did show correlation of efficacy and p53 function (Heise *et al.*, 2000) and a phase I clinical trial of direct intratumoural (i.t.) injection in head and neck cancer demonstrated significant anti-tumour activity (Ganly *et al.*, 2000). Following these findings a phase I trial with i.p. delivery in ovarian cancer patients was performed (Vasey *et al.*, 2002). The treatment was found to be well tolerated and side-effects were described as “flu-like”, including pyrexia and head-aches, and their severity was not correlating to dosage. However, no therapeutic effect could be demonstrated. Nevertheless, evaluation of Onyx-015 eventually resulted in the approval of a very similar adenovirus construct (H101) in China in 2006 for the i.t. treatment of head and neck cancer (Garber, 2006) demonstrating that adenovirus virotherapy can achieve high efficacy, at least in the context of local administration.

1.3.2.2 Emerging impediments to i.p. adenovirus in ovarian cancer

The phase II / III clinical trial investigating p53 replacement with SCH58500 and the Onyx-015 trial highlighted the most prominent obstacles faced by i.p. administration of adenovirus. In both studies the lack of anti-tumour activity was attributed to low transduction efficiency of target cells and it appeared that this was due to properties of the therapeutic agents employed as well as the treatment site itself.

Initially, it was thought that ovarian cancer was privileged for successful treatment via the i.p. route. Even late-stage ovarian cancer predominantly remains confined to the peritoneal cavity and it was thought that i.p. administered agents would be able to reach all sites of disease. However, pre-treated ovarian cancer patients are often affected by peritoneal scarring and adhesion formation due to both surgery and the disease process. Hence, it appears that one reason for the failure of these trials was that many areas of the cavity were inaccessible even when employing large volumes (500 ml) of excipient. Not all mechanisms in fluid transport in the cavity are currently understood, but it has been demonstrated that the use of icodextrin in carrier fluids can increase transduction efficiency in animal xenograft models by increasing i.p. 'dwell time' (Engler *et al.*, 2003), suggesting a way to improve treatment distribution.

A second cause for the failure of the trials appeared to arise from interactions of the Ad5-derived treatments and host factors within the peritoneal cavity. Local administration was thought to ameliorate inflammatory responses to the adenovirus treatment in comparison to observations made in gene therapy trials with systemic administration. Indeed, systemic recombinant Ad5 had induced a fatal inflammatory syndrome in one patient enrolled in an early gene transfer trial (Raper *et al.*, 2003). However, while overall side-effects in both clinical trials of i.p. adenovirus discussed above (section 1.3.2.1) were mild, the p53 replacement trial was terminated after serious local inflammatory responses such as bowel adhesions, perforation and obstruction had been observed. While some of these reactions were due to i.p. catheter placement, it appeared that the Ad5-derived agent was equally causative (Stephen Chang – unpublished personal communication). Severe inflammatory responses after i.p. Ad5 were also observed in mice with xenograft models of ovarian cancer (Morrison *et al.*, 2008) highlighting a possible detrimental interaction between the peritoneal cavity and the virus.

Two other reasons for the low anti-tumour activity due to low target cell transduction were hypothesised to be due to the use of Ad5-derived constructs specifically. First, a lack of the Ad5 entry receptors CAR and integrin $a_V\beta_3$ and $a_V\beta_5$ has been proposed as one of the main reasons for the limited success of Ad5-based cancer gene therapy in the clinics in general (Hermiston, 2006) and the failure of SCH58500 in ovarian cancer in particular (Zeimet and Marth, 2003).

Indeed, it has been demonstrated that CAR and integrin $a_V\beta_3$ and $a_V\beta_5$ expression on cryosections of primary ovarian tumours is limited, showing a highly heterogenic focal pattern which was most pronounced in advanced and undifferentiated tumours (Zeimet *et al.*, 2002). Furthermore, loss of $a_V\beta_3$ expression on ovarian cancer cells has been shown to limit Ad5 transduction (Brüning *et al.*, 2001). Thus, the inability of Ad5 to infect ovarian tumours in patients appears to be one reason why data from the clinical trials did not match reports of high efficacy *in vitro* and in animal models.

Second, neutralisation of the Ad5 vector is likely to be another important reason for decreased efficacy of Ad5-derived therapies. Indeed, high prevalence of anti-Ad5 antibodies in serum from healthy volunteers (Vogels *et al.*, 2003) and in the ascitic fluid of ovarian cancer patients (Stallwood *et al.*, 2000) has been demonstrated and is thought to impede infection and transduction of target cells with Ad5. Furthermore, recent reports have shown that Ad5 virions can be sequestered by non-target cells such as erythrocytes (Carlisle *et al.*, 2009) and platelets (Othman *et al.*, 2007) through binding to CAR on their cell surfaces. Importantly, CAR is not expressed on murine erythrocytes, highlighting a significant restriction to correctly assess pharmacokinetics of Ad5 in murine models. Hence, in the case of blood leakage or wound repair in the peritoneal cavity, substantial amounts of an Ad5-derived agent could be inactivated through these interactions in humans, which could not have been predicted from studies in animal models.

1.3.2.3 New strategies for i.p. adenovirus

Two decades of research of adenovirus as a gene therapy and oncolytic agent for ovarian cancer have created a vast amount of knowledge regarding its behaviour as a therapeutic agent in this setting. Data gathered from laboratory work and both clinical gene therapy and virotherapy trials enabled the intelligent design of adenovirus-derived agents and resulted in a set of strategies intended to overcome obstacles encountered in earlier studies. Approaches employing genetic engineering and chemical modifications of viruses seek to improve efficacy and reduce toxicity of treatments by increasing virus replication and oncolytic efficacy in a tumour specific manner, while reducing interaction with the host's immune system.

One recent clinical trial employed an Ad5-derived infectivity-enhanced CRAd termed Ad5-Δ24-RGD (Kimball *et al.*, 2010), constructed by deletion of 24 base-pairs (bp) in its E1A gene and introduction of a 27-bp sequence, encoding an RGD motif, in the fibre gene (Suzuki *et al.*, 2002) (see Table 1-3). The deletion in E1A confers selectivity of replication to cells with a deficient Rb pathway. Introduction of RGD into the fibre allows enhanced infectivity through CAR-independent infection of cells through integrins. It had previously been shown that this modification increased transduction efficacy in ovarian tumour cell lines and primary samples, but not mesothelial tissue (Vanderkwaak *et al.*, 1999). A subsequent phase I trial in patients with gynaecological (predominantly ovarian) cancers demonstrated limited grade 1 / 2 and no vector-related grade 3 / 4 toxicities. However, clinical efficacy was limited with 14 of 19 patients presenting with stable disease and no complete or partial responses (Kimball *et al.*, 2010).

Improved tumour selectivity via deletion of the same 24-bp deletion in E1A as Ad5-Δ24-RGD was also employed in other Ad5 constructs. In addition, these CRAds carry non-adenoviral genes which are meant to enhance their tumour killing efficacy and are therefore termed “armed oncolytic adenoviruses”. For instance, Ad5/3-Δ24-TK-GFP is an Ad5-derived construct in which the E3 domains encoding the proteins gp19k and 6,7k were replaced by Herpes simplex virus thymidine kinase (TK) and green fluorescent protein (GFP) cDNA (Raki *et al.*, 2007). TK is a prodrug-converting enzyme which converts ganciclovir into its cytotoxic metabolite, hence, enhancing and extending cell killing beyond virus innate cell-lysis via ganciclovir’s reported bystander-effect. Furthermore, the Ad5 fibre knob domain was replaced by the corresponding Ad3 sequence in order to improve target cell infection. Ad3 was reported to infect cells via CD46 (Sirena *et al.*, 2004) which has been found to be widely over-expressed on tumour tissues (Fishelson *et al.*, 2003). However, *in vivo* studies in ovarian cancer xenografts in mice demonstrated no additional benefit of TK expression and ganciclovir treatment over the strong oncolytic efficiency of the construct itself (Raki *et al.*, 2007).

Another small trial used the same Ad5/3-Δ24 backbone, however, E3 domains encoding the proteins gp19k and 6.7k were replaced by the cDNA of human granulocyte-macrophage colony-stimulating factor (GMCSF) (Koski *et al.*, 2010). As GMCSF has been shown to induce tumour-reactive cytotoxic T-lymphocytes and natural killer cells (Arellano and Lonial, 2008), this construct is intended to stimulate local anti-tumour immune responses. Four out of 21 patients in this study suffered from ovarian cancer. Due to the small sample size and wide variety of treated tumours results are hard to interpret and, while only seven grade 3 and no grade 4 / 5 toxicities were reported, overall, no clear benefit of this treatment could be observed. Two months after treatment three of the four ovarian cancer patients were found to have progressive disease according to tumour marker analysis (Koski *et al.*, 2010).

These new advances in the intelligent design of adenovirus constructs for ovarian cancer virotherapy make use of lessons learned from early clinical trials and attempt to increase clinical efficacy in particular, by enhancing infection through the use of capsid-chimaeras or arming constructs with the ability to express immune stimulatory molecules or suicide genes. However, no clinical benefits of these treatments have been demonstrated so far. Furthermore, the increasing complexity of these vectors might limit their applicability in the clinic, due to limitations in manufacturing of high titres and increasing genomic instability.

1.4 Aims and scope of this thesis

Taking into account the lessons learned from earlier studies using Ad5 (discussed in section 1.3.2.2) this thesis seeks to overcome current limitations to i.p. adenovirus virotherapy of ovarian cancer. Notably, all explored agents described above were employing Ad5 as their construct backbone. However, the use of alternative serotypes in an ovarian cancer setting has not been sufficiently investigated. While the Ad5 to Ad3 fibre knob exchange was used as a means to increase target cell infection (Raki *et al.*, 2007) this modification does not address the issue of strong Ad5-specific neutralisation by pre-existing antibodies and blood components. Furthermore, it remains unclear, if serotypes other than Ad5 might be inherently better suited for oncolytic virotherapy. Hence, in order to achieve increased efficacy and lower toxicity of adenovirus virotherapy for ovarian cancer two main approaches were explored: the use of alternative adenovirus serotypes and polymer-coating of adenovirus capsids.

Alternative adenovirus serotypes

Limitations to clinical efficacy due to insufficient infection of target cells and neutralisation by pre-existing anti-Ad5 antibodies as well as induction of intraperitoneal inflammatory responses were noted in previous clinical trials. We hypothesised that the use of adenovirus serotypes other than Ad5 might help to overcome these obstacles to efficient i.p. adenovirus virotherapy.

Both Ad3 and Ad11 are group B adenoviruses, which have been shown to infect cells via the complement regulatory receptor CD46 (Gaggar *et al.*, 2003; Segerman *et al.*, 2003; Sirena *et al.*, 2004). While low expression of CAR and integrins on advanced ovarian tumours limits cellular uptake of Ad5, it has been demonstrated that CD46 is highly expressed on ovarian tumour samples in a homogenous distribution pattern (Bjørge *et al.*, 1997). This might allow efficient Ad3 / Ad11 infection of target tissues and possibly also confer tumour selectivity, as studies suggest over-expression of CD46 on malignant in comparison to non-transformed cells (Fishelson *et al.*, 2003). Additionally, CD46, in contrast to CAR, was found to not be expressed on human erythrocytes (Liszewski *et al.*, 1991). Hence, less sequestration of group B adenoviruses via this interaction could be expected.

Previous studies could show that, globally, the prevalence of antibodies in healthy volunteers directed against uncommon serotypes such as Ad11 or Ad35 was markedly lower than against Ad5 (Vogels *et al.*, 2003; Nwanegbo *et al.*, 2004). Hence, the use of Ad11 as a vector platform or oncolytic agent was hypothesised to be advantageous over Ad5 (Holterman *et al.*, 2004; Stone *et al.*, 2005). Ad11 might encounter no or lower levels of pre-existing antibodies in patients allowing more efficient target cell infection, at least for first administration.

Inflammatory responses partly due to the Ad5-derived vector construct were the reason for the termination of the p53-replacement trial described above (section 1.3.2.1) (Stephen Chang – unpublished personal communication). Severe inflammatory responses after i.p. Ad5 were also observed in xenograft models of ovarian cancer in mice (Morrison *et al.*, 2008). However, preliminary observations from *in vivo* experiments in our group had suggested that i.p. Ad11 caused less toxicity in the form of peritoneal inflammation than Ad5 (N. Green, unpublished data). Hence, the use of alternative serotypes, such as the group B adenoviruses Ad3 or Ad11, might be advantageous in comparison to Ad5 in terms of their inflammatory stimulation in the peritoneal cavity.

Polymer-coating

Neutralisation of Ad5 by pre-existing antibodies (Stallwood *et al.*, 2000; Vogels *et al.*, 2003) and blood components (Othman *et al.*, 2007; Carlisle *et al.*, 2009) might be one of the reasons for low efficacy of Ad5-derived agents in previous clinical trials. However, chemical shielding of adenovirus capsids might provide a way to overcome this and other obstacles to virotherapy such as low target transduction and induction of inflammatory signalling. Polymer coating of virions with hydrophilic reactive polymers based on poly(N-[2-hydroxypropyl]methacrylamide) (pHPMA) has previously been explored. This versatile approach has been shown to offer a degree of protection from antibody binding (Fisher *et al.*, 2001) and has displayed major advantages over non-coated Ad in terms of pharmacokinetics and bioavailability in murine *in vivo* models (Green *et al.*, 2008). In order to achieve greater target cell infection the natural tropism of adenovirus could be modified by covalent linkage of ligands like the EGF-receptor

inhibitor Cetuximab to the polymer shield (Morrison *et al.*, 2009). Hence, adenovirus coating should allow retargeting of the virus to chosen receptors and could thereby serve as a mechanism to improve target specific infection, thus improving patient safety through lower treatment doses and decreased side-effects. In this context it was also observed that polymer coated virus decreased peritoneal adhesion formation in a murine model of ovarian cancer (Morrison *et al.*, 2008). However, while data generated with Ad5 coated with conventional pHPMA have been promising, complete resistance to neutralisation cannot be accomplished with these polymers. The use of novel positively-charged polymers, derived from conventional pHPMA polymers (Subr *et al.*, 2009), could present a means to allow improved oncolytic efficacy in Ad-neutralising environments. Hence, this thesis seeks to evaluate if adenovirus coated with positive polymers would give better shielding from neutralisation than conventionally coated adenovirus without preventing cytotoxicity.

1.4.1 Hypothesis

- group B adenoviruses achieve higher oncolytic activity in ovarian cancer than group C adenoviruses
- group B adenoviruses cause less intraperitoneal inflammatory response than group C adenoviruses
- group B adenoviruses are less susceptible to neutralisation by pre-existing antibodies in cancer patients than group C adenoviruses
- improved polymer-coating will shield adenoviruses against neutralisation by immune components

1.4.2 Aims

The overall aim of this thesis is to assess if group B adenoviruses Ad3 and Ad11 are better suited as oncolytic agents in ovarian cancer than the group C adenovirus Ad5 and if improved polymer-coating can enhance protection from neutralisation in order to develop safe and efficient intraperitoneal virotherapy for ovarian cancer and will:

- evaluate the oncolytic activity of Ad3 and Ad11 in comparison to Ad5 in a panel of ovarian cancer cell lines including investigation of the influence of uptake receptor expression and virion internalisation
- compare the inflammatory response towards Ad3, Ad5 and Ad11 in murine *ex vivo* peritoneal macrophages and after i.p. administration in CD46-transgenic and non-transgenic mouse models
- assess the neutralisation capacity of malignant patient exudates towards Ad3, Ad5 and Ad11 and examine the prevalence of antibodies targeted to adenovirus proteins of the different serotypes
- assess novel positively charged polymers for adenovirus cloaking in terms of their ability to reduce neutralisation of Ad5 in *ex vivo* models of malignant ascites of ovarian cancer origin

2 Materials and Methods

2.1 General laboratory methods

This chapter describes the methods and protocols of experimental studies in this thesis. Methods have been grouped by experimental chapters. If methods were used for studies in different chapters they are listed under the chapter number in which they were first used. Unless otherwise specified, laboratory plastic-ware was purchased from Corning Inc or Fisher Scientific. Cell culture media, fetal calf serum (FCS) and phosphate-buffered saline (PBS) were purchased from PAA-Laboratories and trypsin-EDTA (T/E) from Sigma-Aldrich. Serum positive medium was high glucose Dulbecco's modified Eagle's Medium (DMEM) containing 584 mg/l L-glutamine or Roswell Park Memorial Institute medium (RPMI) variety 1640 containing 300 mg/l L-glutamine supplemented with 10% FCS, unless otherwise specified.

2.1.1 Cell lines and cell culture techniques

2.1.1.1 Cell Passage

Cells were maintained at 37ºC, 5% CO_2 in a humidity-controlled incubator and handled using sterile techniques in a class II laminar-flow cabinet. Cells were split once they were 80-90% confluent. For this, cells were washed with PBS and incubated with 1 – 2 ml T/E at 37ºC, 5% CO_2 for 5 minutes (min). After cells had detached serum-positive medium was added, cells resuspended and split into a new flask containing fresh serum-positive medium. Details of cell lines and their specific growth media are shown in Table 2-1.

Table 2-1 Details of established cell lines

Cell line	*Description*	*Growth medium*	*Split ratio*	*Reference*
A549	Human lung epithelial carcinoma	DMEM 10% FCS	1:10	European Collection of Animal Cell Cultures (ECCAC); (Giard *et al.*, 1973)
SKOV3	Human ovarian epithelial carcinoma	DMEM 10% FCS	1:8	(Fogh, 1975)
IGROV1	Human ovarian epithelial carcinoma	DMEM 10% FCS	1:8	(Benard *et al.*, 1985)
OVCAR3	Human ovarian epithelial carcinoma	RPMI 1640 10% FCS	1:6	(Hamilton *et al.*, 1984)

2.1.1.2 Storage of cell lines

Serum-positive medium was removed from 175 cm^2 flasks of confluent cells and cells washed with PBS before addition of 2 ml T/E and incubation at 37°C, 5% CO_2 for 5 min until cells had detached. Subsequently, serum-positive medium (27 ml) was added to neutralise T/E and the cell suspension centrifuged at 1,000 rpm for 5 min. The resulting cell pellet was resuspended in 6 ml freezing solution (10% sterile dimethyl sulphoxide (DMSO, Sigma-Aldrich), 90% FCS) and 1 ml aliquots in cryovials prepared. After cells had been stored at −80°C in a Mr. Frosty container (Nalgene) overnight cryovials were transferred into storage boxes at -80°C. In order to resuscitate frozen cells cryovials were thawed in a water bath at 37°C, the suspension quickly transferred to 75 cm^2 flasks containing 20 ml of pre-warmed serum-positive medium and cells resuspended. 24 hours later growth medium was renewed and cells passaged, if they were confluent (section 2.1.1.1).

2.1.1.3 Cell plating

For assays that required cells seeded into microplates such as the $TCID_{50}$, MTS or Luciferase assay (sections 2.2.4, 2.2.5 and 2.5.3, respectively) cell suspensions were prepared as described in section 2.1.1.1. The concentration of cells was then determined by counting cells with a haemocytometer (Marienfeld) and adjusted to the concentration required with growth medium. Finally, cells were seeded into wells of microplates at the required density using a multichannel-pipette (Brandt) and incubated overnight before addition of treatments.

2.1.2 Adenoviruses

Viruses were purchased from Hybrid Systems (now The Native Antigen Company). Wild-type adenoviruses and the Ad5, that had been grown in-house (Ad5a, section 5.4.1), had been propagated on A549 cells. Ad5luc (E1/E3-deleted Ad5, expressing firefly luciferase under the cytomegalovirus promoter) had been grown in 293AD cells. All viruses had been purified using double CsCl gradient purification with DNAse treatment and dialysis. Adenovirus serotype 11 was genome type Ad11p.

2.2 Methods of Chapter 3

2.2.1 Photon Correlation Spectroscopy

Photon Correlation Spectroscopy (PCS) or Dynamic Light Scattering (DLS) is a method to analyse the particle size distribution of solutions and suspensions. It allows determination of particle size and polydispersity index through light scattering and was used to examine the quality of virus preparations. Briefly, a monochromatic, coherent laser beam is guided through a cuvette containing particles, in this case adenovirus, in a dispersant. The beam is scattered by the particles and interference occurs. As the particles move in the solvent, due to Brownian motion, interference fluctuates, which is measured by a detector system. As the velocity of particle movement is dependent on particle size, it can be calculated using the Stokes-Einstein relationship. This method calculates the hydrodynamic diameter of a particle, assuming it was a sphere behaving in the same manner as the actual observed particle, and is dependent on its surface structure and properties of the dispersant. Measurements with the PCS method will therefore report different results from other size measurement techniques like Transmission Electron Microscopy, where the particle is not dispersed in a solvent.

Samples were prepared by dilution of virus in PBS to a concentration of approximately $3x10^9$ virus particles (vp) / ml and 700 µl transferred into a polystyrene semi-micro cuvette (Fisher Scientific). Measurements were performed with a Zetasizer 3000HS (Malvern Instruments). Scattered light was detected at a 90º angle to the beam path. Each sample was measured with automatic settings in triplicate of which each consisted of 10 subruns. Data was analysed with PCS software v1.52 Rev.1 (Malvern instruments) using automatic analysis settings.

2.2.2 PicoGreen® assay

The fluorescent cyanine dye PicoGreen® binds to double-stranded DNA (dsDNA) resulting in an increased fluorescence signal (Singer *et al.*, 1997). By extrapolation from a standard curve of fluorescence intensities of known amounts of dsDNA the amount of dsDNA in a virus preparation can be determined. If the virus has been prepared with benzonase to remove free virus DNA, the number of vp can then be calculated, assuming 1 µg/ml of DNA is equivalent to $2.7x10^{10}$ vp (Murakami and McCaman, 1999). The Quant-iT™ PicoGreen® assay kit (Invitrogen) with a modified protocol was used. Specifically, virus dilutions were prepared in TRIS-EDTA-buffer (TE) / 0.5% Sodium dodecyl sulfate (SDS) and incubated at 56°C for 30 min to disrupt virus capsids. A logarithmic dilution series of known amounts of bacteriophage λ DNA prepared in the same medium served as a standard curve. 50 µl of sample or standard curve dilution were dispensed in wells of a black 96 half-well microplate and 50 µl of PicoGreen® reagent (Molecular Probes, Invitrogen; diluted 1:200 in TE) added. The plate was incubated at room temperature (RT) for 2 min before fluorescence measurement in a Wallac 1420 Victor^2 multilabel counter (PerkinElmer) at an excitation and emission wavelength of 485 nm and 535 nm, respectively. A standard curve was generated from signals of DNA standards and the amount of DNA in samples extrapolated.

2.2.3 Plaque assay

The plaque assay is a method to determine the number of active virus particles in a virus stock preparation. For this, the number of particles in a particular volume of stock solution capable of forming plaques on a cell monolayer is determined (plaque-forming units, pfu). In contrast to the PicoGreen® assay, which quantifies the total amount of vp, the plaque assay represents a functional measurement, since defective vp do not produce a plaque and will not be quantified.

Cells ($5x10^4$) were seeded into 6 well flat-bottomed tissue culture plates in serum-positive medium. After overnight incubation at 37°C, 5% CO_2 medium was carefully exchanged for 500 µl of fresh serum-positive medium to prevent detachment of the cell layer. Serial logarithmic dilutions from 10^{-6} to 10^{-10} of each adenovirus serotype were prepared in medium

containing 2% FCS and 500 µl of each virus dilution or virus-free control were added to wells in triplicate. While cells were incubated for 90 min at 37°C, 5% CO_2, a solution of 5% w/v Noble agar (Sigma-Aldrich) in H_2O was prepared and 3 ml aliquots incubated at 42 – 45°C until needed. Growth medium containing 2% FCS and pipettes used for the subsequent agar overlay were incubated at 37°C. When the virus had been incubated on cells for 90 min 12 ml of

2% FCS / DMEM were mixed with one 3 ml aliquot of agar. The virus containing supernatant was removed from cells and 2 ml of the agar mixture quickly, but carefully, added to wells by gentle pipetting against well walls. The gel was left to set for approximately 10 min before another 2 ml of agar mixture were added. After the overlay had set plates were incubated for up to 10 days at 37°C, 5% CO_2 with one additional ml of the agar mixture being added to wells on day 4 and day 8. On day 10 plates were prepared for visual assessment of plaque formation. For this the overlay gel was carefully removed from cells without disrupting the cell monolayer using a spatula. The cells were then fixed and stained for better contrast with a crystal violet solution containing 60% ethanol, 3.3% formalin, 4.3% acetic acid and 1 g / 100 ml crystal violet. After staining for 1 min the wells were thoroughly rinsed with water and left to dry. The number of plaques in wells of a virus dilution, which resulted in well isolated plaques, was counted using an inverted microscope (Axiovert 25, Zeiss). The concentration of active virus particles expressed as plaque-forming units per ml (pfu/ml) was then calculated by dividing the number of counted plaques in a well of a particular virus dilution (n) by the dilution factor of that virus dilution (d) and the volume of virus solution originally inoculated on that well (V).

For example:

26 plaques were counted in a well inoculated with 500 µl of a 10^{-8} dilution of stock virus.

→ $n = 26$

$d = 10^{-8}$

$V = 0.5$ ml

→ $n / (d \cdot V) = 26 / (10^{-8} / 0.5 \text{ ml}) = 5.2 \times 10^{9}$ pfu / ml

2.2.4 $TCID_{50}$ assay

Similar to the plaque assay, the $TCID_{50}$ assay is a method to determine the number of active particles in a virus stock preparation. As it does not require agar overlay of cells it was used to determine activity of the different adenovirus serotypes on cell lines which did not tolerate the plaque assay method.

Cells ($1x10^4$) were seeded into wells of a 96 well flat-bottomed plate in 100 µl of serum-positive medium prior to overnight incubation at 37°C, 5% CO_2. Serial logarithmic dilutions from 10^{-5} to 10^{-12} of each adenovirus serotype were prepared in medium containing 2% FCS. Serum-positive medium was removed from cells and 100 µl aliquots of each dilution of virus or a virus-free control was added to 10 wells of the 96-well plate. Plates were incubated for up to 7 days at 37°C, 5% CO_2 with an additional 100 µl of medium being added to wells on day 4. Development of cytopathic effect (CPE) was assessed using an inverted microscope (Axiovert 25, Zeiss) with a heated stage (temperature set to 37°C). For each dilution the number of wells showing CPE was counted and the ratio of wells with CPE to CPE-free wells calculated. The $TCID_{50}$ was determined using the KÄRBER statistical method (see Equation 2-1).

Equation 2-1 Calculation of $TCID_{50}$ and plaque forming units

$$\text{titre } (TCID_{50}/ml) = 10^{\,1 + D\,(S - 0.5)}$$

$$D = \log(d);\ d = \text{dilution factor}$$

$$S = \text{sum of ratios of wells with CPE to CPE-free wells (starting from the } 10^{-1} \text{ dilution)}$$

For example: 100% CPE at all dilutions below 10^{-9}, 90% CPE at 10^{-10} and 30% CPE at 10^{-11}

$$S = (1+1+1+1+1+1+1+1+1+ 0.9 + 0.3) = 10.2$$

$$D = \log (10) = 1$$

$$\text{titre } (TCID_{50}/100\ \mu l) = 10^{\,1 + 1\,(10.2 - 0.5)} = 10^{\,10.7} \quad \rightarrow \quad \text{titre } (TCID_{50}/ml) = 10^{\,11.7} = 5.0 \times 10^{11}$$

The virus titre measured by $TCID_{50}$ is 0.7 log higher than by plaque assay (Wagner, 2008) and so to transform $TCID_{50}$/ml into pfu/ml:

$$\text{titre (pfu/ml)} = 10^{(1 + D\,(S - 0.5)) - 0.7}$$

$$\text{virus titre (pfu/ml)} = 10^{(11.7 - 0.7)} \rightarrow \text{virus titre (pfu/ml)} = 1.0 \times 10^{11}$$

2.2.5 MTS assay

The MTS assay is a colourimetric method for determining metabolic activity as a surrogate for the amount of viable cells in a cytotoxicity assay (Promega). MTS [3-(4,5-dimethylthiazol-2-yl)-5-(3-carboxymethoxyphenyl)-2-(4-sulphophenyl)-2H-tetrazolium] is a tetrazolium compound which live cells can reduce into a soluble, coloured formazan product (Figure 2-1). The amount of product can be measured by its absorption at a wavelength of 490nm.

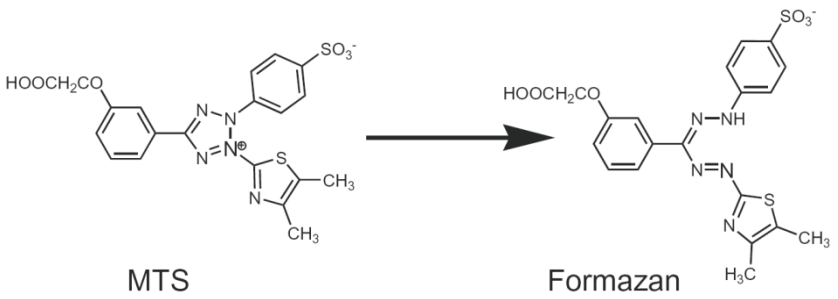


Figure 2-1 Conversion of the MTS reagent by viable cells

MTS-reagent was thawed and mixed with serum-positive growth medium in a ratio of 1:6 (MTS:medium). Cells were washed with PBS and 120 µl of MTS-medium added per well. Background controls were generated by adding 120 µl MTS-medium mixture to wells without cells. The plate was incubated at 37°C, 5% CO_2 for 30 min and absorbance measured in a Wallac 1420 Victor^2 multilabel counter (PerkinElmer) at 490 nm. Viability was calculated by dividing the absorbance of treated cells by the absorbance of non-treated cells after subtracting readings of the background control wells.

2.2.6 Analysis of cell receptor status by flow cytometry

Serum-positive growth medium was removed and cells washed with PBS before 2-3 ml of enzyme-free cell dissociation buffer (Invitrogen) were added to flasks. Cells detached during incubation at 37°C for 5-10 min when 17-18 ml staining medium (DMEM containing 10% FCS and 5% heat-inactivated (56°C for 30 min) rabbit serum (abcam)) was added to flasks and the resulting suspension vigorously pipetted to break up cell clumps. The suspension was then centrifuged at 500 g for 5 min at 4°C, the pellet re-suspended in staining medium and 50 µl containing $5x10^5$ cells were added to wells of a V-bottom 96 well plate. Primary antibodies (Table 2-2) were prepared by diluting to double their final concentration in staining medium and 50 µl primary antibody solution were added to wells. The plate was incubated for 40 min at 4°C on a plate shaker and subsequently washed once by centrifuging at 500 g for 5 min at 4°C, removing the supernatant and re-suspending in 100 µl of staining medium. The secondary antibody was diluted in staining medium and 100 µl used to resuspend cells following the wash. The plate was incubated for a further 40 min in the dark at 4°C on a plate shaker. Another wash step was performed before cells were resuspended in 100 µl 4% paraformaldehyde solution in PBS. The plate was stored at 4°C in the dark until analysis by flow cytometry using a FACSCalibur machine (BD Biosciences). $2x10^4$ cells were counted for each antibody / cell line combination.

Specificity of primary antibodies was evaluated by preparing control samples of cells incubated with staining medium containing either no primary antibody, secondary antibody only or an isotype control antibody. In order to take into account the number of positive cells per tested sample as well as their expression levels, flow cytometry data was analysed by multiplying the percentage of positive cells (cells demonstrating fluorescence above background, gated in region M1) with the geometric mean of their fluorescence intensity as previously reported (Bottini *et al.*, 1993; You *et al.*, 2001).

Table 2-2 Antibodies used for flow cytometry

Antibody [clone]	Species, clonality	dilution	Company
anti-α_V-integrins [272-17E6]	mouse, monoclonal	1:200	abcam
anti-CAR [RmcB]	mouse, monoclonal	1:100	Chemicon Millipore
anti-CD46 [MEM-258]	mouse, monoclonal	1:100	abcam
IgG isotype control	mouse, monoclonal	1:100	AbDSerotec
anti-mouse FITC-conjugate	rabbit, polyclonal	1:100	abcam

2.2.7 Real time Q-PCR for measurement of virus particle uptake

Serum-positive growth medium was removed and cells washed with PBS before 2-3 ml of enzyme-free cell dissociation buffer (Invitrogen) were added to flasks. Cells detached during incubation at 37°C for 5-10 min when 17-18 ml of DMEM containing 2% FCS were added to flasks. The resulting suspension was vigorously resuspended and after centrifugation cells were washed with PBS (centrifugation: 800 g / 5 min / 4°C) before the pellet was resuspended in the required medium. $2x10^5$ cells were then aliquoted into microreaction tubes and 5 µl of virus treatment ($2x10^7$ vp/ml) added before incubation at 37°C, 5% CO_2 for 90 min on a rotator. Cells were pelleted, washed twice with 800 µl PBS (800 g / 3 min / 4°C) to remove non-internalised virus, resuspended in 200 µl PBS and frozen at -20°C until extraction of genomic DNA. To create standard curves for Q-PCR aliquots of cells were treated as described above, however without the addition of virus before incubation. Instead, a dilution series of vp was prepared and aliquots containing known amounts of virus were added to these samples directly before freezing at -20°C.

Genomic DNA was extracted from samples using the NucleoSpin 8 Tissue kit (Macherey-Nagel) according to the manufacturer's instructions. Briefly, samples were thawed and lysed in buffer containing SDS and Proteinase K at 56°C for 20 min before adding ethanol and guanidine-hydrochloride containing buffer. Samples were transferred onto columns containing a DNA

binding silica membrane and the liquid phase removed by vacuum-assisted filtration. Subsequently, membranes were washed with guanidine-hydrochloride and isopropanol containing buffer once, and ethanol containing buffer twice. Purified DNA was eluted by flushing membranes twice with alkaline buffer before storage at -20°C. For real time Q-PCR a TaqMan® detection system was used. FAM-TAMRA labelled probe, primers (both Eurogentec) and ROX (Invitrogen) were added to SensiMix NoRef master mix (Quantace) and topped up with distilled water to 20 µl per well to obtain final concentrations of 125 nmol/l, 800 nmol/l and 500 nmol/l respectively. 5 µl of sample were added and Q-PCR performed with a StepOnePlus™ Real-Time PCR System (Applied Biosystems). The amplification cycle was set to start with 50°C for 2 min and 95°C for 10 min followed by 40 cycles of 15 sec at 95°C for denaturation and 60°C for 60 sec for annealing and extension. Data was analysed with StepOne™ Software (Applied Biosystems) using automatic analysis settings.

TaqMan® method primers and probe used for detection of Ad5wt and Ad5luc in the study described in section 3.2.3 were specific for an 84 base-pair sequence of the Ad5 fibre gene (KT, knob turn, Table 2-3) (Green *et al.*, 2004). The probe was labelled with FAM at the 3' end and TAMRA at the 5' end. The reaction followed the PCR cycling protocol described above.

Table 2-3 KT-primer sequences for Ad5

name	location in genome	sequence
KT - fw primer	nt 32350 - 32370	**5' -** T G G C T G T T A A A G G C A G T T T G G **- 3'**
KT - rv primer	nt 32433 - 32411	**5' -** G C A C T C C A T T T T C G T C A A A T C T T **- 3'**
KT - probe	nt 32372 - 32404	**5' -** T C C A A T A T C T G G A A C A G T T C A A A G T G C T C A T C T **- 3'**

Primers for Ad3, Ad5 and Ad11 were designed according to a published set of universal primers for a conserved region in the hexon sequence of adenovirus (consensus sequences in Table 2-4) (Heim *et al.*, 2003). However, as these primers were not sensitive enough in this method, individual primers for the three serotypes were designed by altering bases to exactly match the serotype-specific sequences (serotype-specific sequences, bases different from the consensus in red). The probe was sensitive enough for all three serotypes (consensus probe). The probe was labelled with FAM at the 3' end and TAMRA at the 5' end. The reaction followed the PCR cycling protocol described above.

Table 2-4 Universal and individual primer sequences for Ad3, Ad5 and Ad11

specification		sequence
consensus **forward primer**	AQ1	**5'-** G C C A C G G T G G G G T T T C T A A A C T T **-3'**
serotype specific sequence	Ad3	**5'-** G C C A C **T** G T G G G G T T T C T A A A **T** T T **-3'**
	Ad5	**5'-** G C C A C **C** G T G G G G T T T C T A A A C T T **-3'**
	Ad11	**5'-** G C **T** A C G G T G G G **A** T T T C T A A A C T T **-3'**
consensus **reverse primer**	AQ2	**5'-** G C C C C A G T G G T C T T A C A T G C A C A T C **-3'**
serotype specific sequence	Ad3	**5'-** G C C C C A **A** T G G **A** C **A** T A C A T G C A C A T C **-3'**
	Ad5	**5'-** G C C **G** C A G T G G T C T T A C A T G C A C A T C **-3'**
	Ad11	**5'-** G C C C C A **A** T G G **G** C **A** T A C A T G C A C A T C **-3'**
consensus **probe**	AP	**5'-** T C G G A G T A C C T G A G C C C G G G T C T G G T G C A **-3'**
serotype specific sequence	Ad3	**5'-** T C G G **G** G T A C C T **C** A G **T** C C G G G T C T G G T G C A **-3'**
	Ad5	**5'-** T C G G A G T A C C T G A G C C C **C** G G **G** C T G G T G C A **-3'**
	Ad11	**5'-** T C G G A G T A C C T G A G **T** C C G G G T C T G G T G C A **-3'**

2.3 Methods of Chapter 4

2.3.1 Generation and treatment of elicited murine peritoneal macrophages

Elicited murine peritoneal macrophages were generated as previously described (Cash *et al.*, 2008) and kindly provided by Professor David Greaves, Dunn School of Pathology, University of Oxford. Briefly, BALB/c mice were injected i.p. with Bio-Gel P100 polyacrylamide beads (Bio-Rad) in PBS (2% wt/vol). After four days mice were harvested and peritoneum lavaged with PBS containing 2 mmol/l EDTA. Cells were pelleted and resuspended in OptiMEM (Invitrogen) and plated into 6-well tissue culture plates ($1x10^6$/well). After incubation for 2 hours at 37°C, 5% CO_2 non-adherent cells were removed by three washes with PBS and macrophages treated with virus, PBS or lipopolysaccharide (LPS) (100 ng/ml) (Sigma-Aldrich) / interferon gamma (IFNγ) (20 ng/ml) (Peprotech). After incubation for up to 24 hours supernatants were collected and stored at -80°C until analysis.

2.3.2 ELISA for quantification of murine RANTES

ELISAs for RANTES cytokine levels were performed as per manufacturer's instructions on 96 well plates pre-coated with a monoclonal anti-murine RANTES antibody (Quantikine®, R&D Systems). Briefly, after preparation of reagents, standard curve dilutions and samples, 50 µl of Assay Diluent RD1-40 were dispensed into wells before addition of 50 µl of standard, control or sample. Plates were incubated for 2 hours at RT and washed five times with Wash Buffer. After addition of 100 µl of mouse RANTES Conjugate to wells and further incubation for 2 hours at RT, followed by five washes, 100 µl of Substrate Solution were added to wells and incubated for 30 min at RT. The chromogenic reaction was stopped by addition of 100 µl of Stop Solution and absorbance measured at 450 nm using a Wallac 1420 Victor^2 multilabel counter (PerkinElmer) with 595 nm as correction wavelength. RANTES concentration of samples was extrapolated from a standard curve of optical densities (ODs) of known amounts of recombinant murine RANTES using a 4-parameter logistic curve-fit.

2.3.3 Cytokine analysis using a multiplex suspension array (BioPlex®)

The Bio-Plex® assay (Bio-Rad) is a bead-based ELISA system that allows simultaneous assessment of multiple cytokines on a single sample of serum or cell supernatant. The system uses an array of beads, each internally dyed with different ratios of two fluorophores to assign it a unique spectral address, enabling multiple bead populations to be distinguished from each other in a flow-cytometry-based system. Cytokines are detected similar to a standard 'sandwich' ELISA. First, cytokines are captured by specific antibodies coupled to beads followed by detection of cytokines by another specific biotinylated antibody and avidin-coupled R-Phycoerythrin (R-PE). Beads with individual spectral signatures are gated separately and fluorescence from R-PE for each bead set measured to allow quantification of cytokine amounts. Supplied with the kit is a standard that contains known amounts of cytokines allowing production of standard curves. Labelling and assay analysis was performed according to manufacturer's instructions except that beads and detection antibody were diluted 2x that recommended (Dr Moghaddam, Dunn School of Pathology, University of Oxford - personal communication).

2.3.4 Animal studies

Studies involving laboratory animals were conducted in accordance with the UK Home Office Animals (Scientific Procedures) Act 1986 under the project licenses PPL 70/006 (KCL-I, KCL-II and KCL-III) or PPL 30/2333 (OX-I) and personal license PIL 30/8216. Experiments KCL-I – III were performed in collaboration with Dr Linda Klavinskis and Dr Veronique Bachy (King's College London). For all animal studies participating investigators were blinded to the type of treatment until after analysis of cytokine and cellular responses.

2.3.4.1 Housing conditions and diet

Mice were housed in temperature and humidity-controlled conditions (20-22°C) at KCL Biological Services Unit (BSU), London (KCL-I, KCL-II, KCL-III) or Biomedical Services, John Radcliffe Hospital, Oxford (OX-I). Mice were given free access to sterile tap water and formulated diets, housed in environmentally-enriched, individually ventilated cages with no more than 6 mice per cage, and exposed to a 12-hour light-dark cycle.

2.3.4.2 Short-term i.p. infection and sample collection

Immune competent mice (CD46-transgenic or non-transgenic mice of C57BL/6 background (Yannoutsos *et al.*, 1996) or C57BL/6 mice) were injected i.p. with 500 µl of PBS containing $5x10^{10}$ (KCL-I) or $2.5x10^{10}$ (KCL-II) vp of Ad5 or Ad11 or no virus. Mice were monitored for acute toxicity for 30 min. After 6 hours mice were sacrificed by cervical dislocation. After confirmation of death, a small hole in the abdominal wall and parietal peritoneum was made and 2 ml PBS instilled. The mouse was gently agitated and i.p. wash fluid aspirated with a Pasteur pipette. Blood was taken by cardiac puncture and allowed to clot at RT for 30 min, centrifuged at 14,000 rpm for 5 min, serum aspirated and stored at −80°C. The i.p. wash was centrifuged at 2,000 rpm for 2 min and the supernatant collected, its volume measured and stored at −80°C. The cell pellet was resuspended in PBS at an equal volume to the previously removed supernatant for each sample. 50 µl aliquots of cells were spun onto polylysine coated microscope slides (VWR) using a Cytospin2 at 1,250 rpm for 2 min and fixed with Shandon Cell Fixx (Thermo).

2.3.4.3 Long-term i.p. infection, sample collection and adhesion scoring

Long-term studies to examine the effect of i.p. Ad5 and Ad11 were designed according to previously published methods (Morrison *et al.*, 2008). Immune competent mice (CD46-transgenic or non-transgenic mice of C57BL/6 background (Yannoutsos *et al.*, 1996) or C57BL/6 mice) were injected i.p. with 250 µl of virus storage buffer (vsb) containing $1x10^{10}$ vp of Ad5 or Ad11 or no virus three times with an interval of 72 hours. After each injection mice were

monitored for acute toxicity for 30 min. 18 days after the first injection mice were sacrificed and samples were prepared as described in section 2.3.4.2. In addition, after cardiac bleeds peritoneal cavities were opened and organs and peritoneum inspected and scored for symptoms of inflammation and adhesion formation (Table 2-5) as previously reported (Morrison *et al.*, 2008).

Table 2-5 Scoring of inflammation and symptoms of adhesion formation

Observation	**Adhesion score**
No adhesions / inflammation	*none*
Mild filmy adhesions or inflammation	*mild*
Denser adhesions, still able to dissect out loops of bowel	*moderate*
Dense adhesions causing bowel matting, dilatation or subacute obstruction; unable to dissect out bowel loops	*severe*
gross liver deformity = increase of score by one step	

2.3.5 Assessment of neutrophil and macrophage infiltration

Immunohistochemical staining was performed using the ABC-alkaline phosphatase (ABC-AP) kit (Vector). After each incubation step at RT, slides were washed twice with PBS. Cytospin samples of i.p. cells were soaked in PBS and incubated for 60 min with a 1:100 dilution of rabbit serum (VECTOR) in PBS before incubation with rat anti-F4/80 antibody (AbD Serotec), rat anti-NIMP-14 (abcam) or an isotype control (abcam) at 2.5 µg/ml for 60 min. Samples were then incubated with mouse adsorbed, biotinylated anti-rat antibody (VECTOR) for 30 min and with Vectastain ABC-AP reagent for further 30 min. Vector Red AP substrate was prepared in Tris-HCl pH 8.2, added to samples and incubated for 30 min. Samples were then washed with water, counterstained with Hematoxylin (Shandon) for 10 min, dehydrated with ethanol, cleared in Histoclear (RA Lamb) and mounted in p-Xylene-bis-N-pyridinium bromide (DPX) mounting

medium (RA Lamb). Slides were left to dry overnight before examination. Three high power fields per slide were imaged (x20 objective lens) on a Nikon Eclipse 80i microscope with a Nikon DS-5M camera using Nikon Imaging Software AR 3.0. On each image the number of all cells and positively stained cells was counted.

2.4 Methods of Chapter 5

2.4.1 Collection of primary pleural effusions

Samples of malignant pleural effusions were collected at the Oxford Centre for Respiratory Medicine, Churchill Hospital, Oxford under the ethics approvals REC 05/Q0301/61, REC 07/Q1603/2, REC 09/H0604/5 or REC 07/Q1607/20 (NHS, National Research Ethics Service) from patients with different primary tumours, who were having therapeutic drainage performed, after obtaining written informed consent. Vacutainer® tubes (BD) were used for collection and subsequent storage at -80°C. For experiments, samples were thawed at 37°C, heat-inactivated (56°C / 25 min) and cleared of particulates by centrifugation (800 g / 5 min / RT).

2.4.2 Protein Assay

Protein concentrations of cell lysates used for luciferase assays (section 2.5.3) and of other solutions were determined with the Advanced Protein Assay (Cytoskeleton, Inc.). Briefly, bovine serum albumin (Sigma-Aldrich) was used to create a dilution series of known protein concentration in lysis buffer (Promega) to serve as a standard curve. 5 µl of sample, standard curve sample or lysis buffer only (background control) were added to wells of a clear 96 well plate and incubated with 250 µl Advanced Protein Assay Reagent (Cytoskeleton, Inc.) (diluted 1:5 with deionised H_2O) at RT for 1 min. Absorbance was measured with a Wallac 1420 Victor^2 multilabel counter (PerkinElmer) at 595 nm. Protein concentration was quantified by subtracting the mean absorbance of wells serving as background controls from unknown samples and extrapolating resulting OD values from the standard curve.

2.4.3 Anti-adenovirus antibody ELISA

An ELISA system for indirect detection and quantification of anti-adenovirus antibodies in malignant patient samples was developed (Figure 2-2). Generally, ELISA plates were sealed with plate sealers (Greiner bio-one) before each incubation step and washed four times with PBS / 0.05% Tween20 using a Nunc-Immuno™ Wash 12 (Nunc) after each incubation step. First, 50 µl of Ad3, Ad5 or Ad11 antigen solution (diluted to 2 µg/ml protein concentration as determined by protein assay (section 2.4.2)) or purified preparations of Ad3, Ad5 or Ad11 virus particles (diluted to $2x10^9$ vp/ml) were added to each well of a MaxiSorp™ flat bottom microplate (Nunc) and incubated overnight at 4°C. 50 µl of blocking buffer (washing buffer containing 2% bovine serum albumin (BSA)) were added to wells and incubated at RT for 90 min. Clinical samples were diluted 1:100 in PBS, 50 µl added to wells and incubated for 2 hours at 4°C. For assays, where antigen solutions served as capture antigens, polyclonal rabbit anti-human IgG-HRP conjugate (abcam) in a 1:1,000 dilution in blocking buffer was used as detection antibody. For assays employing whole virus as capture antigen, polyclonal goat anti-human IgG−HRP conjugate (Santa Cruz) was used at a 1:200 dilution, matching the final protein concentration of the abcam antibody. After washing 50 µl of detection antibody were dispensed per well and incubated at RT for one hour. After washing six times with washing buffer, 50µl of substrate solution (H_2O_2 / TMB (tetramethylbenzidine), Alpha Diagnostics International Inc.) were added to each well and plates left to develop at RT for 4 min. 50 µl of stop solution (diluted sulphuric acid) (Alpha Diagnostics International Inc.) were added to each well and absorbance measured at 450 nm on a Wallac 1420 Victor^2 multilabel counter (PerkinElmer).

2.4.4 Adenovirus neutralisation capacity of patient samples

Assays to assess the neutralisation capacity of samples were performed as depicted in Figure 2-3. First, 100 µl of medium (DMEM / 2% FCS) were added to all wells of a flat-bottom 96 well plate and a 2-fold dilution series of sample across the plate was prepared by adding 100 µl of patient sample to column 2, mixing and transferring 100 µl to column 3, mixing and so forth to column 10. The surplus of 100 µl from column 10 was discarded and column 11 left to contain medium only (serving as a negative control for neutralisation). Subsequently, dilutions of Ad3, Ad5 or Ad11 at a concentration to attain 1,000 vp/cell were prepared and 25 µl added to wells before incubation at 37°C / 5% CO_2 for 90 min. Meanwhile, a suspension of A549 cells was prepared and incubated at 37°C / 5% CO_2 for 60 min to allow receptor recovery. After incubation of plates containing patient sample and virus 25 µl of A549 suspension containing $1x10^4$ cells were dispensed into wells and the plate incubated 37°C / 5% CO_2 for 48 hours when viability was assessed by MTS assay (see section 2.2.5). After normalisation of viability between 0% and 100% to compensate for the varying maximum cytotoxicity of the different serotypes nonlinear regression curves following a sigmoid dose response model with variable slope and constraints for the top and bottom values as 100% and 0%, respectively, were calculated using GraphPad Prism 4 software. In assays investigating if increased virus doses can overcome the neutralisation capacity of patient samples logarithmic dilution series of vp/cell concentrations, instead of a fixed concentration of 1,000 vp/cell, were incubated with patient sample dilutions.

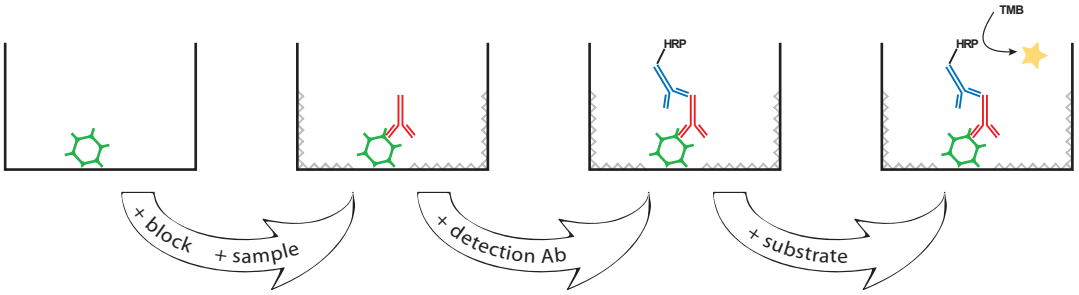


Figure 2 - 2 Schematic of ELISA to quantify total anti-Ad antibody content

Whole Ad or Ad antigen solution (green) was adsorbed to microplates. After blocking nonsaturated binding sites (grey), heat inactivated sample (red) was added. After incubation, detection antibody (polyclonal goat anti-human IgG−HRP; blue) was allowed to bind to captured anti-Ad antibodies. Finally, substrate solution (H_2O_2 / TMB) was added and, after termination of the chromogenic reaction, absorption at 450nm was assessed as a measure for the amount of bound anti-Ad antibodies (red).

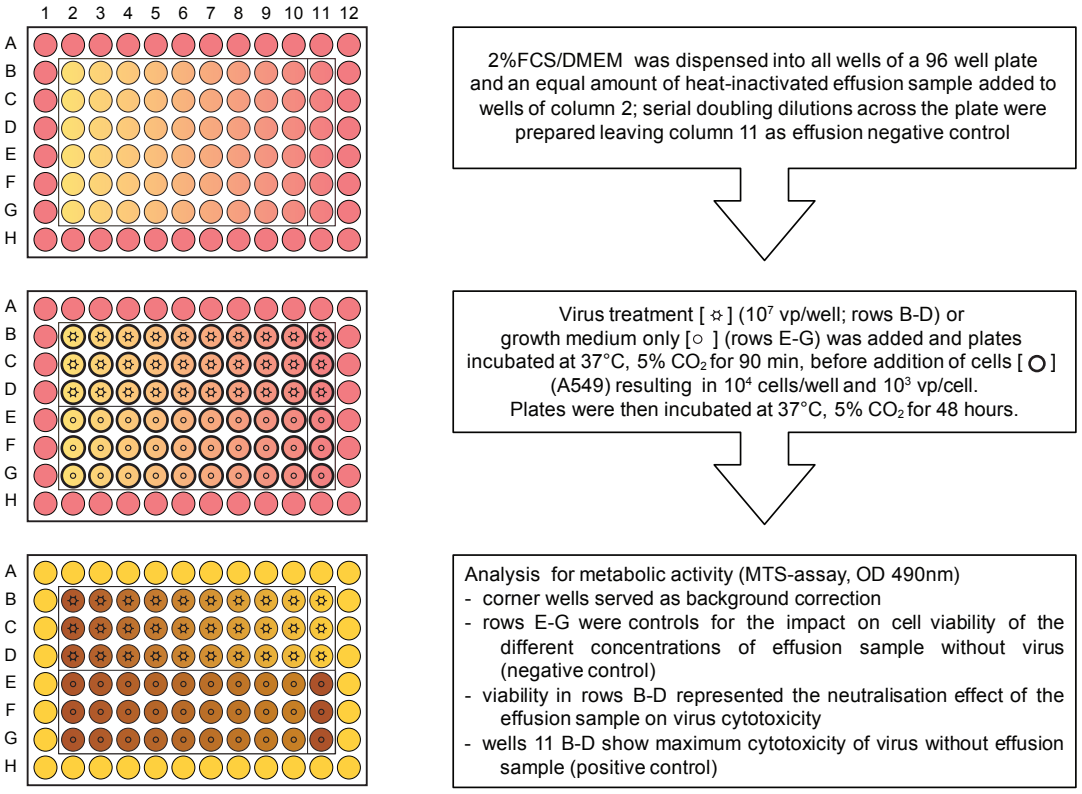


Figure 2 - 3 Method to determine the neutralising capacity of patient samples

2.4.5 SDS-PAGE and Western blot

Running buffer (10x)	**Transfer buffer (10x)**	**Transfer buffer (1x)**
TRIS-HCl 30 g Glycine 144 g SDS 10 g Deionised H_2O ad 1000 ml To be diluted 1:10 with deionised H_2O before use.	TRIS-HCl 30 g Glycine 144 g Deionised H_2O ad 1000 ml To be diluted before use (see Transfer buffer (1x)).	Transfer buffer 100 ml Methanol 100 ml 20% SDS 0.5 ml Deionised H_2O 799.5 ml

Sample loading buffer (3x)	
1 mol/l TRIS-HCl pH 6.8	2.4 ml
Glycerol	3 ml
20% SDS	3 ml
β-Mercaptoethanol	1.6 ml
Bromophenol blue	6 mg

Sample and gel preparation

Precast 4-15% gradient TRIS-HCl gels (BioRad) were placed in a Mini-PROTEAN III electrophoresis cell, sample wells flushed with running buffer and left to condition for 30 min. Virus samples were prepared by diluting the appropriate amount vp/lane (in the screening experiments described in section 5.4.2: Ad3: $4.33x10^9$ vp, Ad5: $2.5x10^9$ vp, Ad11: $3.55x10^9$ vp) in PBS and adding sample loading dye. After incubation at 95°C for 10 min for disintegration of the virus structure, 12 µl of sample were loaded per lane. Some lanes were used for prestained protein molecular weight markers (Precision Plus Protein Dual Color Standard, Bio-Rad or Rainbow™ molecular weight marker, GE Healthcare). Gels were run at 200 V for 35 - 40 min at RT.

Silver stain

Protein bands on SDS-PAGE gels were detected by sliver stain (Silver Stain Plus, Bio-Rad) as per manufacturer's instructions. Briefly, after electrophoresis gels were placed in Fixative Enhancer Solution and incubated for 20 min at RT with gentle agitation. Subsequently, gels

were washed three times with deionised H_2O before staining in a mixture of deionised H_2O, Silver Complex Solution, Reduction Moderator Solution, Image Development Reagent and Development Accelerator Solution (35%, 5%, 5%, 5%, 50% (v/v) respectively) for 20 min at RT. The staining reaction was stopped by incubation in 5% (v/v) acetic acid for 15 min.

Coomassie stain

Gels that were used for identification of protein bands by mass-spectrometry (section 2.4.6) were stained using a Coomassie-based method. After electrophoresis gels were incubated in a fixing solution (25% (v/v) methanol and 10% (v/v) acetic acid in deionised H_2O) for 30 min before incubation with staining solution (0.006% (w/v) Coomassie Brilliant Blue and 10% (v/v) acetic acid in deionised H_2O) overnight at RT with gentle agitation. Subsequently, background staining was reduced by brief incubation with fixing solution followed by incubation in 10% (v/v) acetic acid for 2 hours.

Nitrocellulose transfer

Nitrocellulose membrane (Bio-Rad), filter papers (Bio-Rad) and fibre pads (Bio-Rad) were pre-soaked in transfer buffer. A transfer sandwich was assembled in the following order: fibre pad - filter paper - gel - nitrocellulose membrane - filter paper - fibre pad and placed in the transfer cassette with the gel facing the negative electrode. Electro-transfer was performed for 1.5 hours at 300 mA, 4°C in a BioRad mini-gel Western transfer cell.

Western blot development

The nitrocellulose membrane was removed from the transfer sandwich and stained for proteins with Ponceau solution (0.1% (w/v) Ponceau S in 5% (v/v) acetic acid) to verify efficient transfer. The membrane was destained in deionised water and cut into parts, if incubation with different primary antibodies was required. While blocking in 5% skimmed milk (Sigma-Aldrich) at RT for 10 min, 1:100 dilutions of heat-inactivated patient samples in 5% skimmed milk were prepared. The membrane was then incubated with these dilutions at 4°C overnight with gentle agitation. After washing three times with PBS/0.1% Tween20 the membrane was incubated with a 1:5,000 dilution of goat anti-human IgG-HRP antibody (Santa Cruz), diluted in 5% skimmed milk, with

gentle agitation at RT for 20 min. Subsequently, the membrane was washed with PBS / 0.1% Tween20 twice and chemiluminescence developed with Amersham ECL™ Western Blotting Detection Reagents (GE Healthcare). Chemiluminescence was detected by exposure to X-ray film (SuperRX, Fujifilm) in a fast speed cassette. Exposed X-ray films were developed and fixed in an automatic developer (CP1000, Agfa). Densitometric analysis of band intensity was performed with AlphaView® Software 3.0 (AlphaInnotech).

2.4.6 Mass-Spectrometry

In order to identify unknown protein bands of Ad3, Ad5 and Ad11 SDS-PAGE gels were stained using the Coomassie method (section 2.4.5), detected bands excised and stored in 10% methanol (v/v) until analysis. Further sample preparation and LC - MS / MS were performed by Georgina Berridge and Rod Chalk (Structural Genomics Consortium, University of Oxford) using MS / MS protocols previously published (Berridge *et al.*, 2011). For identification of proteins a database of 185 protein sequences of Ad3, Ad5 and Ad11 was created using published data listed in the RefSeq database (Pruitt *et al.*, 2009) (http://www.ncbi.nlm.nih.gov/RefSeq/ access date 15/06/2010). Peptide sequences detected by MS / MS were analysed and scored according to this database using the following software: data acquisition: Hystar 3.2 (Bruker Daltonik GmbH), peak picking and deconvolution: DataAnalysis 4.0 (Bruker Daltonik GmbH), query and batch submission: Biotools 3.2 (Bruker Daltonik GmbH) and ion search: Mascot 2.3 (Matrix Science Ltd.). Mascot 2.3 software scores the detected peptide according to the MOWSE algorithm (Pappin *et al.*, 1993).

For each band analysed the top three hits according to Mascot Protein Scores which are derived from the individual Ion Scores of detected peptide sequences were examined. To decide if hits were true, the MASCOT Ion Scores of individual peptides, sequence coverage and whether the molecular weight of the identified protein matched the expected molecular weight according to gel migration were considered. A total of two gels were analysed and hits were nearly identical.

2.5 Methods of Chapter 6

2.5.1 Polymer coating virus

Polymers based on poly(N-[2-hydroxypropyl]methacrylamide) (pHPMA) (Subr *et al.*, 2009) (Table 2-6, for structure see Figure 2-4) were dissolved in 20 mmol/l HEPES buffer (pH 7.4). Polymer solution and 20 mmol/l HEPES buffer (pH 7.4) were added to virus stock in storage buffer (50 mmol/l HEPES, pH 7.8, 0.1 g/l $CaCl_2$ and $MgCl_2$, 10% Glycerol) to achieve required polymer concentrations (20 – 0.2 mg/ml) and incubated at RT for two hours. Subsequently, formulations were aliquoted and stored at -80°C.

Table 2-6 Panel of investigated polymers

ID	Reducible TT	QA (amount)
EC193	No	No
EC234	No	Yes (6.5%)
EC235	Yes	Yes (6.5%)
EC236	Yes	Yes (1.5%)

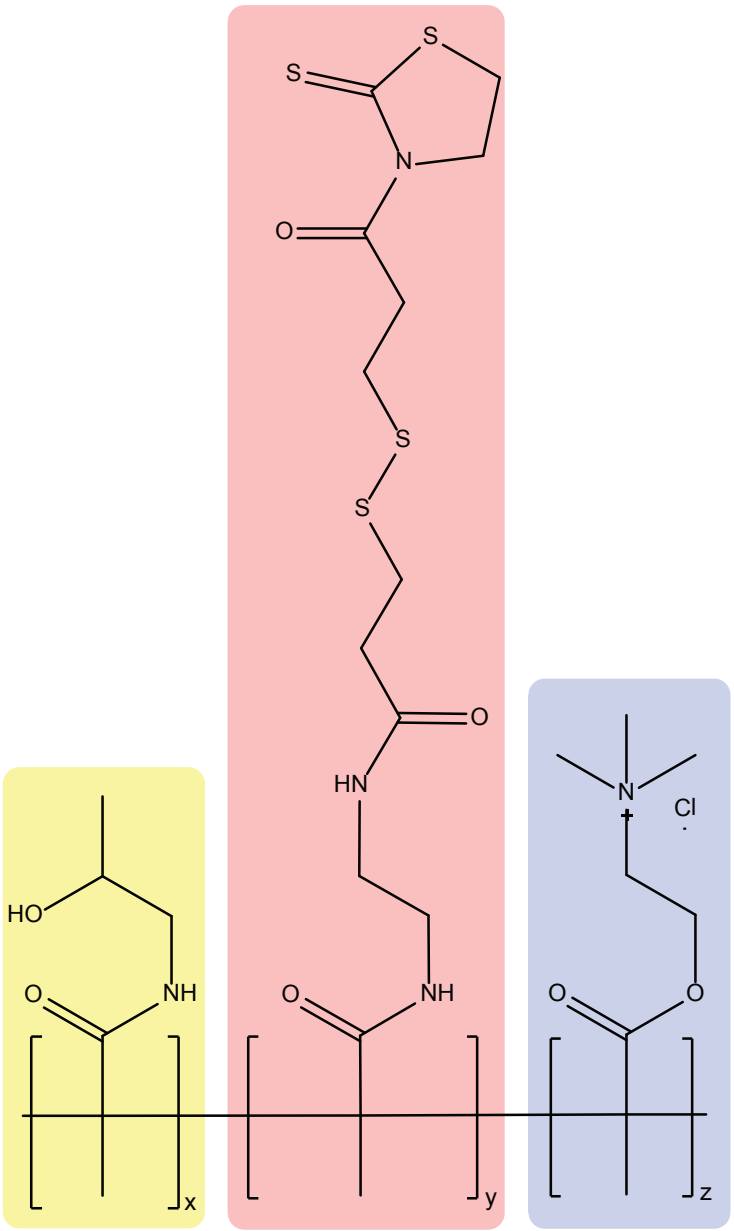


Figure 2 - 4 The chemical structure of a positively charged polymer (EC236)

The graphic illustrates the chemical structure of the positively charged polymer EC236. This terpolymer is composed primarily of N-(2-hydroxypropyl)methacrylamide (HPMA, yellow box, ~ 90 mol%), copolymerised with monomers bearing reducible (—S–S—) amino-reactive thiazolidine-2-thione active esters (TT, red box, ~ 8 mol%) and a monomer bearing a positively charged quaternary amine (QA, blue box, ~ 2 mol%). Covalent attachment of the polymer to the virus capsid is achieved by reaction of the TT-ester with exposed primary amino groups on the capsid surface, and is assisted by electrostatic interaction of the QA groups with negatively charged regions on the capsid.

2.5.2 Adenovirus capsid protection ELISA

Generally, ELISA plates were sealed with plate sealers (Greiner bio-one) before each incubation step and washed ten times with PBS using a Nunc-Immuno™ Wash 12 (Nunc) after each incubation step. An ELISA plate (MaxiSorp™, NUNC) was prepared by coating wells with 50 µl of a 1:500 dilution of polyclonal rabbit anti-adenovirus antibody (abcam) in coating buffer (Alpha Diagnostics International Inc.) and incubated at 4°C overnight. Non-specific binding sites were blocked for 60 min at 37°C with blocking buffer (coating buffer containing 5% heat-inactivated (56°C, 25 min) goat serum (Vector)). 50 µl of polymer-coated or non-coated virus samples at a concentration of $1x10^{10}$ vp/ml were added to wells and incubated overnight at 4°C. 50 µl of a 1:100 dilution of polyclonal biotinylated goat anti-adenovirus antibody (AbD Serotec) in blocking buffer was added to wells. After incubation for 60 min at RT a 1:1,000 dilution of HRP-coupled avidin (eBioscience) in blocking buffer was added and the plate incubated at RT for 30 min. Substrate solution (H_2O_2 / TMB, Alpha Diagnostics International Inc.) was added and the plate incubated for 10-30 min before the chromogenic reaction was stopped by adding diluted sulphuric acid (Alpha Diagnostics International Inc.). Absorbance was measured using a Wallac 1420 Victor^2 multilabel counter (PerkinElmer) at 450 nm.

2.5.3 Luciferase assay

The Luciferase Assay System (Promega) was used to analyse luciferase expression after transduction of cells with a non-replicating adenovirus mutant encoding the firefly luciferase transgene (Ad5luc, section 2.1.2). Monolayers of cells were incubated with virus formulations (500 vp/cell) in the presence or absence of factor X (FX, 8 µg/ml) in serum-free medium for 90 min at 37°C, 5% CO_2 followed by incubation for another 24 hours in serum-positive medium. Then serum-positive medium was removed and cells washed with PBS before addition of lysis buffer (100 µl / well, bicine buffer and Tween). To aid cell lysis plates was frozen at −80°C overnight. After plates had thawed to room temperature well contents were vigorously resuspended and 25 µl of cell lysate added to a luminometer tube and placed in a luminometer (Lumat LB 9507, Berthold Technologies) where luciferase assay substrate (25 µl) (beetle luciferin) was injected. Luciferin was then converted into a luminescent product, oxyluciferin, by

the firefly luciferase using ATP·Mg^{2+} as co-substrate and, after 2 seconds, luminescence (as relative luminescence units (RLU)) was measured for 10 sec. Cells which had not been transduced with Ad5luc served as a negative control to determine background luminescence, which was deducted from readings of Ad5luc-transduced samples. All values were corrected for the amount of cells present in analysed wells by dividing RLU by protein content of wells as determined by protein assay (section 2.4.2).

2.5.4 Uptake and cytotoxicity study of polymer-coated Ad5

Uptake studies were essentially performed as described in section 2.2.7 using $1.5x10^5$ cells per sample replicate infected at a virus concentration of 1,000 vp/cell. However, after incubation of cells in suspension with virus formulations and washing to remove non-cell-associated virus, aliquots of each test sample (corresponding to $1.125x10^4$ cells) were transferred into microplates. After incubation at 37°C, 5% CO_2 for four days cell viability was measured using the MTS assay (section 2.2.5).

2.5.5 Primary ascites culture

Samples of primary ascites from ovarian cancer patients were collected during routine paracentesis at the Oxford Cancer Centre, Churchill Hospital, Oxford after obtaining written informed consent under the ethics approval REC 91/03L (NHS, Berkshire Research Ethics Committee). Samples were immediately transferred to the tissue culture laboratory and handled under sterile conditions in a dedicated class II laminar-flow cabinet. First, cells were separated from fluid by centrifugation (1,500 rpm / 5 min / RT) and the supernatant collected and stored at -80°C. Cell pellets were resuspended in RPMI 1640 and combined (total volume less than 10 ml). Erythrocytes were lysed by addition of Red Blood Cell Lysing Buffer Hybri-Max™ (Sigma-Aldrich) at twice the volume of the cell suspension. After mixing and incubation for 2 min the suspension was centrifuged (1,500 rpm / 5 min / RT) and the cell pellet washed with PBS twice (1,500 rpm / 5 min / RT). Finally, the cell pellet was resuspended in an equal volume of freezing solution (10% sterile dimethyl sulphoxide (DMSO, Sigma-Aldrich), 90% FCS) and handled as described in section 2.1.1.2.

For experiments cells were resuscitated by thawing at 37°C and resuspension in growth medium (10% FCS, 90% RPMI 1640) followed by centrifugation (1,500 rpm / 5 min / RT) to clear samples of DMSO. Cells were then plated into microplates as described in section 2.1.1.3. Subsequently cells were infected with titrations of EC265-coated Ad5 or non-coated Ad5 (10-fold dilution steps, range: 20,000 - 2 vp/cell or 10,000 - 1 vp/cell) in the presence or absence of 10% autologous ascitic fluid (heat-inactivated at 56°C for 25 min). After incubation for seven days cell viability was measured with the MTS assay (section 2.2.5). Treatment efficacy was calculated by extrapolating the IC_{50} values from sigmoid dose response curves fitted to the extent of oncolysis at the different treatment doses using GraphPad Prism4 software.

2.6 Data processing and statistical analysis

Data was processed using Microsoft Office Excel 2007 (Microsoft Corporation) or GraphPad Prism4 Software (GraphPad Software, Inc.). Statistical analysis was performed using GraphPad Prism4. The identities of statistical tests employed have been indicated in figure legends, where applicable.

3 Oncolytic activity of Ad3, Ad5 and Ad11 in human tumour cell lines

3.1 Introduction

In non-immunocompetent animal models Ad5-derived conditionally replicating Ads can eradicate tumour xenografts after intratumoural, intraperitoneal, or even intravenous administration (Heise *et al.*, 1997; Bauerschmitz *et al.*, 2002). In humans, high efficacy of locally administered H101 led to its approval by Chinese authorities for the treatment of head and neck cancers by intratumoural injection (Garber, 2006). However, the efficacy of Ad5-based virotherapeutics after systemic or compartmental delivery in humans is limited. Neutralisation by pre-existing antibodies (Stallwood *et al.*, 2000) and sequestration onto erythrocytes (Carlisle *et al.*, 2009) or platelets (Othman *et al.*, 2007) reduce activity of Ad5. In addition, in the treatment of ovarian cancer, low expression levels of CAR and integrins, two of the receptors used by Ad5 to achieve cell attachment and entry (Wickham *et al.*, 1993; Bergelson *et al.*, 1997), limit target cell infection (Zeimet *et al.*, 2002).

The use of group B adenoviruses, such as Ad3 and Ad11, might present a way to overcome these obstacles. In a global study population the prevalence of pre-existing antibodies against group B adenoviruses, such as Ad11, was low in comparison to Ad5 (Holterman *et al.*, 2004). Importantly, it has been demonstrated that Ad3 and Ad11 mainly infect cells via the CD46 receptor (Gaggar *et al.*, 2003; Fleischli *et al.*, 2007) which has been shown to be highly expressed on ovarian tumours (Bjørge *et al.*, 1997). This might translate into increased target cell infection and oncolytic activity in comparison to Ad5. Furthermore, over-expression of CD46 on tumour cells might also confer inherent cancer selectivity to Ad3 and Ad11.

The aim of the studies described in this chapter was to assess whether Ad3 and Ad11 are better suited for virotherapy of ovarian cancer than Ad5. The oncolytic activity of Ad3, Ad5 and Ad11 was assessed on three human ovarian cancer cell lines and one human lung cancer cell line after assuring the quality of the investigated virus preparations. Furthermore, the relationships between the expression of adenovirus uptake receptors, extent of internalisation of virus particles and oncolytic activities of Ad3, Ad5 and Ad11 were investigated with the aim of prioritising the most efficacious serotype for further development.

3.2 Characterisation of the oncolytic activity of Ad3, Ad5 and Ad11

3.2.1 Physical and biological characterisation of virus preparations

In order to ensure that the virus preparations used to assess and compare oncolytic activity on different cell lines met required quality standards, their physical and biological properties were characterised. The same three adenovirus preparations were used for the studies described in this thesis unless otherwise indicated.

3.2.1.1 Assessment of particle size distribution

One method to assess the quality of virus batches is by analysing the physical properties of the virus particles. A solution of single particles with a monodisperse distribution profile is required to obtain reproducible and scientifically valid data from studies examining their biological properties. For this, Photon Correlation Spectroscopy (PCS), also termed Dynamic Light Scattering (DLS), was used to determine the size distribution profile of virus preparations (section 2.2.1). Briefly, in this method, monochromatic and coherent laser light is scattered by particles in suspension in a dispersant. These particles move in the liquid phase due to Brownian motion, whose speed is dependent on particle size, which leads to fluctuations in the light scattered from the particles. The velocity of Brownian motion can be calculated from these fluctuations and from this the particle size can be deduced using the Stokes-Einstein relationship. Particle sizes measured with PCS differ from (and are usually greater than) values generated with, for example, electron microscopy. This is due to PCS measuring the hydrodynamic radius or diameter of a particle, which depends on the surface structure of the measured particle as well as the dispersant, while these environmental factors do not influence electron microscopy measurements.

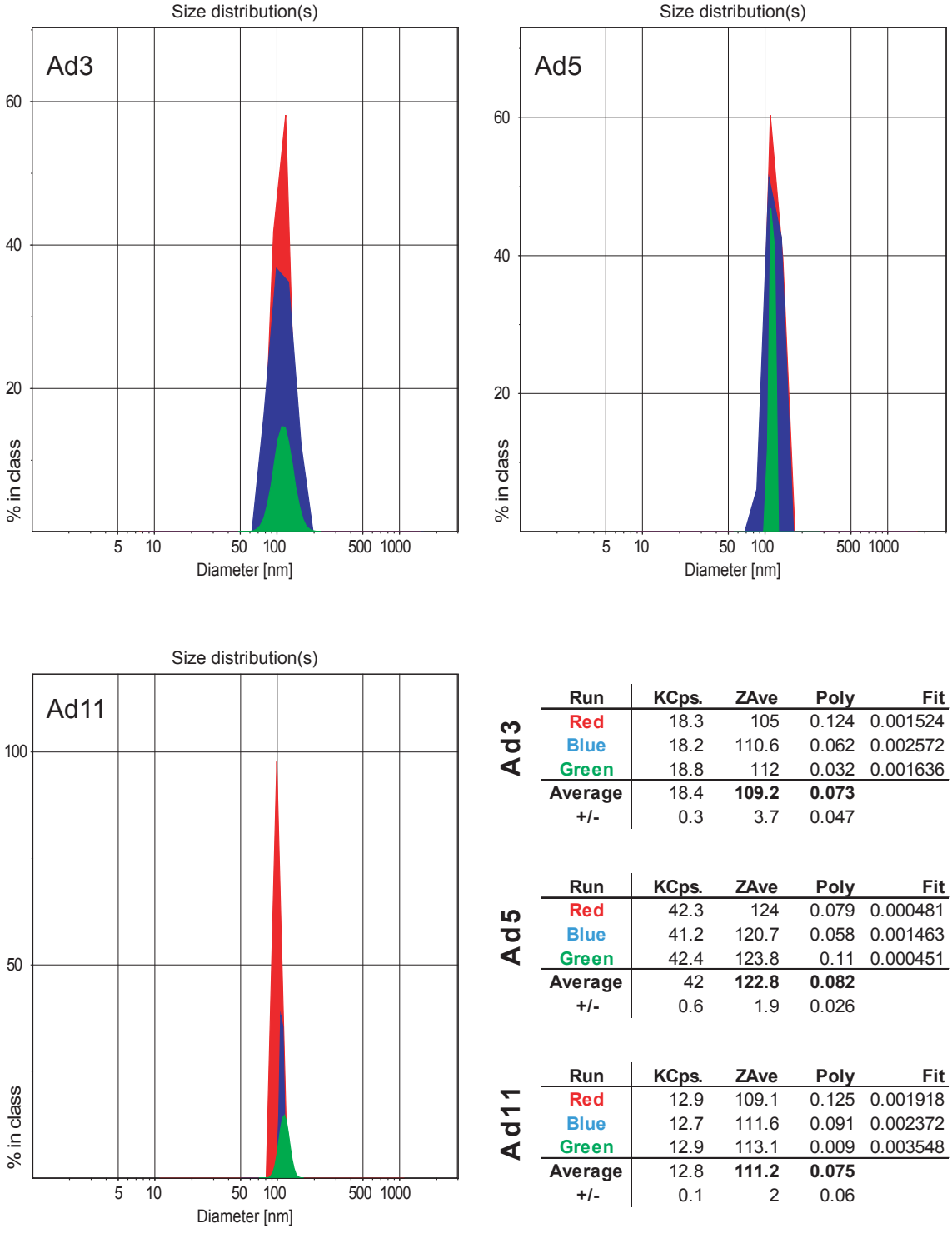
The particle size distributions of virus preparations of Ad3, Ad5 and Ad11 were analysed (Figure 3-1). All three virus preparations appeared to be monodisperse and free of virus particle

aggregates indicated by polydispersity indices below 0.1. The determined hydrodynamic diameters were in the range expected for adenovirus (Oliver *et al.*, 1976), measuring 109.2 ± 3.7 nm, 122.8 ± 1.9 nm and 111.2 ± 2 nm for Ad3, Ad5 and Ad11 respectively. The observed differences between the three serotypes might be attributed to different virus surface charges and structures, such as varying fibre length (Rux and Burnett, 2004), influencing the interaction with solvent molecules.

3.2.1.2 Determination of virus particle concentration

Concentrations of virus particles of adenovirus preparations used in this thesis were determined with the PicoGreen® method (section 2.2.2). This assay quantifies the amount of double-stranded DNA using a fluorescent dye, which gives an increased signal after intercalation with DNA. The concentration of virus particles per millilitre (vp/ml) was calculated by converting the measured amount of double-stranded DNA into the number of whole adenovirus genomes. The removal of free DNA, which was not encapsidated during virus amplification, through incubation with benzonase during virus preparation is a prerequisite for valid results from this method.

Graph A of Figure 3-2 shows the concentration in vp/ml measured from a 1:100 and a 1:500 dilution of the major virus stocks used in this chapter. Concentrations of the viruses were $1.9x10^{12} \pm 2.5x10^{10}$, $3.7x10^{12} \pm 28.8x10^{10}$ and $7.2x10^{11} \pm 4.87x10^{10}$ vp/ml for Ad3, Ad5 and Ad11, respectively. These values were used to calculate virus dilutions in all subsequent experiments. Graph B shows the means of three independent experiments proving that values were reproducible.



Ad3

Run	KCps.	ZAve	Poly	Fit
Red	18.3	105	0.124	0.001524
Blue	18.2	110.6	0.062	0.002572
Green	18.8	112	0.032	0.001636
Average	18.4	**109.2**	**0.073**	
+/-	0.3	3.7	0.047	

Ad5

Run	KCps.	ZAve	Poly	Fit
Red	42.3	124	0.079	0.000481
Blue	41.2	120.7	0.058	0.001463
Green	42.4	123.8	0.11	0.000451
Average	42	**122.8**	**0.082**	
+/-	0.6	1.9	0.026	

Ad11

Run	KCps.	ZAve	Poly	Fit
Red	12.9	109.1	0.125	0.001918
Blue	12.7	111.6	0.091	0.002372
Green	12.9	113.1	0.009	0.003548
Average	12.8	**111.2**	**0.075**	
+/-	0.1	2	0.06	

Figure 3 - 1 Size distribution of virus particles

The distribution of virus particle sizes of the major preparations of Ad3, Ad5 and Ad11 used in this chapter were analysed via Photon Correlation Spectroscopy (section 2.2.1). Virus stock solutions were diluted to approximately $2x10^9$ vp/ml in PBS and aliquots measured in triplicate. Each of the three measurements consisted of 10 subruns. The graphs show the particle distributions of the three measurements for Ad3, Ad5 and Ad11. The tables depict the measured and analysed values. The acronyms stand for: KCps: thousand counts per second [should be > 10], ZAve: mean Z average as determined using cumulants analysis as per ISO 13321, Poly: polydispersity as determined by the width of the peak at its halfmaximal height [should be < 0.1], Fit: indicates the success of the measurement and analysis [should be < 0.01].

3.2.1.3 Biological activity of adenovirus preparations

The PicoGreen® assay cannot distinguish between functional and inactive viruses, as this method only quantifies the amount of virus DNA present in a virus preparation but does not give evidence of biological activity. Hence, a series of plaque assays was used to determine the biological activity of the three virus preparations (section 2.2.3). As it was unclear if the viruses would display equal activity on different host cells three human ovarian cancer cell lines (IGROV1, OVCAR3 and SKOV3) and one human lung cancer cell line (A549), all of epithelial origin, were used in these assays.

3.2.1.3.1 Plaque assay method

Despite three attempts to gather data from plaque assays performed on the ovarian cell lines, it was not possible to maintain these in a viable and confluent condition during the ten to twelve day incubation period. It was only possible to generate data from assays performed with A549 cells (Figure 3-3, graphs A and B). The highest number of plaques could be observed on cells infected with a 10^{-9} dilution of Ad5 stock translating into a value of $5x10^{10}$ plaque forming units per millilitre (pfu/ml) of parent stock dilution, the highest value of all three serotypes. Ad3 created a lower number of plaques at this dilution resulting in a value of $1.9x10^{10}$ pfu/ml, while Ad11 only yielded plaque formation at the lower dilution of 10^{-8}, equating to $7.0x10^{9}$ pfu/ml.

In order to be able to directly compare the activity of the different serotypes it was necessary to take into account differences in their virus particle concentrations. Therefore, pfu/ml values were normalised by the vp/ml values determined with the PicoGreen® assay (section 3.2.1.2). The resulting particle to infectious unit ratio (P/I) describes how many particles of a specific virus preparation are required to achieve one cytolytic event on a specific cell line. As shown in Figure 3-3 graph B all three serotypes appeared to have very similar oncolytic activity on A549 cells. Approximately 1 in 100 particles in these virus preparations was active on this cell line.

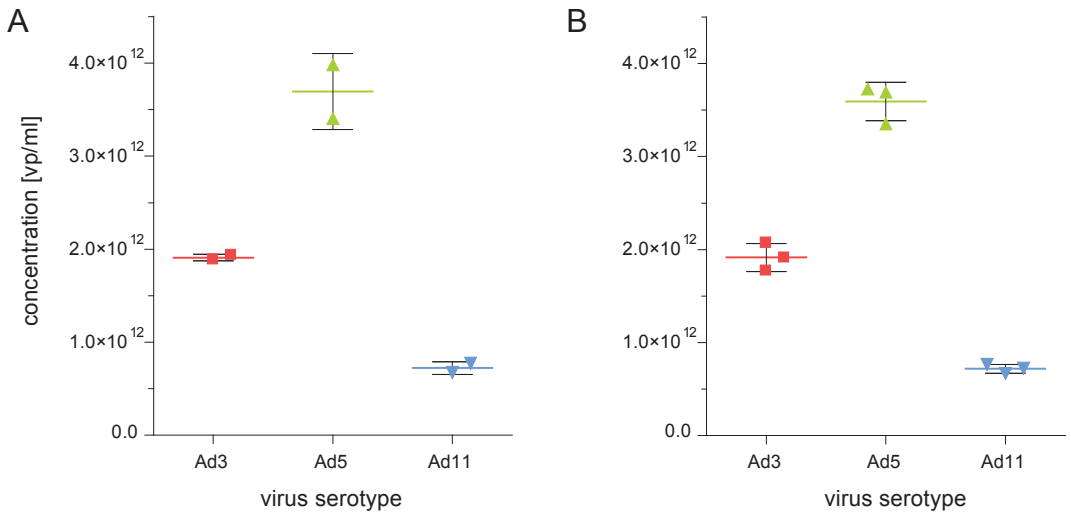


Figure 3 - 2 Determination of virus particle number

The vp concentrations of the preparations of Ad3, Ad5 and Ad11 used in this chapter were determined with the PicoGreen® method (section 2.2.2). Virus dilutions were prepared in SDS containing buffer and incubated at 56ºC for 30 min to disrupt virus capsids. A dilution series of known amounts of bacteriophage λ DNA served as a standard curve. Fluorescence was measured after addition of PicoGreen® reagent. After extrapolation of DNA concentrations of samples from the standard curve the number of vp was calculated assuming 1µg/ml of DNA equaled $2.7x10^{10}$ vp (Murakami and McCaman, 1999). Graph A shows the vp/ml concentrations calculated from triplicate measurements of a 1:100 and a 1:500 dilution of Ad3, Ad5 and Ad11 stock (n = 3). Graph B shows the means of three independent subsequent experiments corroborating the data presented in Graph A (graphs A and B: means and standard deviations).

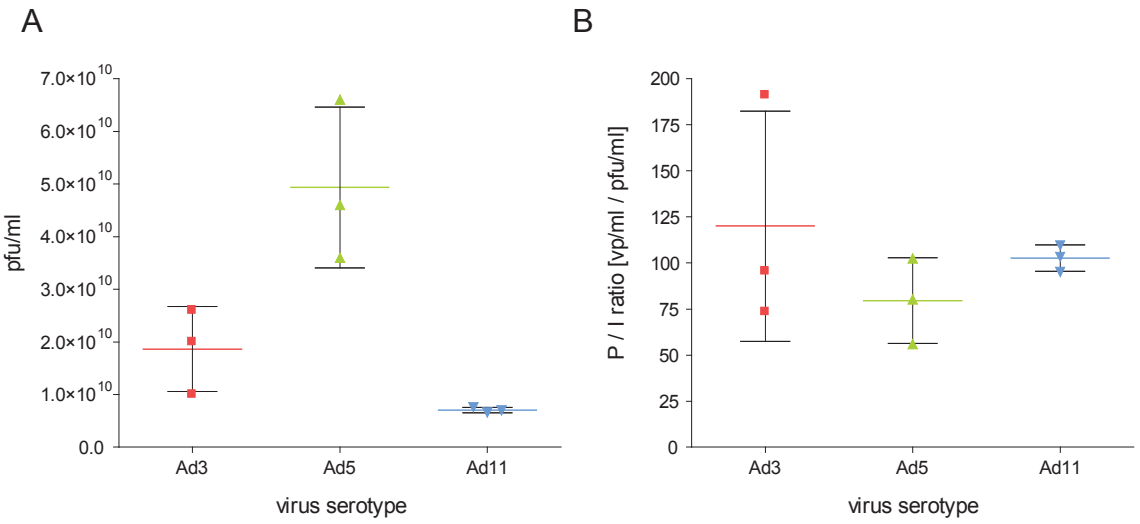


Figure 3 - 3 Virus activity determined by plaque assay

Plaque assays (section 2.2.3) were used to evaluate biological activity of Ad3, Ad5 and Ad11. A549 cells ($5x10^4$/well) were seeded into 6 well tissue culture plates and after overnight incubation serial logarithmic dilutions from 10^{-6} to 10^{-10} of Ad3, Ad5 or Ad11 or a virus-free negative control were added to wells. After 90 min cells were overlayed with agar solution and plates incubated for up to 10 days. After fixing and staining cells with crystal violet the number of plaques in wells of the virus dilution, that resulted in well isolated plaques, was counted. The concentration of active vp (plaque-forming units per ml (pfu/ml)) was then calculated by dividing the number of counted plaques by the dilution factor and the volume of virus solution originally inoculated on that well. Graph A depicts the number of pfu/ml per tested virus preparation. Graph B shows P/I ratios calculated by normalising pfu/ml values by the vp/ml values determined with the PicoGreen assay (Figure 3-2). Differences in calculated P/I ratios between the serotypes on A549 cells were not statistically different (graphs A and B: individual values of triplicate measurements, means and standard deviations; statistical analysis: one-way ANOVA with Tukey post-tests to compare all pairs of data).

3.2.1.3.2 $TCID_{50}$ method

As it was not possible to establish the plaque assay method on the ovarian tumour cell lines, the $TCID_{50}$ (50% Tissue Culture Infectious Dose) method (section 2.2.4) was chosen as an alternative. This method determines the amount of virus required to generate cytopathic effect (CPE) in 50% of a set number of confluent tissue culture wells of cancer cells. The $TCID_{50}$/ml can then be used as a measure of potency of a specific virus preparation. Unlike the plaque assay, it does not require an agar-overlay of cells, which appeared to have a detrimental effect on long-term viability of the ovarian cell lines. Furthermore, the incubation period lasts only seven days as opposed to 10 days, which considerably lowers the risk of cell overgrowth.

Graphs A, B and C in Figure 3-4 show the $TCID_{50}$/ml of virus preparations of Ad3, Ad5 and Ad11 on the four cell lines tested. Notably, virus activity strongly depended on the host cell type for all three virus batches. In A549 cells Ad3 exhibited high activity reflected in a high $TCID_{50}$/ml, whereas its performance on all three ovarian cancer cell lines was weak. Ad5 demonstrated high activity on A549, IGROV1 and OVCAR3, but not on SKOV3 cells. The pattern demonstrated by Ad11 was similar to Ad3, divergent from Ad5, which might be due to both Ad3 and Ad11 belonging to adenovirus group B, whereas Ad5 is a group C adenovirus.

As described in section 3.2.1.3.1 it was necessary to normalise the measured $TCID_{50}$/ml values by the vp/ml values determined with the PicoGreen® assay in order to be able to compare the potency of the different viruses directly. The resulting particle to infectious unit ratio (P/I) for the three virus serotypes on all four cell lines are shown in Graph D, Figure 3-4. A low P/I ratio signifies high virus activity, whereas high P/I values indicate that many virus particles are required to achieve induction of CPE. A549 cells were easily killed by all three serotypes. It appeared that (in accordance with results from the plaque assay, Figure 3-3) between 1 in 100 and 1 in 500 of particles present in each virus preparation was active. In contrast, the three ovarian cancer cell lines exhibited a diverse pattern of susceptibility to induction of CPE. While Ad5 showed high activity on IGROV1 cells, similar to the level on A549 cells, approximately 1,000 times more Ad3 or Ad11 particles were required to achieve CPE on these cells. Interestingly, Ad5 appeared to lose this advantage in the OVCAR3 and SKOV3 cells.

In both of these cell lines CPE formation required more Ad5 than Ad3 or Ad11. OVCAR3 cells seemed to be specifically more susceptible to Ad11, reflected in a P/I ratio which was approximately three times or five times lower than that of Ad3 or Ad5, respectively. SKOV3 cells appeared to be particularly resistant to Ad5-killing. P/I ratios of Ad3 and Ad11 were ten times and four times lower than the one of Ad5, respectively.

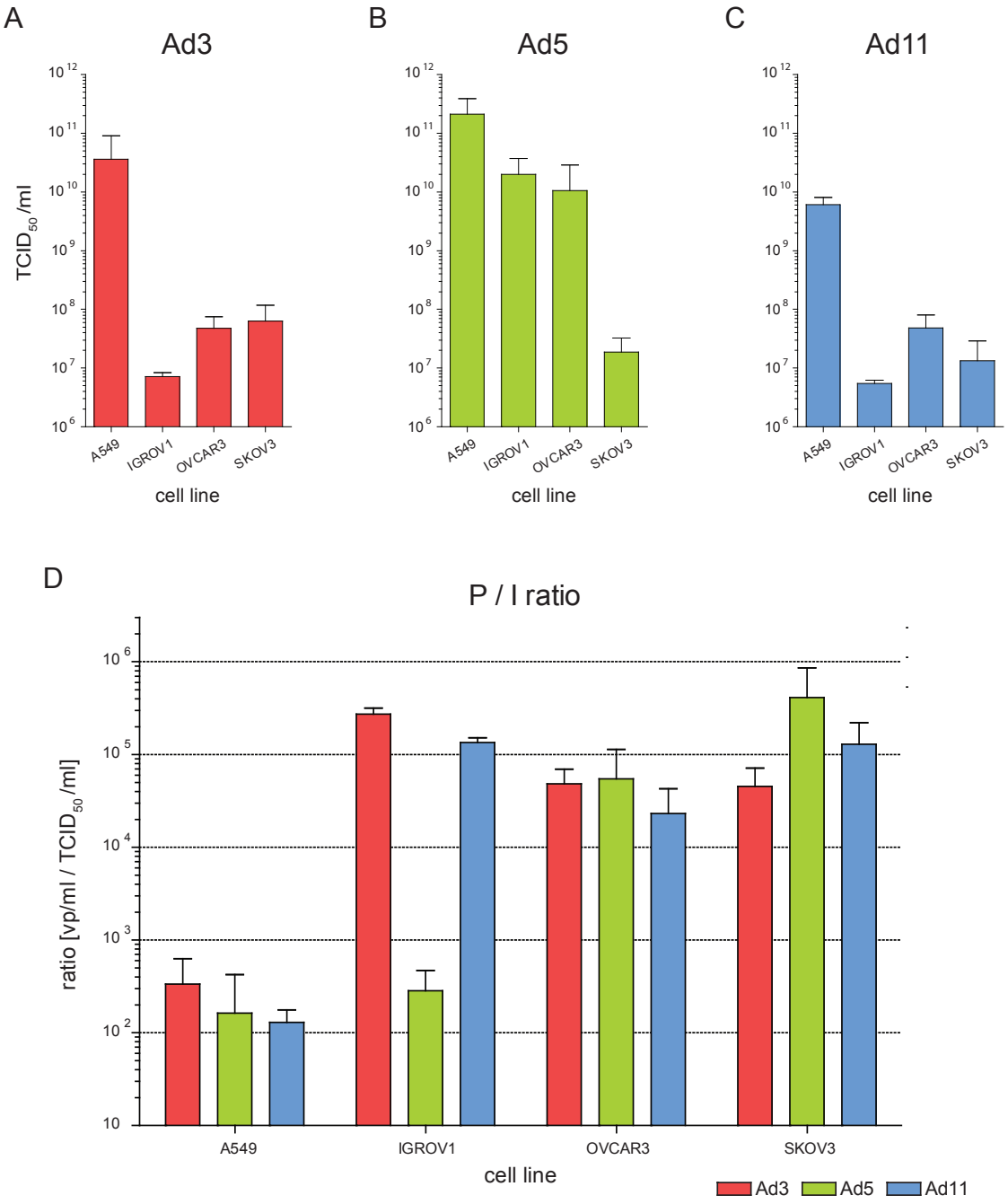


Figure 3 - 4 Virus activity determined by the $TCID_{50}$ method

The activity of Ad3, Ad5 and Ad11 was determined on the four human tumour cell lines A549, IGROV1, OVCAR3 and SKOV3 using the $TCID_{50}$ method (section 2.2.4). Cells (10^4/well) were seeded into tissue culture plates prior to overnight incubation. After removal of media aliquots of serial logarithmic dilutions from 10^{-5} to 10^{-12} of each virus or a virus free negative control were each added to 10 wells and plates incubated for up to 8 days. For each dilution the number of wells showing development of CPE was counted and the ratio of wells affected by CPE versus non-affected wells calculated. The $TCID_{50}$ was then determined using the KÄRBER statistical method. Graphs A, B and C show the $TCID_{50}$ /ml of Ad3, Ad5 or Ad11 on the four cell lines tested. Strong oncolytic activity is reflected in a high $TCID_{50}$ /ml value.

In order to be able to compare the activity of the different serotypes directly, it was necessary to normalise the measured $TCID_{50}$ /ml values by the vp/ml values determined with the PicoGreen® assay (Figure 3-2). The resulting particle to infectious unit ratios (P/I) for the three serotypes on all four cell lines are shown in Graph D. A low P/I ratio signifies strong virus activity, whereas high P/I values indicate that much virus was needed to achieve induction of CPE (graphs depict the mean of three independent experiments and standard deviations).

3.2.2 Assessment of oncolytic potency through cytotoxicity measurements

The MTS assay system was chosen for these and subsequent cytotoxicity studies as it constitutes a more convenient and practical way to study larger sample sets. Through colourimetric measurements the metabolic activity of cells is determined as a surrogate assessment for the number of viable cells in a tissue culture plate well (section 2.2.5). In all studies performed in this section, the amount of virus added to cells was based on the concentration of virus particles as determined with the PicoGreen® method (section 3.2.1.2).

3.2.2.1 Time-course of oncolytic effect and virus production

In general, results from cytotoxicity measurements with a certain compound strongly depend on the duration of its exposure to the host. In order to characterise the influence of incubation time on the cytotoxic effect of the different adenovirus serotypes, oncolytic toxicity was assessed on the same four human tumour cell lines as employed above by measuring viability over a time-course. This would inform subsequent experiments about the optimal time-points for assessment of cytotoxicity. Previous reports had demonstrated completion of one replication cycle of adenovirus on HeLa cells after 36 hours (Fields *et al.*, 2007) and observations in our group demonstrated cell lysis of Ad5-infected A549 cells after 48 hours (unpublished data). Hence, a time-course duration of 120 hours was chosen to allow for at least 2 replication cycles of Ad5 on A549.

For this study, stock cell suspensions were infected with virus at a concentration of 100 vp/cell for 90 minutes, before removing non-internalised virus through one wash with PBS and dispensing cells into 96 well tissue culture plates. This would ensure that wells contained the same amount of cells and virus. Results showed that measurements of virus activity were not only influenced by the type of cells or type and amount of virus, but that they were also highly time-dependent (Figure 3-5). Significant differences in the extent of cytolysis were found for the different cell lines at the different time-points. A549 cells succumbed to virus-induced lysis by Ad5 and Ad11 within 48 hours of infection, which correlates with one full virus replication cycle

and indicates similar kinetics of Ad5 and Ad11 on this cell line. However, when inoculated with Ad3, a proportion of A549 cells remained viable even after 48 hours. This residual viability for Ad3 was seen in several subsequent experiments and might be explained by a sub-population of infection-resistant A549 cells or cells, which were infected but resistant to oncolysis and retained metabolic activity. Overall, the ovarian tumour cell lines IGROV1 and OVCAR3 demonstrated a similar pattern of rapid and extensive cell lysis after 48 hours. However, some serotype / cell line combinations did not lead to immediate cell death. Ad3 seemed to require a second round of replication to kill all IGROV1 cells and there were similar observations with Ad5 on OVCAR3 cells. Interestingly, SKOV3 cells displayed a completely different pattern in comparison to the other cell lines: oncolysis was significantly delayed with Ad11, diminished and incomplete with Ad3 and absent with Ad5 at the virus concentration used.

To investigate if the lysis resistance of SKOV3 cells was due to poor virus replication, cell supernatants, which had been collected at each time-point, were extracted for genomic DNA and the number of virus genomes measured by real time Q-PCR (compare sections 2.2.7 and 3.3.2.1) (Figure 3-6). Genome copy number rose from less than 10^4 per well at 24 hours after infection to a range of 10^5 to 10^6 in the following 24 hours, correlating with the expected first cycle of virus replication. A second significant increase in particle number was observed at around 78 hours leading to a final genome copy number of approximately 10^8 per well. Notably, progeny virus was produced for all three serotypes, although cells infected with Ad3 or Ad5 exhibited very little or no decrease in viability, respectively.

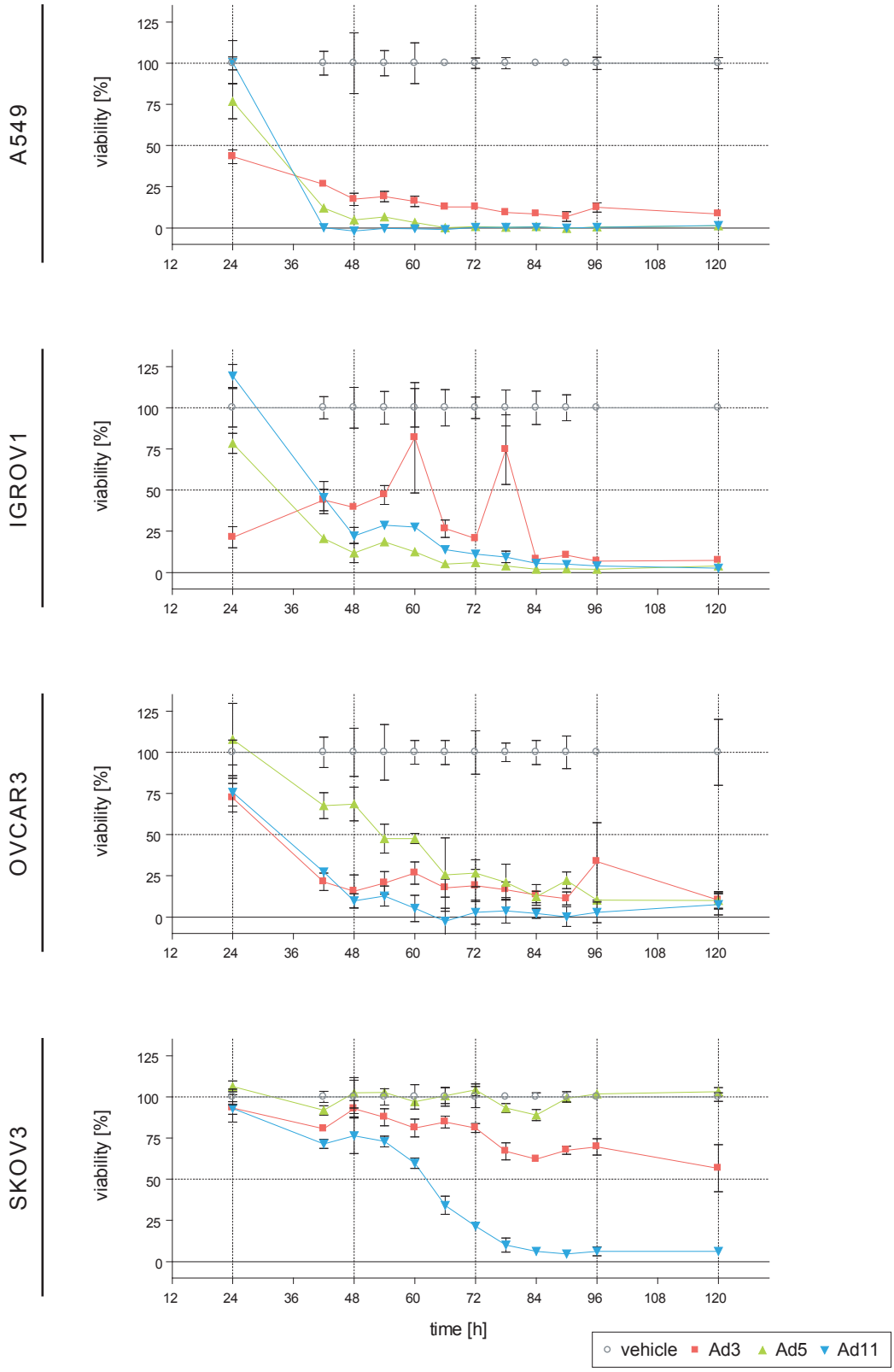


Figure 3 - 5 Time-course of oncolytic effect determined by viability assays (MTS)

In order to clarify the influence of incubation time on the cytotoxic effect of Ad3, Ad5 and Ad11, oncolytic toxicity was assessed through viability measurements over 120 hours using the MTS assay (section 2.2.5). For this, suspensions of cells were incubated with virus (100 vp/cell) or vehicle only for 90 min, before removing non-internalised virus through one wash with PBS and dispensing cells into 96 well microplates. Cell viability was assessed via MTS assay at indicated timepoints. Graphs show viability measurements as a function of time for Ad3, Ad5 and Ad11 and mock-treated controls on A549, IGROV1, OVCAR3 and SKOV3 (means of triplicate values and standard deviations).

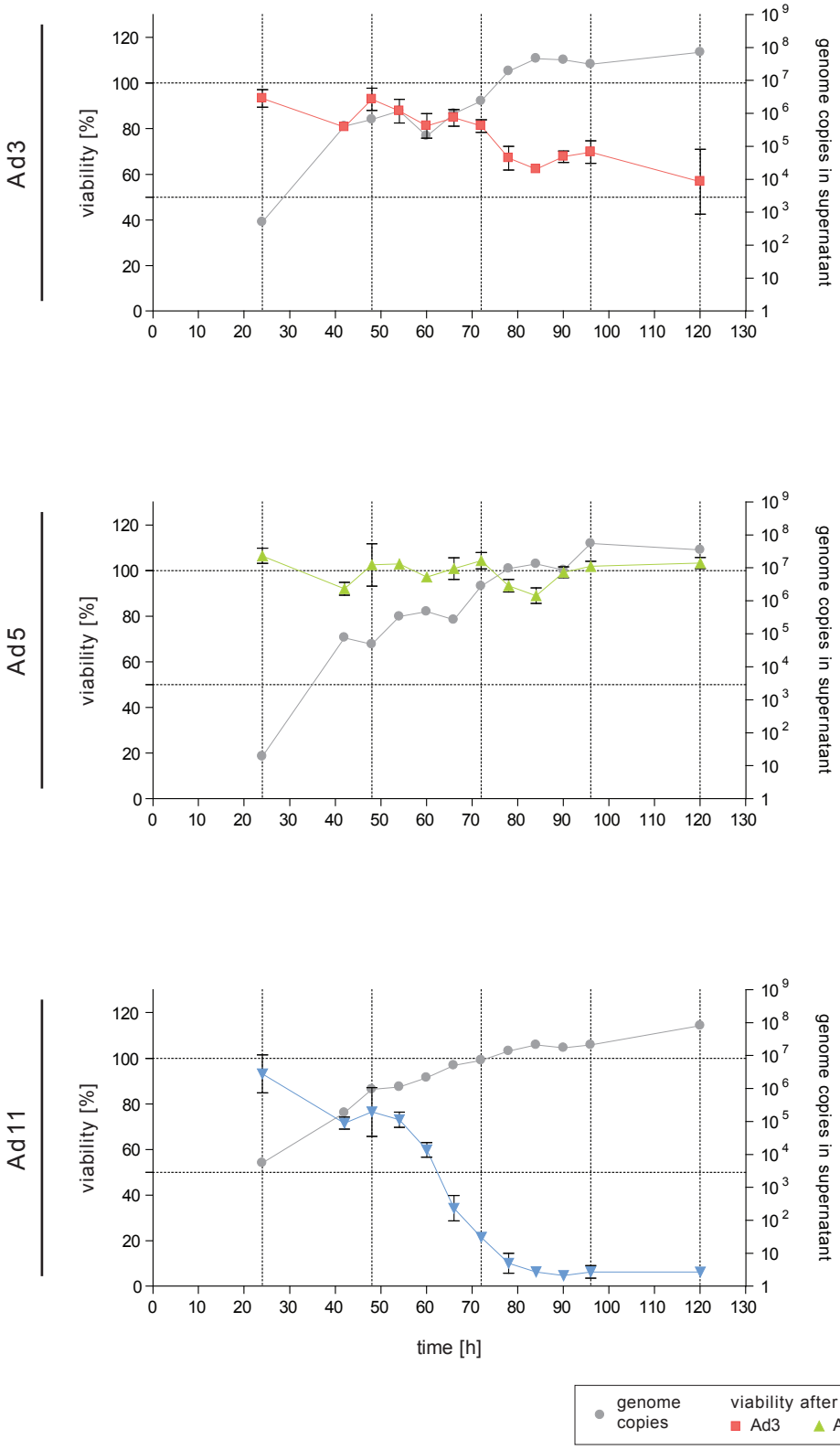


Figure 3 - 6 Time-course of oncolytic effect and virus replication in SKOV3 cells

SKOV3 cell supernatants from the time-course experiment (Figure 3-5), which had been collected at each time point, were extracted for genomic DNA and the amount of virus genomes at each time point measured by real time Q-PCR (section 2.2.7). Graphs depict the viability of cells (left ordinate; compare Figure 3-5) overlayed with the number of virus genome copies in the supernatant (right ordinate, as a measure for virus replication) as a function of incubation time (means of triplicate (viability) or duplicate (genome copy number) measurements and standard deviations).

3.2.2.2 Assessment of oncolytic activity of Ad3, Ad5 and Ad11 with MTS-assays

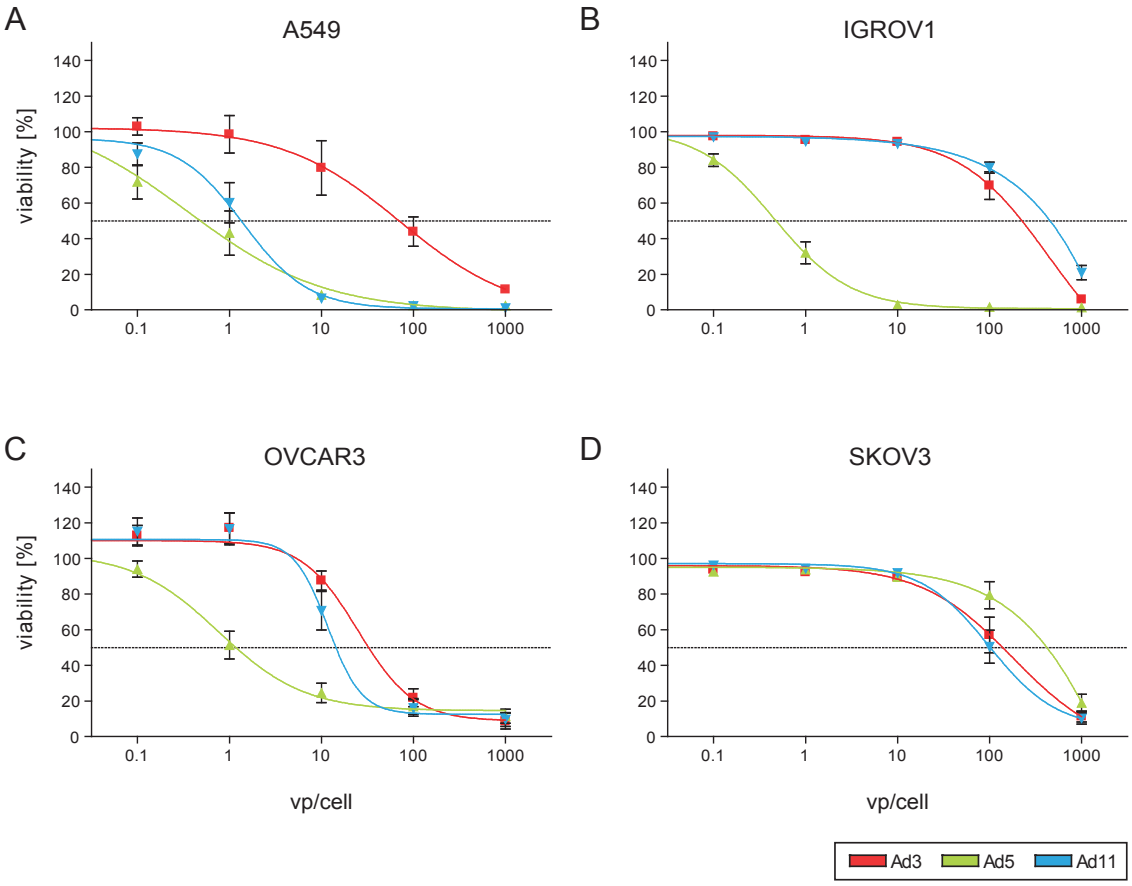
It was deemed essential to corroborate the results gained from plaque assay and $TCID_{50}$ studies and test their transferability to a different assay system, which would allow more convenient study of the oncolytic effect of adenovirus in larger sample sets. This was particularly important in regard to prospective experiments investigating the neutralisation capacity of clinical samples (section 5.3), as these studies would require screening of a large number of microplates. Therefore, oncolysis studies, using titration of the infection dose of virus assessed through viability measurements with the MTS reagent (section 2.2.5), were used as a second approach to assess the oncolytic activity of the three serotypes on the different cell lines.

For these studies, logarithmic dilution series of the different viruses were prepared according to their vp/ml concentration, as previously determined with the PicoGreen® assay (section 3.2.1.2). After infection of cell monolayers, tissue culture plates were incubated for five days, when cell survival was determined by MTS assay. In order to be able to easily compare the activity of the serotypes on the different cell lines, the half maximal inhibitory concentration (IC_{50}) for each virus on each cell line was determined. To this end, a sigmoid dose response model with variable slope was used to fit the calculated viability data to nonlinear regression curves (Figure 3-7, graphs A – D) and the concentration of virus required to reduce viability of cells to 50% (IC_{50}) was extrapolated from the dose response curves (Figure 3-7, table E). Graphing the determined values (Figure 3-8, graph A) revealed a very similar pattern to that observed with the $TCID_{50}$ method (Figure 3-4, graph E) with considerable differences in susceptibility to oncolysis observed between cell lines.

Comparison of the performance of the alternative serotypes on each cell line demonstrated that A549 cells were highly susceptible to killing by Ad5 and Ad11 with approximately 10 vp/cell required for complete cell lysis. Ad3 demonstrated similar activity in two of four independent experiments on this cell line, while around 30 times more virus was needed in the other two experiments. IGROV1 cells were particularly sensitive to Ad5 infection but up to 1,000-fold

more of the group B viruses Ad3 or Ad11 was needed to kill these cells. A similar pattern could be observed on the OVCAR3 cells but the group B viruses were approximately ten times more active than on the IGROV1 cells. The high activity of Ad5 on OVCAR3 cells was in contrast to results from the $TCID_{50}$ study, possibly because OVCAR3 cells, in general, showed the highest variability of growth properties among cell lines. Of all cell lines SKOV3 demonstrated most resistance to virus-induced cell death consistently requiring 500-1,000 vp/cell of Ad3, Ad5 or Ad11 for complete cell kill, making them least susceptible to adenovirus-induced cytotoxicity of all cell lines tested (consistent with results from the $TCID_{50}$ assay (Figure 3-4)). Also similar to the $TCID_{50}$ data, Ad3 and Ad11 were more active on SKOV3 than Ad5.

Graphing the IC_{50} values separated for each of the alternative serotypes (Figure 3-8, graphs B – D) and comparing activity across the different cell lines revealed that Ad3 exhibited similar potency on all four investigated cell lines. Contrarily, significantly less Ad5 was needed to achieve 50% cell killing on A549, IGROV1 and OVCAR3 in comparison to SKOV3 cells ($p < 0.05$). Ad11 performed particularly poorly on IGROV1 cells demonstrated by a highly significant difference in IC_{50} in comparison to A549 and OVCAR3 cells ($p < 0.01$).



E

	A549			IGROV1			OVCAR3			SKOV3		
	mean	**SD**	**N**	**mean**	**SD**	**N**	**mean**	**SD**	**N**	**mean**	**SD**	**N**
Ad3	**108.8**	145.0	4	**290.5**	188.8	4	**43.9**	30.8	4	**330.1**	325.5	4
Ad5	**1.5**	1.7	4	**0.5**	0.2	4	**3.2**	4.7	4	**508.9**	410.2	4
Ad11	**1.5**	1.1	4	**474.8**	247.2	4	**24.8**	20.4	4	**229.5**	235.9	4

Figure 3 - 7 Virus activity determined by viability assays (MTS)

Logarithmic dilution series of Ad3, Ad5 and Ad11 were prepared according to their vp/ml concentration as previously determined with the PicoGreen® assay (Figure 3-2) and after infection of monolayers of A549, IGROV1, OVCAR3 or SKOV3 cells, microplates were incubated for five days, when virus activity was determined by assessing the amount of viable cells using the MTS assay (section 2.2.5). A sigmoid dose response model with variable slope was used to fit the viability data to nonlinear regression curves (Graphs A - D; means of triplicate measurements of four independent experiments and standard error of the mean). In order to be able to easily compare the potency of the serotypes on the different cell lines, the half maximal inhibitory concentration (IC_{50}) value for each serotype on each cell line was calculated. For this, the concentrations of virus required to reduce viability of cells to 50% (IC_{50}) was extrapolated from the dose response curves for each of the four individual experiments and their mean calculated (Table E; means of extrapolated IC_{50} values of four independent experiments and standard deviations).

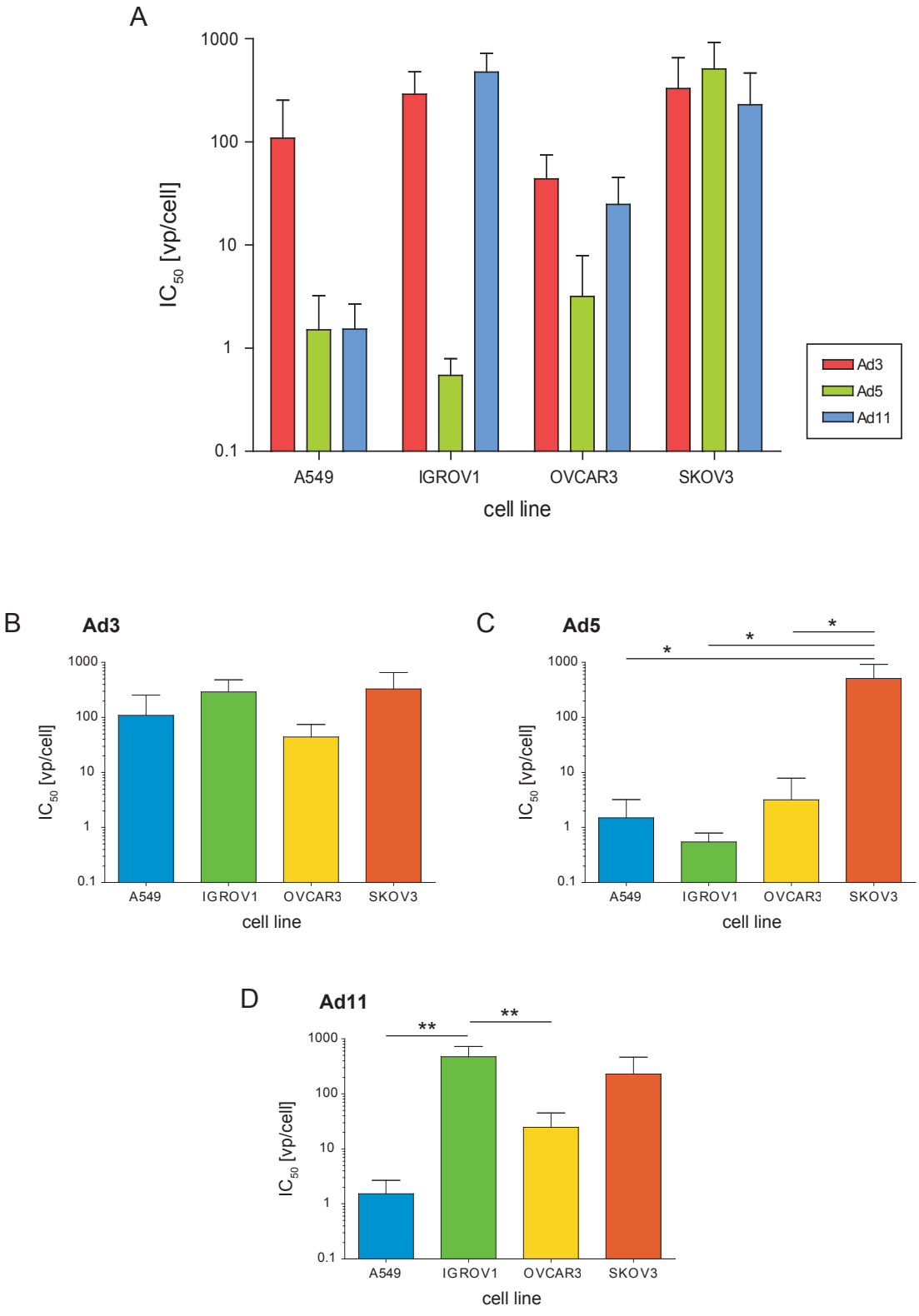


Figure 3 - 8 Comparison of serotype activity expressed as IC_{50} values

The concentration of virus needed to reduce viability of cells grown as monolayers to 50% (IC_{50}) after five days was extrapolated from dose response curves shown in Figure 3-7. Graph A depicts the mean IC_{50} values of four independent experiments and corresponding standard deviations of Ad3, Ad5 and Ad11 on A549, IGROV1, OVCAR3 and SKOV3 cells. Graph B - D show the IC_{50} values separated for each of the alternative serotypes comparing activity across the four cell lines (means of four independent experiments and standard deviations; statistical analysis: repeated measures one-way ANOVA with Tukey post-tests to compare all pairs of columns (** = $p < 0.01$, * = $p < 0.05$)).

3.2.3 Replication dependence of cytotoxicity

In order to ensure that the observed cytotoxicity was caused by virus replication and lysis of cells and was not a reaction to the presence, adsorption or entry of adenovirus, cells were inoculated with serial logarithmic dilutions of wild-type Ad5 (Ad5) and an E1A-deleted Ad5-derived vector construct which expresses luciferase under the control of a CMV promoter (Ad5luc). Due to the deletion of the E1A gene this virus construct is replication-deficient, since E1A gene products are essential to transactivate other sequences of the adenovirus genome and induce S phase entry of the host cell (Frisch and Mymryk, 2002). Hence, this virus acted as a negative control for replication-induced cytotoxicity.

Cells were treated as described in section 3.2.2.2 and viability assessed at two or six days after infection (Figure 3-9). Two days after virus inoculation viability of A549, IGROV1 and OVCAR3 cells incubated with 100 or 1,000 vp/cell of Ad5 had dropped significantly in comparison to Ad5luc-incubated cells. SKOV3 cells showed resistance to oncolysis by Ad5 at this time-point in accordance with earlier experiments (see section 3.2.2). After six days of incubation, allowing for two to three adenovirus replication cycles, even the lower virus particle concentration of 10 vp/cell resulted in complete cell death on A549 and IGROV1 cells, whereas OVCAR3 cells exhibited a residual 35% viability. SKOV3 cells showed a decrease to 50% viability only at the highest vp/cell concentration. Interestingly, a small decrease in viability could be observed for Ad5luc at a concentration of 1,000 vp/cell at this time-point, which was particularly pronounced in A549 and IGROV1 cells. In order to clarify whether this was due to a fraction of the Ad5luc preparation having replication competency, supernatants of wells infected with 1,000 vp/cell of Ad5 or Ad5luc were extracted for genomic DNA and subjected to real time Q-PCR (section 2.2.7) (Figure 3-10). Virus particle numbers measured for Ad5luc remained below or just above the input dose. Replication of Ad5 for six days had resulted in 100- to 200-fold higher virus particle numbers than were originally inoculated. Intriguingly, in accordance with results from the time-course experiment (see section 3.2.2), the same amount of Ad5 progeny virus was produced on all four cell lines, although viability of SKOV3 cells had only decreased by 50%.

In summary, the cytotoxic effects seen after wild-type Ad5 infection were not related to presence, adsorption or entry of virus particles, but were due to adenovirus replication and subsequent cell lysis. The small decreases in viability for Ad5luc infected cells might reflect toxicity related to general particle toxicity, prolonged CMV promoter activity or high levels of expressed luciferase.

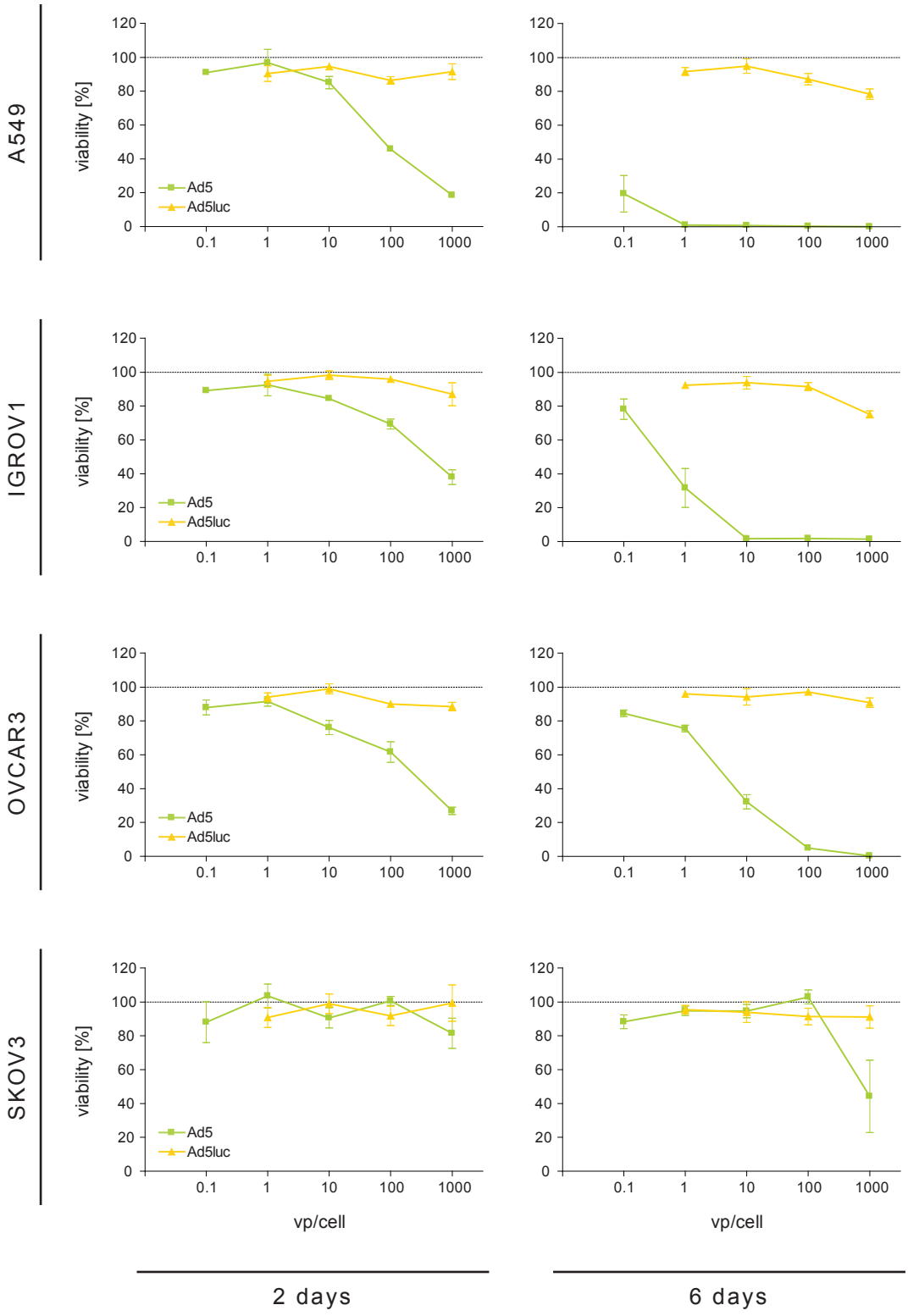


Figure 3 - 9 Cytotoxicity of replicating and non-replicating Ad5

The cytotoxicity of wild-type Ad5 (Ad5) and an E1A-deleted replication-deficient Ad5 (Ad5luc) was measured after two days and six days incubation at a range of vp/cell concentrations. For this, cells (10^4/well) were grown in monolayers in 96 well microplates overnight. After removing media and washing cells with PBS aliquots of serial logarithmic dilutions of Ad5 (green) or Ad5luc (yellow) or a virus-free negative control were added to wells in triplicate and plates incubated for two or six days, when plates were analysed with the MTS assay (section 2.2.5). Graphs show the viability of cells determined by dividing the measured AU of infected wells by values of the non-infected negative control (means of triplicate values and standard deviations).

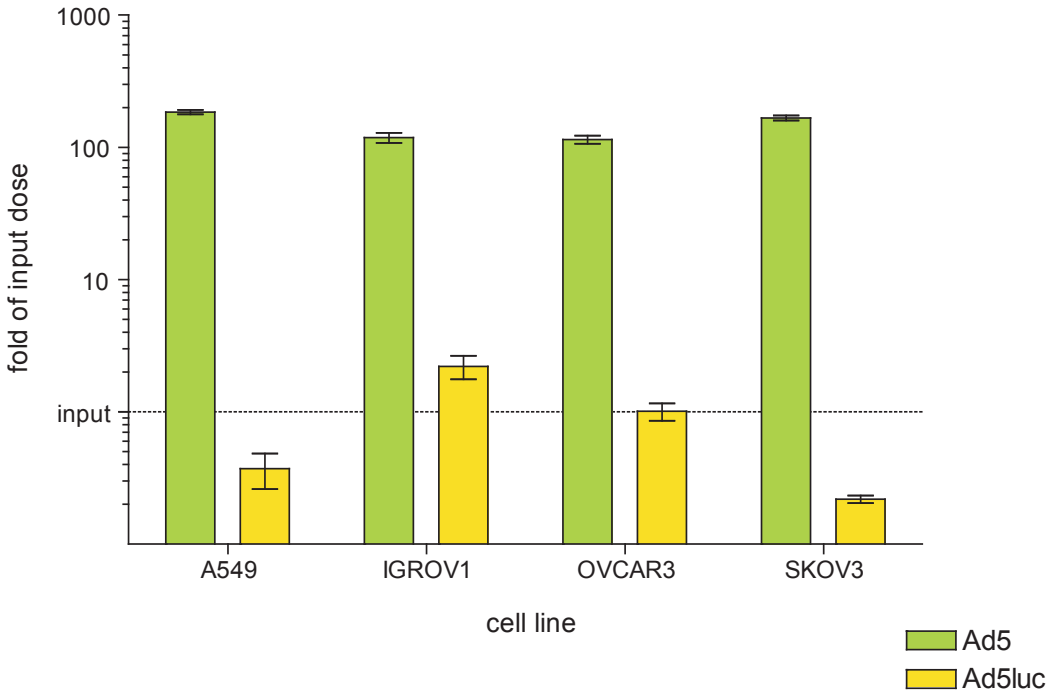


Figure 3 - 10 Progeny genome number of replicating and non-replicating Ad5

Virus replication of wild-type Ad5 (Ad5) and an E1A-deleted replication-deficient Ad5 (Ad5luc) on A549, IGROV1, OVCAR3 and SKOV3 was measured after incubation for six days (compare Figure 3-9). For this, supernatants of cells initially infected with 1,000 vp/cell were extracted for genomic DNA and subjected to real time Q-PCR (section 2.2.7). The graph shows the fold increase of virus genomes over the input dose of 10^7 vp/well (means of triplicate values and standard deviations).

3.2.4 Confirmation of findings with other adenovirus batches

In order to confirm that above results constituted principles which were innate features of the different adenovirus serotypes and were not artefacts of the investigated virus preparations the oncolytic activities of two other batches of Ad5 and Ad11 were tested on the different cell lines (Figure 3-11). Studies were performed as described in section 3.2.2.2.

For both Ad5 and Ad11 viability curves obtained from alternative batches (batch 1 and 2 for Ad5; batch 3 and 4 for Ad11) closely followed the curves from the original virus preparations, with slightly higher variability for Ad5. As the virus dose inoculated on cells is dependent upon results obtained from PicoGreen® assays, variations in toxicity might be attributed to the inter-assay variations of this quantification method. However, the differential pattern of oncolytic activity demonstrated in the original preparations of the two serotypes on the different cell lines could also be observed for the other batches. A549 cells showed little resistance to oncolysis by both Ad5 and Ad11, while IGROV1 cells were more permissive for lytic replication by Ad5. SKOV3 cells exhibited oncolysis resistance similar to previously described data (section 3.2.2.2). Equally, Ad11 again showed greater oncolytic activity in SKOV3 than Ad5. Overall, the two other virus batches tested for each of the serotypes performed very similar to the original virus preparations. The distinct oncolytic activities on the different cell lines were therefore likely to be an intrinsic attribute of the serotypes.

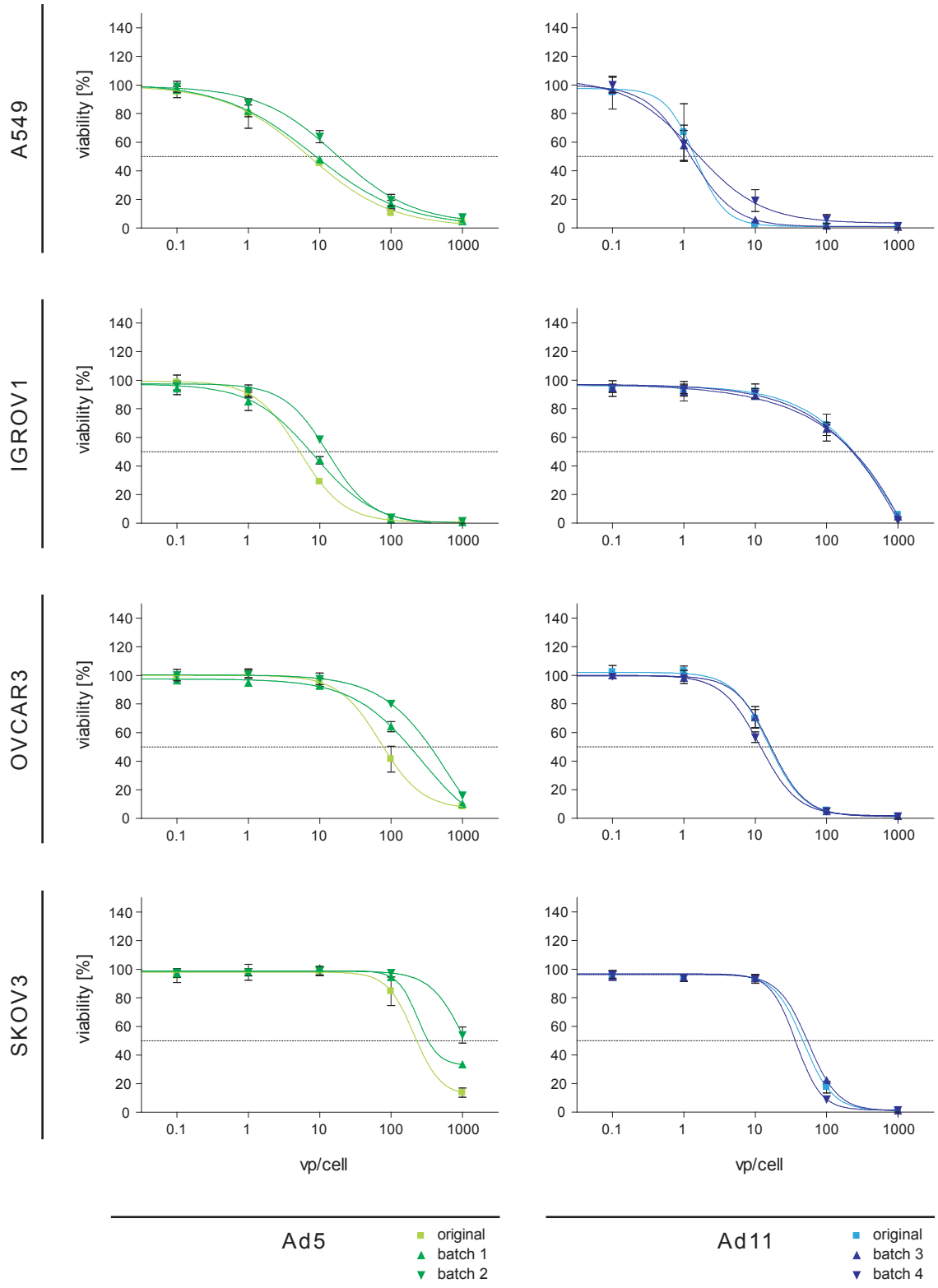


Figure 3 - 11 Confirmation of differential activity of Ad5 and Ad11

The cytotoxicity of different batches of Ad5 and Ad11 was measured at a range of vp/cell concentrations. A549, IGROV1, OVCAR3 and SKOV3 cells (10^4/well) were grown in monolayers in 96 well microplates overnight. After removing media and washing cells with PBS aliquots of serial logarithmic dilutions of Ad5 (green) or Ad11 (blue) or a virus-free negative control were added to wells in triplicate and plates incubated for five days, when plates were analysed with the MTS assay (section 2.2.5). Graphs show the viability of cells determined by dividing the measured AU of infected wells by values of the non-infected controls (means of triplicate values and standard deviations).

3.3 Factors influencing oncolytic activity in tumour cell lines

The experiments discussed in section 3.2 demonstrated that the activity of different adenovirus serotypes on different cell lines was diverse and no serotype had overall increased potency. The potency of Ad3 was mediocre on all of the tested cell lines. Ad5 was the most oncolytic serotype on A549 and the two ovarian cancer cell lines, IGROV1 and OVCAR3. However, Ad5 had the least oncolytic activity in SKOV3 cells. In contrast, Ad11 was particularly weak on IGROV1 cells while its activity was similar to Ad5 on A549 and OVCAR3 cells. Interestingly, Ad11 was the most potent serotype on SKOV3 cells. Hence, these *in vitro* studies did not demonstrate overall better suitability of a particular serotype for virotherapy of ovarian cancer. In particular, the originally proposed higher oncolytic activity of group B adenoviruses (due to higher expression levels of their uptake receptor CD46 in ovarian tumours (see section 3.1)) had not been observed. However, as the receptor status of the cell lines used in these experiments had not been evaluated, it was unclear if these findings were due to varying amounts of receptor expression between cell lines.

3.3.1 Receptor expression of human tumour cell lines

As a first step to elucidate whether the discrepancies in oncolytic activity of the three serotypes described in section 3.2 were caused by differences in uptake receptor expression levels, the relative expression of their main uptake receptors was analysed by flow cytometry (section 2.2.6). A549, IGROV1, OVCAR3 and SKOV3 cells were stained with antibodies specific for the integrin subunit α_V, which forms part of the integrin heterodimers $\alpha_v\beta_3$ and $\alpha_v\beta_5$, CAR, CD46 or an isotype control. The important role of Desmoglein 2 in uptake of Ad3 and Ad11 (Wang *et al.*, 2011) had only been reported at the end of this thesis project, hence this receptor had not been included in this study. A polyclonal FITC-labelled secondary antibody recognising murine IgG antibodies was used for detection of bound primary antibodies (Figure 3-12). Controls treated with the unspecific isotype showed little elevation of fluorescence intensity above background levels for unstained cells or cells incubated with the secondary antibody only.

In order to take into account the number of positive cells per tested sample as well as their expression levels, flow cytometry data was analysed by multiplying the percentage of positive cells with the geometric mean of their fluorescence intensity (Figure 3-13) as previously reported (Bottini *et al.*, 1993; You *et al.*, 2001). Furthermore, in order to be able to compare expression levels of the different receptors on cell lines it was assumed that the binding efficiencies of primary antibodies to their epitopes and secondary to primary antibody binding were similar for all antibodies (Shashkova *et al.*, 2009).

CD46 had the highest expression of the three cell-surface receptors on all four cell lines. While the ovarian cancer cell lines expressed similar amounts of CD46, the lung carcinoma cell line, A549, showed lower levels of expression. The integrin α_v subunit was the second most abundant receptor. Here, the pattern observed for CD46 was reversed, with A549 expressing the highest levels of the subunit. CAR demonstrated the lowest staining levels of the three receptors on all four cell lines. While A549 and IGROV1 cells showed higher levels of CAR cell-surface expression, OVCAR3 and SKOV3 cells had significantly lower CAR levels. Indeed, the intensity measured on SKOV3 cells hardly exceeded the value of the unspecific isotype, indicating no or very low expression of this receptor in this cell line. The contrast between CAR and CD46 expression on SKOV3 cells is in accordance with previously published results, while the similar pattern of expression on OVCAR3 cells, seen here, was in contrast to previous observations (Shashkova *et al.*, 2009). The universally high expression of the complement receptor, CD46, in the ovarian cancer cell lines is likely due to its protective role against complement-mediated lysis, thereby giving an selective ‘evolutionary’ advantage during development of malignant characteristics (Fishelson *et al.*, 2003).

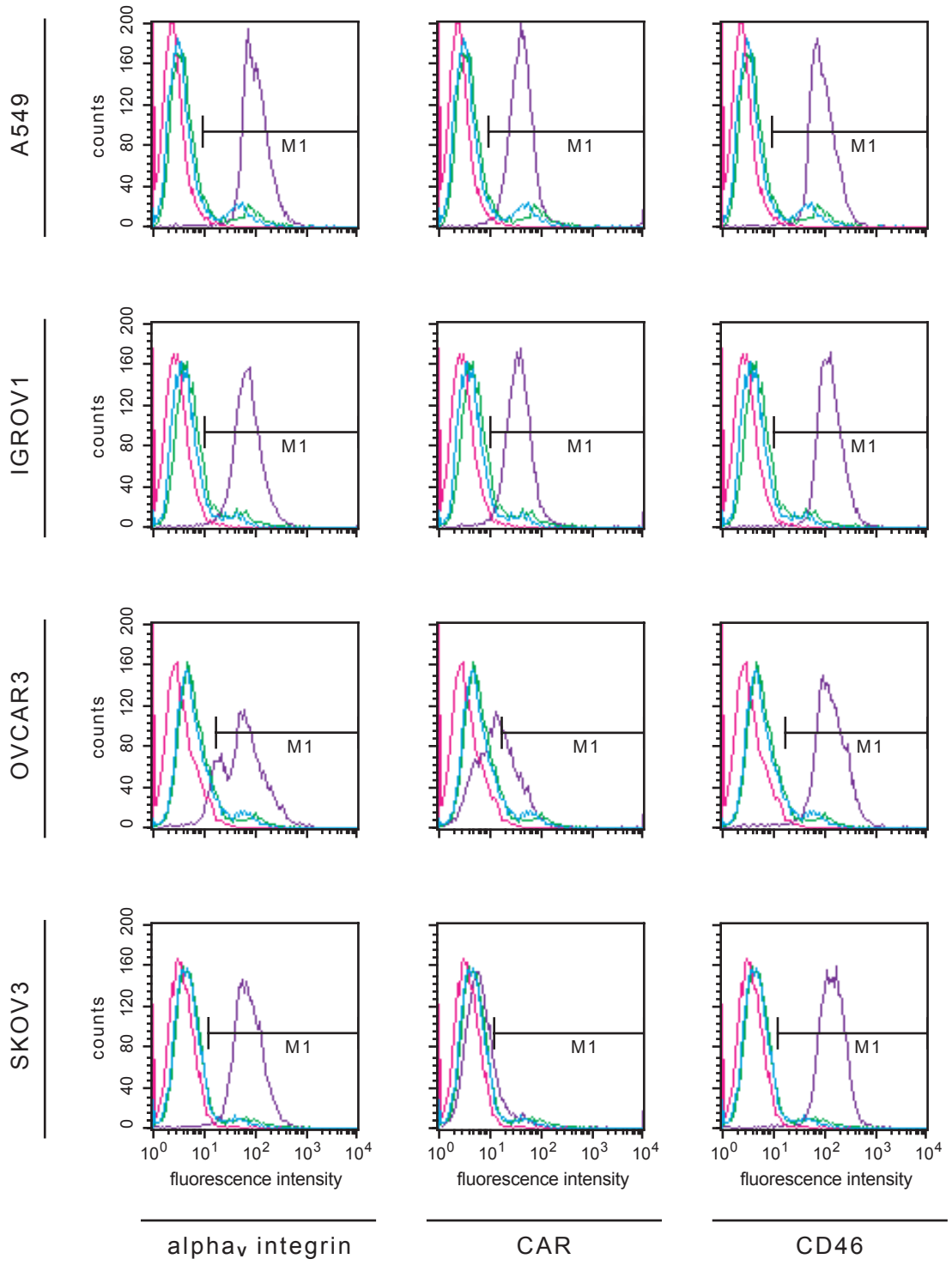


Figure 3 - 12 Adenovirus receptor expression profiles of investigated cell lines

Relative expression of the main adenovirus uptake receptors was analysed by flow cytometry (section 2.2.6). $5x10^5$ cells of A549, IGROV1, OVCAR3 and SKOV3 were stained with antibodies specific for the integrin α_v subunit, CAR, CD46 or an unspecific isotype control. A polyclonal FITC-labelled secondary antibody recognising murine IgG antibodies was used for detection of bound primary antibodies. $2x10^4$ cells were analysed per antibody / cell line combination. Histograms depict the number of detected cells per intensity of fluorescence equalling the amount of receptor expression (pink: unstained cells, green: cells incubated with unspecific isotype, blue: cells incubated with secondary antibody only, purple: cells stained with receptor specific antibodies). Cells demonstrating fluorescence above background were gated in region M1. Data representative of three independent experiments are shown.

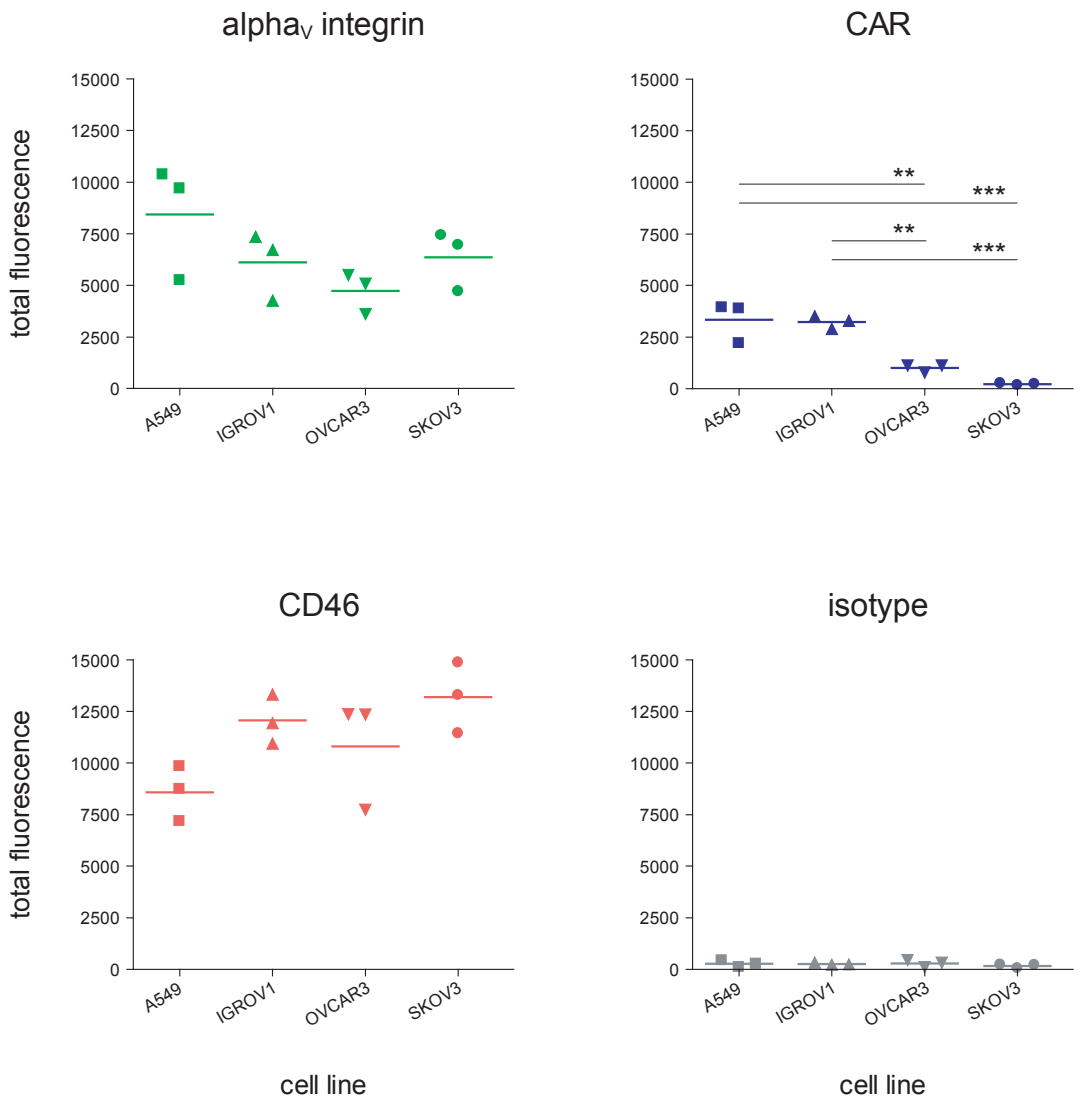


Figure 3 - 13 Levels of adenovirus receptor expression of investigated cell lines

In order to take into account the number of receptor-positive cells as well as the expression levels of receptors, flow cytometry data was analysed by multiplying the percentage of positive cells with the geometric mean of their fluorescence intensity as shown in Figure 3-12 (compare section 2.2.6). Graphs show the total fluorescence (% positive gated cells (M1) x GeoMean fluorescence) of A549, IGROV1, OVCAR3 and SKOV3 cells for alpha$_V$ integrin, CAR, CD46 and isotype control antibody. Points represent measurements from three independent experiments with the line indicating their mean. For statistical analysis one-way ANOVA with Tukey post-tests to compare all pairs of datasets was performed (*** = $p < 0.001$, ** = $p < 0.01$).

3.3.2 Quantification of adenovirus uptake into cells

The second important factor affecting virus activity, apart from the availability of uptake receptors, is the efficiency of virus internalisation. To this end, experiments to determine the amount of virus particle uptake into the cells were designed. This would help to understand whether the amount of internalised virus was correlated to the level of receptor expression on the cell surface and whether oncolytic activity was directly related to adenovirus uptake.

3.3.2.1 Development of probe and primers for real time Q-PCR

As all members of the Adenoviridae family carry a double stranded DNA genome, they can be directly detected and quantified using real time Q-PCR. To this end, probes and primers to detect all three serotypes were designed. Initially, a consensus probe and primer set, which would detect all three serotypes, was investigated. These sequences were developed for quantification of adenovirus infection and virus load in clinical samples using a TaqMan® real time Q-PCR strategy targeting a conserved region in the hexon sequence of the adenovirus genome (Heim *et al.*, 2003). Experiments employing genomic DNA, extracted from cancer cell line samples spiked with known amounts of virus, revealed that this system was not sensitive enough for detection of Ad3 and Ad11 (data not shown). Therefore, in order to optimise performance, the primer sequences were altered to exactly match the individual sequences of the different serotypes. The probe sequence remained unchanged and a universal probe was used for detection of all three serotypes (compare section 2.2.7).

Efficiency of the Q-PCR reactions with the three serotype-specific primer sets was verified by assaying serial logarithmic dilutions of DNA extracted from cancer cell samples spiked with known amounts of adenovirus, creating a standard curve (Figure 3-14). The coefficients of determination (R^2; 1.0, 1.0 and 0.999 for Ad3, Ad5 and Ad11, respectively) show that the calculated regression lines approximate the real data points sufficiently, indicating that samples containing virus DNA in a range between 10^4 and 10^8 could be quantified by this method. The efficiencies of the amplification reaction were calculated from the slopes of the determined regression lines and are below 100% for all three serotypes. While this illustrates that the

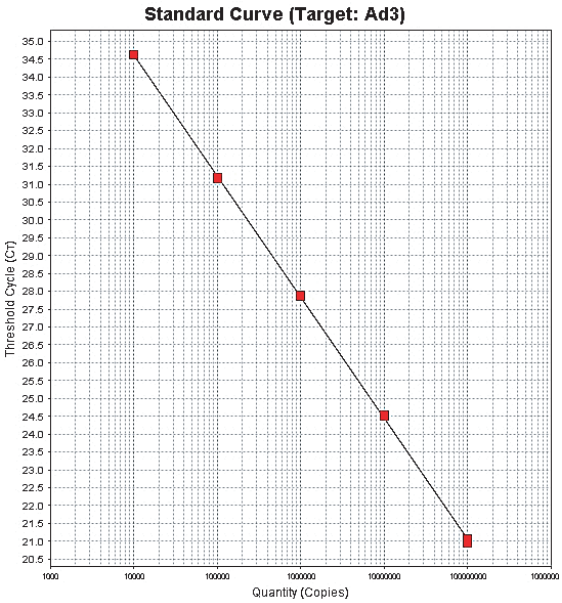
amount of DNA amplified in each cycle is less than the expected double, this is not critical in this context, as long as all values of samples containing unknown amounts of DNA fall within the range of the standard curve.

3.3.2.2 Measurement of virus particle uptake into cells

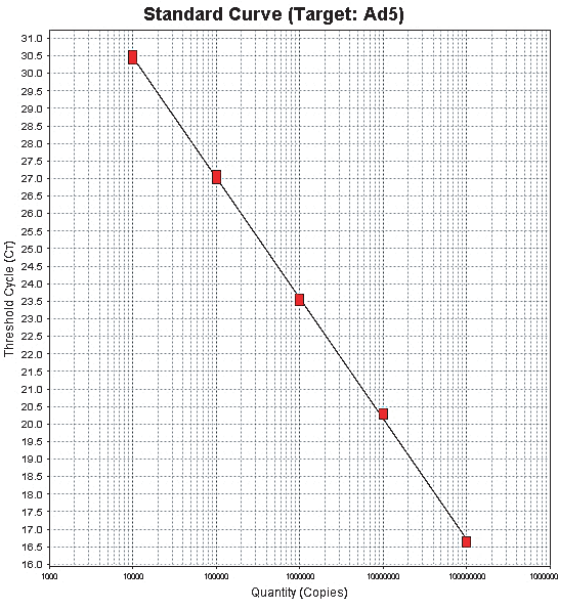
In order to measure uptake of adenovirus, cells in suspension were incubated with virus for ninety minutes, when non-cell-associated virus was eliminated by two washes with PBS. After cell lysis and DNA extraction, samples were subjected to real time Q-PCR quantifying virus genome content. Standard curves were prepared by spiking samples of cells with logarithmic serial dilutions of virus. These standards were lysed and their DNA extracted in the same way as the samples before Q-PCR was performed on samples and standards (section 2.2.7)

Figure 3-15 shows the amount of virus internalised as a fraction of the total amount incubated with the cells from three independent experiments. As cells were incubated with 100 vp/cell, the percentage of internalised virus also represents the number of vp associated with a single cell. Overall, Ad3 and Ad11 demonstrated higher uptake than Ad5. On average, between ten and forty vp were associated with each cell for Ad3 and Ad11, while it were less than ten vp for Ad5. For the group B viruses, differences in uptake between the cell lines were small. However, Ad3 tended to be less efficiently internalised on OVCAR3 cells (significantly in comparison to A549 cells ($p < 0.05$)), whereas Ad11 appeared to have increased uptake into A549 and OVCAR3 cells in comparison to the other cell lines. In contrast to Ad3 and Ad11, uptake of Ad5 was reduced. Comparing differences in uptake between cell lines revealed that A549 internalised significantly more Ad5 than the other cell lines ($p < 0.05$ vs IGROV1 and $p < 0.01$ vs OVCAR3 and SKOV3).

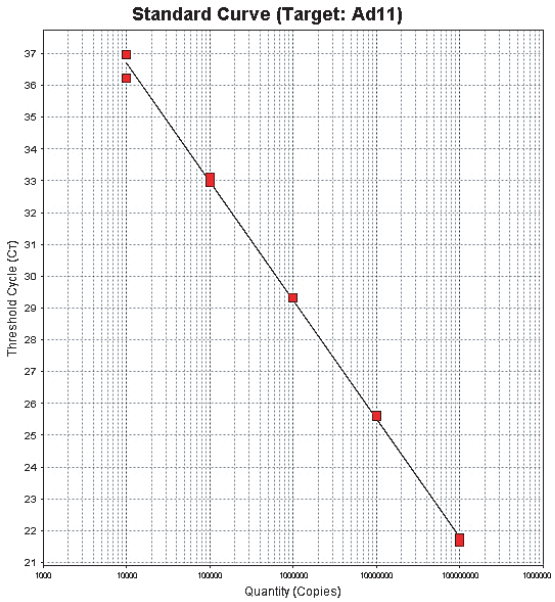
Ad3



Ad5



Ad11



	slope	Y-Intercept
Ad3	-3.386	48.16
Ad5	-3.44	44.232
Ad11	-3.72	51.576

	R^2	Eff%
Ad3	1.0	97.378
Ad5	1.0	95.298
Ad11	0.999	85.69

Figure 3 - 14 Performance of real time Q-PCR setup

Performance of TaqMan® primers individualised for Ad3, Ad5 and Ad11 was assessed by analysing logarithmic dilutions of standard samples containing known amounts of Ad3, Ad5 or Ad11 virus particles via real time Q-PCR (section 2.2.7). The graphs show the cycle number at which the fluorescence level of the individual samples crossed the threshold (C_T) for each of the serotypes. Baseline and threshold values were automatically defined by the real time Q-PCR software. The table depicts the slope, Y-Intercept and correlation coefficient of the regression line fitted on the actual C_T values (R^2) as well as the amplification efficiency (Eff%), which is calculated from the regression line slope. The R^2 values show that the calculated regression lines fit the individual data points, indicating that samples containing virus DNA in a range between 10^4 and 10^8 can be quantified with this method. The calculated efficiencies are below 100%, which illustrates that the amount of DNA amplified in each cycle is less than the expected double.

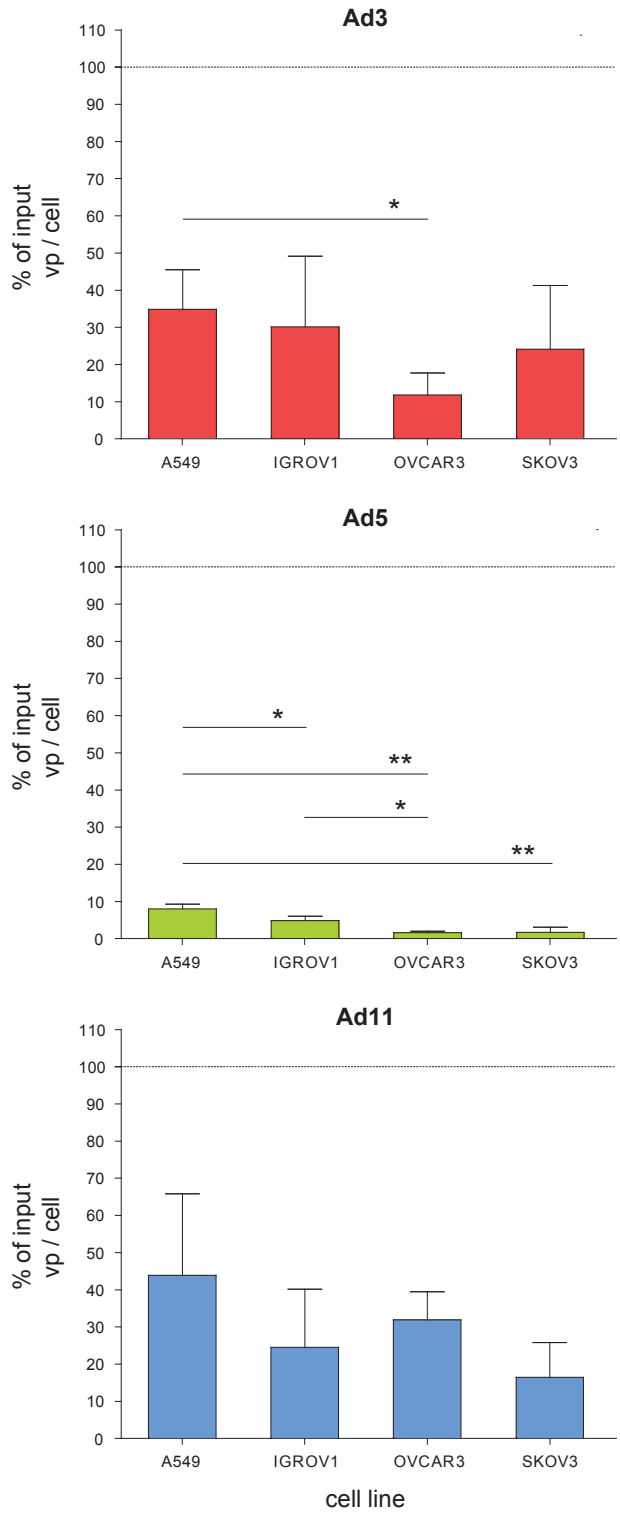


Figure 3 - 15 Uptake of Ad3, Ad5 and Ad11 into investigated cell lines

The amount of uptake of particles of Ad3, Ad5 and Ad11 into A549, IGROV1, OVCAR3 and SKOV3 cells was assessed through measurement of adenovirus genome number associated with the cellular fraction (section 2.2.7). Briefly, cells in suspension were inoculated with Ad3, Ad5 or Ad11 at a concentration of 100 vp/cell and incubated for 90 min with constant movement of reaction tubes. After two washes with PBS cells were lysed and stored at -20°C until extraction of genomic DNA and quantification of virus genome number via real time Q-PCR. The graphs show the mean percentage of vp of the input dose (means of three measurements from three independent experiments and standard deviations; statistical analysis: repeated measures one-way ANOVA with Tukey post-tests to compare all pairs of columns (** = $p < 0.01$, * = $p < 0.05$)). As the input dose was 100 vp per cell, depicted values also represent the number of vp associated with a single cell.

3.3.3 Correlation of virus particles uptake to receptor expression levels on cell lines

In order to investigate whether the differential uptake of the two virus groups and the trends observed for the different cell lines were directly influenced by the amount of uptake receptor expression on cell surfaces, the data were subjected to correlation analyses (Figure 3-16). Examining uptake receptor expression levels it was found that CD46 was the most abundantly expressed receptor of the three investigated markers on all four cell lines screened followed by the integrin α_v subunit, while CAR demonstrated the lowest staining. Virus particle internalisation determined by real time Q-PCR demonstrated overall higher uptakes rates of Ad3 and Ad11 in comparison to Ad5. Hence, there appeared to be a link between receptor expression levels and amount of particle internalisation. Greater CD46 expression resulted in higher uptake of the CD46 exploiting group B viruses, whilst lower CAR expression appeared to be a limiting factor for Ad5 internalisation.

Detailed investigation by comparing the receptor levels of the individual cell lines to the extent of uptake revealed that the uptake pattern of Ad5 and the expression levels of its attachment and uptake receptors, CAR and integrin α_v, followed a positive correlation. A549 cells which expressed the highest levels of integrin α_v and CAR also showed the highest virus load in the uptake experiments. While IGROV1 expressed levels of CAR similar to A549 cells, the slightly lower level of internalised virus might be attributable to the decreased expression of integrin α_v. Both OVCAR3 and SKOV3 had very low levels of CAR expression, presumably hampering virus attachment to those cells and significantly limiting virus uptake.

As described above, CD46 was strongly expressed on all investigated cell lines, which indeed appeared to be associated with increased uptake of the group B adenoviruses Ad3 and Ad11 in comparison to Ad5. However, the number of internalised virus particles did not correlate to receptor expression for the individual cell lines. While highest uptake levels for Ad3 and Ad11 could be observed on A549 cells, these expressed the lowest amount of CD46 on their surface. While further results for Ad3 were variable internalisation of Ad11 appeared to follow a negative

correlation. Highest uptake was observed on A549 cells, which expressed the lowest levels of CD46, whereas uptake on SKOV3, which expressed the highest levels of CD46, was lower than for any other cell line.

These observations might be founded in a lack of knowledge regarding receptors involved in group B adenovirus uptake. The complement receptor CD46 has initially been implicated as a common receptor for group B adenoviruses (Gaggar *et al.*, 2003). While it has been proven that it constitutes one of the main entry pathways for serotype 11 (Segerman *et al.*, 2003) and has also been advocated as the uptake receptor for Ad3 (Sirena *et al.*, 2004), this has subsequently been challenged by other groups. Heparan sulfate proteoglycans (HSPGs), CD80 and CD86 in addition to the, until recently, unknown receptor X, which has now been identified as Desmoglein 2 (Wang *et al.*, 2011), have been proposed as entry pathways for the two group B adenoviruses (Tuve *et al.*, 2006; Tuve *et al.*, 2008; Hall *et al.*, 2009). In addition, the RGD motif in the adenovirus penton base protein, which has been found to mediate internalisation of Ad5 through attachment to integrins (Wickham *et al.*, 1993), is conserved throughout adenovirus groups, with the exception of those from group F, suggesting a putative role in the uptake process of group B adenoviruses (Arnberg, 2009). Interestingly, it has recently been demonstrated that integrin $\alpha_v\beta_5$ alone can mediate Ad5 uptake, without the need for prior virion attachment to CAR (Lyle and McCormick, 2010), challenging a longstanding consensus and suggesting this pathway could also be available for group B viruses. However, a correlation between integrin α_v expression and Ad3 or Ad11 uptake was not found in our studies. In addition, the recent identification of above mentioned group B Ad receptor X as Desmoglein 2 (Wang *et al.*, 2011), highlights the current insufficiency in knowledge about Ad uptake receptors and employed pathways. Similarly, the emergence of studies demonstrating that Ad5 uptake into cells can be mediated through HSPGs in the presence of adaptor proteins like Factor IX or X (Jonsson *et al.*, 2009), emphasises discrepancies between *in vitro* and, indeed, *in vivo* animal studies and clinical settings.

Consequently, as it appears that not all cell receptors participating in adenovirus attachment and internalisation are currently known, correlating receptor expression levels to the amount of

adenovirus uptake remains difficult. Accordingly, receptor expression was not compared to oncolytic activity of the different viruses. Investigation of the relationship between oncolytic activity and amount of virus uptake, a measure independent from knowledge of all uptake receptors, thus avoiding aforementioned issues, was thought to be a better way to elucidate the reason behind the differential potency of Ads observed in *in vitro* settings.

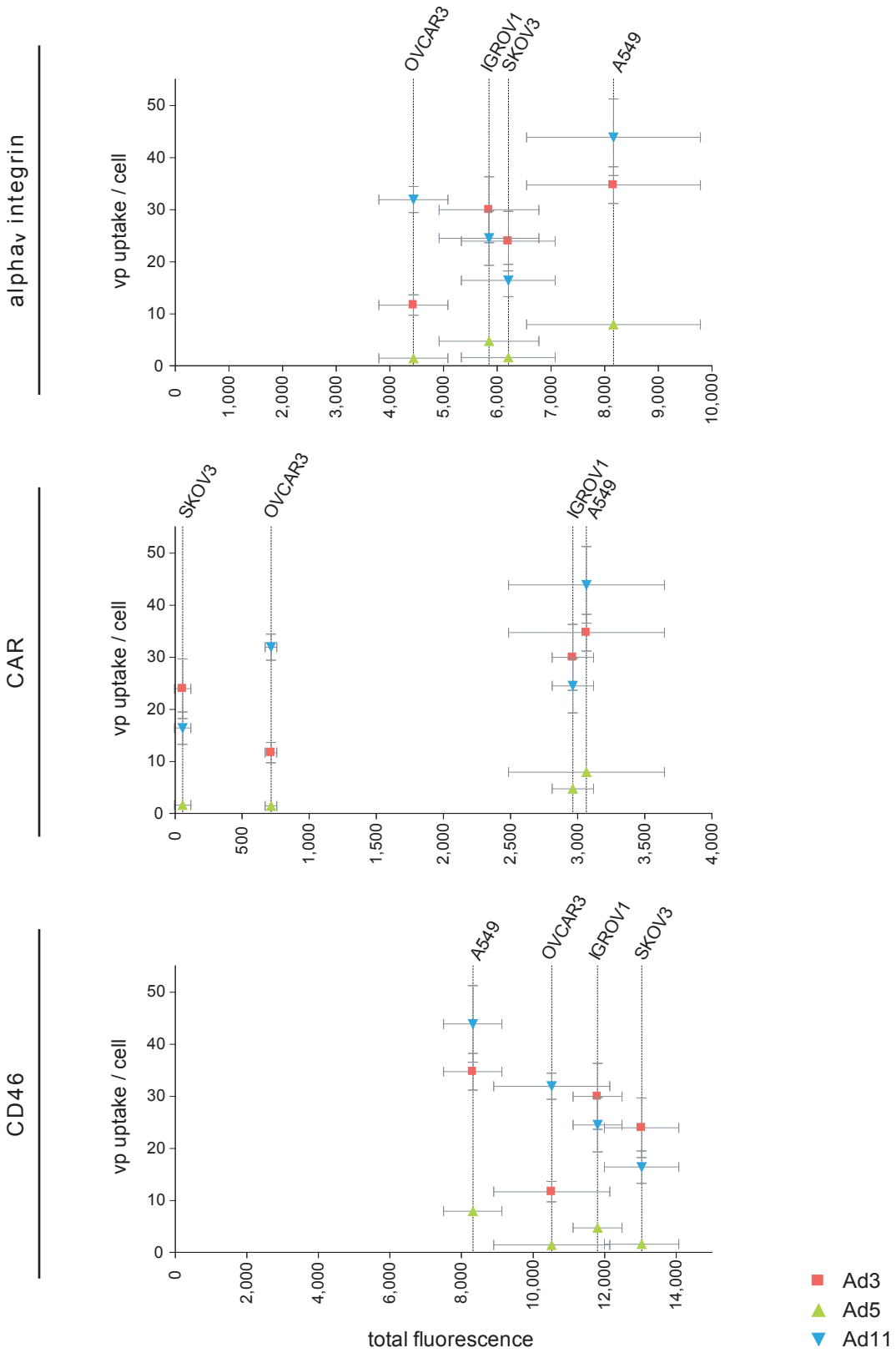


Figure 3 - 16 Correlation of virus uptake to receptor expression

The graphs show the amount of virus particles of Ad3, Ad5 and Ad11 internalised on the investigated cell lines (A549, IGROV1, OVCAR3 and SKOV3; Figure 3-15) plotted against the receptor expression levels of these cell lines (Figure 3-13). Each graph represents one of the receptors investigated (α_v integrin, CAR and CD46; error bars: standard error of the mean). While the charts for α_v integrin and CAR are predominantly relevant for uptake of Ad5 (green), the bottom diagram for CD46 applies to Ad3 (red) and Ad11 (blue) uptake.

3.3.4 Correlation of virus particle uptake to IC_{50} values

In order to eliminate the uncertainties regarding adenovirus uptake receptors discussed in section 3.3.3, numbers of internalised virus particles (section 3.3.2.2) were compared to IC_{50} values (section 3.2.2.2) (Figure 3-17). This would help to clarify whether the diverse oncolytic activity in the different cell lines solely originated from the amount of virus particles entering the cells, or whether other cell line-specific properties played a role in determining the success of viral killing. High IC_{50} values, corresponding to a greater amount of virus required to achieve an oncolytic effect, would be expected where low levels of virus were internalised by cells and vice versa.

Examining the correlation for Ad3 and the three cell lines SKOV3, IGROV1 and A549, it appeared that a higher IC_{50} corresponded to uptake of fewer particles. This trend was not supported by the data for OVCAR3 cells, which were most easily killed by this serotype despite low virus particle uptake. Similarly, Ad5 was a potent oncolytic agent on all cell lines investigated, apart from SKOV3 cells, even in the presence of generally low virus uptake (see section 3.3.2.2). These data suggest that Ad5 is intrinsically better suited to mediate cell lysis than Ad3 and Ad11 except in SKOV3 cells. SKOV3 seem to harbour an inherent resistance to Ad5, which relates not to the entry of the virus or its replication but the step of cell lysis (as shown in section 3.2.2.1). Ad11, with uptake levels comparable to those of Ad3, exhibited the strongest oncolytic activity on OVCAR3 and A549 cells, which correlated with highest levels of virus uptake. In contrast, IGROV1 cells were most resistant to Ad11-mediated lysis, despite higher virus uptake than SKOV3 cells, which were more easily killed by Ad11.

Overall, it appeared that while cells internalising the highest amount of virus particles demonstrated the highest susceptibility to adenovirus-mediated lysis, some cells carried an intrinsic resistance to adenovirus-mediated lysis, which furthermore appeared to be serotype-specific.

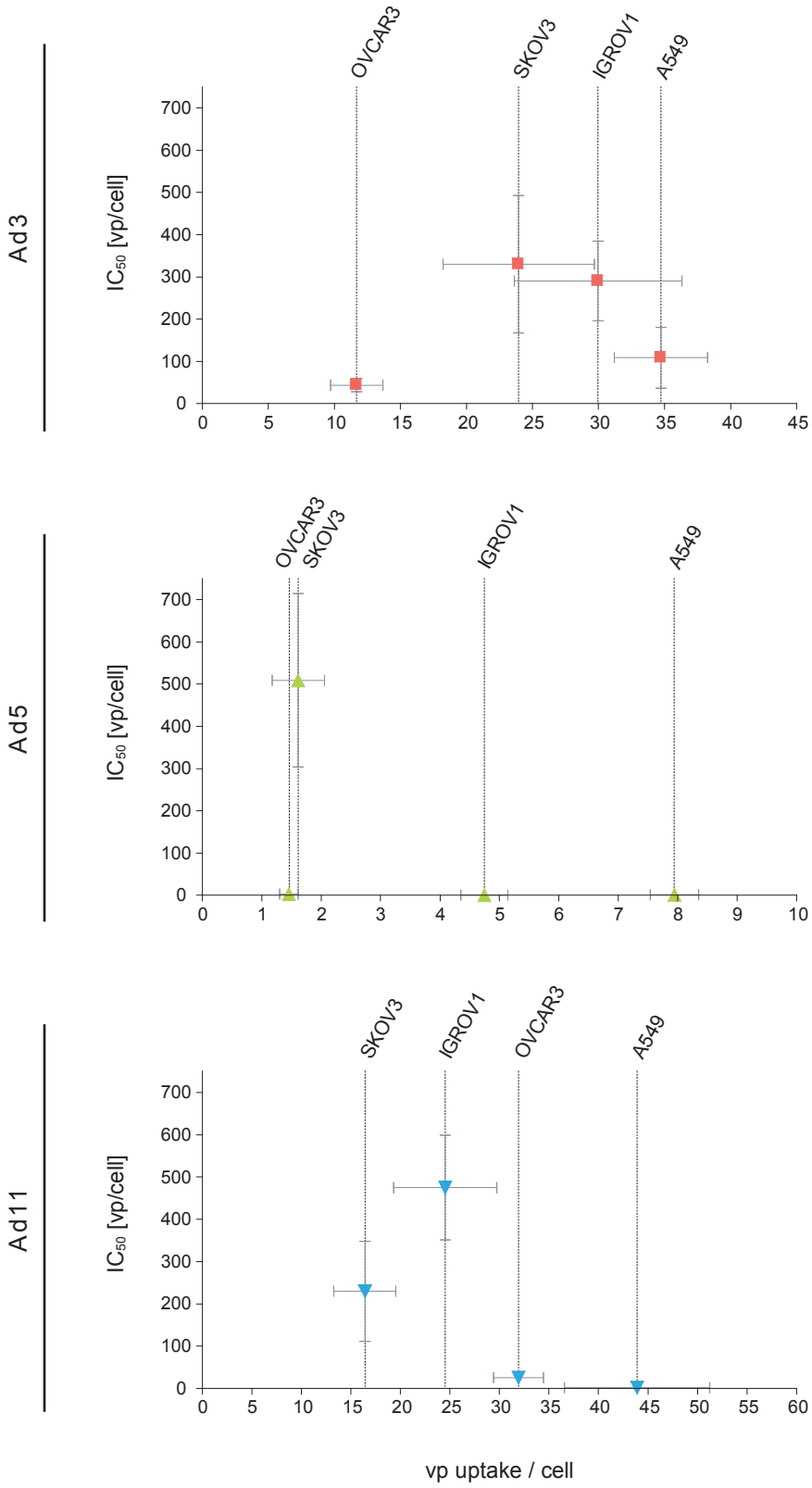


Figure 3 - 17 Correlation of IC_{50} values (oncolytic activity) to virus uptake

The graphs show the IC_{50} values of Ad3, Ad5 and Ad11 on the investigated cell lines (A549, IGROV1, OVCAR3 and SKOV3; Figures 3-7, 3-8) plotted against the amount of virus particles of the different serotypes internalised by these cell lines (Figure 3-15). Each graph represents one of the investigated adenovirus serotypes (Ad3, Ad5 and Ad11; error bars: standard error of the mean).

3.4 Conclusion

Data from this chapter demonstrated that none of the investigated adenovirus serotypes (Ad3, Ad5 and Ad11) had overall greater oncolytic activity on the investigated tumour cell lines. Instead, investigation of the relationships between receptor expression levels, uptake of adenovirus particles and oncolytic activity highlighted the complexity of the interplay between virus and cells. While receptor expression and particularly virus uptake data from section 3.3 would have suggested low oncolytic potency of Ad5 in comparison to the group B adenoviruses Ad3 and Ad11, similar to what had been proposed in the literature (Hermiston, 2006), this was not observed in cell kill assays (section 3.2). Overall, Ad5 appeared to be better suited for efficient oncolysis in three of the four investigated cell lines than Ad3 or Ad11, despite low internalisation of this serotype. Notably, however, some cell lines carried an intrinsic resistance to adenovirus-mediated lysis, which appeared to be serotype-specific. Ad3 on IGROV1 and SKOV3, Ad5 on SKOV3 and Ad11 on IGROV1 cells were unable to mediate efficient cell kill despite virus uptake comparable to or even higher than other, more easily killed cells (OVCAR3 for Ad3 and Ad5, SKOV3 for Ad11) (section 3.3.4). Hence, it appears that cellular characteristics other than uptake receptor expression or even virus uptake levels can be the dominant factors determining virus activity and consequently susceptibility to oncolysis by a specific serotype.

Recent studies are addressing the role of cellular proteins in adenovirus replication and lytic activity and there is increasing evidence that these are major factors in the determination of post-entry adenovirus fate. For instance, the carcinoembryonic antigen–related cell adhesion molecule 6 (CEACAM6), whose roles in affecting cell polarity, differentiation and tumour invasion have implicated it as a factor of tumourigenesis, has been shown to inhibit adenovirus trafficking to the nucleus, ultimately lowering oncolytic activity (Wang *et al.*, 2009). Two main implications of this study are that CEACAM6 expression could be used as a biomarker to identify non-responders to adenovirus oncolytic therapy, but also that interference with CEACAM6 expression in cancer cells could improve anti-cancer activity. Importantly, a second study focused on the cyclin dependent kinase inhibitor 1 (p21), a protein controlling cell-cycle

progression from G_1- to S-phase under the control of p53. Flak and colleagues could demonstrate that p21 expression is a marker for adenovirus activity and cells expressing no or low levels of the protein showed significantly lower expression of E1A, the first adenovirus protein to be expressed after infection, and reduced progeny virus production (Flak *et al.*, 2010).

These cellular factors affecting susceptibility to oncolysis, may be determined by the cancer cell stage, i.e. how far malignant transformation has progressed (Shashkova *et al.*, 2009). Shashkova and colleagues demonstrated variable cytotoxicity of replication-competent adenovirus serotypes on prostate cancer cell lines. It had previously been shown that these cell lines might represent differently advanced cancers, as suggested by cell-surface molecule analysis (Liu, 2000). It would be expected that more advanced cancers would accumulate mutations affecting surface receptor expression levels, accessibility of intracellular trafficking pathways, control of the cellular replication cycle, metabolic rate or replication frequency. All of these processes are required for adenovirus replication, thus their alteration could increase or decrease oncolytic activity. In a similar manner, different lengths of 'evolution' and artificial selection for cells adapted to the *in vitro* environment, for instance, cells suited to adherence to plastic culture bottles and those responding to bovine serum supplemented tissue culture media, might further diversify cellular properties that influence virus replication and oncolysis.

However, adenovirus serotype-specific properties may also play a role. For example, Ad5 expresses the Adenovirus Death Protein (ADP) (Tollefson *et al.*, 1996), which is thought to aid in cell lysis after progeny virus production and accelerate the oncolytic effect. The expression of this protein or a variant with similar function has not yet been shown for Ad11 (Lichtenstein *et al.*, 2004). Another important difference between serotypes, which might affect oncolytic activity, has been found regarding their intracellular trafficking properties. While group C adenoviruses appear to rapidly travel to the nuclear envelope upon internalisation, group B viruses accumulate in lysosomes, which is thought to be dependent on properties of the different virus capsids (Leopold and Crystal, 2007). One study, which compared intracellular trafficking of Ad5 and the group B adenovirus Ad7, found that Ad5 capsids co-localise with the nuclear envelope one hour after inoculation, while group B viruses were located in the

cytoplasm at this time-point and slowly accumulated at a nuclear location over a duration of eight hours (Miyazawa *et al*., 1999). It was proposed that this effect is due to pH-dependency of the ability of the virus capsid to lyse the endosomal lipid bilayer. Group B adenoviruses require a lower pH than those in group C to achieve release from the endosomal compartment, which is only encountered in late endosomes / lysosomes, therefore delaying endosomal escape and virus trafficking to the nucleus (Leopold and Crystal, 2007). These serotype-specific differences, combined with the individual mutations accumulated by the tumour cell lines, might amalgamate to constitute the basis for the observed diversities in oncolytic activity in these *in vitro* studies.

In a clinical setting, tumours, including ovarian tumours, are highly diverse neoplasms and characteristics differ not only between patients, but also within tumour areas of individual patients. They might show distinct uptake receptor expression profiles and, as discussed above, contain a range of diverse mutations. These might affect the permissiveness of post-internalisation steps, such as intracellular trafficking, nuclear uptake and subversion of the cellular replication machinery, which is likely to have an extensive impact on the oncolytic activity of a particular adenovirus serotype. The results presented in this thesis indicate that this can already be observed *in vitro*, as for instance, the studies described in this chapter found that IGROV1 and SKOV3 cells demonstrate unique resistance to Ad11- and Ad5-mediated killing, respectively, uncorrelated to virus internalisation. In this context, a recent study demonstrating the dispensability of CAR expression for Ad5 uptake found that T47D cells, despite expressing both CAR and integrins, were highly resistant to Ad5 infection (Lyle and McCormick, 2010).

In order to better understand why some cells show resistance to adenovirus-mediated lysis it seems necessary to identify more of the proteins, both viral and cellular, that play important roles in the adenovirus infection cycle. Manipulation of these by engineering better recombinant adenoviruses and / or by virotherapy concomitant drug treatment of tumours could lead to greatly increased oncolytic efficacy. If protein target selectivity is achieved, cancer selectivity should be maintained, as non-transformed cells have redundancy in many of the pathways, which adenoviruses need to disturb to allow replication and cell lysis.

In summary, it appears that there are numerous factors determined by both cellular and viral properties, which influence the oncolytic activity of different adenovirus serotypes on different cell lines. Therefore, classification of serotypes according to their oncolytic potency, as found *in vitro,* in order to help improve performance of oncolytic virotherapy in the clinic, is difficult. The large diversity appears to call for a patient-tailored assessment to determine the susceptibility of the respective tumour to oncolysis by a certain adenovirus serotype. Hence it appears, that the use of virotherapy in humans may be yet another area where therapy could and should be personalised to the patient to fully optimise patient responses.

4 The inflammatory response towards Ad3, Ad5 and Ad11

4.1 Introduction

One of the major constraints to successful application of adenovirus-based therapies in the peritoneal cavity has been the interaction of the treatment with the immune system. A phase II/III clinical trial of i.p. gene therapy with an Ad5-based vector had to be halted at interim analysis due to complications in the treatment group. Side-effects observed included bowel adhesions, perforation and obstruction and, while some were due to i.p. catheter placement, were mainly caused by an inflammatory reaction against the virus (Stephen Chang – unpublished personal communication). Furthermore, transduction of cancer cells was found to be poor and much of the treatment dose was detected in peritoneal macrophages (Zeimet and Marth, 2003).

The central role of macrophages as mediators of the innate inflammatory response against adenovirus has, indeed, been shown in different animal models. In C57BL/6 mice, intravenous injection of a high dose of a non-replicating Ad5-derived vector prompted a strong inflammatory response in the first 24 hours after application, characterised by expression of cytokines, such as IL-6 and IL-12 (Zhang *et al.*, 2001). Further investigation in *ex vivo* cultures of isolated spleen cells revealed that dendritic cells (DCs) and macrophages, but not lymphocytes, produced IL-6 and IL-12. Furthermore, *in vivo*, elimination of DCs and macrophages through administration of Cl_2MBP-liposomes markedly decreased IL-6 and IL-12 levels in serum. These results demonstrated that DCs and macrophages have a pivotal function in the immediate inflammatory response both *ex vivo* and *in vivo* (Zhang *et al.*, 2001). Interestingly, a second study investigating the *in vivo* cytokine response through liver mRNA measurements one hour after i.v. administration of a non-replicating Ad5-based vector demonstrated similar levels of cytokine expression between Kupffer cell- (KC, resident liver macrophage) depleted animals and non-depleted animals (Zaiss *et al.*, 2002). These observations, divergent from results by Zhang *et al.*, might be due to the use of gadolinium chloride ($GdCl_3$) instead of Cl_2MBP-liposomes for KC depletion, possibly resulting in differing cell type depletion patterns. Furthermore, macrophages might be responsible for more prolonged expression of cytokines, which was not addressed in the study performed by Zaiss *et al*.

Notably, a study in male rhesus macaques (Macaca mulatta) demonstrated that intraportal administration of Ad5-based vectors stimulated an immediate reaction which was characterised by increased serum IL-6 and IL-12 levels (Schnell *et al.*, 2001), similar to what has been described in murine models. Analysis of splenocytes for populations of transduced cells indicated strongest transgene expression in monocytes / macrophages. While the authors point out that there are considerable differences in the extent of the immune response towards adenovirus between species, it would appear that the immediate response to Ad5 is similar, characterised by inflammatory cytokine expression through macrophages.

As this project sought to advance oncolytic therapy for ovarian cancer, which might be most successful using direct i.p. administration, experiments investigating the inflammatory response to adenovirus focused on the peritoneal cavity. Previous studies demonstrated that i.p. application of Ad5 can have deleterious long-term effects to peritoneal homeostasis. Significant long-term inflammatory reactions in the form of adhesion formation were observed in mice treated with unmodified Ad5 (Morrison *et al.*, 2008; Morrison *et al.*, 2009) similar to the observations that led to the suspension of the clinical trial described above. Importantly, these *in vivo* experiments were performed in ovarian tumour xenograft models in athymic nude mice, which are not able to develop an adaptive immune response. Therefore, adhesion formation in these mice was likely to be caused by activation of the innate immune system through cellular responses by macrophages and DCs.

Inflammatory signalling against Ad11 was similar to that seen with Ad5, following i.v. injection into mice (Stone *et al.*, 2007). However, it remains unclear if this response would be altered after i.p. application due to the different physiological setting and primary target cells. Furthermore, preliminary observations from *in vivo* experiments in our group had suggested that i.p. Ad11 inoculation caused less toxicity in the form of peritoneal inflammation than Ad5 inoculation (Dr Nicola Green, unpublished data). Hence, the studies described in this chapter sought to investigate possible advantages to the use of alternative adenovirus serotypes, such as Ad3 or Ad11, in comparison to Ad5 in terms of their inflammatory stimulation in the peritoneal cavity.

4.2 Cytokine responses of ex vivo murine macrophages towards adenovirus

Monocytes and macrophages constitute the most abundant cell population in human peritoneal fluid (Kubicka *et al.*, 1996) and they appear to be pivotal in the recruitment of neutrophils to sites of inflammation through cytokine signalling (Cahill and Redmond, 2008). While it has been reported that mesothelial cells, which are the main functional constituent of the peritoneal lining, are equally capable of cytokine production and concomitantly influencing inflammatory responses (Mutsaers, 2002), selective depletion of peritoneal F4-80 cells (a marker for murine macrophages (Austyn and Gordon, 1981)) lead to markedly reduced CXC chemokine production and prevented neutrophil influx in an experimental peritonitis model (Cailhier *et al.*, 2005). Furthermore, it has been shown that macrophages play a direct role in repair of the peritoneal surface after surgical injury (Haney, 2000).

These results suggest a central role for macrophages in the initiation of inflammatory responses in the peritoneum. Therefore, an *ex vivo* macrophage model of adenovirus infection was chosen to assess the immediate peritoneal inflammatory response towards different adenovirus serotypes *in vitro*. Murine macrophages were obtained from BALB/c mice after induction of sterile peritonitis through injection of polyacrylamide beads and harvest of cells after four days, as previously described (Cash *et al.*, 2008), and kindly provided by Professor David Greaves, Dunn School of Pathology, University of Oxford. After incubation of cells in tissue culture plates and several wash steps to remove platelets and leukocytes adherent macrophages were treated with virus and supernatants collected during the following 24 hours (section 2.3.1).

4.2.1 Selection of markers to assess inflammatory signalling

Initial experiments were designed to investigate the cytokine response of *ex vivo* murine macrophages towards adenovirus over a 24 hour time-course. A bead-based multiplex system (Bio-Plex®), which allows simultaneous assessment of multiple cytokines in a single sample of serum or cell supernatant (section 2.3.3), was used to determine time-points of strong cytokine

expression and select one indicative marker with a large dynamic range, which could be used in an ELISA system for future experiments. Adherent murine macrophages were treated with Ad5 (10^3 vp/cell) or vehicle (PBS) and cell supernatant collected and frozen at 2, 4, 8, 16 and 24 hours after inoculation for subsequent analysis of cytokine concentration (Figure 4-1). As separate sets of wells had been prepared for each of the time-points, concentrations represent cumulative values at each time-point. Supernatants were screened for the concentrations of nine different cytokines (IL-1β, IL-6, IL-10, IL-12, MIP-1β, MIP-2, KC, RANTES and TNF-α), which have previously been shown to be secreted after adenovirus stimulation (Muruve *et al.*, 1999; Zhang *et al.*, 2001).

Time-dependent increase or decrease of concentrations could be observed for all cytokines. Overall, 16 to 24 hours of incubation were required to accumulate cytokine quantities, which were significantly higher than levels measured 2 hours after Ad5 inoculation. Notably however, the concentrations measured varied greatly between the different cytokines. IL-1β, IL-6 and IL-12 were expressed at concentrations below 100 pg/ml. IL-10, KC and TNF-α showed slightly higher amounts of up to 400 pg/ml, while MIP-1β, MIP-2 and RANTES were detected at concentrations between 500 and 3,500 pg/ml. As it was the aim of this experiment to define inflammatory markers, which could be used to determine an inflammatory response in subsequent experiments, cytokines demonstrating a significant difference in expression between Ad5- and mock-treated cells were identified. For IL-10, IL-12, MIP-2 and TNF-α no differences in cytokine expression were found for the two treatment groups at later time-points. In contrast, IL-1β, IL-6, MIP-1β and RANTES were expressed at significantly higher levels in Ad5- than in vehicle-treated cells. Specifically, expression of MIP-1β was 3.5-fold and RANTES expression 10-fold higher in Ad5- in comparison to mock-treated wells. Based on these findings RANTES was selected as a marker of inflammatory responses for further experiments utilising bench-top-based ELISAs.

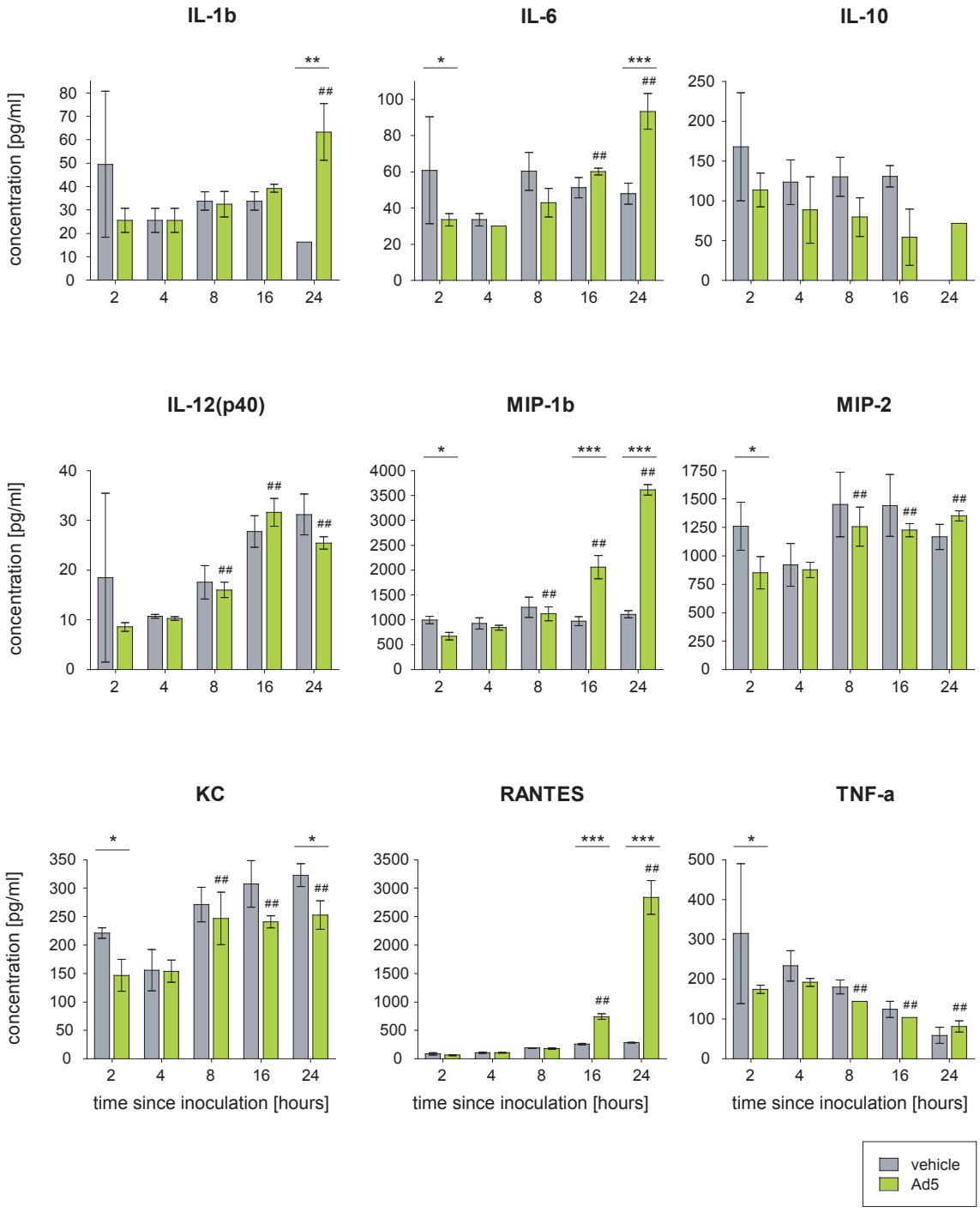


Figure 4 - 1 Time-course of cytokine expression of peritoneal murine macrophages following *ex vivo* incubation with Ad5

Elicited peritoneal macrophages from Balb/c mice were incubated *ex vivo* with Ad5 (10^3 vp/cell) or vehicle (PBS) and supernatants harvested at specified time-points (2, 4, 8, 16, 24 hours after treatment). Supernatants were stored at -80ºC until cytokine levels were analysed with a Bio-Plex® system (section 2.3.3). Bars represent mean concentration values (n=3) of accumulated cytokines until the indicated time-point and standard deviations. In order to analyse the time dependency of cytokine expression of Ad5-treated cells over the incubation period one-way ANOVA with Dunett's multiple comparison post-tests versus a control column (2 hour time-point) was performed (## = $p < 0.01$). To be able to identify time-points with significant differences between Ad5- and mock-treated cells measurements were analysed with a two-way ANOVA with Bonferroni post-tests (*** = $p < 0.001$, ** = $p < 0.01$, * = $p < 0.05$).

4.2.2 *Ex vivo* cytokine response towards different adenovirus serotypes

Previous *in vivo* experiments in our group had suggested that Ad11 caused less toxicity in the form of peritoneal inflammation after i.p. Ad11- than after Ad5-treatment (N. Green, unpublished data). Therefore, following establishment of the experimental *ex vivo* macrophage model, including identification of RANTES as a marker for macrophage-driven inflammatory signalling after adenovirus stimulation, studies to assess the inflammatory response towards Ad11 in comparison to Ad5 were performed. For these experiments murine macrophages were treated with Ad5 or Ad11 (both 10^3 vp/cell) (Figure 4-2 A). Control wells were treated with vehicle (PBS) or LPS/IFNγ (100 and 20 ng/ml, respectively), serving as a negative or positive control of macrophage activity, respectively. Supernatant was collected 2, 8, 16 or 24 hours after inoculation from separate sets of wells, therefore measured values represent cumulative amounts as described above. RANTES concentration was analysed by a commercial ELISA system (section 2.3.2).

Overall, the values measured with this method were much lower than those read with the Bio-Plex® system. As the same experimental layouts and virus preparations were used in both experiments this disparity might have been caused by the different analysis methods or differences in the murine macrophage preparation. Cells treated with a combination of LPS and IFNγ did, however, demonstrate high levels of RANTES expression (OOR = out of range), demonstrating that cells were alive and could be activated. A greater increase in RANTES expression in response to Ad5, in comparison to vehicle or Ad11 treatment, could be observed over the incubation period leading to an 8-fold increased cytokine concentration in the cell supernatant after 24 hours. Intriguingly, values measured in Ad11- did not differ from mock-treated wells at any time-point. This suggests that the immediate cytokine signalling following adenovirus stimulation is serotype-specific and that i.p. administration of Ad11-based treatments might not induce the same inflammatory responses as observed after Ad5 application.

A subsequent study employing the same experimental model included the adenovirus serotype 3 (Figure 4-2 B). Ad3, a group B adenovirus like Ad11, was used to investigate, if the results described above were common to adenoviruses of the same group or if they were Ad11 specific. The cytokine concentrations measured in this experiment were even lower than the ones observed before, which might be due to changes in *in vitro* plate layout. As fewer macrophages were available for this experiment only $2x10^5$ cells instead of $1x10^6$ cells were plated. However, analogous reduction of supernatant volume in order to compensate for the lower cell numbers was not possible. Intriguingly, despite the low values the findings regarding the differential stimulation by Ad5 and Ad11 confirmed findings from the previous experiment (Figure 4-2 A). RANTES expression at 8 and 24 hours after Ad11 was significantly lower than after Ad5 inoculation. Differences between mock- and Ad11-treated cells were not significant at any of the time-points. These observations were representative of at least three independent experiments. Interestingly, Ad3 did not show decreased cytokine signalling similar to Ad11. Measured values were not significantly different from Ad5-treated cells and higher than mock-treated cells after 4, 16 and 24 hours of incubation. This observation suggests that inflammatory properties do, indeed, differ between serotypes and are not necessarily shared by members of an adenovirus group.

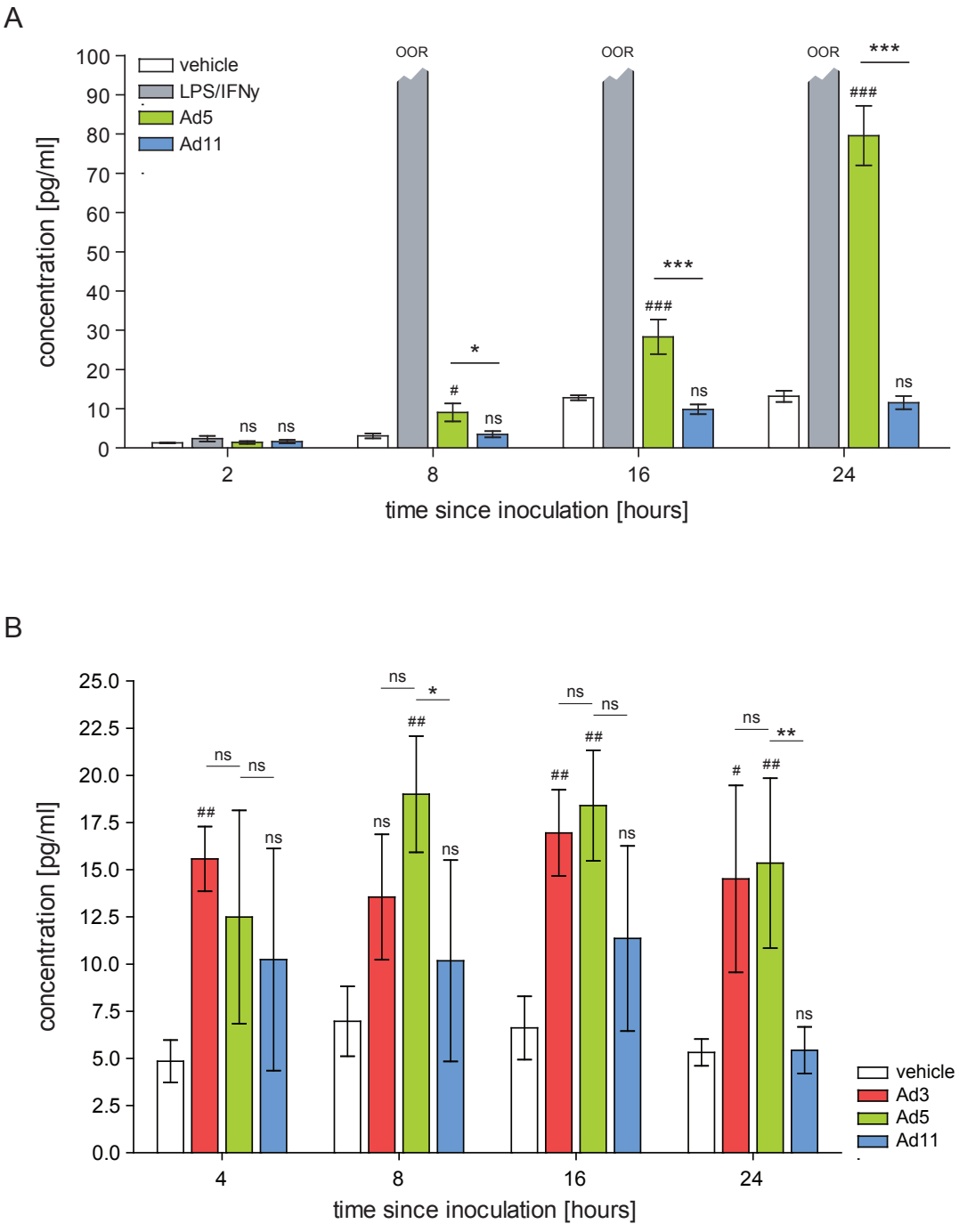


Figure 4 - 2 RANTES expression following *ex vivo* incubation of peritoneal murine macrophages with Ad3, Ad5 or Ad11

Peritoneal murine macrophages were treated with Ad5 or Ad11 (1,000 vp/cell). Vehicle (PBS) and LPS/IFNγ (100 and 20 ng/ml, respectively) served as negative and positive control, respectively (A). A subsequent experiment included the group B adenovirus Ad3 (B). Supernatants were collected at indicated time-points and the concentration of accumulated RANTES concentration measured by ELISA (section 2.3.3). The graphs show means of triplicate measurements and standard deviations; statistical analysis by repeated measures two-way ANOVA with Bonferroni post-tests (ns = not significant, *** = $p < 0.001$, ** = $p < 0.01$, * = $p < 0.05$; # symbols on top of bars represent p-values versus mock-treated cells (ns = not significant, ### = $p < 0.001$, ## = $p < 0.01$, # = $p < 0.05$); OOR = out of range).

4.3 Immune responses towards Ad5 and Ad11 in murine models of intraperitoneal administration

The encouraging results of minimal cytokine induction after Ad11, in comparison to Ad5 treatment of *ex vivo* murine macrophages, prompted the design of animal studies to further investigate this differential immune response. While macrophages are one of the dominant mediators of inflammatory reactions towards infectious agents in the peritoneal cavity, the immune response in the peritoneum is a co-ordinated response by a variety of cell types. Hence, it was important to examine if *ex vivo* results would correspond to responses *in vivo*; an environment much more closely related to the situation in a clinical setting.

Mice, unlike humans, do not express CD46, the main uptake receptor of Ad11. It was therefore not clear whether the differences between serotypes observed in the *ex vivo* experiments performed on peritoneal macrophages from BALB/c mice were due to reduced uptake of Ad11, or even the possibility that Ad11 may achieve non-receptor-mediated uptake in CD46-negative cells, trafficking to non-immune-stimulatory cellular compartments. Therefore, experiments were performed using CD46-transgenic mice, in a C57/BL6 background (Yannoutsos *et al.*, 1996) in collaboration with Dr Linda Klavinskis and Dr Veronique Bachy (King's College London), who had a colony of CD46-transgenic mice available at that time (section 2.3.4). As it was not possible to use these mice to obtain peritoneal macrophages to repeat the *ex vivo* experiments described above in a CD46-positive model, due to restrictions of the Home Office Animal Licence, it was decided to perform experiments *in vivo*. This was expected to give a more complete picture of the immune responses, as described above.

4.3.1 Short-term *in vivo* inflammatory responses to i.p. adenovirus

Previous studies investigating inflammatory signalling after intravenous injection of Ad5-based adenoviral vectors into C57BL/6 mice demonstrated a strong inflammatory response in the first 24 hours after application characterised by expression of cytokines like IL-6 and IL-12 (Zhang *et al.*, 2001). It was therefore apparent that strong reactions occurred soon after i.p. adenovirus inoculation. It was hypothesised that these initial signalling events, with their corresponding cellular activation and migration patterns, were determining detrimental long-term effects of Ad-based treatments and experiments were designed to investigate whether short-term responses might be used to predict delayed toxicity.

Studies sought to investigate two aspects of the intraperitoneal immune response. First, the activation of the inflammatory response was to be analysed through cytokine measurements in both blood and i.p. fluid samples. Second, the cellular response in terms of migration patterns was to be examined by quantification of neutrophil and macrophage numbers in the peritoneal cavity (section 2.3.4.2).

An unpublished preliminary experiment (data not shown) performed by Dr Joanne Morrison had investigated the timing and range of the inflammatory response after i.p. delivery of Ad5 in Balb/c mice over a 24 hour time-course. This study notably informed the subsequently described studies about the timing and range of the inflammatory response towards i.p. adenovirus and helped to considerably minimise the use of laboratory animals. In Dr Morrison's experiment the cellular response after Ad5 application was characterised by decreased macrophage numbers after 4 hours followed by an increase until 24 hours, when the number of macrophages counted was double that in 0 hour samples. The neutrophil count appeared to be a two phase response, starting with an initial peak in cell numbers at 8 hours, followed by a nadir at 16 hours and a second peak at 24 hours. The concentrations of 9 cytokines involved in intraperitoneal inflammatory signalling were assayed in peritoneal and serum samples, all of which showed some degree of time-dependent increase. Hence, it was decided to assess immediate inflammatory reactions 6 hours after virus injection as a distinct decrease of

macrophages, marked increase of neutrophils and peaks of cytokine expression were to be expected by this time-point, as informed by Dr Morrison's preliminary experiments (data not shown).

Accordingly, studies examining the short-term *in vivo* inflammatory response towards i.p. Ad were performed (compare section 2.3.4.2). Mice were injected i.p. with adenovirus, or vehicle as a negative control, and after 6 hours animals were sacrificed by cervical dislocation. Peritoneal cavities were rinsed with PBS and i.p. lavage fluid prepared through separation of cells through centrifugation. Blood samples were taken by cardiac bleed immediately after i.p. lavage and serum prepared through centrifugation. Serum and i.p. lavage fluid were stored frozen until analysis for cytokines with a Bio-Plex® system. Cytospins were prepared from cells after separation from i.p. lavage fluid and resuspension in PBS. Fixed cells were then subjected to immunohistochemistry for the murine macrophage marker F4/80 or the neutrophil marker NIMP with an unspecific isotype antibody as negative control.

Assessment of the immediate i.p. response to adenovirus was performed in two independent experiments. The first experiment (KCL-I) consisted of three treatment groups (Ad5, Ad11 (previously tested for absence of LPS) and vehicle (PBS) as negative control) of CD46-positive mice. The treatment dose was $5x10^{10}$ vp per mouse. An immediate reaction to virus injection could be observed for mice treated with Ad5, but not Ad11. Animals appeared slow or immobile with a hunched posture for up to 20 minutes after injection. Hence, it was decided to decrease the treatment dose to $2.5x10^{10}$ vp per mouse in the second experiment (KCL-II) to minimise animal distress and amelioration of these immediate effects of virus injection was noted. Furthermore, the second experiment included two groups of mice in the Ad11 treatment arm, which were not CD46-positive. The first group consisted of non-transgenic littermates of the CD46-positive animals and, as there were insufficient numbers of these mice, the second group consisted of C57/BL6 mice. These were included in this study, in order to investigate, if results observed with Ad11 in the first experiment were due to CD46 expression or represented immune responses specific to the *in vivo* setting, influenced by additional cell types and the unique intraperitoneal environment in comparison to the *ex vivo* experiments. For all animal

studies participating investigators were blinded to the type of treatment until after analysis of cytokine and cellular responses.

As discussed above, mice were sacrificed 6 hours after virus administration. Cytokine responses (IL-1β, IL-6, IL-10, IL-12(p40), IFNγ, MCP-1, RANTES and TNFα) of both experiments (KCL-I and KCL-II) were analysed with the Bio-Plex® system in both serum and i.p. lavage samples (Figure 4-3). Notably, there was a marked increase in cytokine expression in all animals treated with adenovirus when compared to mock-treated animals. Figure 4-3 shows concentrations of cytokines with significant changes to mock-treated animals (IL-6, MCP-1 and RANTES). Intriguingly, Ad11 did show stimulation of these cytokines to levels equal to or in some cases even significantly above Ad5, in contrast to data obtained in the *ex vivo* experiments (section 4.2). Furthermore, this effect was not restricted to the CD46-transgenic animals, but increased inflammatory signalling was also observed in the non-transgenic littermates and C57/BL6 mice. The cytokine concentrations measured in both experiments were very similar for both serum and i.p. lavage samples. A significant difference in cytokine levels between serum and i.p. samples was observed for MCP-1 and RANTES, with markedly lower concentrations in serum. This observation appears to correspond with localised production of these cytokines in the i.p. cavity, with little leakage from the original site of the inflammatory stimulus, in keeping with their roles as chemotactic cytokines. In contrast, the elevated levels of IL-6 measured in serum conform to its function as an acute phase protein in inflammation with systemic effects.

Cellular responses were investigated through analysis of numbers of neutrophils and macrophages (Figure 4-4). The microphotographs in Figure 4-4 A are representative of immunohistochemistry slides from these experiments. A significant difference in the amount of cells for both macrophages and neutrophils between virus- and mock-treated animals could be observed. More cells stained positive (red) for the vehicle- than for the virus-treated animals when labelling macrophages (F4/80), while there were fewer cells positive for the neutrophil-specific NIMP antibody. Although the unspecific isotype antibody did show some staining, possibly due to unspecific attachment of the heavy chains of the immunoglobulin to

Fc receptors on some cells, the stained cells were minimal and the pattern of staining different and easily distinguishable from true positive staining with the specific antibodies. One slide per mouse was prepared for each of the antibodies. After taking photographs of three randomly selected areas per slide, positively stained cells were counted manually. Figure 4-4 B depicts the amount of macrophages or neutrophils as a percentage of the whole cell population from both experiments (KCL-I and KCL-II). As indicated by the microphotographs, macrophage and neutrophil numbers 6 hours after treatment were significantly lower or higher in adenovirus- than in mock-treated animals, respectively. In accordance with the data from the cytokine analysis, there was no difference between Ad5- and Ad11-injected animals. Equally, non-transgenic and C57BL/6 mice demonstrated the same levels as Ad11-injected CD46-transgenic animals, suggesting that C57/BL6 animals were a suitable CD46-negative control.

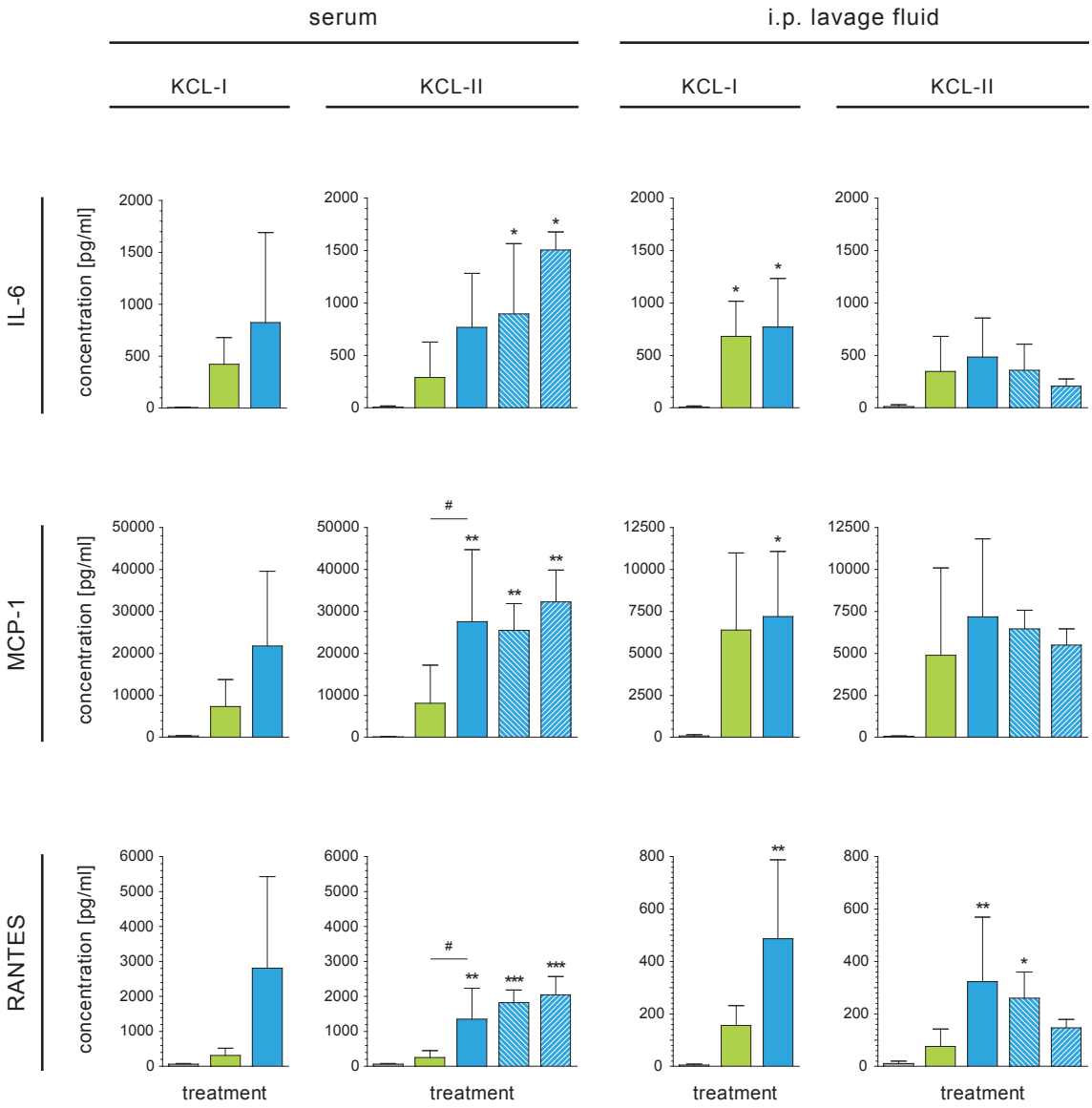


Figure 4 - 3 Short-term *in vivo* cytokine response to i.p. adenovirus

Six hours after i.p. injection of $5x10^{10}$ vp (KCL-I) or $2.5x10^{10}$ vp (KCL-II) of Ad5, Ad11 or PBS (vehicle) into CD46-transgenic (tg), non-transgenic litter-mates (ntg) or C57BL/6 mice animals were sacrificed and peritoneal cavities were rinsed with PBS and i.p. lavage fluid prepared through separation of cells through centrifugation. Blood samples were taken by cardiac bleed immediately after i.p. lavage and serum prepared through centrifugation (section 2.3.4.2). Serum and i.p. lavage fluid were stored frozen until analysis for cytokines using a Bio-Plex® system (section 2.3.3). The graphs depict the concentrations of cytokines (IL-6, MCP-1 and RANTES) in serum or i.p. lavage fluid from two independent experiments (KCL-I and KCL-II). Bars and error bars represent the mean of duplicate (KCL-I) or triplicate (KCL-II) measurements for each treated animal and standard deviations. The number of treated animals is noted in the figure legend. For statistical analysis one-way ANOVA with Bonferroni post-tests to compare pairs of treatments was performed (*** = $p < 0.001$, ** = $p < 0.01$, * = $p < 0.05$ vs vehicle; # = $p < 0.05$ Ad5 vs Ad11).

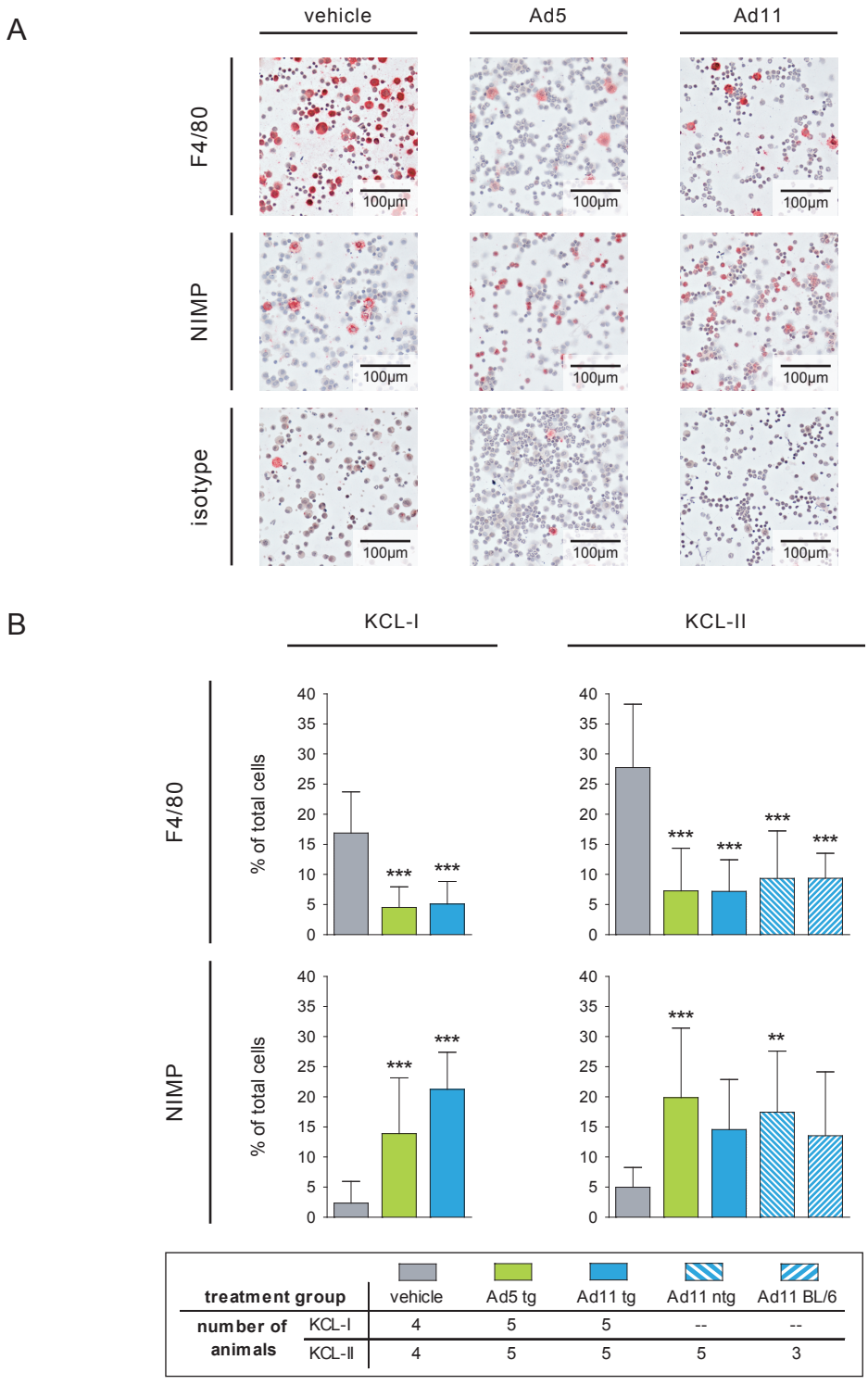


Figure 4 - 4 Short-term cellular *in vivo* response to i.p. adenovirus

Six hours after i.p. injection of $5x10^{10}$ vp (KCL-I) or $2.5x10^{10}$ vp (KCL-II) of Ad5, Ad11 or PBS (vehicle) into CD46-transgenic (tg), non-transgenic litter-mates (ntg) or C57BL/6 mice animals were sacrificed and peritoneal cavities rinsed with PBS. Cytospins were prepared from fresh cells after centrifugation and resuspension in PBS (section 2.3.4.2). Fixed cells were then stained for the murine macrophage marker F4/80 or the neutrophil marker NIMP (section 2.3.5). An isotype antibody served as a negative control. Figure A shows representative microphotographs of stained slides. Positive signal (red) indicates macrophages (F4/80), neutrophils (NIMP) or false positive staining (isotype). Figure B depicts the amount of macrophages or neutrophils as a percentage of the whole cell population from two independent experiments (KCL-I and KCL-II). Bars and error bars represent the mean of triplicate countings for each treated animal and standard deviations. The number of treated animals is noted in the figure legend. For statistical analysis one-way ANOVA with Bonferroni post-tests to compare pairs of treatments was performed (*** = $p < 0.001$, ** = $p < 0.01$).

4.3.2 Long-term *in vivo* inflammatory responses to i.p. adenovirus

The finding that Ad11 caused a significant inflammatory response, equal to Ad5 in the short-term *in vivo* experiments (section 4.3.1), raised concerns about the feasibility of using Ad11 clinically as a means of avoiding the immune responses generated by Ad5. However, the mechanisms and pathways linking the acute response to long-term inflammatory signalling and fibrotic tissue remodelling and the role of CD46 expression in that context remained unclear. Furthermore, previous unpublished data had suggested that i.p. Ad11 caused less long-term toxicity than Ad5 (Dr Nicola Green, unpublished data). It was, therefore, of interest to examine whether the similar acute inflammation caused by Ad5 and Ad11 would ultimately also lead to the same long-term toxicities previously observed with Ad5 (Morrison *et al.*, 2008).

Similar to the short-term experiments, these long-term studies sought to investigate the inflammatory response in terms of cytokine signalling as well as cellular responses. Additionally, in order to assess long-term pathologic effects, peritoneal cavities were to be examined for signs of tissue remodelling and formation of adhesions (section 4.3.2). Experiments were performed in CD46-transgenic mice (KCL-III) and in a second experiment C57/BL6 mice as non-transgenic controls (OX-I). In both studies animals were assigned to the different treatment arms randomly (by cage) and assessors blinded to treatments until after analysis of results. Previous experiments had shown, that three i.p. adenovirus administrations of $5x10^{10}$ vp per mouse with intervals of three days between injections caused long-term inflammatory sequelae and the onset of adhesion formation after 18 days (Morrison *et al.*, 2008). In order to keep pain and distress for the animals at the lowest level possible, virus doses were reduced to $1x10^{10}$ vp per mouse. Accordingly, animals were injected i.p. with $1x10^{10}$ vp of Ad5 or Ad11 per mouse or vehicle (virus storage buffer) as negative control three times with an interval of 72 hours between injections. 18 days after the first inoculation animals were sacrificed by cervical dislocation. Subsequently, peritoneal lavage and serum samples were prepared as described above (section 4.3.1) and peritoneal cavities visually examined and scored for signs of inflammation and adhesion formation (as per a pre-determined scoring system (Morrison *et al.*, 2008)).

Figure 4-5 A shows photographs from experiment OX-I representative for the appearance of peritoneal cavities of mice treated with Ad5, Ad11 or vehicle. Notably, while organs of mice treated with Ad11 were equal in appearance to vehicle-treated mice, gross changes in liver architecture (blunting of liver edges and reduced size, possibly due to liver capsule fibrosis) and matting of organs were observed in Ad5-treated animals. Furthermore, in some Ad5-treated animals the peritoneal lining appeared inflamed and red. All animals were scored for signs of inflammation as reported previously (Morrison *et al.*, 2008) (Figure 4-5 B). While five of six CD46-transgenic animals treated with Ad11 did show mild long-term inflammatory symptoms, no statistical difference was found between Ad11- and vehicle-treated animals in the experiment using CD46-transgenic as well as in the second experiment with non-transgenic C57/BL6 mice. It appears that, while CD46 expression did not have an effect in the short-term experiments (section 4.3.1), in the long-term study a slightly greater response could be observed in CD46-positive in comparison to CD46-negative mice. In contrast, Ad5 induced significantly greater long-term pathologic effects in the form of moderate to severe adhesions and profound liver toxicity in all animals of both experiments ($p < 0.001$ vs Ad11- or vehicle-treated).

Measurement of cytokine levels (IL-6, IL-10, IL-12(p40), IFNγ, MCP-1, RANTES and VEGF) of intraperitoneal lavage and serum samples, overall, demonstrated little difference between treatment groups for most cytokines (data not shown). However, analysis of peritoneal fluid from CD46-transgenic mice showed significant elevation of IL-12 and RANTES in Ad11- in comparison to vehicle-treated ($p < 0.05$) or vehicle- ($p < 0.01$) and Ad5-treated ($p < 0.05$) animals, respectively. In contrast, Ad5-treated mice expressed significantly higher levels of IFNγ and VEGF than both Ad11- or vehicle-treated animals ($p < 0.05$ or $p < 0.01$) (Figure 4-6). While the same pattern could be observed in C57BL/6 CD46-negative mice, these results did not reach significance (data not shown).

As in the short-term experiments (section 4.3.1), levels of neutrophils and macrophages in the peritoneal lavage samples of all mice were measured by staining cytospins with the mouse neutrophil marker NIMP and the macrophage marker F4/80 (Figure 4-7). No samples demonstrated cells positive for NIMP (data not shown), suggesting that there were very low levels of free neutrophils in the cavity at this time-point regardless of treatment type. Notably however, F4/80-positive macrophage levels were significantly lower in Ad5- than in vehicle- or Ad11-treated mice ($p < 0.001$). Similarly, the total amount of free cells in the cavity was significantly lower after Ad5 treatment in both CD46-transgenic ($p < 0.001$) and non-transgenic animals ($p < 0.05$).

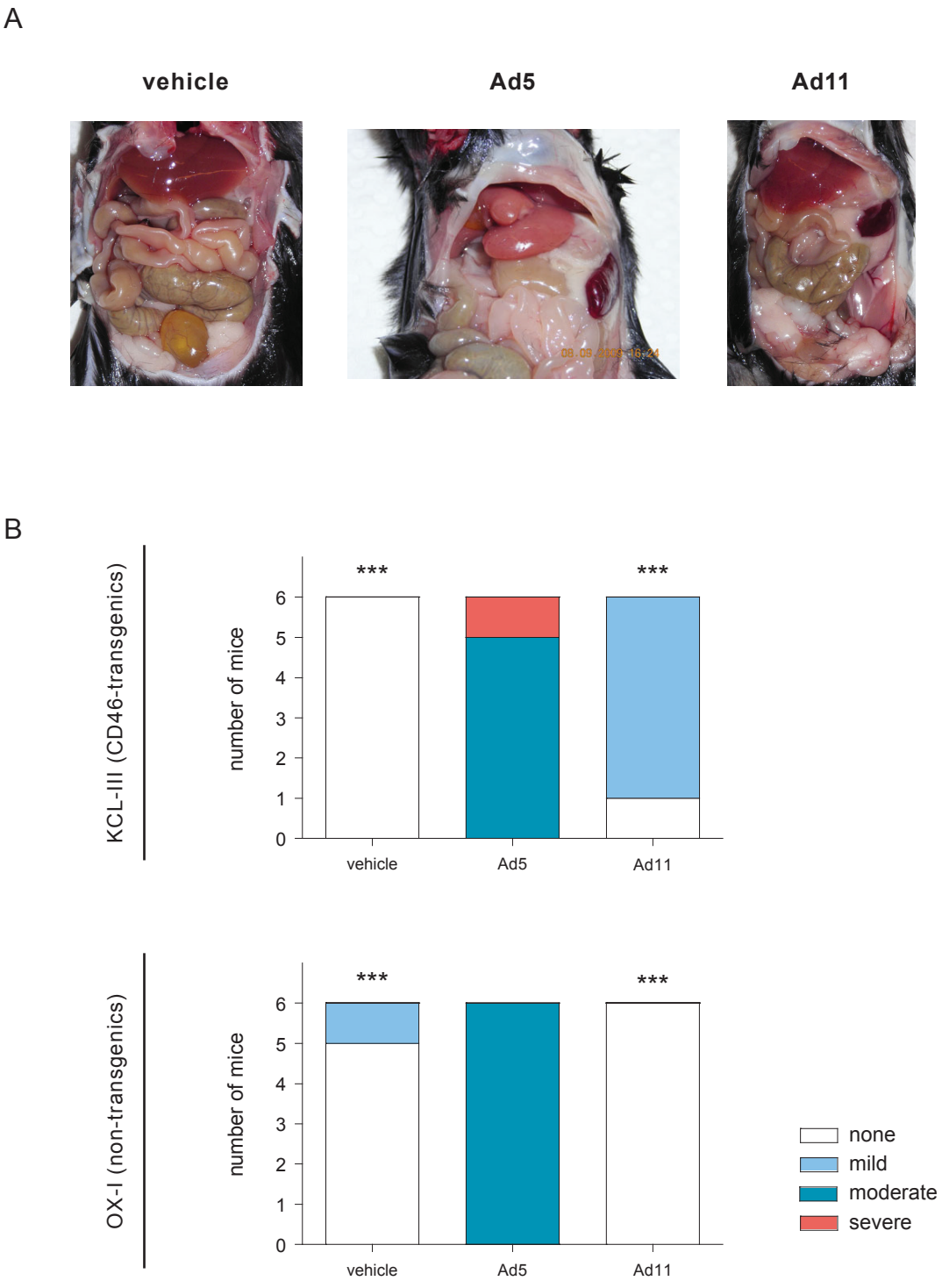


Figure 4 - 5 Long-term *in vivo* pathologic effects after i.p. adenovirus

CD46-transgenic (KCL-III) or non-transgenic C57BL/6 mice (OX-I) were injected with Ad5 or Ad11 (10^{10} vp/mouse) or virus storage buffer (vehicle) as negative control three times with an interval of 72 hours between injections. 18 days after the first injection animals were sacrificed. After preparation of samples for cytokine and cell analysis peritoneal cavities were visually examined for signs of inflammation and adhesion formation (section 2.3.4.3). Photographs show peritoneal cavities from experiment OX-I representative for the appearance after treatment with Ad5, Ad11 or vehicle (A). Animals of experiment KCL-III and OX-I were scored for signs of inflammation (none, mild, moderate or severe) as reported previously (Morrison *et al.*, 2008) (B). The graphs show the number of animals for each scoring group per treatment. For statistical analysis Chi-square tests to compare pairs of treatments were performed (*** = $p < 0.001$).

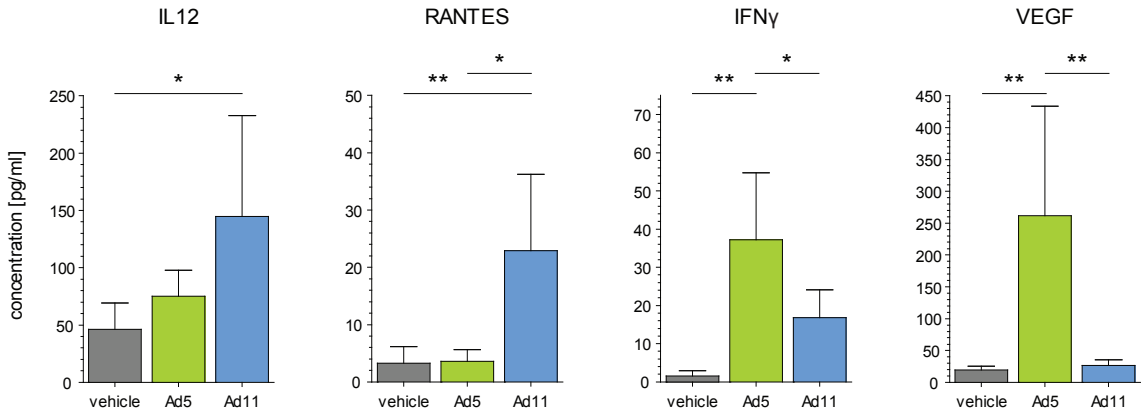


Figure 4 - 6 Long-term *in vivo* cytokine response to i.p. adenovirus

CD46-transgenic mice (KCL-III) were injected with Ad5 or Ad11 (10^{10} vp/mouse) or virus storage buffer (vehicle) as negative control three times with an interval of 72 hours between injections. 18 days after the first injection animals were sacrificed. Peritoneal cavities were rinsed with PBS and i.p. lavage fluid prepared by separation of cells through centrifugation (section 2.3.4.3) and stored frozen until analysis using a Bio-Plex® system (section 2.3.3). The graphs show the concentration of cytokines (IL-12, IFNγ, RANTES and VEGF) in i.p. lavage fluid, bars and error bars represent the mean of single measurements for each treated animal and standard deviations (n = 6). For statistical analysis one-way ANOVA with Bonferroni post-tests to compare pairs of treatments was performed (** = $p < 0.01$, * = $p < 0.05$).

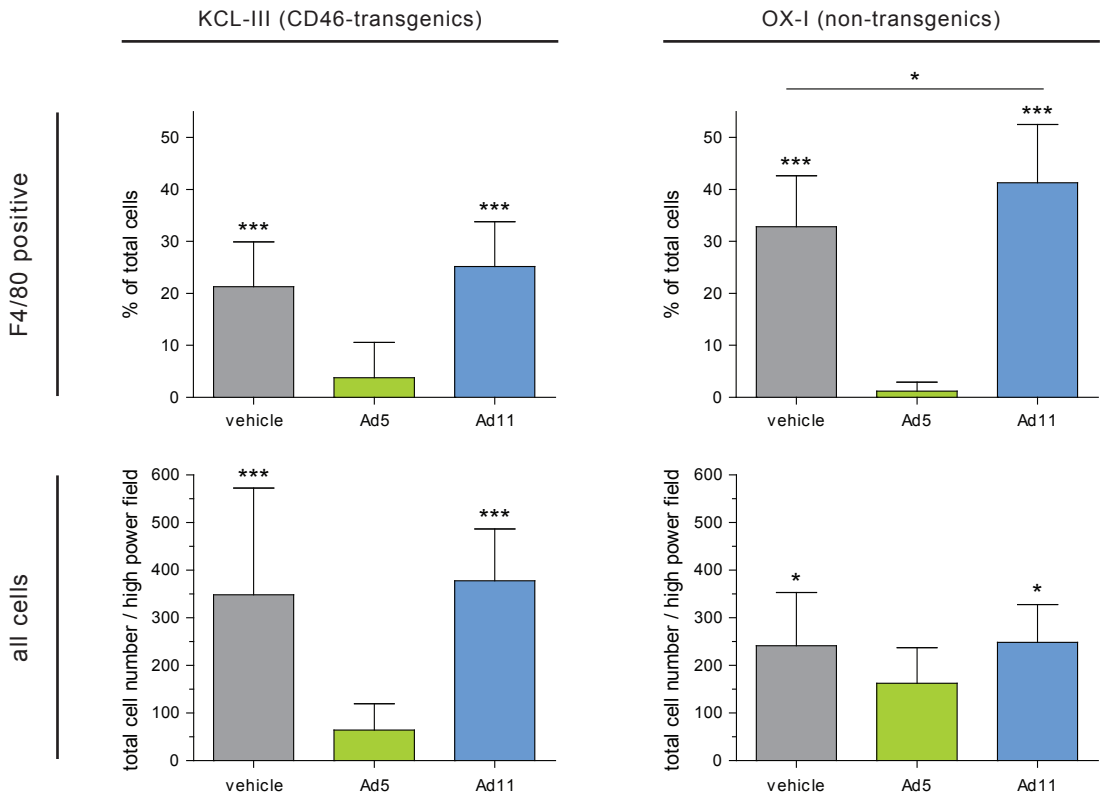


Figure 4 - 7 Long-term cellular response to i.p. adenovirus

CD46-transgenic (KCL-III) or non-transgenic C57BL/6 mice (OX-I) were injected with Ad5 or Ad11 (10^{10} vp/mouse) or virus storage buffer (vehicle) as negative control three times with an interval of 72 hours between injections. 18 days after the first injection animals were sacrificed and peritoneal cavities rinsed with PBS. Cytospins were prepared from fresh cells after centrifugation and resuspension in PBS (section 2.3.4.3). Fixed cells were stained for the murine macrophage marker F4/80 (section 2.3.5). The graphs show the amount of macrophages as a percentage of the whole cell population of two independent experiments (KCL-III and OX-I). Bars and error bars represent the mean of triplicate countings for each treated animal and standard deviations (n = 6). For statistical analysis one-way ANOVA with Bonferroni post-tests to compare pairs of treatments was performed (*** = $p < 0.001$, ** = $p < 0.01$).

4.4 Discussion

Previous studies had demonstrated that Ad5 treatment of ovarian tumour xenografts in nude mice provoked strong long-term inflammatory reactions in the form of adhesion formation (Morrison *et al.*, 2008; Morrison *et al.*, 2009). Similar observations had led to the suspension of a phase II/III clinical trial of i.p. gene therapy with an Ad5-based vector (Zeimet and Marth, 2003) at interim analysis (Stephen Chang – unpublished personal communication). However, previous *in vivo* experiments in our group had suggested that i.p. Ad11 caused less peritoneal toxicity than Ad5 treatment (Dr Nicola Green, unpublished data). Hence, the experiments presented in this chapter investigated the inflammatory response towards different adenovirus serotypes in order to identify possible advantages of the use of Ad3 or Ad11 in comparison to Ad5 in future virotherapy of ovarian cancer.

Experiments in an *ex vivo* model of peritoneal inflammation using elicited peritoneal macrophages from BALB/c mice (section 4.2) demonstrated up to 8-fold higher RANTES expression after Ad5 in comparison to Ad11 treatment, while values of Ad11- did not differ from mock-treated cells (Figure 4-2). Interestingly, Ad3 did not show the effect of decreased cytokine signalling like Ad11. Indeed, measured values were not significantly different from Ad5-treated cells. These observations suggest that the immediate cytokine signalling following adenovirus stimulation is serotype-specific and that i.p. administration of Ad11-based treatments might not induce the same inflammatory responses as observed after Ad5 application. While it was thought that inflammatory properties might be common among members of the same adenovirus group, there was a differential response towards Ad3 and Ad11, both group B adenoviruses. Ad3 has been classified as a subspecies B1 adenovirus, while Ad11 belongs to subspecies B2 (Wadell *et al.*, 1980) with both subgroups showing different tissue tropisms. It is uncertain, if this might be the reason for the diverging stimulatory patterns. Also, as described in section 3.4, Ad3 appears to use additional uptake receptors in comparison to Ad11, which might lead to the observed stimulation of inflammatory signalling in macrophages.

Due to the promising results of low inflammatory stimulation after Ad11 in comparison to Ad5 treatment in the *ex vivo* model, animal studies were designed to investigate this differential

immune response further. This was particularly important as the immune response in the peritoneal cavity is regulated by a variety of cell types and influenced by its unique physiological setup. As mice, unlike humans, do not express CD46, the main uptake receptor of Ad11, CD46-transgenic, alongside non-transgenic C57BL/6 mice were used in these studies (Yannoutsos *et al.*, 1996). Notably, short-term experiments, where animals were sacrificed 6 hours after treatments, revealed that Ad11 did show stimulation of cytokines to levels equal to or in some cases even significantly above Ad5 (Figure 4-3), in contrast to data obtained in the *ex vivo* experiments. This was in accordance to previously published data of the cytokine expression after i.v. Ad5 or Ad11 injection into CD46-transgenic mice (Stone *et al.*, 2007). Hence, acute inflammatory responses to these adenovirus serotypes appear to be similar for both administration routes. However, it was surprising to observe the same reaction of increased inflammatory signalling for Ad5 and Ad11 in the non-transgenic littermates and C57/BL6 mice, as the *ex vivo* model would have predicted a lower response towards Ad11. It is possible (although unlikely), that these differing data are due to the different mouse strains used in the *ex vivo* and *in vivo* models. However, more importantly, it appears that the *ex vivo* model of isolated macrophages was not able to represent the more complex peritoneal *in vivo* environment. These data suggest that the immediate intraperitoneal inflammatory reaction is not only triggered by macrophages, but develops through the interplay with other resident cell populations like the mesothelial lining cells as well as chemotacticly attracted immune cells, such as neutrophils. Indeed, a significant difference between adenovirus- and mock-treated animals regarding the cellular components of their i.p. fluid was observed. The number of macrophages was significantly lower, while the number of neutrophils was significantly higher in Ad5- or Ad11- in comparison to mock-treated mice, in both CD46-transgenic and non-transgenic animals (Figure 4-4 B).

The significant decrease in the number of macrophages in the peritoneal cavity followed the pattern, which has previously been described as the ‘macrophage disappearance’ reaction. Previous studies had demonstrated that macrophages adhere to the peritoneal wall at sites of injury and after challenge with inflammatory agents like LPS or, indeed, Herpes simplex virus, possibly due to chemokine signalling from mesothelial cells (Barth *et al.*, 1995; Cheong *et al.*,

2001). Furthermore, monocytes and macrophages, after contact with the pathogen, could withdraw from the peritoneal cavity in order to home to adjacent lymph nodes for further immunological signalling and antigen presentation (Bellingan *et al.*, 1996). The significant increase in the amount of neutrophils has previously been described (Knudsen *et al.*, 2002; Cailhier *et al.*, 2005) and is one of the hallmarks of the early reaction to intraperitoneal inflammatory stimulation.

While the short-term *in vivo* experiments revealed that Ad5 and Ad11 had similar inflammatory short-term effects, previous unpublished data had suggested that i.p. Ad11 caused less long-term toxicity than Ad5 (Dr Nicola Green, unpublished data). To further investigate this observation, studies were designed, based on the protocols used in experiments that had previously shown strong long-term toxicities after i.p. Ad5 administration (Morrison *et al.*, 2008). Notably, Ad5 induced significantly more severe long-term pathologic effects in the form of adhesions and liver toxicity in all animals, in comparison to Ad11. It was found that this was accompanied by significantly higher levels of IFNγ and VEGF expression and a significantly reduced number of macrophages and, indeed total cell number, in the i.p. fluid of Ad5- than in Ad11- or vehicle-treated animals (Figure 4-6).

The formation of adhesions after traumatic interventions in the peritoneal cavity continues to be a great concern in the clinic and considerable effort is put into research clarifying the mechanisms involved. Studies have revealed a complex system of cellular and molecular events. It appears that peritoneal adhesions are the result of an inordinate wound repair involving mesothelial cells, monocytes and macrophages as well as neutrophils, whose localisation and function are mutually regulated by cytokine and chemokine signalling (Cahill and Redmond, 2008). During this process cell numbers of resident macrophages in the peritoneal fluid drop due to adherence to the peritoneum (Cheong *et al.*, 2001). Ultimately, a pathologically altered fibrin/plasmin-ratio, leads to profuse depositions of fibrin, which can grow to become well-organized, vascularised and innervated tissues (Sulaiman *et al.*, 2002). One of the key-players of these processes appears to be VEGF. Apart from its angiogenic properties, VEGF has been implicated in tissue remodelling and wound healing processes. In the process

of adhesion formation in particular, its effect of increased vascular permeability and concurrent deposition of fibrin-rich matrices appears to be of particular importance (Cahill and Redmond, 2008). Hence, the increased VEGF and diminished macrophage levels observed in the long-term studies described in this chapter appear to indicate that similar tissue remodelling processes occur after Ad5- but not Ad11-treatment. The presence of large surfaces with adhesive properties might explain the generally decreased cell numbers in Ad5-treated animals.

Previous reports investigating the liver toxicity of Ad5 and Ad11 after i.v. injection into CD46-transgenic mice demonstrated that Ad11 did not induce increased serum levels of liver enzyme alanine aminotransferase (ALT) on day 3 after administration in comparison to Ad5 (Shashkova *et al.*, 2009). It was reasoned that this might be due to a lack of interaction of Ad11 with FX and the consequent absence of hepatocyte infection. Furthermore, the authors could show that predosing of animals with Ad5, but not Ad11, lead to increased hepatocyte transgene expression after subsequent administration of an Ad5-derived vector, concluding that Ad11, in contrast to Ad5, did not kill liver-resident Kupffer cells. These findings might explain the absence of long-term i.p. toxicities after Ad11 treatment in the experiments presented in this chapter. First, the severe hepatotoxicity after Ad5 administration, which was also observed in the present study, might cause secondary inflammatory effects in the peritoneal cavity, unbalancing its regular inflammatory responses. Second, if the toxic effect of Ad5 on Kupffer cells is also occurring in resident peritoneal macrophages, the absence of this pivotal cell type and its influence on the inflammatory signalling cascade might lead to aberrant cytokine expression from mesothelial cells and neutrophils and subsequent inordinate inflammatory effects resulting in symptoms of adhesion formation as observed in the long-term experiments presented here. Hence, while Ad11 caused short-term responses similar to Ad5, the absence of hepatotoxicity and the availability of i.p. macrophages to control inflammatory responses prevented excessive long-term toxicity.

The present i.p. *in vivo* studies revealed that the use of Ad11, in contrast to Ad5, might have a major advantage in future applications of adenovirus virotherapy of ovarian cancer. If these findings are translatable to the human setting, patient safety would be considerably increased.

5 Neutralisation of Ad3, Ad5 and Ad11 by malignant exudates

5.1 Introduction

A dose of therapeutic adenovirus, after either systemic or regional delivery, encounters a range of obstacles that diminish the number of particles reaching the target site. Apart from loss of particles due to sequestration by non-target cells such as erythrocytes (Carlisle *et al.*, 2009), and activation of the innate immune response, including interaction with serum proteins and immune cells, the main mechanism responsible for abrogation of a treatment dose are pre-existing anti-adenovirus antibodies (Zaiss *et al.*, 2009). The low toxicity and rapid spread of naturally occurring adenovirus infections in healthy individuals (Gonçalves and de Vries, 2006) contributes to its high prevalence in the population (Vogels *et al.*, 2003). Hence, the majority of patients will have encountered adenovirus in the environment prior to possible virotherapy and will have developed antibodies, which can effectively neutralise both wild-type virus and virotherapy vectors before they achieve any notable efficacy. Hence, a large proportion of current research into adenovirus-based virotherapy is concerned with strategies to overcome this type of neutralisation (Zaiss *et al.*, 2009). In this context, some previous studies suggested that, globally, the prevalence of antibodies directed against more uncommon serotypes, such as 11 or 35, was markedly lower than against Ad5. However, this appeared to be partly dependent upon on the population investigated (Vogels *et al.*, 2003; Nwanegbo *et al.*, 2004). These findings sparked an interest in alternative serotypes that might encounter no or lower levels of pre-existing antibodies and might have a significant advantage over common serotypes.

The majority of earlier work examining adenovirus neutralisation investigated serum samples from healthy adult volunteers. Hence, it was of interest to study whether findings from those studies were applicable to a prospective virotherapy patient population. In the present study it was decided to investigate this in a more clinically relevant setting using samples from cancer patient exudates, rather than serum samples from healthy adults. In particular, it was questioned whether the amount of antibodies present in patient fluid samples was correlated to and could, indeed, be predictive for their neutralising capacity. This would constitute a simple and quick way to assess a patient's neutralisation status and potentially allow prediction of virotherapy efficacy with a specific Ad serotype. To this end, an ELISA system was developed that would detect the total amount of antibodies in exudates. Neutralising capacity, i.e. the

amount of neutralising antibodies, in contrast to total amount of antibodies, was investigated by assaying the inhibition of oncolysis in the presence of different concentrations of exudates, effectively determining the neutralising titre of samples. Furthermore, it was questioned whether antibodies elicited by different Ad serotypes were directed to different structural Ad proteins. In an attempt to answer this question, an immunoblot system was explored, where Ad was subjected to gel electrophoresis and patient samples used as primary detection antibodies. Intensity of detected bands would reveal the amount of antibodies directed towards different Ad proteins. These results would inform future research about which specific structural proteins require shielding or alteration in order to escape antibody-mediated neutralisation in a serotype-specific manner.

5.2 Total antibody content against different adenovirus serotypes of patient samples

In order to measure the total amount of antibodies against Ad serotypes in malignant exudates from patients, an indirect ELISA system was developed. It was of interest to investigate whether antibodies were predominantly directed against capsid proteins or whether patients had also developed immunoglobulins against internal proteins or proteins produced during synthesis of progeny virus. To this end, purified preparations of adenovirus particles were used to test for exposed capsid proteins only, in addition to supernatants obtained during Caesium chloride banding of virus, which will present a range of proteins including internal as well as early and intermediate Ad proteins. Ultimately, this might help to understand better the scope of the antibody response towards Ad and specifically whether physical shielding of virus capsids (Fisher *et al.*, 2001) alone would be sufficient to overcome neutralisation or whether oncolytic efficiency was hampered by additional antibody interactions with virus proteins, that are only available following cell entry and virion disassembly. All serum or exudate samples investigated in this study had been heat-inactivated prior to experimental use in order to minimise neutralisation effects of other serum proteins, such as complement.

5.2.1 ELISA development

The ELISA was developed as an indirect detection system (section 2.4.3). Briefly, a known amount of antigen (purified wild-type Ad3, Ad5 or Ad11 or antigen solution of Ad3, Ad5 or Ad11) was directly adsorbed to MaxiSorp™ microplates. After blocking of free binding sites, diluted patient samples were added. Subsequently, bound antigen-specific antibodies were detected by HRP-coupled anti-human IgG antibodies, whose amount was quantified by measurement of absorbance after conversion of TMB substrate. Several presumptions have to be met, to allow for valid results from this method, for example: a) capture antigens bind to the plate surface in equal amounts, regardless of serotype origin; b) binding does not alter the antigen's three-dimensional structure in a way to alter or obstruct access to epitopes; c) non-Ad-specific antibodies in the patient fluid do not bind the capture antigens; d) the amount of Ad-specific

antibodies in the patient fluid lies in the dynamic range of the assay; e) the efficiency of binding between the detection antibody and the different captured antigen-specific antibodies is similar for all antigen-specific antibodies. In order to address the most important of these issues several assay development experiments were performed.

5.2.1.1 Adenovirus antigen solutions

The first development experiments were designed to determine optimal concentrations of capture antigen, patient sample and detection antibody to be used in subsequent assays (Figure 5-1). Protein concentrations of Ad3, Ad5 and Ad11 antigen solutions were determined by a modified Bradford assay (section 2.4.2, data not shown) and serial doubling dilutions from 0.5 to 8 µg/ml used to coat ELISA wells. A patient sample, which was known to have high neutralising capacity, was used to investigate maximum possible signal and signal/noise ratio. The patient sample was used in a 1:10 and a 1:100 dilution. The HRP-coupled detection antibody was tested at a 1:500 and a 1:1,000 dilution. It was determined that a coating concentration of 2 µg/ml protein of antigen solution gave maximum signal at smallest possible reagent use for antigen solutions of all three serotypes, regardless of sample or detection antibody concentration (Figure 5-1 A, B and C). Wells that were not incubated with antigen solution, but blocked and incubated with patient sample and detection antibody, revealed that a 1:10 dilution of sample or 1:500 dilution of detection antibody lead to high background readings, minimising the dynamic range of the assay (Figure 5-1 D). Therefore, dilutions of 1:100 for patient samples and 1:1,000 for the detection antibody were chosen for further assays.

In a second experiment these results were corroborated employing human serum samples. In order to establish the dynamic range of the assay, serial dilutions of human serum pooled from 20 healthy volunteers (pool20) were used, which was intended as a possible standard curve for future assays (Figure 5-2 A). This was tested alongside a second human serum sample (serum1) known to have high neutralising capacity (Figure 5-2 B). Serial dilutions of samples were incubated on plates coated with 2 µg/ml antigen solution and detected with a secondary antibody dilution of 1:1,000, as established in the first experiment (Figure 5-1). Figure 5-2 A and B show that it was possible to measure Ad antigen directed antibodies in dilutions between

1:50 to 1:3,200 for both samples tested. It was concluded that the detection range of the assay system should allow measurement of a wide variety of antibody concentrations as would be expected in an array of patient samples. These results also indicated that neither of the two samples carried equal amounts of antibodies against Ad3, Ad5 and Ad11. Hence, it was not possible to use these serum samples as standards, which the readings from the patient sample screen could be correlated to. Furthermore, as it could not be demonstrated that the amount of capture antigen bound to the plate was the same for Ad3, Ad5 and Ad11, it was not possible to directly compare the raw absorption readings for the three serotypes in the subsequent screens.

5.2.1.2 Whole purified adenovirus

For assays to determine the amount of immunoglobulins directed against Ad capsid epitopes only, first, the virus particle concentration of purified virus preparations was determined by PicoGreen® assay (section 2.2.2, data not shown). The amount of virus used to coat well surfaces was evaluated according to this measurement rather than whole protein measurements, since values from protein assays of purified virus preparations were exceedingly low and thought not to be as reliable as the PicoGreen® results. However, comparison of protein content to DNA content by PicoGreen® assay revealed good correlation for all three virus preparations (data not shown) and the amount of protein per well was in the range of previously reported studies (Stallwood *et al.*, 2000).

In order to determine the correct amount of vp to be used in this assay, plates were coated with a range of vp per well and the magnitude of signal tested after incubation with pooled human serum. Figure 5-3 shows that the signal rises in a linear fashion across the range of $1x10^7$ to $1x10^9$ vp/well. Hence, a coating concentration of $1x10^8$ vp/well was chosen for further experiments, as this should allow a high enough dynamic range of the ELISA, while minimising adenovirus use. As the aim of this assay was also to compare amounts of antibodies in patient samples directed against different Ad serotypes, it was important to ensure that binding of these serotypes to the plates was equally efficient. Therefore, wells were coated with a range of vp numbers and, after incubation and washing, the amount of bound vp was assessed by PicoGreen® assay. Figure 5-4 A shows that the number of vp dispensed per well correlates to

the number of vp recovered from wells over a range from $1x10^7$ to $1x10^9$ vp/well. Importantly, the amount of virus recovered from wells at a concentration of $1x10^8$ vp/well was the same for all three serotypes, demonstrating that these bind the plate surface with the same efficiency (Figure 5-4 B). Hence, subsequent experiments were performed using $1x10^8$ vp/well coating concentration for all three serotypes. Furthermore, having established that all three serotypes bind the plate with equal efficiency, it was then possible to compare amounts of antibodies directed against Ad3, Ad5 or Ad11 by their raw absorption readings.

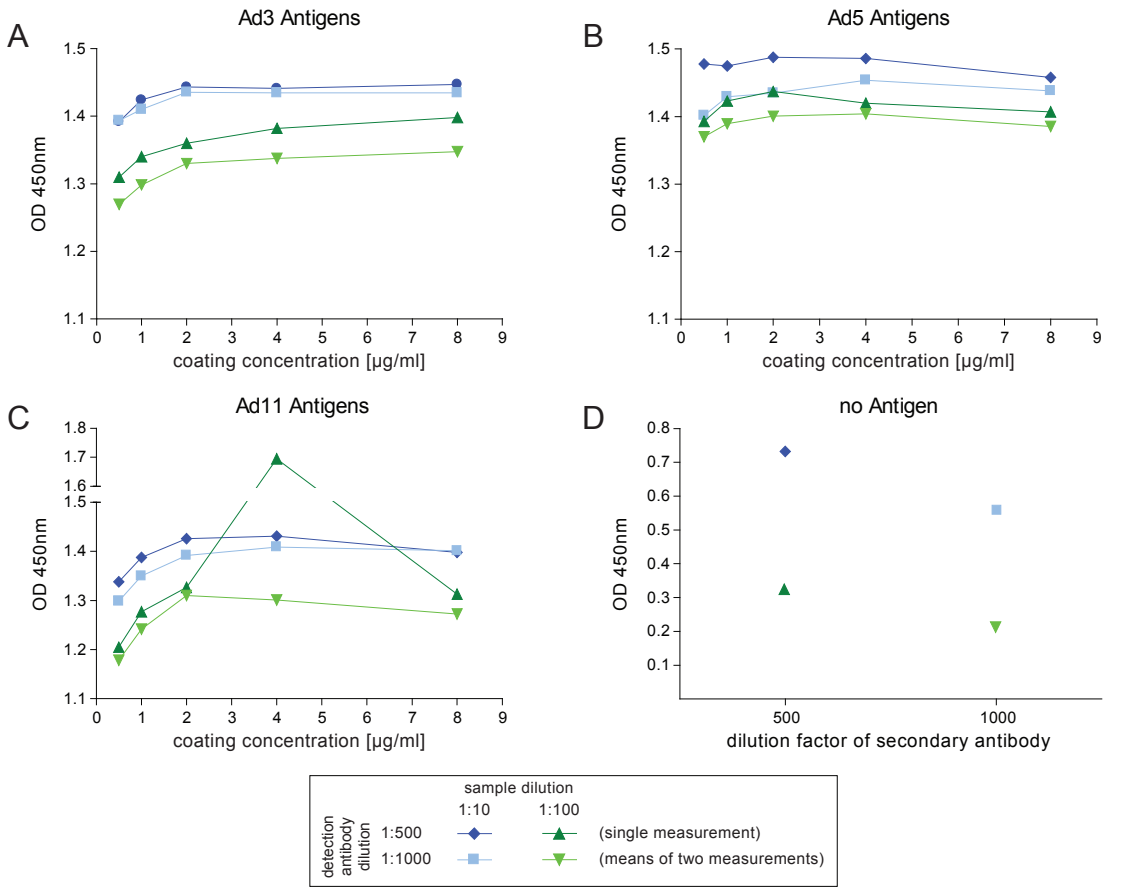


Figure 5 - 1 Determination of optimal concentrations of capture antigen, sample and detection antibody

Antigen solutions of Ad3, Ad5 or Ad11 in serial doubling dilutions in a range from 0.5 to 8 µg/ml of protein were used to coat ELISA plates (graphs A, B or C, respectively, single or means of two measurements). Wells were incubated with a 1:10 (blue) or 1:100 (green) dilution of sample with high neutralising capacity before addition of HRP-coupled detection antibody at a 1:500 (dark colour) or a 1:1,000 (light colour) dilution. OD was assessed at 450nm after signal development (substrate: H_2O_2 / TMB). Wells that were not incubated with antigen solution, but sample and detection antibody were used to determine background signal caused by these components alone (graph D, single or means of two measurements).

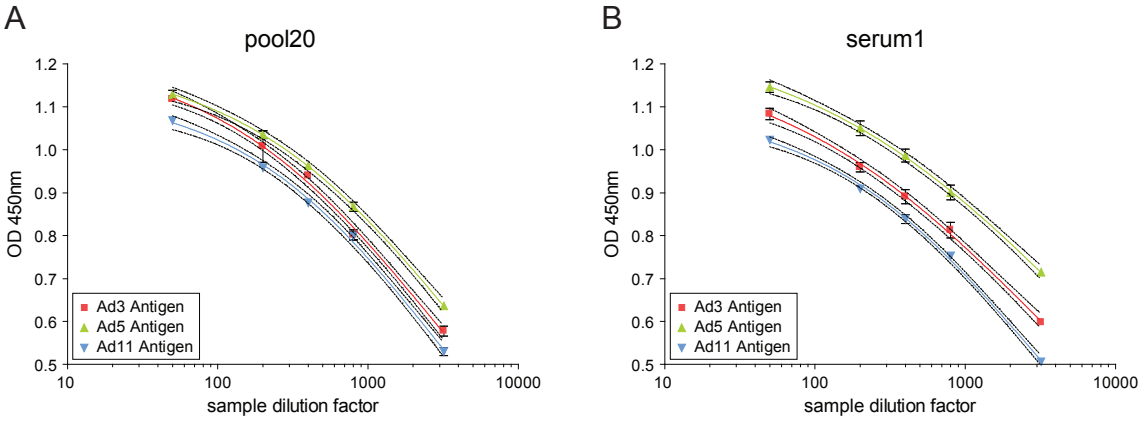


Figure 5 - 2 Dynamic range of ELISA system

In order to establish the dynamic range of the assay serial dilutions of human serum pooled from 20 healthy volunteers (pool20, graph A) and a second human serum sample known to have a high neutralising capacity (serum1, graph B) were incubated on plates coated with 2 µg/ml antigen solution and detected with a secondary antibody dilution of 1:1,000. Nonlinear regression curves were calculated for all sets of values in order to investigate whether measurements were different for the three serotypes and whether one of the tested samples could be employed as a standard curve in subsequent assays (means of triplicates and standard deviations, nonlinear regression curve fits and corresponding 95% CI).

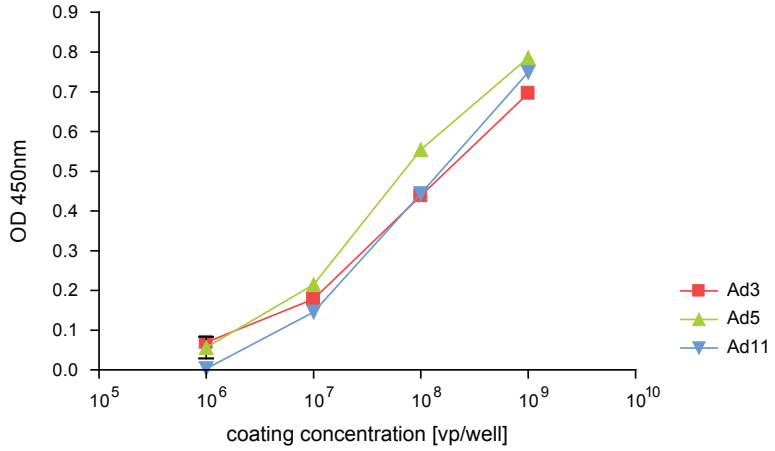


Figure 5 - 3 Determination of optimal adenovirus concentration for well coating

In order to determine the optimal amount of vp to be used in subsequent ELISAs, plates were coated with a range of vp/well from 10^6 to 10^9 vp/well. After incubation with a 1:100 dilution of pooled human serum (pool20) and detection antibody optical density was assessed at 450nm (OD 450nm) after signal development (substrate: H_2O_2 / TMB) (means of triplicate measurements and standard deviations after subtraction of the mean of background readings from wells containing no virus).

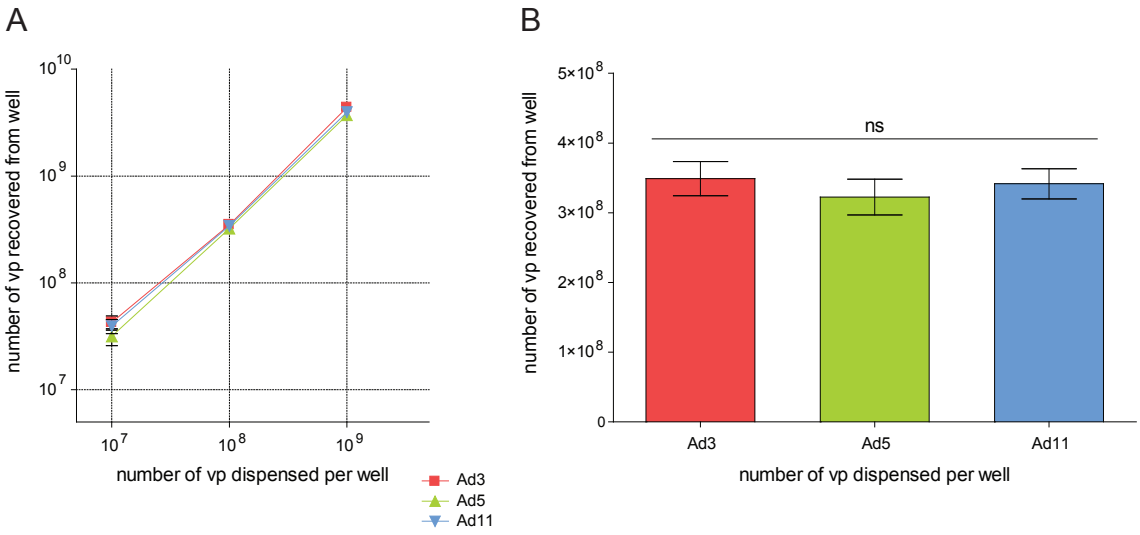


Figure 5 - 4 Well coating efficiency of Ad3, Ad5 and Ad11

The binding efficiencies of Ad3, Ad5 and Ad11 were tested by coating wells with a range of vp from 10^7 to 10^9 vp/well (number of vp dispensed per well) and, after incubation and washing, assessing the amount of bound vp by PicoGreen® assay (section 2.2.2) (number of vp recovered from well). The number of vp dispensed per well correlates to the number of vp recovered from wells over the tested range (graph A). There were no statistical differences between the amount of vp per well for the different serotypes at the designated assay concentration of 10^8 vp/well (graph B) (graphs A and B: means of six measurements and standard deviations; statistical analysis: one way ANOVA with Tukey post-tests to compare differences between all columns (ns = not significant)).

5.2.2 Sample screen

After the assay system had been developed as described in section 5.2.1, 22 pleural exudate samples from patients with varying malignant diseases and 6 samples of ascitic fluid from ovarian cancer patients were screened for their anti-adenovirus antibody content. The screen was performed on plates coated with antigen solutions and on plates coated with whole virus.

Whole purified adenovirus

Figure 5-5 A shows the amount of antibodies in patient samples cumulated for their specificity against whole purified Ad3, Ad5 or Ad11 virions. Importantly, the amount of antibodies directed against Ad11 was significantly lower than the amount against Ad3 ($p < 0.05$). However, significance could not be demonstrated for differences in amount between Ad3 / Ad5 or Ad5 / Ad11. Nevertheless, the difference between Ad5 and Ad11 appeared greater than the difference between Ad3 and Ad5, suggesting a lower prevalence or overall amount of antibodies against Ad11 in the study population. Interestingly, no samples appeared to be negative for antibodies against any of the three serotypes. It is unclear whether this is due to unspecific binding of antibodies or cross-reactivity of antibodies across serotypes. Unfortunately, serum or even exudate samples with proven negative antibody status to further investigate these questions could not be obtained. Interestingly, some samples demonstrated lower content of antibodies against one particular serotype than against the others. It appears that in these patients the therapeutic use of this serotype might be advantageous by allowing higher efficacy.

Adenovirus antigen solutions

As it was not demonstrated that the amount of capture antigen bound to the plate using the antigen solutions was the same for Ad3, Ad5 and Ad11, it was not possible to directly compare the raw absorption readings for the three serotypes in these screens. Figure 5-5 B shows the cumulative raw readings for Ad3, Ad5 and Ad11. A very similar trend, as described above, towards a lower amount of antibodies against Ad11 could be observed, under the assumption that the amount of antigen bound to the plate surface was the same for the three serotypes.

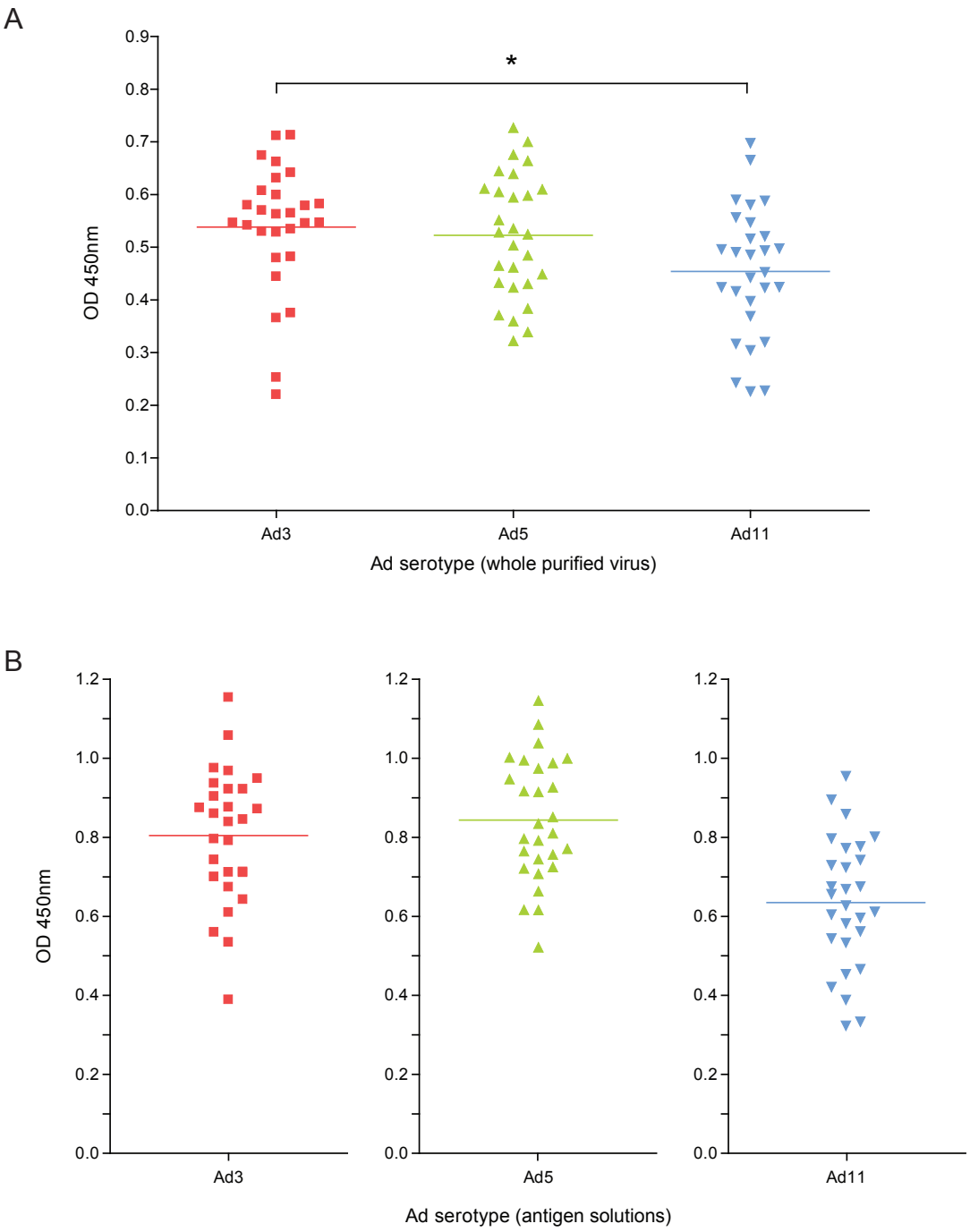


Figure 5 - 5 Antibody content of malignant exudates against Ad3, Ad5 and Ad11

Pleural exudate samples (n = 22) from patients with varying malignant diseases and samples of ascitic fluid (n = 6) from patients with ovarian cancer were screened for their anti-adenovirus antibody content. The screen was performed on plates coated with antigen solutions and on plates coated with whole purified virus (section 2.4.3). Briefly, ELISA plates were coated with whole purified Ad3, Ad5 or Ad11 (10^8 vp/well, graph A) or serotype specific antigen solutions (2 µg/ml protein, graph B). Wells were then incubated with 1:100 dilutions of samples and, after washing, HRP-coupled anti-human IgG detection antibodies. The amount of bound detection antibodies was quantified after chromogenic reaction (substrate: H_2O_2/TMB). Direct comparison of measurements from assays using antigen solutions for plate coating was not possible, due to unknown binding efficiencies of the different serotype specific antigens (graph B). Both graphs show means of duplicate or triplicate measurements of each sample and the mean of readings of all samples for the three investigated serotypes; statistical analysis: one-way ANOVA with Tukey post-tests to compare differences between all groups (* = $p < 0.05$).

5.2.3 Discussion

The original idea behind comparing purified virus and a mixture of virus peptides as capture antigens was to investigate whether the antibody response towards Ad also comprised specificity towards internal or intermediate Ad proteins, which would not be found on the virus capsid. This might indicate the possibility of neutralisation after virus internalisation. Although higher raw readings were taken for the antigen solution coated plates, it was unclear if this was due to a higher amount of detected antibodies or overall higher background readings, as it was not possible to determine the background values and to equalise measurements of both assays, due to a lack of a negative control sample, which would not contain Ad-directed antibodies. Hence, it was not possible to identify, whether antigen solution coated plates captured more antibodies than plates coated with purified virus alone.

Although the statistically significant difference between antibody amounts directed against whole purified virions of Ad3 and Ad11 could not be observed in assays using antigen solutions, comparison of results from both assays demonstrated highly significant correlation of readings (data not shown). Therefore, it appears that antigen solutions, which are normally a waste by-product of adenovirus production, could be a very cost effective way to substitute for the costlier purified Ad preparations, if these types of assays would be used to assess patient neutralisation status in the future.

Only immunoglobulins of the G isotype have been investigated in this study. However, the development of this assay system provides a platform, which should easily be adaptable to evaluate amounts of other isotypes through the use of a detection antibody with different immunoglobulin specificity. It would be interesting to investigate whether the three tested serotypes do show varying profiles of immunoglobulin isotypes, which might be the case, due to their differing pathophysiology (Russell, 2009). Due to limited availability of plate coating reagents at the time of study these questions were not addressed during this project.

Overall, it appeared that all samples contained antibodies against all three investigated Ad serotypes. However, due to a lack of an antibody negative sample, this finding could not be fully corroborated. Notably however, it could be demonstrated that more samples in this study population contained less antibodies directed towards Ad11 than towards Ad3 or Ad5. This is in accordance with previously published data (Vogels *et al.*, 2003; Thorner *et al.*, 2006) and highlights a possible advantage in using Ad11 as a platform for future adenovirus-based virotherapy approaches.

5.3 Neutralisation capacity of patient samples

While the ELISA system described in section 5.2 quantified the total amount of antibodies present in patient samples, it did not allow prediction of the neutralising capacity of these antibodies. To this end, experiments testing the functionality of antibodies by investigating the capability of malignant pleural effusion and peritoneal ascitic fluid samples to neutralise oncolysis by different wild-type Ad serotypes and maintain viability of tumour cells were performed. The studies were designed to resemble antibody titre detection assays. Hence, virus would be incubated with serial dilutions of samples before addition of cells followed by incubation until oncolysis could be observed in wells that did not contain pleural sample. It was decided to use A549 cells for these studies. This cell line had demonstrated least variability of P/I ratios across the different serotypes (section 3.2) thereby minimising inter-serotype dependent differences in activity. Comparison of results from this study with data obtained from the ELISAs for total amount of antibody might reveal, if the ELISA system could serve as a simple and quick way to predict the neutralising capacity of patient fluids, which would be a simple method to determine the appropriate Ad serotype for treatment in a clinical setting.

5.3.1 Assay development

Pleural fluid samples were routinely collected in Vacutainer® tubes which were pre-treated with anticoagulants. Preliminary experiments had shown that different types of anticoagulants could affect *in vitro* cell viability (data not shown). Hence, a study was designed to investigate these effects and to determine which anticoagulant would least impact on downstream screening procedures. Two different pleural fluid samples (pf1 and pf2), which had been collected in Vacutainer® tubes containing either no anticoagulant, sodium citrate, EDTA or Heparin were tested in this experiment. A549 cells were incubated overnight with dilution series of fluid samples in growth medium. After changing supernatants to fresh medium without pleural fluids, cells were incubated for a further 96 hours when cell viability was assessed using the MTS assay (section 2.2.5). Figure 5-6 shows that EDTA is highly toxic to cells when supernatants contain more than 20% of pleural fluid. At the highest tested concentration of 80% fluid,

EDTA levels were high enough to reduce cell viability by about 80% in comparison to cells treated with fluid without anticoagulant. Citrate appeared to be mildly toxic at concentrations above 40% of fluid showing reduction of viability of approximately 20% to 40% at the highest concentration tested. Heparin did not appear to have an effect on cell viability in this assay. Although it appeared that Heparin would least impact on cell viability, it was decided to use samples containing citrate in this study as only for this anticoagulant a large number of samples could be obtained.

Notably, all cells incubated with the two samples of pleural fluid investigated demonstrated a profound increase in viability in comparison to cells left untreated, which, furthermore, seemed to be a concentration dependent effect. Hence, it appeared that the samples contained growth factors which strongly stimulated cell growth during the initial 24 hour incubation phase. This highlighted the importance of defining appropriate controls in the subsequent screening experiments. For each screened sample, cells incubated with the same dilution range, but without virus infection, would be required to serve as background controls for effects of the different samples, and indeed sample concentrations, on cell viability.

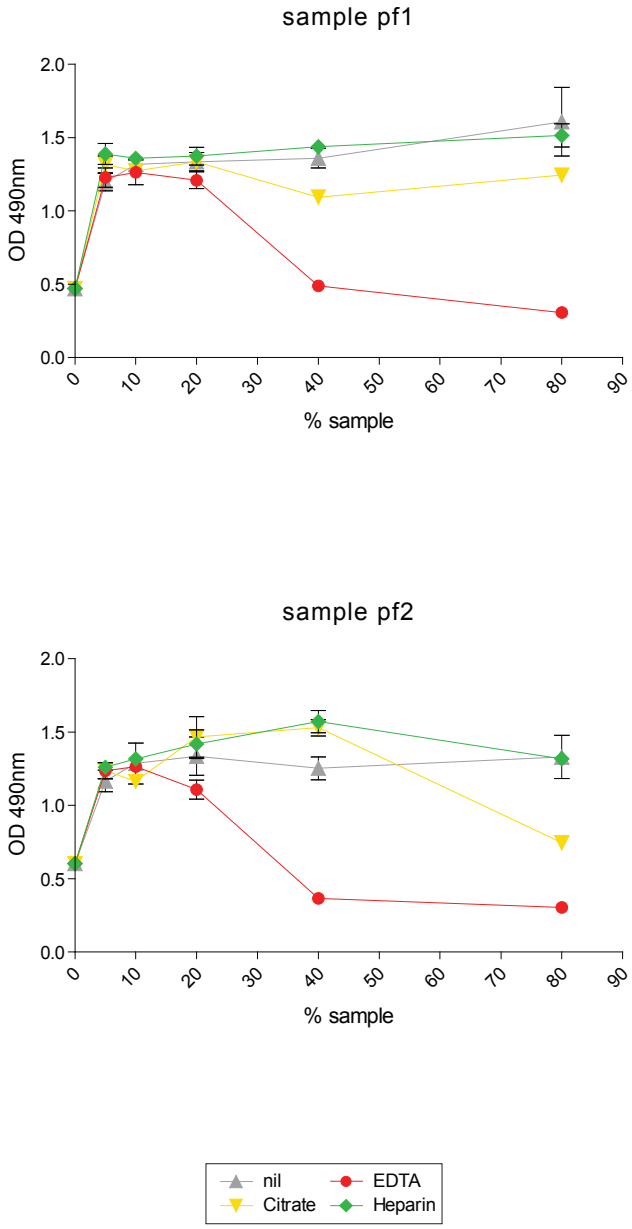


Figure 5 - 6 Effects of anticoagulants on cell viability

Monolayers of A549 cells were incubated overnight with dilution series of two pleural fluid samples (pf1 and pf2), which had been collected in Vacutainer® tubes containing either no anticoagulant, sodium citrate, EDTA or Heparin in growth medium. After changing supernatants to fresh medium without pleural fluids, cells were incubated for a further 96 hours when cell viability was assessed with the MTS assay (section 2.2.5) (means of triplicate measurements and standard deviations).

5.3.2 Sample screen

The assay format used in this study was developed to allow screening of a large number of samples in a reproducible manner (compare section 2.4.4). To this end, it was decided that the first step should be to prepare serial dilutions of samples in growth medium directly in 96 well microplates, followed by addition of Ad3, Ad5 or Ad11 to result in a final concentration of 1,000 vp/cell. After 90 minutes incubation at 37ºC cells were added and plates left to incubate for 48 hours before assessment of cell viability. This incubation period was chosen to put emphasis on the neutralisation of the parental virus and to minimise effects of infection of cells with progeny virus. As shown in section 3.2.2.1 a profound oncolytic effect in A549 cells could be observed after this incubation time, giving the assay a large dynamic range.

Figure 5-7 depicts the viability curves of A549 cells over the range of tested sample concentrations separated for the three tested Ad serotypes. 22 pleural exudate samples from patients with varying malignant diseases and 6 samples of ascitic fluid from ovarian cancer patients were screened. Viability of cells was calculated by dividing the reading of a well containing a dilution of sample and virus by the readings of wells containing the same dilution of sample without virus (negative control). Wells containing virus alone were used to assess maximum cytotoxicity of the serotypes (positive control). After normalisation of viability between 0% and 100% nonlinear regression curves following a sigmoid dose response model with variable slope and constraints for the top and bottom values as 100% and 0%, respectively, were calculated. For most curves a steep rise from strong oncolytic effect (low viability) to complete loss of effect (high viability) could be observed. It appeared that neutralisation of virus cytotoxicity occurred relatively instantly, once a threshold value of functional virus had been neutralised. It could be observed that, consistently, low concentrations of samples were required for neutralisation for Ad3, while neutralisation curves for Ad5 were dispersed over a wider range of concentrations. In contrast, neutralisation of Ad11 appeared to occur at higher concentrations of samples.

In order to make the neutralisation capacity of samples more easily comparable, the amounts of samples required to restore 90% normalised viability was extrapolated from the regression curves. This value was chosen in accordance with previously published studies as a threshold measure of effective neutralisation of virus (Vogels *et al.*, 2003). Figure 5-8 shows the concentration of sample required to obtain neutralisation of virus oncolysis resulting in a viability of cells of 90%. Significantly more samples required higher concentrations to neutralise Ad11 than Ad3. No statistical difference was found between Ad5 and Ad11, due to the diversity of extrapolated concentrations for Ad5. Importantly however, the concentration of sample at which Ad (regardless of serotype) was effectively neutralised equated to concentrations lower than 10% for the majority of samples. This indicated that all tested samples had high neutralising capacity towards all evaluated Ad serotypes.

In order to investigate the patterns of neutralisation of the different serotypes at low concentrations of patient fluid, where differential effects could be expected, cell viability values at sample concentrations below 5% were examined (Figure 5-9). It appeared that the lower neutralisation of Ad11 in comparison to Ad3 was only apparent at concentrations of 2.5%, 1.25% and 0.625% of samples. In addition, it appeared that Ad5 was neutralised by significantly less samples than Ad3 at a sample concentration of 5%. At lower amounts of fluids antibody concentrations had dropped below levels that could neutralise Ad (at the vp concentration tested) and cell lysis was efficiently mediated by all three serotypes.

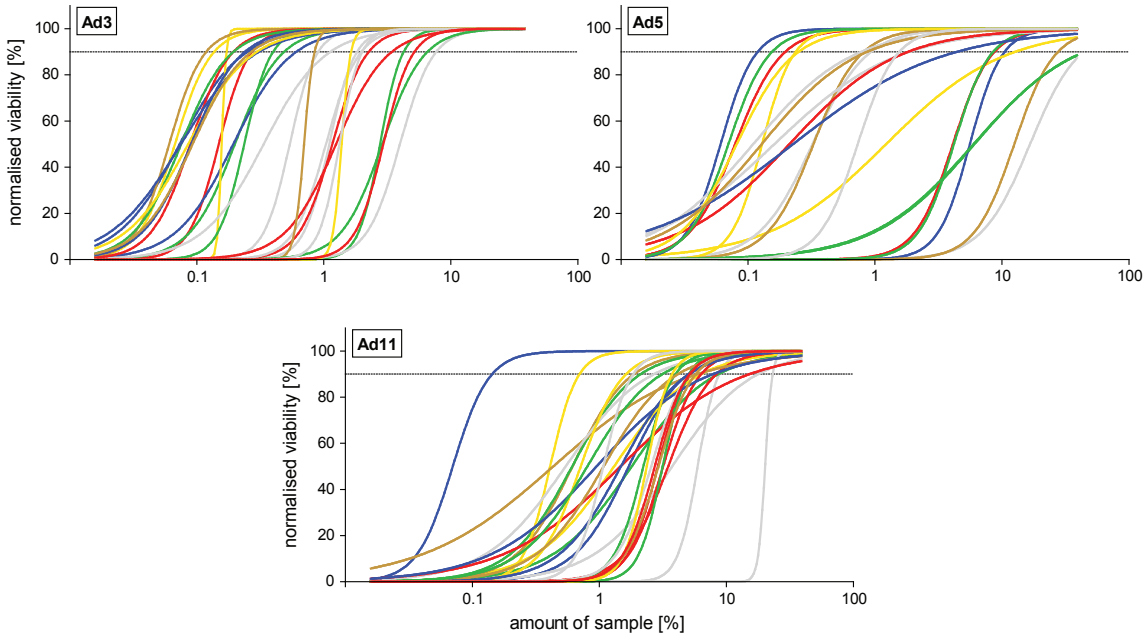


Figure 5 - 7 Viability of cells incubated with Ad3, Ad5 or Ad11 in the presence of malignant exudates

The viability of A549 cells incubated with Ad3, Ad5 or Ad11 (1,000 vp/cell) in the presence of a dilution range of exudates was assessed with MTS assays (section 2.4.4). Viability of cells was calculated by dividing the reading of triplicate wells containing sample and virus by the readings of triplicate wells containing the same dilution of sample without virus (negative control). Wells containing virus alone were used to assess maximum cytotoxicity of the serotypes (positive control). After normalisation of viability nonlinear regression curves following a sigmoid dose response model were calculated. Neutralisation capacity was determined by extrapolating the amount of sample required to restore 90% viability (dashed line).

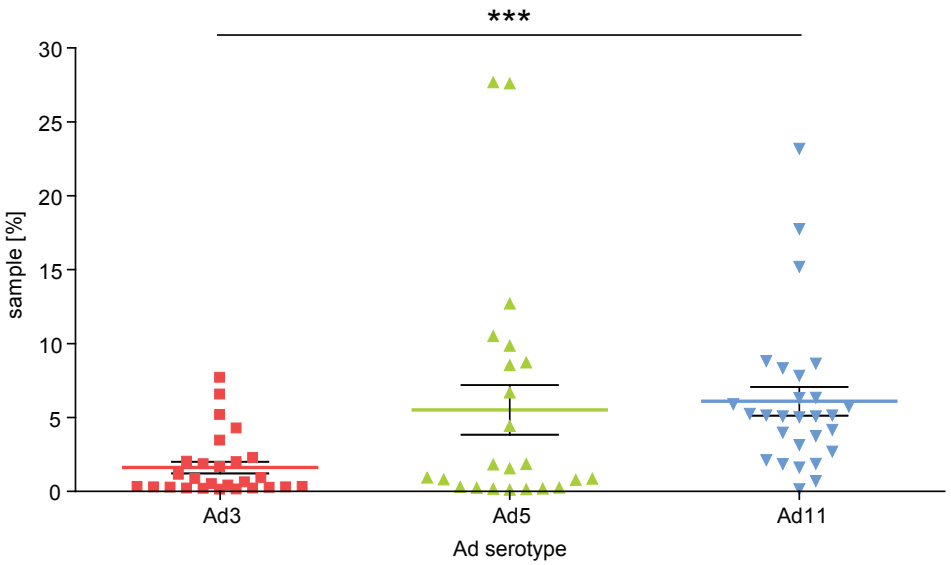


Figure 5 - 8 Neutralisation capacity of malignant exudates

The amount of sample required to restore 90% normalised viability was extrapolated from regression curves (Figure 5-7). This value was chosen in accordance with previously published studies as a threshold measure of effective neutralisation of virus (Vogels *et al.*, 2003). The graph depicts the extrapolated concentrations of samples that restored 90% viability for Ad3, Ad5 and Ad11 (line: mean value of all samples per serotype; error bars: standard error of the mean) As extrapolated values did not follow a Gaussian distribution data was statistically analysed with a Kruskal-Wallis test and Dunn's multiple comparison post-tests to compare all pairs of groups (*** = $p < 0.001$).

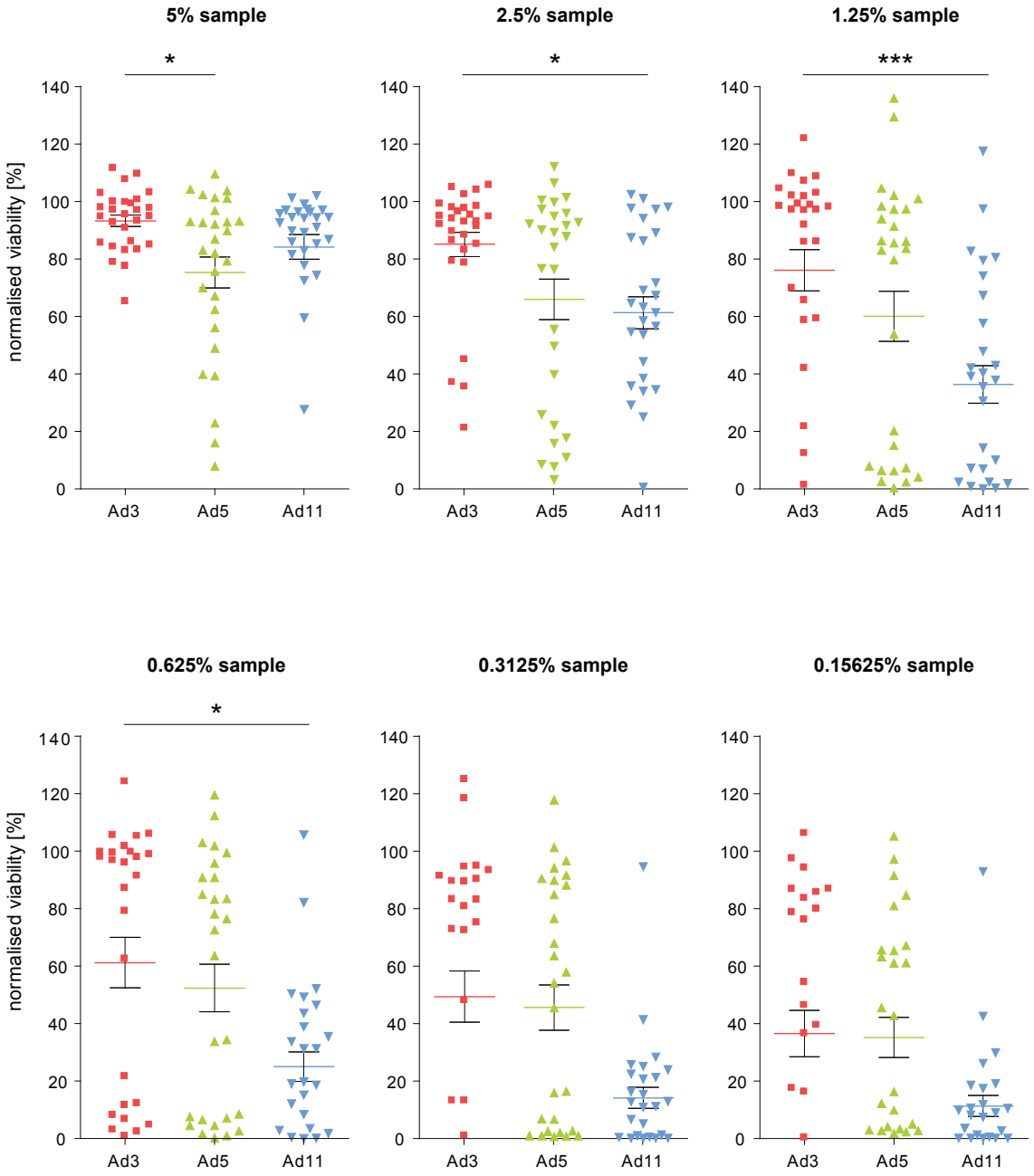


Figure 5 - 9 Neutralisation capacity at low concentrations of exudates

In order to investigate the neutralisation capacity of exudates towards the different serotypes at low concentrations of patient fluid, where differential effects could be expected, cell viability (Figure 5-7) at sample concentrations below 5% were examined. The graphs show the normalised viability values of A549 cells incubated for 48 hours with Ad3, Ad5 or Ad11, which had been preincubated with sample dilutions of 5%, 2.5%, 1.25%, 0.625%, 0.3125% or 0.15625% in growth medium (means of triplicate measurements for each sample with the line depicting the mean value of all samples and its standard error; statistical analysis: Kruskal-Wallis test with Dunn's multiple comparison post-tests (* = $p < 0.05$, *** = $p < 0.001$)).

5.3.3 Overcoming neutralisation by increased virus doses

The experiments described in section 5.3 were performed at a fixed vp concentration of 1,000 vp/cell with varying amounts of patient samples (dilution range 40% - 0.16%). It was found that samples were highly neutralising to this amount of virus even at concentrations as low as 5% of fluid. To investigate whether the use of higher concentrations of virus could lead to effective oncolysis even in the presence of neutralising samples, experiments were performed, where the amount of virus was titrated against a dilution series of sample. Only Ad5 and Ad11 were studied in these experiments, since previous results suggested exceedingly weak oncolysis by Ad3, even at very low concentrations of neutralising fluids (Figure 5-9). Due to a relatively large volume of exudate required for these experiments, the number of available samples was limited. Five different samples were examined, pooled serum from 20 healthy donors (pool20), two pleural fluid samples and two samples of peritoneal origin. All had shown higher amounts of anti-Ad5 antibodies than anti-Ad11 antibodies in the ELISA assays discussed in section 5.2. Identical to previous experiments, all samples were heat treated at 56ºC for 25 minutes and cleared of particulates by centrifugation. Virus was incubated with dilutions of sample for 90 minutes before addition of cells and after 48 hours cell viability was assessed.

Figure 5-10 depicts the neutralisation pattern of the sample of pooled human serum expressed through the inhibition of oncolysis at different concentrations of sample over a dilution range of Ad5 or Ad11. The two graphs clearly show strong neutralising capacity even at concentrations of 100,000 vp/cell. 40% solutions of pooled serum sufficed to inhibit oncolysis by Ad11 and only 10% solutions were required to neutralise Ad5. These experiments were performed to attempt to estimate the amount of virus that would have to be used to overcome neutralisation in a clinical setting. To this end, oncolytic activity of different virus doses at a sample concentration of 10% was investigated. It was estimated that, in a clinical setting, body cavity drainage and rinsing protocols prior to virus treatment might be able to reduce fluid concentrations to this level. Figure 5-11 shows the oncolytic activity of Ad5 and Ad11 at 10% of different malignant exudate samples or in the absence of exudate over a range of virus particle concentrations. The overall high neutralising capacity of samples and the pattern of higher neutralising capacity

against Ad5 in comparison to Ad11, as described in section 5.3.2, were corroborated in this study. In general, at least 1,000- to 10,000- or 100- to 1,000-fold more Ad5 or Ad11, respectively, was required to mediate oncolysis at a concentration of 10% malignant exudate than in the absence of exudate. Indeed, for most samples a concentration of 10,000 vp/cell of Ad5 was not able to overcome neutralisation at this sample concentration. Overall, these results indicate that around 10-fold less Ad11 than Ad5 might be required for oncolytic efficacy. Notably, the differences in oncolytic activity of Ad5 and Ad11 in the absence of neutralising fluids were much smaller than the differences observed in the presence of fluids. This highlights the fact that the differential lytic activities observed in these neutralisation studies were not due to inherent differential activity of these two serotypes in A549 cells (compare chapter 3).

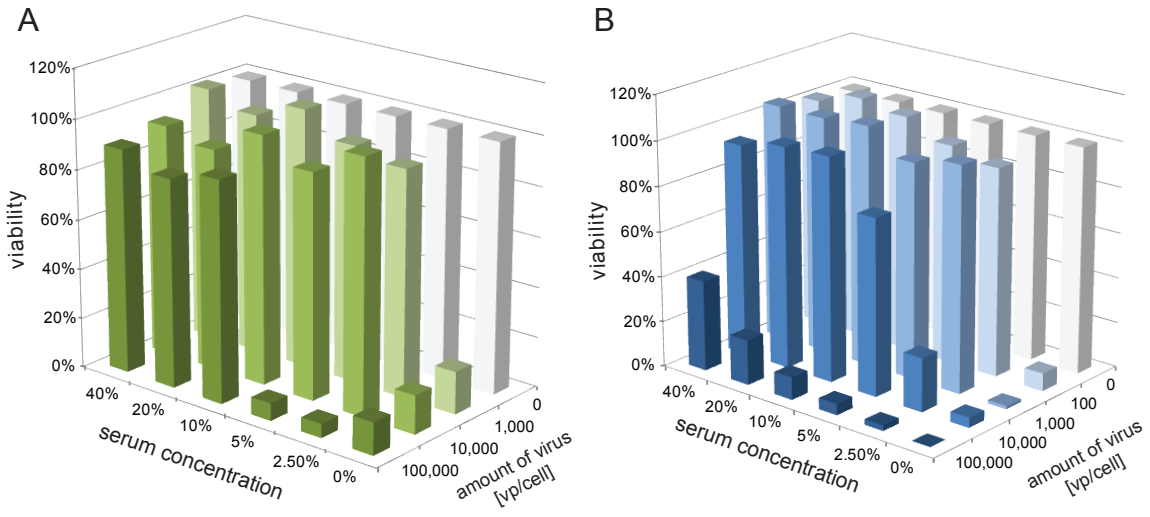


Figure 5 - 10 Effect of increasing virus doses on neutralisation by pooled serum

To investigate whether the use of higher concentrations of virus could lead to effective oncolysis even in the presence of neutralising samples, experiments were performed, which titrated the virus amount against a dilution series of sample (pool20, section 2.4.4). The graphs show the viability of A549 cells incubated for 48 hours with logarithmic dilutions of Ad5 (A) or Ad11 (B), which had been preincubated with sample dilutions of 40%, 20%, 10%, 5% or 2.5% in growth medium (means of triplicate measurements).

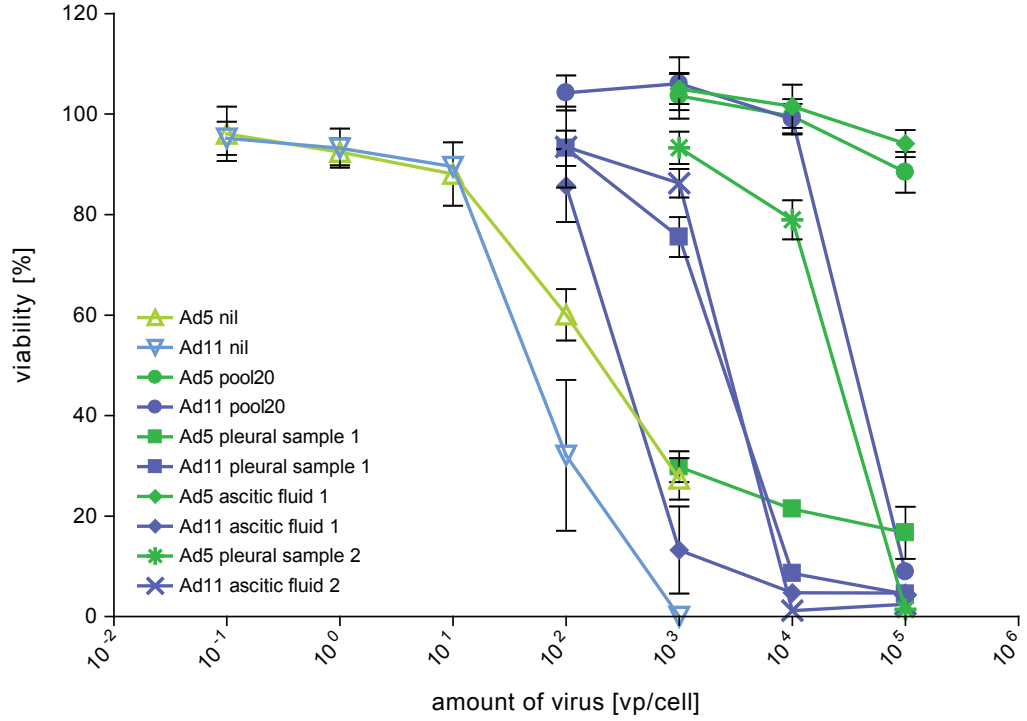


Figure 5 - 11 Overcoming neutralisation of 10% exudate by increasing virus doses

As it was thought that in a clinical setting cavity drainage and rinsing protocols before virus treatment could be able to reduce fluid concentrations to a level equivalent to 10% of exudate, the oncolytic activity of different virus doses at this concentration was investigated. Five different samples were examined: pooled serum from 20 healthy donors (pool20), two pleural fluid samples (pleural sample 1 and 2) and two samples of peritoneal origin (ascitic fluid 1 and 2). The graph shows the viability of A549 cells incubated for 48 hours with logarithmic dilutions of Ad5 (green) or Ad11 (blue), which had been preincubated with a 10% dilution of sample in growth medium (dark colours) or growth medium only (nil, light colours) (means of triplicate measurements and standard deviations).

5.3.4 Discussion

Several published studies have investigated the neutralising capacity of human fluids and the majority were using surrogate endpoint markers, such as transgene expression (Vogels *et al.*, 2003; Nwanegbo *et al.*, 2004; Thorner *et al.*, 2006), to determine the amount of pre-existing antibodies and extrapolated the effect on oncolytic efficacy from these results. Since vector constructs of Ad3 and Ad11 were not available, wild-type adenoviruses were used for the study described here. This might indeed be a more realistic model to assess the neutralising capacity of clinical samples, as it remains unclear how much influence the presence of antibodies exerts on virus replication and cytotoxicity. Using a CMV promoter-driven transgene signal as a surrogate neutralisation readout might underestimate neutralisation effects on virus assembly and cell lysis.

The experiments described in this section were performed using virus amounts according to their particle number rather than values normalised for their P/I ratio. This approach was thought to be more appropriate to assess the amount of neutralising antibodies, as antibody-mediated neutralisation was assumed to occur on a particle basis, i.e. actual amount of epitopes present. In order to minimise the effect of differing oncolytic activity of the different serotypes on cell lines it was, therefore, decided to use A549 cells in these assays, which had shown very similar susceptibility to oncolysis for all three serotypes (section 3.2).

Overall, it was demonstrated that the tested samples had high neutralising capacity towards all evaluated Ad serotypes, as concentrations of samples lower than 10% efficiently neutralised oncolysis for the majority of samples. However, it appeared that at lower sample concentrations Ad11 was less neutralised than Ad3. Experiments to explore if this could translate into a clinical advantage showed that Ad11 might achieve efficiency at a 100- to 1,000-fold lower dose than Ad5.

5.4 Antigen specificity of anti-Ad antibodies

Identification of the most immunogenic proteins of adenovirus is an important component of the development of improved virotherapy. Once main epitopes have been determined, strategies to selectively alter these through genetic engineering or physical shielding may improve pharmacokinetics and result in higher efficacy. This would, in turn, allow a decrease in the required therapeutic dose and result in lower side-effects. It has previously been reported that anti-Ad5 antibodies react with the three major capsid proteins fibre, penton and hexon (Hong *et al.*, 2003; Sumida *et al.*, 2005). We were interested to investigate if clinical samples displayed the same pattern of antibody specificity for Ad3 and Ad11. This might help future research to design methods to overcome neutralisation in a serotype-specific manner.

The following experiments describe the development and results of a method to examine the amount of antibodies directed against the different proteins of the adenovirus particle. Virions of Ad3, Ad5 and Ad11 were subjected to SDS gel-electrophoresis under reducing conditions and heat-inactivated patient samples (the analyte) used as primary antibody mixtures. The amount of bound protein-specific antibodies was detected with an anti-human IgG HRP-labelled secondary antibody, incubation with ECL and X-ray film exposure. Band intensities were quantified as a measure of the amount of bound primary antibodies.

5.4.1 Method development and optimisation

5.4.1.1 Gel electrophoresis migration patterns and protein identification

In order to establish if protein migration patterns of the three serotypes differed $2.5x10^9$ vp/lane of Ad3, Ad5 or Ad11 were subjected to electrophoresis on gradient TRIS-HCl gels under reducing conditions and proteins detected by silver stain (section 2.4.5) (Figure 5-12). Protein molecular weights were assigned according to their position in relation to molecular weight marker ladders. Because of a lack of published data for Ad3 and Ad11 protein migration patterns, it was not possible to determine band identity apart from correlation to Ad5 proteins, which was hampered by the multitude of bands detected for all three serotypes. Overall, while proteins of Ad3 and Ad11 showed very similar migration, bands of Ad5 appeared to display a different pattern. It appeared that the hexon protein of Ad5 migrated slightly further than hexon of Ad3 or Ad11. Also, the distribution of bands around the molecular weight where the penton and fibre proteins would be expected was different for the different serotypes.

Due to these uncertainties regarding the identity of protein bands, further gels were prepared to be analysed by mass-spectrometry (section 2.4.6). For this gels had to be stained with the less sensitive Coomassie stain, which resulted in a reduced number of visible bands (Figure 5-13). Notably, intensity of bands was different after the Coomassie stain than after silver stain. For instance, while not detected with the silver stain, a band at 20 kD was visible after Coomassie stain. Bands were excised from the gel and analysed by mass-spectrometry (LC-MS/MS was performed by Georgina Berridge / Rod Chalk (Structural Genomics Consortium, University of Oxford)). Detected peptide sequences were compared to a database of 185 Ad protein sequences and protein hits accepted according to data interpretation described in section 2.4.6. A total of two gels were analysed and hits were nearly identical. Figure 5-14 shows the allocation of these protein hits to the bands on the Coomassie stained gel. The band pattern and identity of Ad5 was in accordance to previously published results (Blanche *et al.*, 2001). For some bands at low molecular weight and at locations were bands clustered together or were not efficiently separated, more than one significant protein match was found. Overall, migration patterns of proteins from the different serotypes were similar with the exception of the penton

base protein, which migrated further when of Ad3 or Ad11 in comparison to Ad5 origin. Identification of the location of the fibre protein was of particular interest in these experiments as it had been reported that the fibre of Ad11 was of shorter size, and accordingly lower molecular weight, than the Ad5 fibre (Mei *et al.*, 2003). Notably, fibre protein could only be identified in the Ad11 lane. However, it did, indeed, appear to migrate further than the Ad5 equivalent, which would be expected at around the location of protein IIIa.

5.4.1.2 Protein transfer and western blotting

Proteins were electro-transferred onto a nitrocellulose membrane and efficient transfer verified with the reversible Ponceau stain. Apart from the general lane pattern, only hexon, the most abundant protein, could be observed with this method (data not shown). Membranes were then cut into pieces with each piece containing one lane of Ad3, Ad5 and Ad11. Subsequently, membranes were incubated with a 1:100 dilution of a selection of different samples: pooled serum from 20 healthy donors (pool20), which would be used as a standard, to be able to compare band densities between different gels in the subsequent screening study, and two ascitic fluid samples (asc1, asc2). After overnight incubation the membranes were probed with an anti-human-IgG antibody coupled to HRP, developed through addition of ECL and chemiluminescence detected by exposure to X-ray film (Figure 5-15). Overall, it could be observed, that this method gave high signal with low background noise, and that detected bands were specific for individual samples, indicating that binding of the secondary detection antibody was primary antibody dependent. This experiment also highlighted the need to reduce loading volume of virus solutions before electrophoresis in order to decrease the risk of overspill into neighbouring lanes as seen in lanes incubated with pool20 and asc2. Interestingly, Ad5 showed distinctly stronger bands in the area between 75 and 50 kD, whereas this pattern could not be observed for the other serotypes with any of the tested samples. This was similar to the pattern of proteins detected by silver staining (Figure 5-12). It was important to clarify if these additional bands were a characteristic inherent to Ad5 or if the batch of Ad5 used in this experiment was contaminated with non-adenovirus proteins, possibly from its producer cell line, which could potentially lead to unspecific binding of sample antibodies or the detection antibody. Hence, another gel was prepared comparing the batch described above (Ad5) to one batch

prepared in house by a colleague (Ad5a) and another company bought batch (Ad5b). Figure 5-16 shows a silver stain of the gel containing the three different Ad5 preparations. Band profiles were identical for the three tested Ad5 batches. As no difference in protein content between the three batches could be observed, it was unlikely that the additional bands of Ad5 in comparison to the other serotypes on the Western blot were caused by contamination of the Ad5 batch. Hence, the additional signals appeared to be caused by specific antibodies in the tested patient samples.

Further development experiments were concerned with equalising the amount of protein per lane for the different serotypes. As the analyte was the antibody content of patient samples directed at the different proteins of the three serotypes, it was important to guarantee the same amount of target Ad protein (i.e. epitope amount) in each lane to make comparison between serotypes possible. While, in the first experiments, Ad was loaded on gels according to particle number of the serotypes as determined by PicoGreen® assay, it was decided to equalise the amount of protein according to densitometry values of their respective hexon bands after silver staining. Equivalent strength of silver staining would be expected for similar amounts of hexon protein for each virus particle of the different serotypes. Hence, densitometric analysis of hexon bands of gels loaded with equal numbers of vp of Ad3, Ad5 or Ad11 were performed. These values were then used to adjust the vp number per lane to achieve equal amount of hexon for all three serotypes. Figure 5-17 A shows a silver stained gel of one set of lanes of Ad3, Ad5 and Ad11 loaded to obtain equal virus particle number per lane and a second set of lanes where the serotypes were loaded after adjusting their amount to obtain equal hexon protein amount. Quantification of protein amount through densitometry of hexon bands showed that the amount of protein per lane was significantly different between Ad3 and Ad5 ($p < 0.05$) for lanes loaded according to vp number whereas there were no differences for lanes loaded with vp numbers adjusted for hexon band density (Figure 5-17 B).

As the main method of analysis in this study was densitometry of band intensity, it was necessary to determine, which dilution of patient sample should be used to ensure that none of the bands would be saturated by analyte, i.e. band density would not correlate to antibody

amount. To this end, membranes were incubated with a dilution range of pooled human serum (pool20) (i.e. primary antibody) and band densities assessed. Pool20 was chosen as this sample had shown high antibody content against all three serotypes in the ELISA studies (section 5.2). Figure 5-18 A shows the Western blot of this experiment. Increasing band intensity could be observed for increasing concentrations of patient sample. Densitometric analysis of indicated bands revealed that this rise was linear until a dilution of 1:100 (Figure 5-18 B). At the lower dilution of 1:50 band intensity of two bands of Ad5 seemed to be lower than at the 1:100 dilution. Importantly, some bands begin to disappear at dilutions higher than 1:100. From these results it was decided to use a dilution of 1:100 of patient samples in this study in order to minimise the risk of saturating signals while allowing detection of low amounts of antibodies.

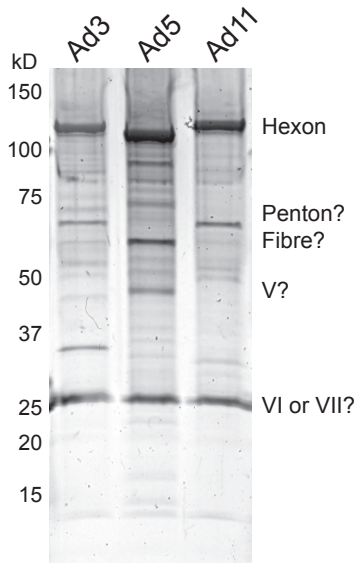


Figure 5 - 12 Silver stain

In order to establish the protein migration patterns of Ad3, Ad5 and Ad11 $2.5x10^9$ vp/lane of each serotype were subjected to electrophoresis on TRIS-HCl gradient gels under reducing conditions and proteins detected by silver stain (section 2.4.5). The figure shows identity of proteins estimated from their band position in correlation to molecular weight markers.

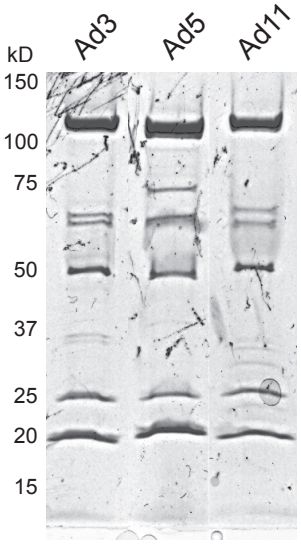


Figure 5 - 13 Coomassie stain

For analysis by mass-spectrometry separated proteins had to be stained with Coomassie stain. $2.5x10^9$ vp/lane of Ad3, Ad5 and Ad11 were subjected to electrophoresis on TRIS-HCl gradient gels under reducing conditions before detection with the Coomassie stain (section 2.4.5). The figure shows band migration patterns of Ad3, Ad5 and Ad11 and molecular weights.

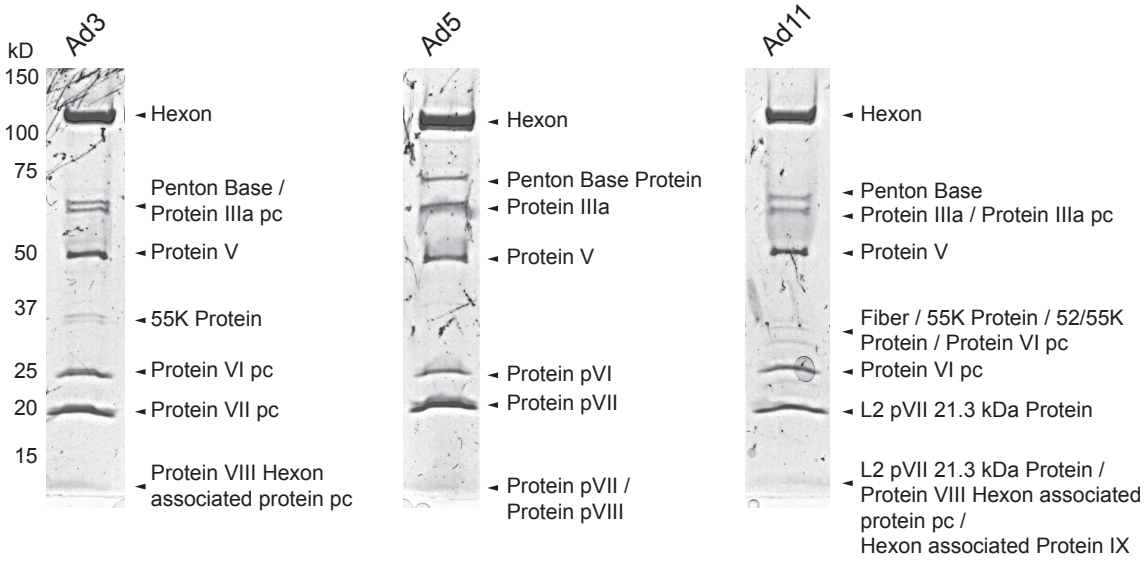


Figure 5 - 14 Identity of protein bands on Coomassie-stained adenovirus gels

Protein bands were excised from Coomassie stained gels prepared as described in Figure 5-13 and prepared for and analysed by mass-spectrometry (section 2.4.6). LC-MS/MS was performed by Georgina Berridge / Rod Chalk (Structural Genomics Consortium, University of Oxford). Detected peptide sequences were compared to a database of 185 Ad protein sequences. Protein hits were accepted according to data interpretation described in section 2.4.6. The figure shows the location and identity of determined bands for Ad3, Ad5 and Ad11 (pc: precursor; cumulative results from two seperately analysed gels).

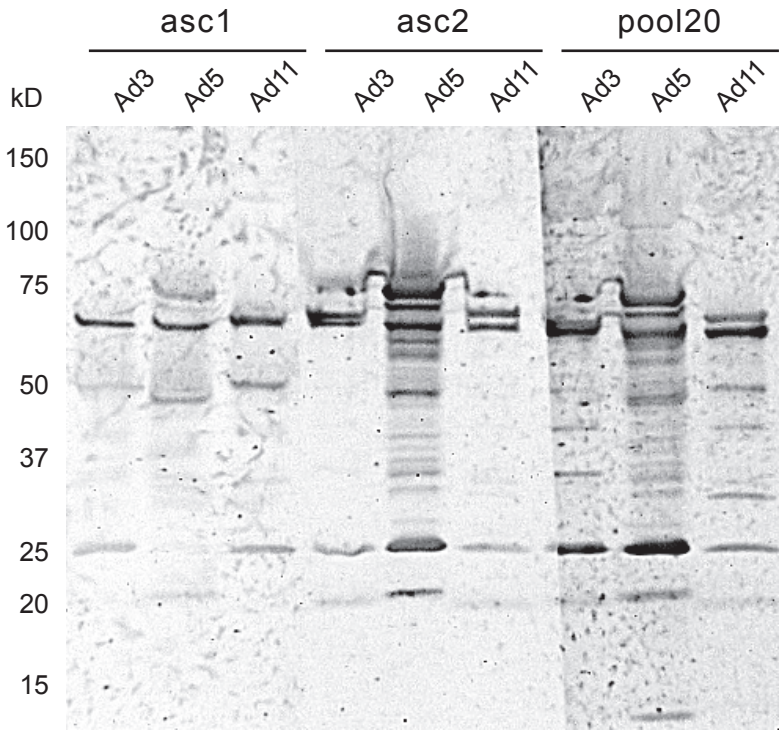


Figure 5 - 15 Western blot of separated adenovirus proteins detected by exudates

After separation of Ad3, Ad5 and Ad11 proteins by electrophoresis under reducing conditions proteins were electro-transferred onto a nitrocellulose membrane. Subsequently, membrane pieces containing one lane of each Ad3, Ad5 and Ad11 were incubated with 1:100 dilutions of different samples: pooled serum from 20 healthy donors (pool20), which would be used as a standard to be able to compare band densities between different gels in the subsequent screening study, and two ascitic fluid samples (asc1, asc2). After overnight incubation the membranes were probed with an anti-human-IgG antibody coupled to HRP, developed through addition of ECL and chemiluminescence detected by exposure to X-ray film (compare section 2.4.5).

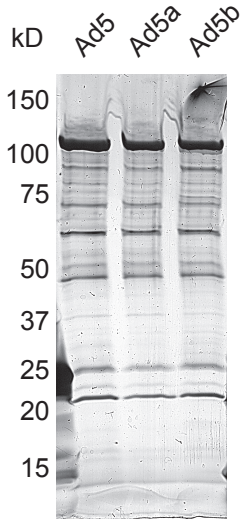


Figure 5 - 16 Purity of Ad5 preparation

Proteins of three different Ad5 preparations (originally used batch (Ad5), a batch prepared in house by a colleague (Ad5a) and a company bought batch (Ad5b)) were separated by electrophoresis under reducing conditions. Bands were detected by silver stain (section 2.4.5). Band profiles were identical for the three tested Ad5 batches by visual comparison.

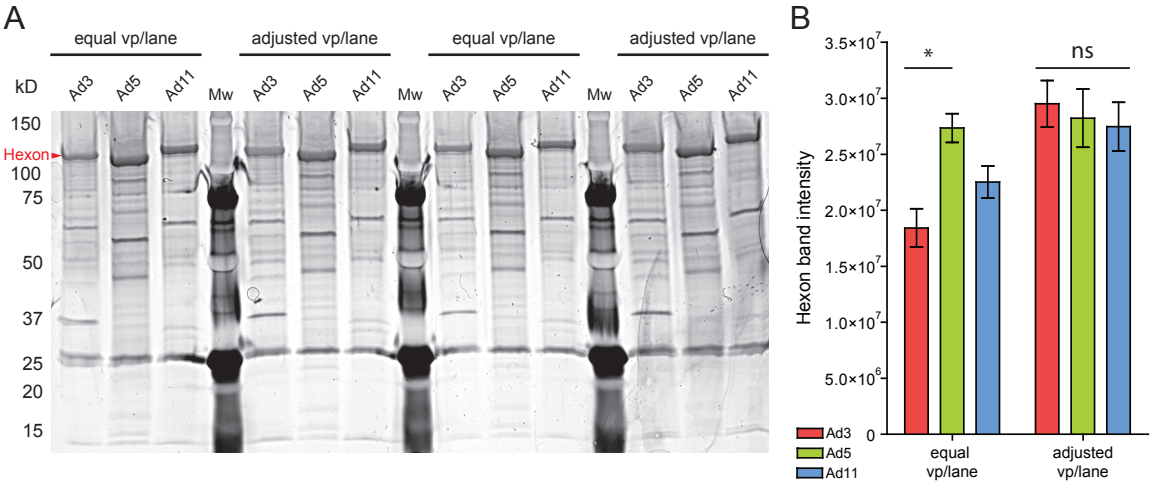


Figure 5 - 17 Equalisation of protein amount per lane

In order to establish equal protein content of lanes of Ad3, Ad5 and Ad11 reducing gels were prepared by loading lanes with either equal amount of vp (equal vp/lane) or amount of vp adjusted to give equal amount of hexon protein (adjusted vp/lane) of the three serotypes. After electrophoresis gels were sliver stained (A) and optical density of hexon bands determined (B) (compare section 2.4.5, B: means of duplicate measurements and standard deviations; statistical analysis: one-way ANOVA with Tukey's post-tests (* = $p < 0.05$, ns = not significant)).

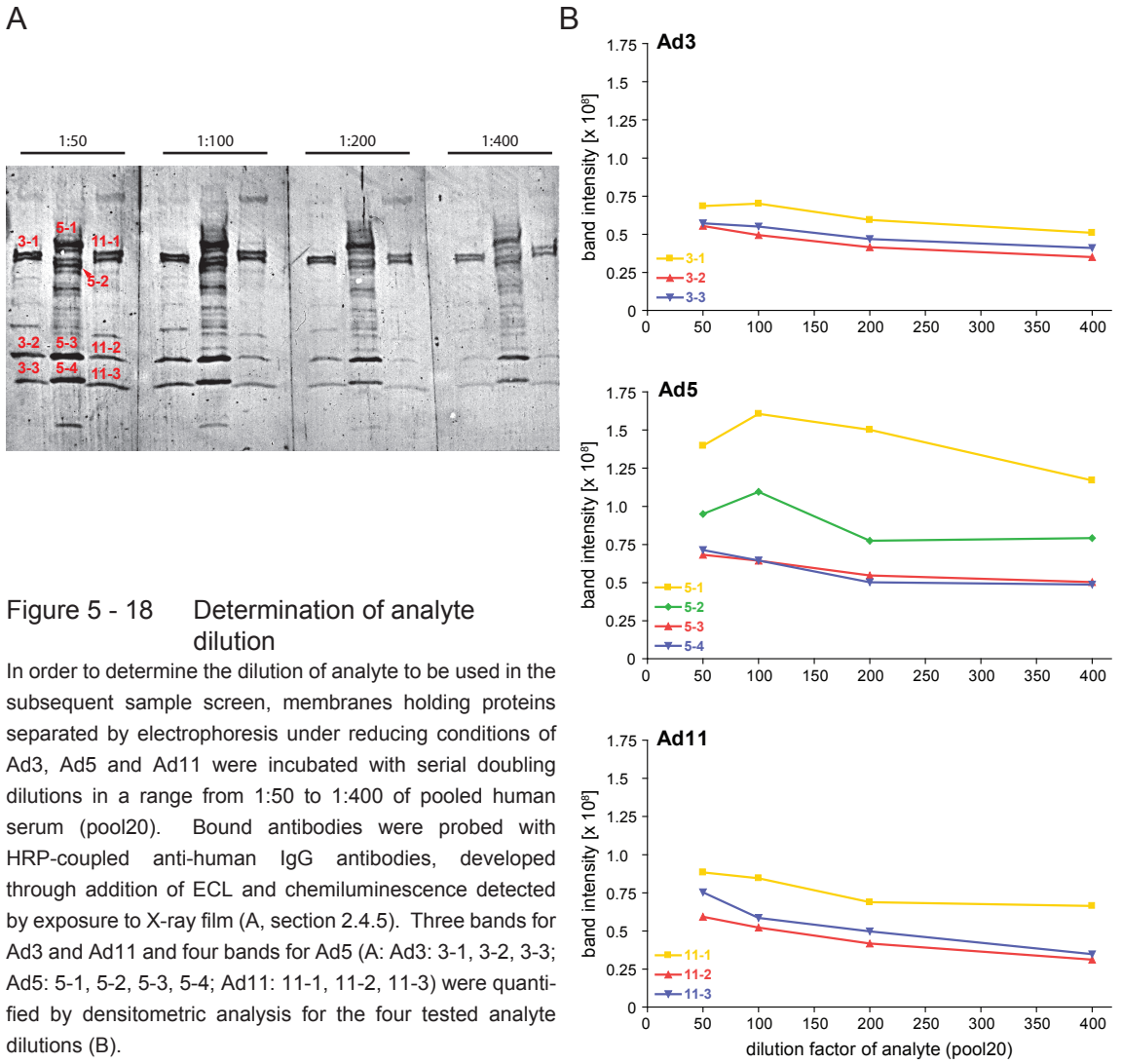


Figure 5 - 18 Determination of analyte dilution

In order to determine the dilution of analyte to be used in the subsequent sample screen, membranes holding proteins separated by electrophoresis under reducing conditions of Ad3, Ad5 and Ad11 were incubated with serial doubling dilutions in a range from 1:50 to 1:400 of pooled human serum (pool20). Bound antibodies were probed with HRP-coupled anti-human IgG antibodies, developed through addition of ECL and chemiluminescence detected by exposure to X-ray film (A, section 2.4.5). Three bands for Ad3 and Ad11 and four bands for Ad5 (A: Ad3: 3-1, 3-2, 3-3; Ad5: 5-1, 5-2, 5-3, 5-4; Ad11: 11-1, 11-2, 11-3) were quantified by densitometric analysis for the four tested analyte dilutions (B).

5.4.2 Sample screen

After establishing protocols and conditions (as described in section 5.4.1) 21 pleural effusion and 6 ascitic fluid samples from patients with varying primary malignancies were analysed for their patterns of antigen specificity. Images, as exemplified in Figure 5-19 A, were used for densitometric analysis of bands. Overall, a distinctly different pattern and lower amounts of antibodies against proteins from Ad3 and Ad11 in comparison to Ad5, displayed through lower band densities and lower number of bands detected, could be observed on most blots.

After cumulating observations made on all blots, a set of band locations to be analysed for each of the serotypes was established (Figure 5-19 B). When bands were present at these locations their intensity was quantified by densitometric analysis (with appropriate background correction). To be able to compare values from all blots, it was necessary to correct via a standard sample. To this end, the band intensities of proteins incubated with pool20 on each of the blots were equalised and the resulting factors for each band was used to normalise values of bands incubated with the patient samples. This procedure would help to minimise variations, caused by differences in incubation times and exposure to X-ray films, between blots prepared on different days. Figure 5-20 A shows the normalised intensities of detected bands for each designated band location for each of the serotypes. As it had been established that equal amounts of capture proteins were present for each of the serotypes (see section 5.4.1.2 and Figure 5-17) comparison of intensities, as a measure of the amounts of antibodies against the different serotypes, was possible. Overall, it appeared that patient samples held more antibodies directed against Ad5 than Ad3 or Ad11 proteins.

By alignment of images of Coomassie-stained gels used for the mass-spectrometry analysis (section 5.4.1.1) with Western blots according to molecular weight marker migration the identity of bands detected on blots was determined. This was hampered by the low number of bands visible after Coomassie stain and, subsequently, identified by mass spectrometry. Notably, gel resolution did not allow identification of the location of the fibre protein band of Ad5. Furthermore, for some bands more than one significant protein match was found (Figure 5-14).

For proteins with unambiguously determined identity direct comparison of antibody amount against (and accordingly immunogenicity of) specific proteins of the different serotypes was performed. Corresponding to Figure 5-19 B, these bands were hexon (band 1 for Ad3, Ad5 and Ad11), protein V (Ad3: band 4, Ad5: band 8, Ad11: band 5) and protein pVI (Ad3: band 8, Ad5: band 12, Ad11: band 9). Figure 5-20 B shows the normalised intensity of bands representing these three proteins of the three serotypes investigated. Surprisingly, the amount of antibodies directed against hexon was very low in comparison to some other proteins, in contradiction to previous reports (Sumida *et al.*, 2005). However, it has been hypothesised that hexon-specific antibodies might be predominantly directed towards epitopes which are conformation-sensitive (Hong *et al.*, 2003), which would have been modified in the denaturing electrophoresis system used in this study. Hence, amounts of antibodies directed against hexon of the three serotypes were not significantly different. For both identified structural proteins V and VI significantly more antibodies were directed against proteins from Ad5 than Ad3 or Ad11 ($p < 0.01$ or $p < 0.001$).

Previous reports had established the molecular weights of the penton base and fibre proteins of all three investigated serotypes. Hence, although the identity of bands representing these two proteins for all three serotypes could not be determined by mass spectrometry, their location was inferred from the expected migration pattern according to published molecular weights (Table 5-1). From a total of four bands detected in the range between 65 and 60 kD after incubation with pool20 two bands had higher intensity. Due to previous reports of their capacity to elicit antibody production (Hong *et al.*, 2003) and their reported molecular weight difference the heavier and lighter band were determined to be penton base protein and fibre, respectively. However, as complete resolution of this area could not be ensured in all analysed immunoblots the possibility of additional signal from antibodies directed against protein IIIa could not be excluded. Hence, graphs comparing the amount of antibodies directed against penton base and fibre for the Ad3, Ad5 and Ad11 show the intensities of two bands for each of the proteins for Ad5 (Figure 5-20 C).

Overall, the amount of antibodies directed against the penton base appeared to be higher than against fibre for both Ad3 and Ad11. Comparing amounts between serotypes revealed that more samples seemed to hold higher amounts of antibodies directed against Ad5 fibre, irrespective of combining the intensities from the pairs of bands (bands 5 + 6), than against Ad3 or Ad11.

In conclusion, these results suggest that, in addition to the major capsid proteins hexon, penton base and fibre, other structural Ad proteins are good antigens for stimulation of antibody development. Overall, the number of samples showing higher antibody amounts against Ad5 was greater than for Ad3 or Ad11. Proteins of these two serotypes displayed a very similar pattern of immunogenicity.

Table 5-1 Molecular weights and immunoblot locations of penton base and fibre proteins

		Ad3	Ad5	Ad11
penton base	**molecular weight**	60 kD (Fender *et al.*, 2005)	63.296 kD (Rux and Burnett, 2004)	62.3 kD (Stone *et al.*, 2003)
	corresponding immunoblot band in Figure 5-19 B	3	3 / 4	3
fibre	**molecular weight**	34.8 kD (Signas *et al.*, 1985)	61.96 kD (Rux and Burnett, 2004)	36.2 kD (Stone *et al.*, 2003)
	corresponding immunoblot band in Figure 5-19 B	6	5 / 6	7

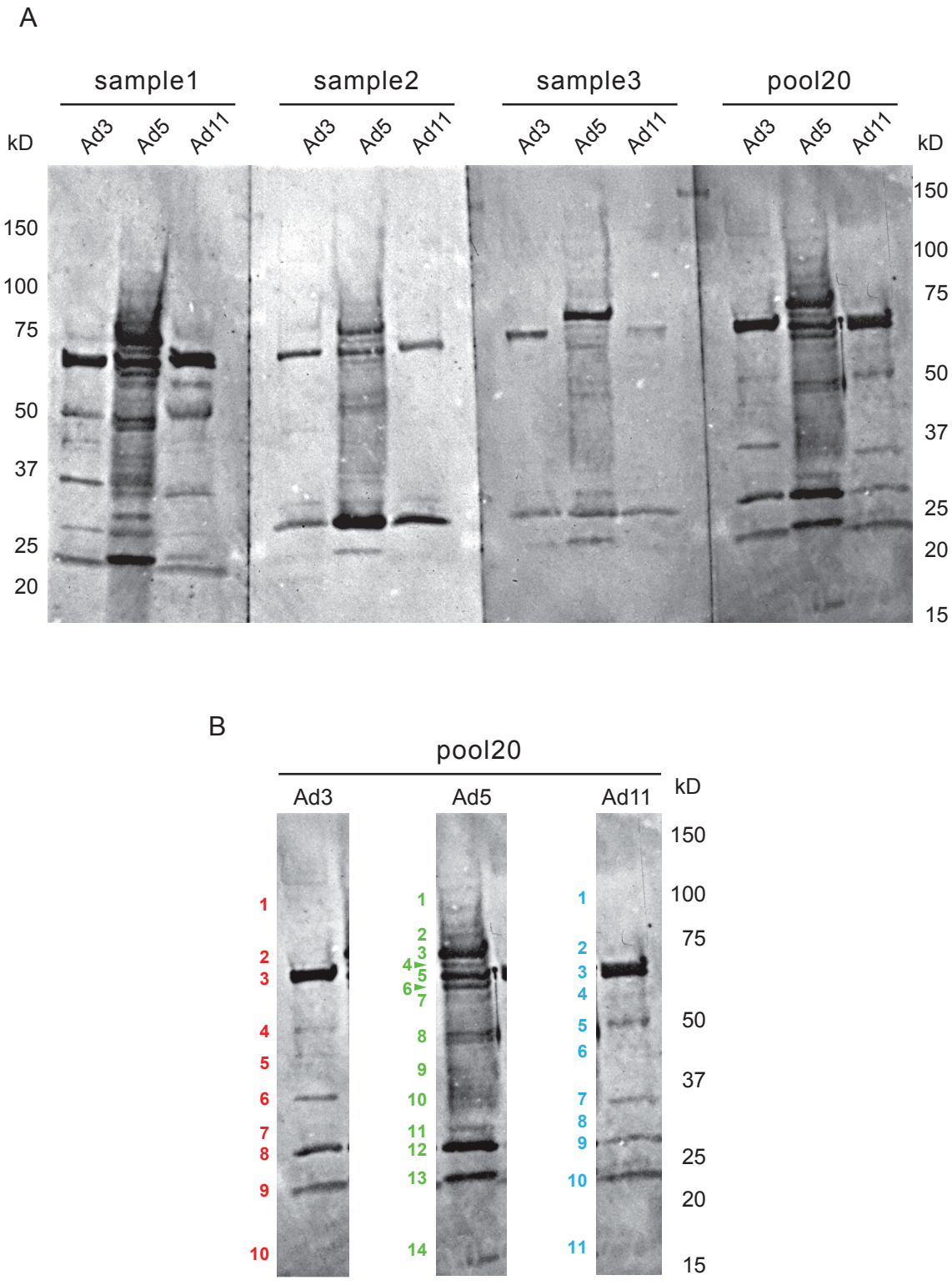


Figure 5 - 19 Western blot example of the sample screen

After establishing protocols and conditions as detailed in section 5.4.1 pleural exudate samples (n = 21) from patients with varying malignant diseases and samples of ascitic fluid (n = 6) from patients with ovarian cancer were analysed for their patterns of antigen specificity. A shows an example of a set of Western blots incubated with three different patient samples (sample1 - 3) or pooled human serum (pool20). After cumulating observations made on blots of all tested samples a set of band locations to be analysed by densitometry for each of the serotypes was established as exemplified on the blot incubated with pool20 from A (B). Ten band locations for Ad3, 14 for Ad5 and 11 for Ad11 were found to be prevalent across all blots. Images as shown in A were used for densitometric analysis of bands (section 2.4.5).

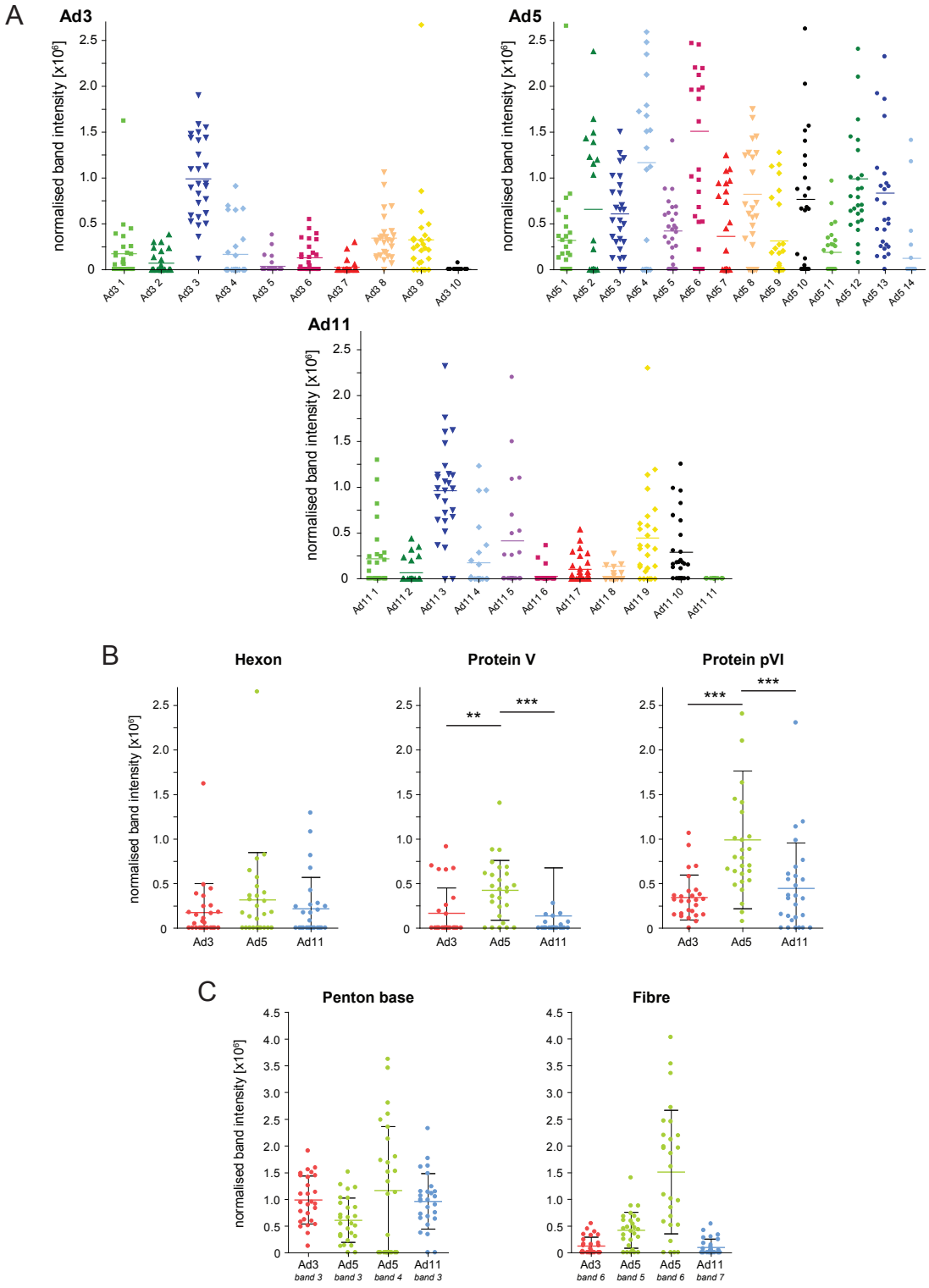


Figure 5 - 20 Comparison of antibody amounts against proteins of Ad3, Ad5 and Ad11

Intensities of bands at designated locations (Figure 5-19) were quantified by densitometry and corrected via a standard that had been used on all blots in order to minimise variations between blots (A). By alignment of images of Coomassie stained gels used for mass-spectrometry analysis (Figure 5-14) with Western blots the identity of three band locations could be determined (Hexon (band 1 for Ad3, Ad5 and Ad11), Protein V (Ad3: band 4, Ad5: band 8, Ad11: band 5) and Protein pVI (Ad3: band 8, Ad5: band 12, Ad11: band 9)) (B). For penton base and fibre the correct bands were inferred from their position corresponding to molecular weight markers. Due to low resolution, for Ad5, two bands for each penton base and fibre were likely to represent these proteins (C). The graphs show the normalised intensity of bands (individual band intensity of each sample, means of intensities and standard deviations; B: statistical analysis: Kruskal-Wallis test with Dunn's multiple comparison test (*** = $p < 0.001$, ** = $p < 0.01$)).

5.5 Conclusion

Twenty-eight samples of exudates from cancer patients have been examined for their antibody content and neutralising capacity towards Ad3, Ad5 and Ad11. ELISAs measuring whole antibody content revealed that samples contained more antibodies towards Ad3 than Ad11. Oncolysis inhibition assays, to investigate neutralising capacity of antibodies, demonstrated greater neutralisation of Ad3 and Ad5 than Ad11 in accordance with previous studies using serum from healthy volunteers (Vogels *et al.*, 2003). Importantly, however, solutions containing less than 10% of sample were able to effectively neutralise all three serotypes for the majority of samples, demonstrating that all samples tested had high neutralising capacity towards all Ad serotypes evaluated, contradicting previous results (Vogels *et al.*, 2003). The lower neutralisation of Ad11 was only apparent at concentrations of 2.5%, 1.25% and 0.625% of samples. It does, indeed, appear that the use of serum samples from healthy volunteers does not completely mirror observations made with malignant exudates. These may have other components that enhance neutralising capacity, such as C-reactive protein and increased levels of soluble forms of CD46 shed by tumour cells (Bjørge *et al.*, 2005), which could act as decoys, reducing the amount of virus available for infection.

Overall, these data suggest that the use of Ad11 may be advantageous over Ad3 or Ad5 in situations where the level of endogenous neutralisation has been reduced. Some clinical protocols may permit reduction of neutralising capacity by fluid drainage and subsequent washing of the peritoneal or pleural cavity before application of the therapeutic virus. It is unclear, if these procedures could lower antibody concentrations to an extent, where advantages of certain serotypes could be relevant. Nevertheless, it appears that, in the light of an overwhelming neutralising capacity of all screened samples, body cavity wash-out would be required for therapeutic protocols with these adenovirus serotypes.

Notably, it could be demonstrated that around 100- to 1,000-fold less Ad11 than Ad5 might be required for oncolytic efficacy in an environment of reduced neutralisation. In a clinical setting this difference could be of great significance, since lower virus input would presumably lead to

lower particle-mediated side-effects, increasing patient safety, and, furthermore, would reduce virus production and patient therapy costs.

While it had been questioned whether the amount of antibodies present in samples was correlated to and could, indeed, be predictive for their neutralising capacity, comparison of results from ELISAs (section 5.2) and oncolysis inhibition assays (section 5.3) did not show a linear relationship (data not shown). Hence, it appears that total antibody amount is not predictive of neutralising capacity of samples and functional assays are necessary to estimate the neutralisation status of patients.

In order to improve protection of possible future virotherapy agents derived from serotypes other than Ad5, the patterns of antigen specificity of antibodies directed against Ad3, Ad5 and Ad11 were investigated with an immunoblot system. It has previously been shown that both Ad3 and Ad11 differ from Ad5 in their structural proteins. For example, both serotypes have considerably shorter fibre length than Ad5 (Signas *et al.*, 1985; Stone *et al.*, 2003). It was unclear, how this would influence their immunogenicity and if Ad3 and Ad11 would show the same high prevalence of antibodies directed towards the three major capsid proteins fibre, penton and hexon as Ad5 (Hong *et al.*, 2003; Sumida *et al.*, 2005). Corroborating the results from the ELISA system and the oncolysis inhibition assays, it appeared that patient samples contained more antibodies directed against Ad5 than Ad3 or Ad11 proteins. The strong immunogenicity of hexon, which had been reported previously (Sumida *et al.*, 2005), was not observed for any of the three serotypes, possibly due to the employed electrophoresis conditions. Analysis was hampered due to ambiguity of the location of the penton base and fibre bands of Ad5. However, results suggested that more samples appeared to hold higher amounts of antibodies directed against Ad5 than against Ad3 or Ad11 fibre. While significantly more antibodies were directed against the structural proteins V and VI from Ad5 than Ad3 or Ad11, differences in antibody amounts directed against the penton base protein of the different serotypes were not as pronounced. Notably, the penton base appeared to be more immunogenic than fibre for both Ad3 and Ad11, corresponding to observations made with Ad5 (Hong *et al.*, 2003).

It remains unclear to what extent the results reported in this chapter were influenced by cross-reactivity of antibodies between different serotypes. In this context, it has previously been demonstrated that the RGD motif of the penton protein, which is important for integrin-mediated uptake (Wickham *et al.*, 1993), is conserved throughout different Ad species (Arnberg, 2009), illustrating one possible site of antibody cross-reaction across serotypes. Due to the lack of samples, which were known to contain antibodies directed against one single adenovirus serotype only, this question could not be addressed further in the present study. However, if anti-adenovirus antibodies did indeed cross-react, this would impact on the usefulness of serotype-switch protocols to increase clinical efficiency, highlighting the need of improved virus cloaking technologies (Fisher and Seymour, 2010).

6 Improved polymer coating to overcome barriers to *in vivo* adenovirus efficacy

6.1 Introduction

Apart from the use of alternative adenovirus serotypes coating of virions with hydrophilic reactive polymers has been explored to overcome prominent obstacles to *in vivo* oncolytic therapy such as antibody-mediated neutralisation, induction of inflammatory signalling and low target transduction. The two main chemical strategies are based on the use of polyethylene glycol (PEG) or poly(N-[2-hydroxypropyl]methacrylamide) (pHPMA) (Fisher and Seymour, 2010).

Modification of adenovirus with PEG-derived molecules has demonstrated partial resistance to neutralisation, improved pharmacokinetics and reduced immune stimulation in comparison to non-modified virus (reviewed in (Wonganan and Croyle, 2010)). In contrast to monovalent PEG-based polymers, pHPMA compounds are multivalent molecules which allow attachment of the polymer chain to multiple sites on the virus capsid. This is thought to allow tighter binding of HPMA polymers and thus better shielding of capsid epitopes and improved detargeting of coated adenovirus (Fisher and Seymour, 2010). Indeed, pHPMA coating has been shown to offer a degree of protection from antibody binding (Fisher *et al.*, 2001) and has displayed major advantages over non-coated Ad in terms of pharmacokinetics and bioavailability in murine *in vivo* models (Green *et al.*, 2008). Furthermore, in order to achieve greater target cell infection the natural tropism of adenovirus has been modified by covalent linkage of ligands such as the EGF-receptor inhibitor Cetuximab to the polymer shield (Morrison *et al.*, 2009). Hence, adenovirus coating with pHPMA may allow retargeting of the virus to chosen receptors, thereby improving target specific infection and enhancing patient safety through lower treatment doses and decreased side-effects. This was exemplified by reduced peritoneal adhesion formation, observed with polymer-coated Ad in a murine SKOV3 xenograft model of ovarian cancer, and was believed to result from attenuated interaction with non-target cells (Morrison *et al.*, 2008).

Although data generated with Ad coated with conventional pHPMA, which carries a slight net negative charge, have been promising, complete resistance to neutralisation could not be accomplished with these polymers (Fisher *et al.*, 2001). Therefore, optimisation of Ad cloaking

was necessary to allow efficient application in neutralising environments. The improved polymers discussed subsequently are derived from previously used HPMA polymers (Fisher *et al.*, 2001; Green *et al.*, 2008; Morrison *et al.*, 2009) and designed to provide better shielding of adenovirus epitopes.

The aims of the studies described in this chapter were to investigate whether coating adenovirus with improved polymers would give better shielding from neutralisation than coating with conventional polymers and whether improved coating would reduce adenovirus activity. The suitability of these novel polymers for the deployment of virotherapy in the treatment of ovarian cancer was examined through efficiency studies performed *ex vivo* in a panel of primary ovarian ascites samples.

6.2 Assessment of different polymer formulations

The polymers evaluated in the experiments presented here are derived from pHPMA which was given further functionality by the introduction of side-chains, which bear positive charges in the form of quaternary amines (QA). It was hypothesised that the addition of positive charges would allow tighter binding of the polymer to negatively charged areas of the virus capsid, especially hexon, which has been reported to be the antigen for the majority of neutralising antibodies (Sumida *et al.*, 2005). In addition, as a means to allow better release of the virion from its polymer cloak following cell entry, reducible disulfide bonds were incorporated into side-chains which covalently bind the polymer to the virus surface (reducible TT). After cell binding and internalisation these linkers should be cleaved in the reducing intracellular environment, restoring adenovirus functionality. These polymers were synthesised by chemists in the group of Prof Ulbrich, Institute of Macromolecular Chemistry, Prague and have previously been demonstrated to provide protection of adenovirus from binding by erythrocytes, coagulation factors and antibodies (Subr *et al.*, 2009).

Three positively charged polymers with different molar percentages of QA and one neutral polymer were assessed and the influence of presence or absence of reducible side-chains investigated in order to elucidate structure / function relationships and prioritise the best formulation for further development (Table 6-1, for chemical structure see 2.5.1).

Table 6-1 Panel of investigated polymers

ID	Reducible TT	QA (amount)
EC193	No	No
EC234	No	Yes (6.5%)
EC235	Yes	Yes (6.5%)
EC236	Yes	Yes (1.5%)

EC193 and EC234 were chosen to investigate how the presence of positive charges and, hence, tighter binding of the polymer to the virus capsid would decrease the activity of the coated virus. EC234 and EC235 should reveal if the presence of reducible TT would allow restoration of activity, due to better uncoating of virus following cell entry. EC236 was included in the panel to assess if a lower amount of QA groups would still provide protection from antibody-mediated neutralisation, whilst ameliorating possible deleterious effects on virus infection activity caused by higher QA levels present in polymers EC234 and EC235

6.2.1 Coating efficiency and virus activity

6.2.1.1 Ad5 capsid shielding

Virus (Ad5) was coated by incubation of aliquots of virus stock with aqueous dilutions (0.2, 1, 5, 20 mg/ml) of the different polymers (EC193, EC234, EC235 and EC236) for two hours at room temperature. In order to determine the concentrations of polymer solutions for virus coating, which would be required to yield efficient virus cloaking and protection of capsid proteins from antibody binding, an ELISA system was used (section 2.5.2). Briefly, wells of 96 well plates were coated with a polyclonal anti-adenovirus antibody and incubated with aliquots of the different virus preparations or non-coated virus (all $5x10^8$ vp/well) before detection of bound virus by a second polyclonal anti-adenovirus antibody.

Figure 6-1 shows the ELISA signal generated by captured virus which had been coated with the different polymer formulations at the tested concentrations. Ad5 coated with the neutral polymer EC193 gave the highest signal of all coated viruses at all polymer concentrations. This indicated that many capsid epitopes were left unshielded by this polymer and that it provided least protection against antibody binding of all investigated compounds. Introduction of QA groups markedly decreased virus capture. EC234, containing 6.5% QA, provided the highest protection of virus epitopes of all polymers, even at the lowest coating concentration of 0.2 mg/ml. The presence of reducible side-chains in EC235 and EC236 decreased shielding efficiency, possibly due to unspecific reduction of disulfide bonds and loss of linkage of these

side-chains to the capsid during the assay. EC236 (1.5% QA) and even EC235, despite containing the higher QA-amount of 6.5%, could only provide shielding similar to EC234 at concentrations of 5 mg/ml. However, at this concentration all positive polymers showed markedly improved protection of the virus capsid from antibody binding in comparison to the neutral polymer EC193. In order to provide best possible cloaking of the virus capsid while minimising the use of polymer it was decided to use coating concentrations of 20 mg/ml of EC193 and 5 mg/ml of EC234, EC235 and EC236 for subsequent experiments.

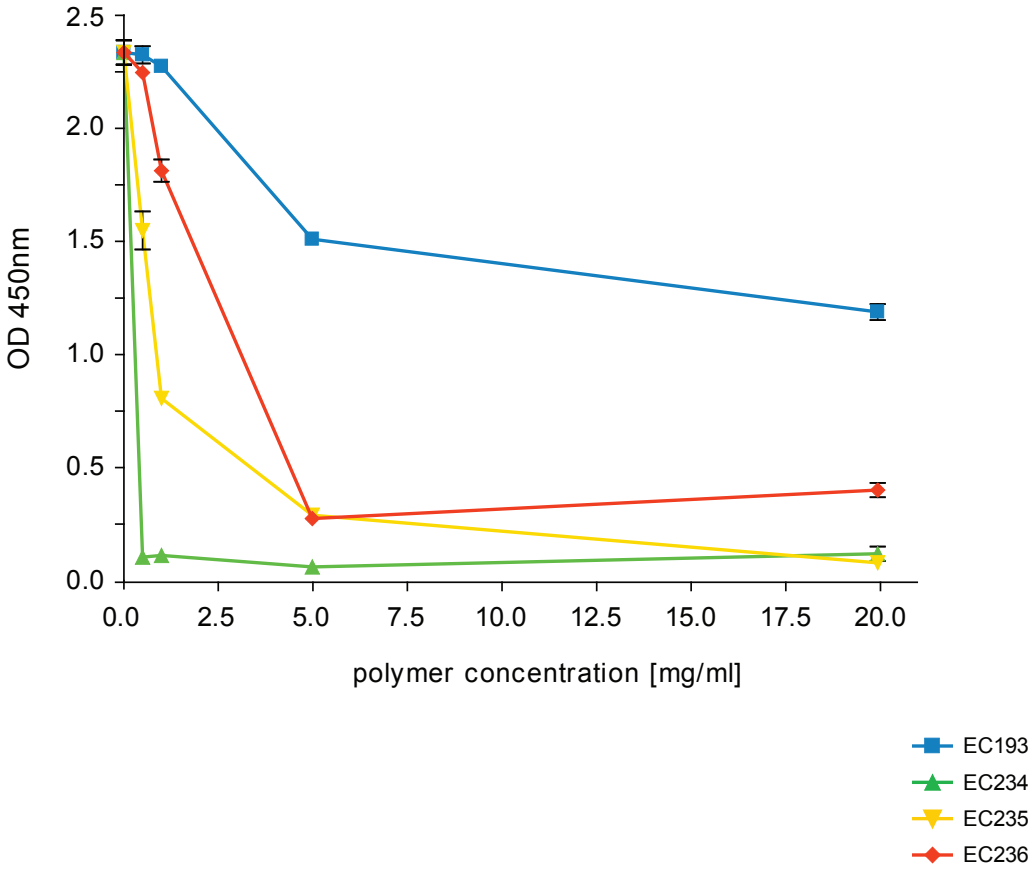


Figure 6 - 1 Determination of optimal polymer concentration for virus coating

Concentrations of polymer solutions required for efficient virus cloaking and protection of capsid proteins from antibody binding were determined with an ELISA system (section 2.5.2). Ad5 was coated by incubation of aliquots of virus stocks with aqueous dilutions (0.2, 1, 5, 20 mg/ml) of the different polymers (EC193, EC234, EC235 and EC236) for 2 hours at room temperature (section 2.5.1). The ELISA was prepared by coating wells of microplates with a polyclonal anti-adenovirus antibody followed by incubation with the different virus preparations or non-coated virus (all $5x10^8$ vp/well). After washing captured virus was detected by a second polyclonal anti-adenovirus antibody coupled to HRP and quantified by a chromogenic reaction. The graph depicts the measured optical density at 450nm (OD 450nm) after background subtraction (means of triplicate values and standard deviations).

6.2.1.2 Biological activity of polymer-coated Ad5luc

As shown in section 3.3.1 SKOV3 cells express little CAR on their surface. In the absence of serum this markedly restricts Ad5 internalisation. However, the addition of factor X (FX) to serum-free medium allows uptake of Ad5 into cells after binding of FX to hexon (Waddington *et al.*, 2008). Hence, on this cell line this mechanism can be used to assess how well a polymer has covered these hexon regions and indicate how efficiently coating ablates natural FX uptake mechanisms (Subr *et al.*, 2009). Furthermore, it has previously been demonstrated that the majority of antibodies against Ad are directed towards hexon proteins (Sumida *et al.*, 2005). Hence, this assay would also indicate how well the different polymers shield against antibody-mediated neutralisation.

For these studies, a non-replicating Ad5 vector expressing luciferase (Ad5luc, section 2.1.2) was coated with the different polymers at the concentrations determined by ELISA (see above). Then SKOV3 cells were incubated with the different virus formulations (500 vp/cell) in the presence and absence of FX in serum-free medium for 90 minutes and after incubation for another 24 hours in serum-positive medium luciferase expression was measured (Figure 6-2 A and B) (section 2.5.3).

As expected, in the absence of FX, luciferase expression after infection with non-coated Ad5luc was not significantly different from mock-treated cells. Equally, cells treated with virus coated with the neutral polymer EC193 and the two positive polymers with high QA content (6.5%; EC234 and EC235) did not exceed values from mock-treated cells. Surprisingly however, EC236-coated virus achieved significant transgene expression ($p < 0.01$ EC236 vs non-coated Ad5luc). The addition of FX (8 µg/ml) to the incubation medium significantly increased the expression of luciferase from non-coated virus ($p < 0.001$, 30-fold increase, Figure 6-2 A and B). Notably, values from the QA polymer-coated viruses remained similar to those measured in the absence of FX with the exception of EC236Ad, which demonstrated lower transgene expression in the presence than in the absence of FX. In contrast, the activity of EC193-coated Ad increased 5-fold upon FX addition. Hence, it appeared that all positively charged polymers, but not the neutral polymer, efficiently covered hexon and could abrogate FX-mediated infection.

To elucidate if the notable enhancement of luciferase expression by EC236 was SKOV3 specific and how it compared to expression in cells expressing higher levels of CAR (compare section 3.3.1) A549 cells were treated with the same Ad5luc formulations as described above (Figure 6-2 C). In contrast to SKOV3, on A549 cells, non-coated Ad5luc demonstrated significantly increased luciferase expression in comparison to mock-treated cells ($p < 0.01$). The values measured for the neutral polymer EC193 and the two positive polymers with high QA content (6.5%; EC234 and EC235) remained on the level of mock-treated cells and significantly restricted virus transgene expression ($p < 0.01$) in comparison to non-coated virus. Notably however, EC236 not only allowed, but significantly increased luciferase expression in comparison to non-coated virus ($p < 0.01$) on A549 cells, similar to results observed on SKOV3 cells. Hence, it appeared that EC236Ad used a highly efficient uptake mechanism, which did not rely on fibre or hexon interaction with the cell-surface receptors. Together with the observations in SKOV3 the results in A549 cells also indicated that, while the neutral polymer EC193 efficiently covered fibre and abrogated CAR infection (Figure 6-2 C), hexon areas remained accessible and FX-mediated uptake was not abolished after coating with EC193 (Figure 6-2 B).

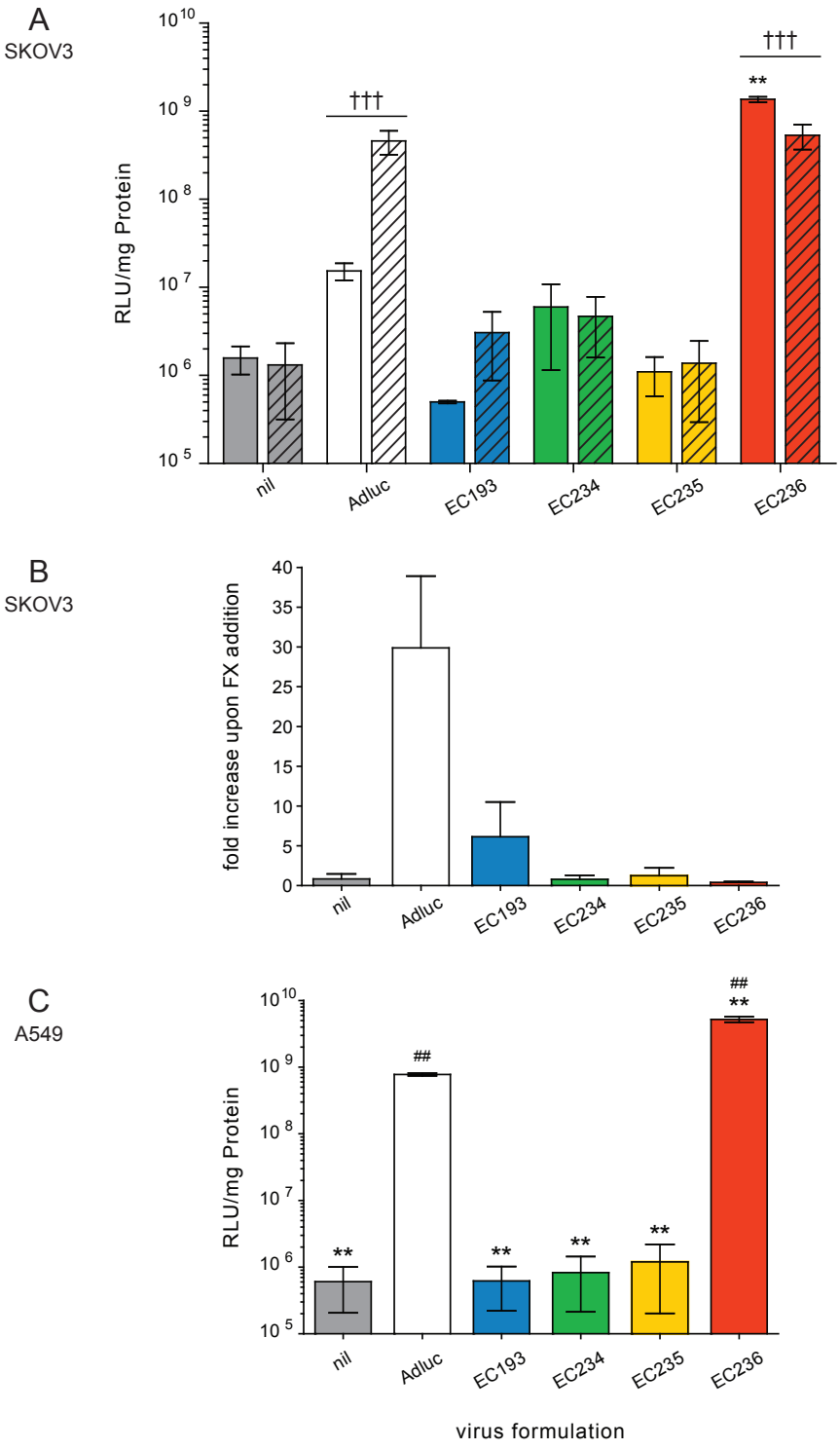


Figure 6 - 2 Activity of coated virus and efficiency of hexon shielding

Transduction efficacy and hexon protein cover of optimally coated Ad (compare Figure 6 -1) was investigated. For this, SKOV3 cells were incubated with non-modified Ad5luc or Ad5luc coated with the different polymers (all 500 vp/cell) in the presence or absence of factor X (FX) (section 2.5.3). Graph A depicts the luciferase expression in the absence and presence (striped bars) of FX during vector incubation (90 minutes) after further incubation for 24 hours. Graph B shows the fold increase of luciferase expression in the presence of FX. Graph C depicts luciferase expression in A549 cells infected with the same formulations in the absence of FX. (Graphs A & B: means of triplicate values and standard deviations; Graph C: means of quadruplicate values and standard deviations; statistical analysis: one-way ANOVA with Dunnett's multiple comparison post-tests: A: ** = $p < 0.01$ vs Adluc (in the absence of FX), C: ** = $p < 0.01$ vs Adluc, ## = $p < 0.01$ vs nil; two-way ANOVA with Dunnett's multiple comparison post-tests: A: ††† = $p < 0.001$ presence vs absence of FX; results representative of two independent experiments)

6.2.1.3 Effect of different polymers on the oncolytic activity of Ad5

This project intended to explore the use of Ad as an oncolytic agent rather than as a gene therapy vector and it was of interest to know whether oncolytic activity of polymer-coated wild-type Ad5 would mirror the effects observed with non-replicating Ad5luc. Hence, experiments using wild-type Ad5 modified with the different polymers were devised. An ELISA to assess coating efficiency (Figure 6-3 A) revealed an overall similar pattern of capsid coverage for the different polymers as previously observed, however, all values were slightly higher than in earlier experiments (Figure 6-1 and other studies (data not shown)). EC236-coated virus in particular appeared to be markedly less well shielded than previously.

Upon discussion with the team of chemists (Prof Ulbrich and colleagues, Institute of Macromolecular Chemistry, Prague) who synthesised these polymers it became apparent that the polymer TT-groups and the reducible disulfide bonds were susceptible to decay during storage. EC236 contains the lowest amount of QA-groups, which allow adherence of the polymer to the virus capsid through electrostatic interaction. Hence, the decreasing availability of TT-groups, which covalently link the polymer with the virus capsid, became most obvious on this polymer. Thus, future experiments would be influenced by suboptimal coating and decreased significance of polymer-mediated effects was expected.

EC236Ad5luc had demonstrated significantly increased luciferase expression on SKOV3 cells in comparison to non-modified Ad5luc in the absence of FX (Figure 6-2 A). However, it remained unclear, whether this was due to increased uptake of EC236-modified virus or an intracellular process such as more efficient intracellular trafficking, for example via more effective endosome lysis. Hence, in order to assess the uptake of coated virus, A549 cells were incubated with the different virus formulations for 90 minutes in suspension and numbers of internalised genome copies determined. Furthermore, aliquots of cells from this study were seeded into microplates and viability assessed after four days (section 2.5.4).

In accordance with previous results (section 3.3.2.2), Figure 6-3 B demonstrates that non-modified Ad5 achieved little uptake into cells (5% of the original infection dose). Unfortunately,

values of sample replicates showed high variability. However, overall, results indicated a trend towards higher uptake of Ad5 coated with polymers bearing positive charges, while Ad5 coated with the neutral polymer EC193 showed low uptake similar to non-modified virus. Notably, EC236-coated virus appeared to achieve highest uptake of all formulations.

Oncolytic activity of the formulations was assessed after incubating the aliquots, which had been seeded into microplates, for four days (Figure 6-3 C). Comparison of cell viabilities as a measure of oncolytic activity between non-coated and polymer-coated Ad5 revealed that EC193 and EC234 coating significantly decreased virus activity ($p < 0.05$ and $p < 0.001$, respectively). Comparison among positive polymers demonstrated that EC235- and EC236-coated Ad5 was significantly more active than EC234-coated virus ($p < 0.01$ and $p < 0.001$, respectively). Hence, there appeared to be a relationship between polymer structure and virus activity. Coating virus with polymers, which did not contain reducible intra-structural disulfide bonds (EC193 and EC234), lead to a reduction of virus activity. In addition, introduction of positive charges in the form of QA-groups (to allow for tighter binding of the polymer to the virus capsid) resulted in a decrease of activity in comparison to neutral polymer. As the uptake experiment in fact indicated higher uptake of EC234- in comparison to EC193-coated Ad, this appeared to be a post-internalisation effect, possibly due to inhibited virus capsid disassembly of EC234-coated Ad. Notably, the introduction of intra-structural disulfide bonds (EC235) allowed restoration of oncolytic activity. Furthermore, a decreased amount of QA-groups (EC236) appeared to ameliorate their activity-diminishing effect resulting in oncolytic activity similar to non-coated Ad5.

Although this experiment was affected by the deterioration of the TT-groups, it appeared to allow an insight into the structure / function relationship of the investigated polymers. Taking into account the extraordinary enhancement of transgene expression achieved with EC236-coated Ad5luc in both A549 and SKOV3 cells, and the strong oncolytic activity of EC236-coated wild-type Ad5, in conjunction with its ability to protect the virus capsid from antibody-capture (Figure 6-1, Figure 6-3 A), it appeared that EC236 could help to significantly increase oncolytic activity of wild-type Ad in neutralising environments.

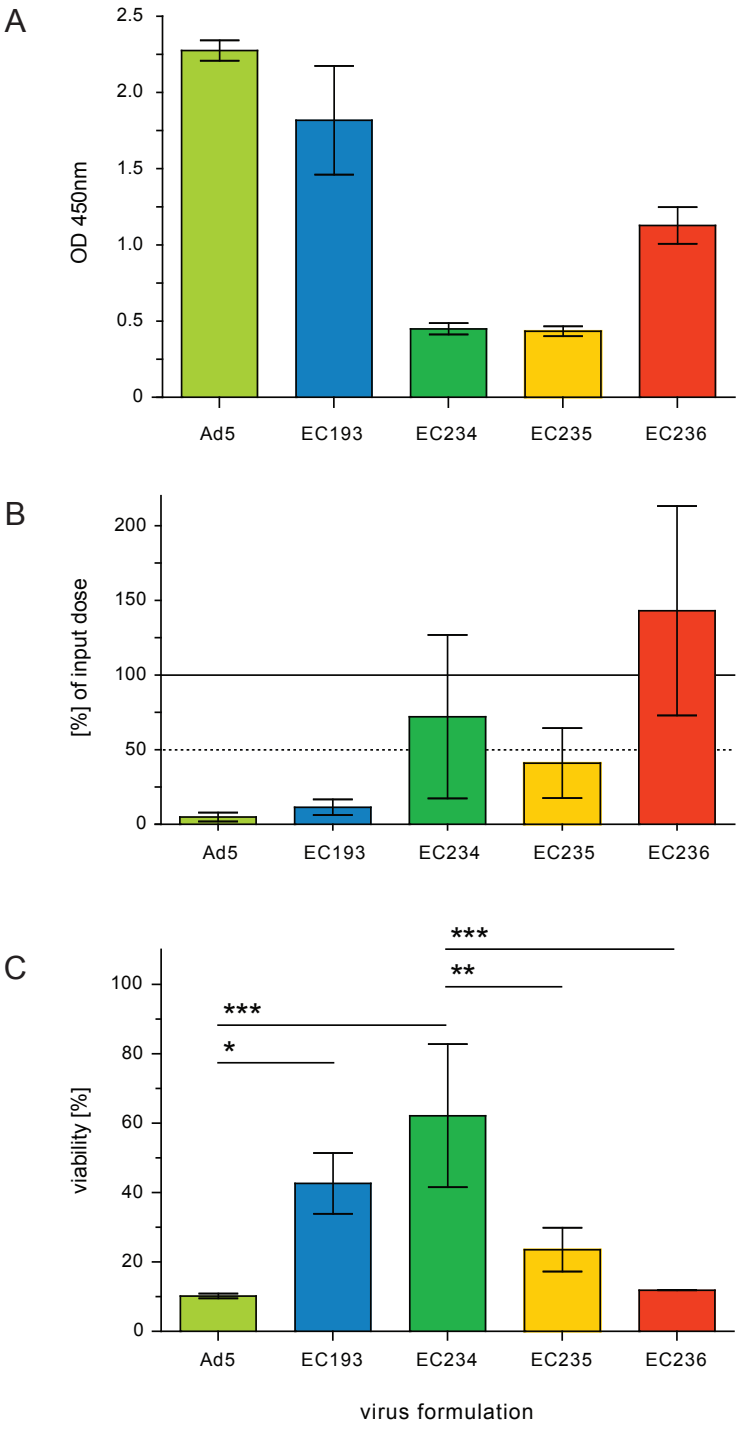


Figure 6 - 3 Evaluation of shielding, uptake and activity of polymer-coated Ad5

In order to investigate if polymer-coated wild-type Ad5 (Ad5) would mirror the results observed with non-replicating Ad5luc (Figure 6-2) a study evaluating coating efficiency on Ad5 and cellular uptake and oncolytic activty on A549 cells was performed. For this, Ad5 was coated with the different polymers at their optimal concentrations and an ELISA to test capsid shielding performed (section 2.5.2, Graph A). Uptake into cells ($1.5x10^5$ cells per replicate) was assessed by incubation with the different virus formulations (1,000 vp/cell) for 90 minutes in suspension and measurement of adenovirus genome number associated with the cellular fraction via Q-PCR (section 2.5.4, Graph B). Furthermore, oncolytic activity was evaluated by seeding aliquots of infected cells into microplates and measurement of cell viability after four days via MTS assay (section 2.5.4, Graph C). (Graphs A, C: means of triplicate values and standard deviations; Graph B: means of triplicate values expressed as percentage of virus genomes recovered from the cellular fraction in comparison to the amount initially inoculated onto cells ($1.5x10^8$ vp per replicate) and standard errors of the mean; Graph C: statistical analysis: one-way ANOVA with Tukey's multiple comparison post-tests (*** = $p < 0.001$, ** = $p < 0.01$, * = $p < 0.05$))

6.2.2 Polymer-coated Ad5 in neutralising environments

As the polymer EC236 was rendered non-functional through decay of its TT-groups and intra-structural disulfide bonds, a new batch of polymer (EC265) with the same specifications was synthesised. Initial tests revealed that this preparation sufficiently mirrored the results achieved with EC236 (data not shown) to further evaluate this polymer in neutralising environments. The following studies were performed in collaboration with Dr Robert Carlisle, who has longstanding experience in the research of polymer-coated viruses.

Both *in vitro* cell lines and freshly isolated primary tumour cells show great variation in properties such as gene expression. Hence, it was of interest to investigate if the remarkable properties of EC236 / EC265 were particular to A549 and SKOV3 cells or might be common across different cell lines and EC265-coated Ad5luc was tested on a panel of ten different cell lines (BHK, B16F10, CT26, HepG2, G43, LNCap, PC3, SKOV3, SW620 & U87, Figure 6-4). In addition, protection of Ad5luc from neutralising antibodies was assessed by comparing transgene expression in the presence and absence of pooled neutralising serum from 20 healthy volunteers (pool20, compare chapter 5). In non-neutralising conditions EC265Ad5luc had higher gene transfer activity than non-modified virus in six cell lines (BHK, B16F10, CT26, G43, PC3 and, as previously observed with EC236, SKOV3). In general, the increase was between 2- and 40-fold, but on BHK and CT26 cells gene transfer activity was enhanced about 100-fold. On two cell lines (HepG2 and SW620) activity of treatments was equivalent, while on two other cell lines (LNCaP and U87) EC265 modification appeared to restrict gene transfer activity.

In the presence of pooled neutralising human serum (1:50 dilution of pool20) the decrease in transgene activity was greater for non-modified Ad5luc than for EC265Ad5luc in comparison to non-neutralising conditions in all cell lines tested. Notably, in six cell lines (BHK, B16F10, CT26, G43, PC3 and SKOV3) even in the presence of neutralising serum, the activity of EC265Ad5luc remained higher than that of non-modified Ad5luc.

Overall, it appeared that the capability of EC265 to increase virus infectivity and / or transgene expression was present in most cell lines. Most importantly, the neutralisation resistance of EC265-modified virus, which had been indicated in the ELISA studies (Figure 6-1 and Figure 6-3 A), was verified in these transgene expression studies. However, it remained unclear if this protection of Ad5 infection would also translate to oncolytic activity. Hence, studies using non-modified or EC265-coated wild-type Ad5 in the presence or absence of human ascitic fluid from ovarian cancer patients were performed. Titrations of virus particle number per cell on ovarian cancer cell lines (A2780, OVCAR3 and SKOV3) revealed that, in neutralising conditions, less EC265Ad5 than non-coated Ad5 was required to achieve equivalent levels of oncolysis (data not shown).

To test the applicability of these results in a system more akin to the clinical situation, studies using wild-type Ad5 were extended to include human malignant primary ascites cells. For this, titrations of virus particle number per cell (10-fold dilution steps, range: 20,000 - 2 vp/cell or 10,000 - 1 vp/cell) of Ad5 or EC265Ad5 were performed (section 2.5.5). In these assays autologous ascitic fluid in a 10-fold dilution was used to recreate a neutralising environment, which might be encountered after peritoneal paracentesis and washout. Treatment efficacy was measured by extrapolating the IC_{50} values from sigmoid dose response curves fitted to the extent of oncolysis at the different treatment doses seven days after infection and comparing values between different treatments (Figure 6-5 A and B).

In non-neutralising conditions non-modified Ad5 demonstrated higher activity than EC265Ad5 in five of the eight samples tested. However, in the presence of autologous fluid, 50% oncolysis was only achieved in two of eight samples for Ad5, while EC236Ad5 achieved 50% kill in six of eight samples in the investigated concentration range. Notably, overall, the presence of autologous fluid had very little effect on the efficacy of EC265Ad5. These results show that although polymer-coating with EC265, overall, decreases oncolytic activity, it efficiently protects Ad5 from neutralisation and enables cell kill in malignant primary samples in a neutralising environment.

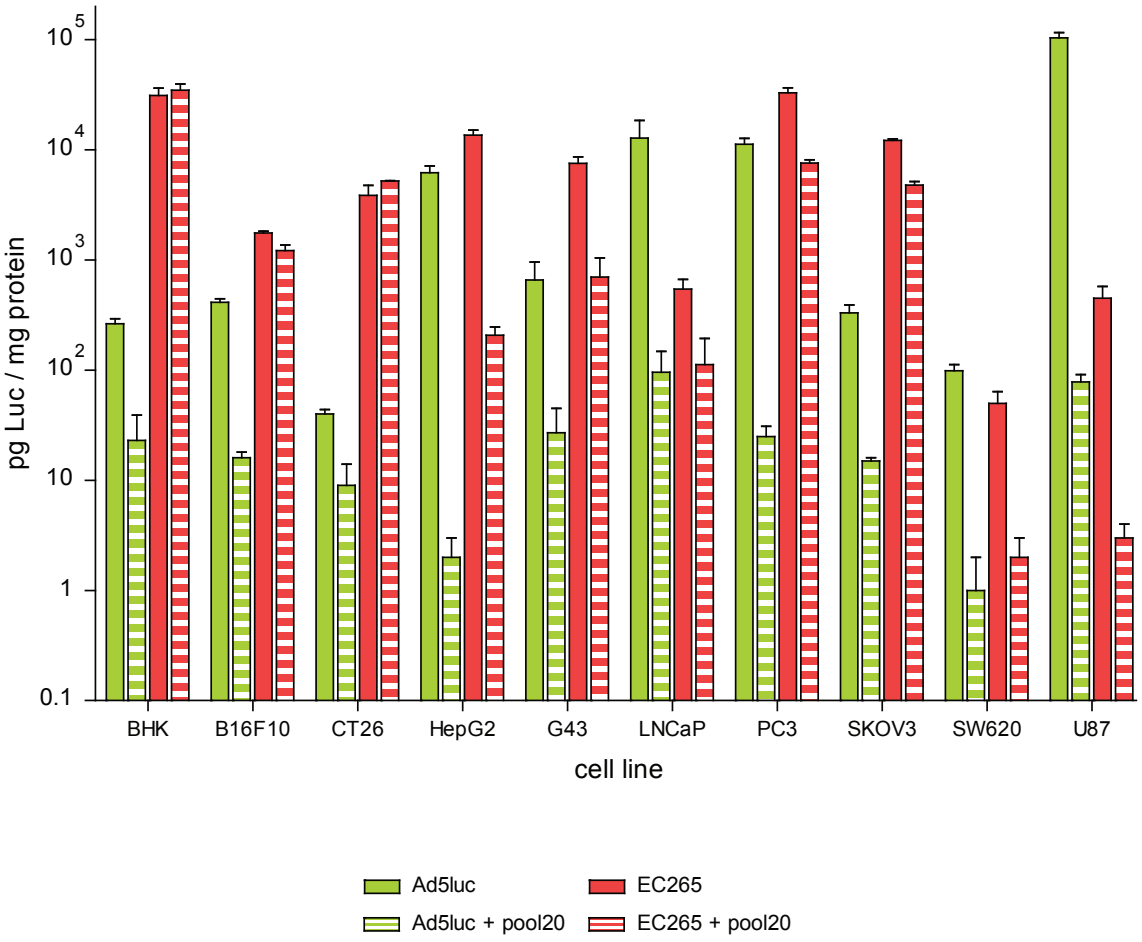
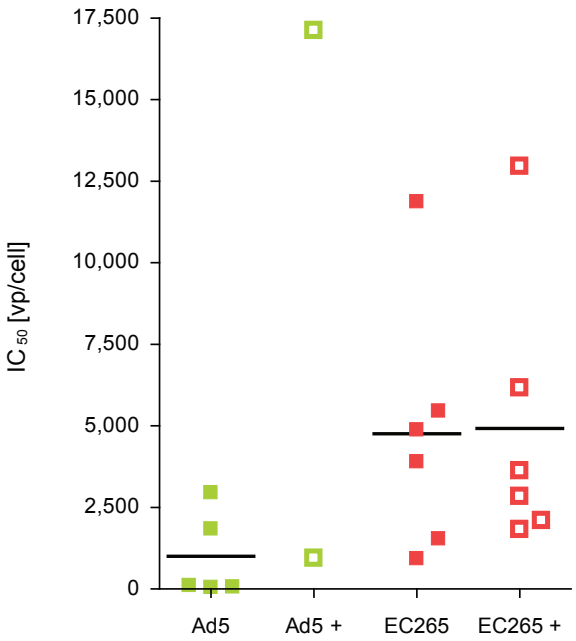


Figure 6 - 4 Transduction efficacy and neutralisation resistance of EC265Ad5luc

To investigate if the transduction properties of EC265-coated Ad5luc were common across different tumour cell lines and its resistance against neutralisation ten different cell lines (BHK, B16F10, CT26, HepG2, G43, LNCap, PC3, SKOV3, SW620 & U87) were inoculated with non-modified (Ad5luc) or EC265-coated Adluc (EC265) (both 500 vp/cell) in the presence or absence of pooled human serum (1:50 dilution of pool20) for 90 minutes. The graph depicts the amount of luciferase in pg per mg total cellular protein expressed after 24 hours incubation for the different cell lines and conditions (section 2.5.3, means of quadruplicate values and standard errors of the mean; results representative of three separate experiments; data obtained through collaboration with Dr Robert Carlisle).

A



B

	Ad5	Ad5 +	EC265	EC265 +
s1	50	17121	3898	6168
s2	60	946	5455	3625
s3	2950	>	4880	12954
s4	106	>	928	2100
s5	1838	>	11868	1823
s6	>	>	1537	2838
s7	>	>	>	>
s8	>	>	>	>

Figure 6 - 5 Oncolytic activity and neutralisation resistance of EC265Ad5 in *ex vivo* human malignant ascites

The oncolytic activity and neutralisation resistance of EC265-coated wild-type Ad5 in human malignant primary ascites cells in the presence and absence of autologous ascitic fluid was investigated (section 2.5.5). For this, cells isolated from eight primary ascites samples from ovarian cancer patients were inoculated with titrations of virus particle number per cell (10-fold dilution steps, range: 20,000 - 2 vp/cell or s4: 10,000 - 1 vp/cell) of Ad5 or EC265Ad5 with or without autologous ascitic fluid in a 10-fold dilution in growth medium. Cell viability was measured after incubation for seven days and treatment efficacy was determined by extrapolating the IC_{50} values from sigmoid dose-response curves fitted to the extent of oncolysis at the different treatment doses (n=5; s4: n=4). Graph A depicts the IC_{50} values of non-modified Ad5 or EC265-coated Ad5 (EC265) from the different patient samples in the presence (+) or absence of respective autologous fluid (the line indicates the mean of values). Table B lists the exact IC_{50} values extrapolated from the fitted sigmoid dose-response curves for the different primary samples (s1 - s8) (> : 50% cell kill not achieved with the highest vp/cell concentration used). Experiments performed in collaboration with Dr Robert Carlisle.

6.3 Discussion

Modification of adenovirus with neutral pHPMA had demonstrated a degree of protection from antibody binding in comparison to non-modified virus. However, it appeared that the polymer coat did not provide sufficient protection from neutralising antibodies as complete resistance to neutralisation could not be accomplished (Fisher *et al.*, 2001). The objective of this chapter was to investigate a panel of novel positively charged HPMA polymers, which were designed to allow tighter binding to the adenovirus capsid, hence providing better shielding against neutralisation, while maintaining intracellular virus activity.

All novel polymers provided better shielding of the adenovirus capsid from anti-adenovirus antibodies than conventional neutral polymers (Figure 6-1). Results demonstrated that the natural adenovirus uptake pathway through CAR could be blocked by positively charged polymers (Figure 6-2 C). This implies that the polymer covers adenovirus fibre, which is required for CAR binding. While this is important in terms of detargeting from undesired sites of infection, it also implies that the modified virus is protected from antibodies directed against fibre epitopes, one of the important antibody-binding sites of the virus capsid (Hong *et al.*, 2003). Furthermore, absence of augmentation of infection through FX (Figure 6-2 B) demonstrated good polymer cover of hexon protein epitopes, another main site of antibody-mediated neutralisation (Sumida *et al.*, 2005). It has been reported that hexon residues are critical for adenovirus attachment to the nuclear pore complexes for nuclear transfer of Ad DNA (Saphire *et al.*, 2000). Indeed, it appeared that the positive polymer without intrastructural reducible disulfide bonds (EC234) inhibited intracellular virus activity (Figure 6-2, Figure 6-3), possibly due to non-availability of these hexon residues. This is supported by the fact that the introduction of reducible groups (EC235), which should allow partial disassembly of the polymer coat in the intracellular reductive environment, could restore virus activity.

Unfortunately, further studies to elucidate the structure / function relationship between polymer composition and virus uptake and activity could not be performed due to the limited stability of the polymer stocks. The TT-groups which form the covalent bonds between the polymer and exposed primary amine groups on the virus capsid were susceptible to hydrolysis and the disulfide bonds prone to spontaneous reduction into thiols. Therefore, while perishability of the polymer structure is an inherent requirement for intracellular virus activity, it appears to also limit the versatility and practicability of these compounds. However, previous experiments had demonstrated that coated virus could be stored at -80ºC and tolerate one freeze- / thaw-cycle without loss of activity (data not shown). Hence, once the configuration of an optimal polymer structure has been determined it should be possible to prepare large batches of modified virus which can then be safely stored and shipped as ready-to-use formulations.

In the present study it was possible to acquire a second batch of polymer EC236 (termed EC265) which appeared most promising for subsequent studies of neutralisation resistance. This compound had demonstrated a remarkable enhancement of transgene expression in comparison to non-modified adenovirus even in SKOV3 cells, which usually demonstrate highly restricted infection with Ad5-derived vectors (Figure 6-2 A). Notably, uptake studies in A549 cells indicated increased uptake of virions modified with EC236 in comparison to non-modified Ad5 (Figure 6-3 B). However, EC236 coating did show good capsid coverage in the ELISA experiments (Figure 6-1, Figure 6-3 A), implying fibre shielding and, therefore, ablation from CAR-mediated uptake. In addition, transduction of SKOV3 cells, expressing low levels of CAR, was significantly enhanced with EC236 and was not increased further by addition of FX, indicating resistance to FX-mediated uptake (Figure 6-2 A, B). Hence, it appears that this formulation uses a distinct mechanism for cell entry, which remains to be further elucidated.

Investigation of the oncolytic activity of EC236-coated wild-type Ad5 demonstrated that this formulation had the highest oncolytic activity of all polymer-coated virus formulations, equal to non-modified Ad5 (Figure 6-3 C). Evaluation of the neutralisation resistance of EC265-modified Ad5luc on a panel of ten different cell lines demonstrated remarkable protection of transduction efficacy in the presence of human serum for most cell lines (Figure 6-4). These experiments

also indicated that some cell lines appear to be resistant to the infection-augmenting properties of this formulation. It is currently unclear if EC265-coated Ad is internalised through specific receptors or by unspecific, possibly electrostatic, interactions with the cell membrane. Hence, it remains to be investigated if the varying amount of transgene expression was due to varying receptor expression levels, cell-surface charges or intracellular reducing potentials of cell lines.

To evaluate if coating with EC265 might also convey resistance to neutralisation while maintaining oncolytic activity in a more clinically relevant model, EC265-coated Ad5 was tested in an *ex vivo* model of malignant ascites from ovarian cancer patients. Indeed, in neutralising environments EC265Ad5 could achieve at least 50% cell kill in six out of eight samples whereas non-modified Ad5 achieved this level in only two of eight samples (Figure 6-5) signifying markedly increased efficacy under these conditions.

Overall, Ad5 coated with polymers EC236 or EC265 appears to present an exciting advancement in overcoming treatment neutralisation in adenovirus virotherapy. However, the high uptake levels and unknown uptake mechanism of these formulations require further investigation since it is unclear whether infection and cytotoxicity are tumour cell specific. We are currently developing a flow cytometry-based assay to distinguish cell populations in the primary ascites samples by staining for cell-surface markers of tumour cells, leukocytes and fibroblasts (data not shown). Monitoring the amount of cells of each population during oncolysis assays will help to elucidate the specificity of oncolysis and undesired non-target cytotoxicity.

In the case of adenovirus coated with neutral polymers, retargeting strategies have been successfully used to enhance efficacy and lower side-effects of Ad-based treatments (Green *et al.*, 2008; Morrison *et al.*, 2008; Morrison *et al.*, 2009). In these protocols the retargeting ligand was incorporated into the Ad-polymer complex after the polymer had been linked to the virus. Initially, it was thought that this approach could also be employed to address current concerns about non-specificity of Ad formulations with positively-charged compounds. However, this method was found to not be feasible in the case of positive polymers, possibly due to electrostatic charge interactions between polymer and ligand. Hence, polymer synthesis was

amended to incorporate ligands such as human EGF in the polymer chain *a priori*. However, while these “retargeted” formulations did demonstrate effective shielding of the virus capsid, efficient cell infection was not observed (data not shown). If non-specificity and high off-target toxicity of EC265-coated virus will, indeed, be limiting its utility *in vivo*, new ways of incorporating retargeting ligands into the Ad-polymer complex will have to be explored.

7 Conclusion

7.1 Preface

Currently, the two major limitations to successful deployment of a virotherapeutic approach using adenovirus for the treatment of ovarian cancer are insufficient efficacy and high toxicity. Both appear to be, at least partly, particular to the use of adenovirus serotype 5 in this setting. Target cell infection is often restricted due to low levels of CAR, the major uptake receptor of Ad5, on ovarian tumour cells (Zeimet *et al.*, 2002). Furthermore, efficacy is limited due to widespread immunity and high titres of neutralising antibodies against Ad5 among patients (Stallwood *et al.*, 2000; Vogels *et al.*, 2003). Intraperitoneal inflammatory responses against Ad5 were among the reasons for the termination of a phase II/III clinical trial of p53 replacement in ovarian cancer (Stephen Chang – unpublished personal communication). In addition, substantial liver toxicity and adhesion formation after i.p. Ad5 administration in mice *in vivo* has been reported (Morrison *et al.*, 2008).

This thesis sought to overcome these obstacles to efficient i.p. adenovirus virotherapy of ovarian cancer. The two main aims were to investigate if group B adenoviruses Ad3 and Ad11 were better suited as oncolytic agents in ovarian cancer than the group C adenovirus Ad5 and if improved polymer-coating could impart enhanced protection from neutralisation. For this, the work presented in this thesis was divided into four objectives:

- evaluation of the oncolytic activity of Ad3 and Ad11 in comparison to Ad5 in a panel of ovarian cancer cell lines including investigation of the influence of uptake receptor expression and virion internalisation;
- comparison of the inflammatory response towards Ad3, Ad5 and Ad11 in murine *ex vivo* peritoneal macrophages and after i.p. administration in CD46-transgenic and non-transgenic mouse models;
- investigation of the neutralisation capacity of malignant patient exudates towards Ad3, Ad5 and Ad11 and the prevalence of antibodies targeted to adenovirus proteins of the different serotypes;
- assessment of novel positively charged polymers for adenovirus cloaking in terms of their ability to reduce neutralisation of Ad5 in *ex vivo* models of malignant ascites of ovarian cancer origin.

7.2 Principal findings

7.2.1 Oncolytic activity of Ad3, Ad5 and Ad11 in human tumour cell lines

Assessment of the oncolytic activity of Ad3, Ad5 and Ad11 in four human epithelial tumour cell lines (A549: lung carcinoma; IGROV1, OVCAR3, SKOV3: ovarian carcinoma) revealed that, while the serotypes demonstrated equal activity on A549 cells, they displayed differential activity in the ovarian cancer cell lines. It appeared that the group B adenoviruses Ad3 and Ad11 shared a similar pattern of activity across cell lines divergent from Ad5.

Investigation of the relationships between virus receptor expression levels, virus uptake and oncolytic activity revealed that, while cells internalising the highest amount of virus particles showed, in general, highest susceptibility to Ad-mediated lysis, some cell lines showed lysis resistance in a serotype-specific manner (IGROV1 for Ad3 and Ad11, SKOV3 for Ad3 and Ad5).

Hence, with regard to their oncolytic activity, none of the investigated adenovirus serotypes (Ad3, Ad5 and Ad11) appeared to be, overall, better suited for virotherapy of ovarian cancer. In fact, it appeared that cellular characteristics other than uptake receptor expression or even virus uptake levels could be the dominant factors determining virus activity. The interplay of cell-specific gene expression and serotype-specific genomes might decide efficacy of oncolysis by an individual serotype.

7.2.2 The inflammatory response towards Ad3, Ad5 and Ad11

Studies to investigate the use of Ad3 and Ad11 in comparison to Ad5 for intraperitoneal virotherapy in terms of their immunostimulatory properties were performed. In an *ex vivo* model using elicited peritoneal macrophages from BALB/c mice Ad11, but not Ad3, demonstrated up to 8-fold lower expression of the inflammatory cytokine RANTES than Ad5 and did not differ from mock-treated cells.

As the immune response in the peritoneal cavity is a complex system regulated by a variety of cell types studies in mice, including CD46-transgenic mice, were performed. Notably, in short-term experiments, where animals were sacrificed 6 hours after i.p. administration, Ad11 stimulated production of IL-6, MCP-1 and RANTES to levels equal to or even significantly above Ad5 in both serum and i.p. lavage fluid. Furthermore, assessment of cell populations in i.p. fluid demonstrated significantly lower or higher numbers of macrophages or neutrophils, respectively, for both Ad5- and Ad11- in comparison to mock-treated mice.

However, in long-term studies of repeated Ad administration, where animals were sacrificed after 18 days, Ad5 induced significantly more severe long-term pathologic effects in the form of adhesions and liver toxicity in comparison to Ad11. This was accompanied by significantly higher levels of IFNγ and VEGF expression and a significantly lower total number of cells and, in particular, fewer macrophages in the i.p. fluid of Ad5- than in Ad11- or vehicle-treated animals. None of these results were dependent on CD46 expression.

These results indicated that the use of Ad11 might ameliorate the side-effects observed in previous clinical trials of Ad5-based treatments in the peritoneal cavity and considerably improve patient safety.

7.2.3 Neutralisation of Ad3, Ad5 and Ad11 by malignant exudates

The neutralisation capacity towards Ad3, Ad5 and Ad11 of 28 exudate samples from cancer patients was examined. ELISAs measuring overall serotype-specific antibody content demonstrated a significantly higher amount of antibodies against Ad3 than Ad11. In assays evaluating the inhibition of oncolysis, greater neutralisation of Ad3 and Ad5, in comparison to Ad11, at concentrations lower than 2.5% of exudate samples, was observed. Notably, 100- to 1,000-fold less Ad11 than Ad5 was required for oncolytic efficacy in experiments titrating virus dose against a sample concentration of 10%.

These data suggest that virotherapy using Ad11-based treatments might have an advantage over Ad3 and Ad5, particularly after reduction of the neutralising capacity of the peritoneal cavity by paracentesis and subsequent wash-out. This would allow reduction of the virus dose and help to decrease particle-mediated side-effects, increasing patient safety, and reducing treatment costs.

The patterns of antigen specificity of antibodies directed against Ad3, Ad5 and Ad11 were investigated with an immunoblot system. Results demonstrated that more samples held higher amounts of antibodies directed against fibre and proteins V and VI of Ad5 than of Ad3 or Ad11. Differences in the amount of antibodies against the penton base protein of the different serotypes were not as pronounced. Notably, penton base appeared to be more immunogenic than fibre for both Ad3 and Ad11. In these experiments, the amount of antibodies directed against hexon was very low in comparison to other proteins for all serotypes.

These observations can help to improve future development of Ad-based therapeutics by selective modification of main epitope sites through genetic engineering or physical shielding in a serotype-specific manner. This may improve pharmacokinetics and result in higher efficacy permitting a decrease in the required therapeutic dose and result in lower side-effects.

7.2.4 Improved polymer coating to overcome barriers to *in vivo* adenovirus efficacy

A panel of novel positively charged polymers for adenovirus cloaking was evaluated to prioritise the compound which provided best shielding against neutralisation while maintaining virus activity. All novel polymers provided better shielding of the Ad5 capsid from anti-adenovirus antibodies than conventional neutral polymers and abrogation of adenovirus uptake through fibre / CAR and hexon / FX interactions. Notably, coating with EC236 resulted in increased uptake and significantly enhanced transgene expression in comparison to non-modified Ad5luc. Furthermore, EC236-coated wild-type Ad5 demonstrated highest oncolytic activity of all polymer-coated virus formulations, equal to non-modified Ad5.

Due to deterioration of polymers during storage, probably due to decay of disulfide bonds and TT-groups, neutralisation resistance was investigated with EC265, which had demonstrated physico-chemical properties equivalent to EC236. Upon addition of neutralising serum the decrease in transgene expression was greater for non-modified Ad5luc than for EC265Ad5luc in all ten cell lines tested. In six cell lines transgene expression of EC265Ad5luc remained even higher than that of non-modified Ad5luc in non-neutralising conditions. In an *ex vivo* model of malignant ascites from ovarian cancer patients, EC265Ad5 could achieve at least 50% cell kill in six out of eight samples, in contrast to two of eight samples for non-modified Ad5.

Coating of Ad5 with polymer EC236 / EC265 demonstrated markedly increased efficacy in neutralising environments and presents an exciting advancement in overcoming treatment neutralisation in adenovirus virotherapy.

7.3 General Discussion

As the four chapters of this thesis explored very different aspects of adenovirus virotherapy in ovarian cancer, respective results were, for the most part, discussed at the end of each of the chapters. This section attempts to highlight and discuss limitations of findings, areas of further work and implications for future research.

7.3.1 The use of Ad11

Combining the findings of reduced inflammatory stimulation and better activity under neutralising conditions of Ad11 in comparison to Ad5, it appears that employing Ad11 or an Ad11-derived vector could be advantageous over Ad5 and its constructs in the treatment of ovarian cancer.

Benefits of the use of Ad11 have also been observed in previous studies. However, although the genome sequence of Ad11 has been published nearly a decade ago (Mei *et al.*, 2003; Stone *et al.*, 2003), in comparison to Ad5, few studies with Ad11 have been reported to date. One publication by Stone *et al.* described the generation of an Ad11-derived vector and evaluation of *in vitro* and *in vivo* properties in comparison to an equivalent Ad5 construct (Stone *et al.*, 2005). A second paper by the same research team investigated biodistribution and safety after i.v. delivery of a range of adenovirus serotypes from species B, C, E and F, which also included Ad11 and Ad5 (Stone *et al.*, 2007). A recent study by Shashkova *et al.* compared the adenovirus serotypes 5, 6, 11 and 35 in terms of their oncolytic activity *in vitro* and *in vivo* and characterised *in vivo* toxicity (Shashkova *et al.*, 2009). In addition, in a proof-of-principle study Sandberg *et al.* examined anti-tumour activity of a replicating GFP-reporter Ad11 construct, which contained the complete Ad11 genome, in a human prostate cancer xenograft model in mice (Sandberg *et al.*, 2009). Overall, these publications demonstrated a favourable toxicity profile and strong *in vivo* anti-tumour activity of Ad11, equivalent to Ad5, after both i.v. and i.t. application. Notably, in accordance with results presented in chapter 4, Ad11 did not induce

severe hepatotoxicity, which has been widely reported following i.v. administration of Ad5 in mice.

No reports of Ad11 constructs employing strategies to increase oncolytic efficacy have been published to date. As discussed in section 1.3.2.3, introduction of GMCSF is currently being explored in an Ad5-derived vector as a way to increase efficacy by stimulation of the intratumoural immune environment (Koski *et al.*, 2010). Indeed, this approach has previously been applied to poxvirus (JX-594) and Herpes simplex type 1 (OncoVEX$^{GM\text{-}CSF}$) and preclinical testing has demonstrated significantly enhanced anti-tumour activity of these constructs (Liu *et al.*, 2002; Kim *et al.*, 2006). While both agents are currently being evaluated in clinical trials, which will determine if their promising preclinical efficacy will translate into patient benefit, they appear to represent one of the most potent strategies to improve tumour oncolysis to date. However, whether a similar approach in a novel Ad11-derived construct for i.p. treatment of ovarian cancer would be useful remains to be proven. As described in chapter 4, the interplay between adenovirus and the immune system in the peritoneal cavity on both a temporal and spatial level appears remarkably complex. The introduction of a potent immunostimulatory protein such as GMCSF might upset a fine balance, which appeared to be maintained after i.p. Ad11 but not Ad5 and could possibly result in the loss of the advantageous inflammatory profile of i.p. Ad11.

It is to be hoped that the recent identification of the long elusive alternative adenovirus species B uptake receptor, termed receptor X, as Desmoglein 2 might help to further interest in this serotype (Wang *et al.*, 2011). Future studies might elucidate so far unresolved questions in the activity and toxicity profiles, biodistribution and pharmacokinetics of Ad11. This would, in turn, allow the systematic development of new Ad11 constructs, which could further improve on the already promising properties of this virus.

7.3.2 New ways of enhancing efficacy

After early clinical trials had indicated a lack of efficiency of Ad5 oncolysis, the need for increased efficacy inspired research into possible strategies to enhance virus activity. These predominantly focused on modification of the viral vector through genetic engineering and a range of novel Ad5 constructs were developed. Many of the methods employed aimed at enhancing vector infection, for instance, through exchange of Ad5 fibre with Ad3 fibre (Raki *et al.*, 2007) or introduction of RGD motifs into Ad5 fibre (Kimball *et al.*, 2010).

However, findings presented in chapter 3 demonstrated that some cell lines display strong resistance against virus induced lysis independent of adenovirus uptake and even replication. It appears that cellular properties other than uptake receptor expression may be the dominant factors determining susceptibility to oncolysis. Importantly, this finding was corroborated by other recently published research, which found that proteins such as CEACAM6 or p21 can greatly influence adenovirus activity (Wang *et al.*, 2009; Flak *et al.*, 2010). It appears that more research into the reasons for lysis resistance of certain tumour cells and identification of cellular proteins that attenuate virus activity is required to be able to improve future vector modification strategies.

One approach, which circumvented the need for exact knowledge of the specific cellular proteins which influence virus activity, but still resulted in adaption of a virus towards greater oncolytic potency through those proteins, was realised by a method termed “directed evolution”. In this strategy a pool of seven adenoviruses from species B, C, D, E and F was passaged on a range of different tumour cell lines in a manner to encourage recombination between serotypes (Kuhn *et al.*, 2008). The most potent progeny was eventually recovered from the colon cancer cell line HT-29. This virus, termed ColoAd1, demonstrated significantly increased activity on a range of other colon cancer cell lines in comparison to Ad5, but also on lines of different origin like the ovarian OVCAR3 cells. DNA sequencing revealed that this virus was a chimera of Ad11p and Ad3 and its genome predominantly consisted of Ad11p sequences with a major and a minor deletion in its E3 and E4 regions, respectively, and an insertion of several sequences from Ad3 in its E2B region. These results appear to indicate that out of the seven serotypes

tested Ad11 has strongest natural oncolytic potency, as the genome of Ad11 is almost entirely conserved in ColoAd1. In addition, areas of the Ad11 sequence where manipulation might yield greater activity were discovered. However, while this approach inherently takes into account cell-specific properties as a driver for evolution (in this case towards increased cytotoxicity), the resulting "strategy" of increasing Ad activity lies in manipulation of the virus genome and, thus, virus properties.

In contrast, a different approach to enhance Ad tumour toxicity might be to manipulate tumour cell properties with the aim of rendering these cells more sensitive to oncolysis. Identification of, first, generally tumour-specific characteristics or, second, properties of certain cancer cell types (as described in chapter 3) that attenuate virus kill could yield targets whose manipulation might sensitise for oncolysis.

Research in this area might focus on distinctive features of tumour biology. For example, many tumours possess areas of insufficient vascularisation resulting in hypoxia in affected areas. This tumour-specific property has previously been employed to increase specificity of Ad replication. In a strategy to restrict Ad replication to hypoxic tissues Ad5 vectors (e.g. AdEH2T and AdEHE2F) were constructed in which E1A transcription was dependent on cellular expression of hypoxia-inducible factor (HIF) (Hernandez-Alcoceba *et al.*, 2002). However, some studies demonstrated general attenuation of Ad activity in these environments. Ad5, but also Ad3 and Ad11, have been found to display diminished virus replication and oncolysis under hypoxic conditions (Pipiya *et al.*, 2005; Shen and Hermiston, 2005; Shen *et al.*, 2006). As chronic hypoxia is a common pathophysiological finding in many advanced tumours, identification and manipulation of proteins that are expressed in hypoxic conditions and attenuate virus activity might allow restoration of regular or even enhancement of oncolytic activity in affected areas and overcome a current obstacle in virotherapy.

Results described in chapter 3 appear to indicate that the diversity of genetic mutations acquired during progression of cells towards a malignant phenotype results in some cell types which possess an inherent resistance to oncolysis whereas others do not, even if they originate from the same parental tissue. The data presented here furthermore suggest that this resistance might be directed towards particular Ad serotypes only. Identification of attenuating pathways / proteins in a cell line-specific, rather than tumour-specific, manner might reveal targets whose manipulation might increase virus activity. These targets could, for instance, encompass proteins involved in interferon-mediated anti-virus immunity, endosomal trafficking or regulation of gene expression.

The increasing availability of large robot-assisted library screening methodologies might significantly accelerate identification of key proteins among relevant signalling cascades. Furthermore, availability of libraries of small-molecule protein inhibitors could open avenues for the development of a new type of “oncolysis enhancing” drug. Evidently, selectivity of augmentation of these novel adjuvant treatments for the cancer phenotype is a prerequisite for their applicability in patient treatment. Many non-transformed cells often have pathway redundancy which, due to mutations during progression to malignancy, is lost in cancer cells. This could be the basis for selective sensitisation of tumour cells to oncolytic treatment even after systemic application of an oncolysis adjuvant.

7.3.3 Protecting adenovirus from neutralisation

In keeping with a pharmaceutical understanding of treatments in virotherapy, the strategy of polymer-coating of adenovirus with positively charged polymers investigated in chapter 6 can be perceived as the development of a sophisticated excipient for virotherapeutics. Findings demonstrated abrogation of adenovirus uptake through fibre / CAR and hexon / FX interactions, while maintaining virus activity. Importantly, coating of Ad5 with polymer EC236 / EC265 demonstrated markedly increased efficacy in neutralising environments in comparison to non-modified virus.

Polymer-coated Ad5 investigated in this thesis was not retargeted with ligands, which convey tumour cell or tumour vasculature selectivity, such as Cetuximab or selectins, respectively (Morrison *et al.*, 2009; Bachtarzi *et al.*, 2011). However, despite demonstrating detargeting from CAR- or FX-mediated uptake, EC265-modified Ad5luc achieved more uptake and significantly enhanced transgene expression in comparison to non-modified virus *in vitro*. The mechanisms which resulted in these findings remain currently unknown and non-selectivity of polymer-coated Ad represents a concern for its applicability *in vivo*. Preliminary *in vitro* data investigating kinetics of cell-attachment, intracellular trafficking and "uncloaking" of coated Ad using fluorescently labelled virions and neutral polymers so far failed to elucidate relevant processes (data not shown).

In an *in vivo* setting the introduction of positive charges onto the virus capsid might increase non-target cell binding and influence *in vivo* pharmacokinetics. Apart from the risk of losing large quantities of the input dose to non-target tissues and possible related side-effects, stimulation of inflammatory signalling through increased interaction with immune cells could preclude the clinical use of positive polymers. Importantly, as discussed in chapter 4, inordinate inflammatory stimulation appears to be particularly detrimental in the peritoneal cavity.

Previous reports and further unpublished data examining the i.p. inflammatory responses towards Ad5 coated with neutral polymer demonstrated decreased adhesion formation and cytokine and cellular reactions compared with non-modified virus, on a par to mock-treated mice (Morrison *et al.*, 2009). In the case of positive polymers, preliminary data investigating uptake and subsequent expression of the inflammatory cytokines IL-6 and RANTES of EC265Ad5 on freshly isolated peripheral blood mononuclear cells (PBMC) demonstrated lower uptake and decreased cytokine signalling of the modified in comparison to non-modified Ad5 both in the presence or absence of autologous plasma (data not shown). However, as exemplified by the findings presented in chapter 4, *in vitro* data is not necessarily a predictor for the situation *in vivo* and studies of i.p. administered EC265Ad are required to be able to characterise its effect on the peritoneal inflammatory system and homeostasis.

In order to avoid possible non-specificity of infection through the introduction of positive charges onto the virus capsid, the QA-groups could be incorporated into the polymer chain using cleavable linkers. This approach would allow utilisation of the preferential coating of the negatively charged immunogenic motifs of hexons through the electrostatic interaction between QA and these regions. However, after formation of the covalent bonds between the TT-groups of the polymer chain and amines on the virus capsid, QA could be removed while the polymer remained to specifically shield negatively charged epitopes.

Chapter 6 solely investigated polymer-modification of Ad5 and derived vectors due to limited experience in the application of this approach for other adenovirus serotypes. However, preliminary data of polymer-coated Ad3 and Ad11 indicated applicability of the coating strategy to alternative serotypes. Protection from antibody binding equivalent to modified Ad5 was observed in ELISA experiments (data not shown). Hence, it appears that polymer-coating can also be employed in future developments of alternative serotypes and allow combination of the protective properties of EC265 with serotype-specific advantages, such as the reduced i.p. inflammatory stimulation of Ad11. However, differences between serotypes in capsid-surface architecture, such as varying fibre length (Signas *et al.*, 1985; Stone *et al.*, 2003), and charge distribution (Russell, 2009) warrant thorough investigation of the resulting virus formulations.

In this context, the positive polymers investigated in this thesis were specifically developed to better shield highly immunogenic epitopes in Ad5 hexon proteins. Results from chapter 5 indicated divergent patterns of antigen specificity of antibodies directed against Ad5 and Ad3 / Ad11. Future polymers could potentially be designed to take these differences into account and protect important epitopes in a serotype-specific manner. Furthermore, while it was important to provide efficient polymer coverage of Ad5 fibre to guarantee detargeting from CAR-expressing non-target tissues, fibre modification might not be beneficial in the case of Ad3 and Ad11, which employ CD46 for cellular uptake, which was found to be highly expressed on malignant ovarian tissues (Bjørge *et al.*, 1997; Fishelson *et al.*, 2003).

7.3.4 Future directions

As an alternative to adenovirus, the Edmonston vaccine strain of measles virus (MV-Edm) has been developed for the i.p. treatment of ovarian cancer (Peng *et al.*, 2002b). In a recently concluded phase I trial, employing a replicating MV-Edm reporter vector for i.p. treatment of recurrent ovarian cancer, this virus was well tolerated and demonstrated efficacy observed in a dose-dependent disease stabilisation of a median duration of 92.5 days in 14 of 21 enrolled patients (Galanis *et al.*, 2010). MV-Edm virus, as opposed to its wild-type variant, infects cells via CD46, similar to Ad3 / Ad11. In addition, it encounters equally widespread antibody-mediated immunity as adenovirus (Russell and Peng, 2009). However, while in the case of Ad this is due to the ubiquity of viruses in the environment, in the case of MV-Edm this is due to its extensive use in vaccination. Hence, it appears the same arguments can be applied for the choice of MV-Edm or Ad3 / 11 as a virotherapeutic agent: first, increased tumour specificity via infection through CD46 and, second, an inherent mechanism guaranteeing patient safety through high prevalence of anti-virus immunity. Evidently, the latter also signifies one of the main obstacles to efficient virus delivery and spread, which affects both viruses.

A valuable lesson can be learned from the two, currently, most promising measles vectors. Early in their development, researchers realised the necessity for an effective way to monitor virus replication, spread and distribution. To this end, two replicating reporter vectors were developed. MV-CEA was engineered to express the soluble extracellular domain of the human carcinoembryonic antigen (CEA) and, thus, allows quantitative assessment of virus replication through blood or exudate monitoring (Peng *et al.*, 2002a). MV-NIS encodes the sodium-iodine symporter gene (NIS) which, after expression in infected cells and application of radioactive isotopes, allows imaging of virus spread through single-photon emission computed tomography (SPECT) or positron emission tomography (PET) (Dingli *et al.*, 2004). These viruses now enable non-invasive assessment of virus pharmacokinetics and correlation of replication and distribution to anti-tumour efficacy measurements. This should elucidate impediments to clinical efficacy of current measles vectors and help in the development of future improved formulations. Clearly, employment of a similar strategy in the development of adenoviral agents would be of significant benefit. If the obstacles to the success of Ad5-derived vectors, such as

SCH58500 and Onyx-015 in their respective clinical trials, would have been better characterised and reported at the time, findings could already have helped to considerably improve present adenovirus virotherapy strategies.

In general, it appears that intelligent development of adenoviral virotherapeutics is currently hampered by inadequate models to test virus efficacy. This is of particular importance as the response to these agents, both in aspects of efficacy and, crucially, safety, largely depends on interaction of the virus with the immune system, particularly in the treatment of disseminated disease, as in the case of late stage ovarian cancer, which requires systemic or intracompartmental administration. The development of transgenic animal models enabled, in part, investigation of treatments in a more "human-like" environment, exemplified by the use of CD46-transgenic mice in studies investigating the i.p. inflammatory response towards Ad11 described in chapter 4. However, current *in vivo* efficacy studies in xenograft tumour models, necessarily, require the use of immune-incompetent mice, making simultaneous assessment of treatment efficacy and safety impossible.

Notably, permissiveness for adenovirus serotype 5 replication has recently been described in organs and tumour cell lines of immunocompetent Syrian hamsters and this animal model has since been employed by several research groups (Toth *et al.*, 2010). While Syrian hamsters now allow a better insight into pharmacokinetics and interaction of adenovirus with the immune system, it remains unclear if efficacy data obtained from tumour models using hamster cell lines are representative of efficacy in human tumours. As discussed in section 7.3.2, varying properties of different human tumour cell lines appear to greatly influence adenovirus activity. Hence, it appears likely that disparities between cells of different species might not allow the application of efficacy data from hamster tumour models to human tumours. Furthermore, it remains currently unclear if Syrian hamsters are also permissive for alternative adenovirus serotypes such as Ad3 and Ad11.

Overall, it appears that intensive patient monitoring and extensive data collection in current clinical trials of adenovirus virotherapy are the prerequisite for the development of future oncolytic adenoviruses, which combine strong efficacy with robust safety.

7.4 Final conclusion

Previous use of Ad5-derived agents for i.p. adenovirus virotherapy of ovarian cancer demonstrated strong inflammatory responses and limited efficacy. The work presented in this thesis sought to overcome these obstacles by investigating the alternative adenovirus serotypes Ad3 and Ad11 and novel adenovirus cloaking techniques.

While none of the alternative adenovirus serotypes demonstrated, overall, greater oncolytic activity than Ad5, cell line-specific resistance to oncolysis in a serotype-specific manner, independent of virus uptake and replication, was observed. This highlights the need for a better understanding of the interactions of adenoviral and cellular proteins to allow future development of virus constructs with enhanced lytic efficacy.

Importantly, both the long-term intraperitoneal inflammatory profile and the performance under neutralising conditions of Ad11 were significantly better than those of Ad5. These results indicate that the use of Ad11 for the i.p. treatment of ovarian cancer might present a way to ameliorate the side-effects previously observed with Ad5-based treatments. The lack of strong inflammation on the one hand combined with the possibility to decrease treatment doses due to less neutralisation, without loss of efficacy, on the other might result in considerably improved patient safety when using Ad11.

Improved polymer-cloaking strategies for Ad5 demonstrated increased oncolytic efficacy under neutralising conditions in comparison to non-modified Ad5. While limited insight into the specificity of polymer-coated Ad for target cells might hamper the utility of current non-retargeted formulations, the significant increase in protection from neutralisation in comparison to previously used compounds, which was achieved through intelligent polymer design, demonstrates the potential of this technology in future strategies of adenovirus virotherapy.

References

AGHAJANIAN, C., FINKLER, N. J. , RUTHERFORD, T. , TENERIELLO, M. G. , YI, J. , PARMAR, H. , NYCUM, L. R. , SOVAK, M. A. . (2011). OCEANS: A randomized, double-blinded, placebo-controlled phase III trial of chemotherapy with or without bevacizumab (BEV) in patients with platinum-sensitive recurrent epithelial ovarian (EOC), primary peritoneal (PPC), or fallopian tube cancer (FTC). J Clin Oncol **29**.

ALVAREZ, R.D., GOMEZ-NAVARRO, J., WANG, M., BARNES, M.N., STRONG, T.V., ARANI, R.B., ARAFAT, W., HUGHES, J.V., SIEGAL, G.P., and CURIEL, D.T. (2000). Adenoviral-Mediated Suicide Gene Therapy for Ovarian Cancer. Mol Ther **2**, 524-530.

ARELLANO, M., and LONIAL, S. (2008). Clinical uses of GM-CSF, a critical appraisal and update. Biologics **2**, 13-27.

ARNBERG, N. (2009). Adenovirus receptors: implications for tropism, treatment and targeting. Reviews in Medical Virology **19**, 165-178.

AUSTYN, J.M., and GORDON, S. (1981). F4/80, a monoclonal antibody directed specifically against the mouse macrophage. European Journal of Immunology **11**, 805-815.

BACHTARZI, H., STEVENSON, M., SUBR, V., ULBRICH, K., SEYMOUR, L.W., and FISHER, K.D. (2011). Targeting adenovirus gene delivery to activated tumour-associated vasculature via endothelial selectins. Journal of Controlled Release **150**, 196-203.

BAILEY, C.J., CRYSTAL, R.G., and LEOPOLD, P.L. (2003). Association of Adenovirus with the Microtubule Organizing Center. J. Virol. **77**, 13275-13287.

BARTH, M.W., HENDRZAK, J.A., MELNICOFF, M.J., and MORAHAN, P.S. (1995). Review of the macrophage disappearance reaction. In *J Leukoc Biol*. *pp*. 361-367.

BAUER, U., FLUNKER, G., BRUSS, K., KALLWELLIS, K., LIEBERMANN, H., LUETTICH, T., MOTZ, M., and SEIDEL, W. (2005). Detection of Antibodies against Adenovirus Protein IX, Fiber, and Hexon in Human Sera by Immunoblot Assay. J. Clin. Microbiol. **43**, 4426-4433.

BAUERSCHMITZ, G.J., LAM, J.T., KANERVA, A., SUZUKI, K., NETTELBECK, D.M., DMITRIEV, I., KRASNYKH, V., MIKHEEVA, G.V., BARNES, M.N., ALVAREZ, R.D., DALL, P., ALEMANY, R., CURIEL, D.T., and HEMMINKI, A. (2002). Treatment of Ovarian Cancer with a Tropism Modified Oncolytic Adenovirus. Cancer Research **62**, 1266-1270.

BELLINGAN, G.J., CALDWELL, H., HOWIE, S.E., DRANSFIELD, I., and HASLETT, C. (1996). In vivo fate of the inflammatory macrophage during the resolution of inflammation: inflammatory macrophages do not die locally, but emigrate to the draining lymph nodes. J Immunol **157**, 2577-2585.

BENARD, J., DA SILVA, J., DE BLOIS, M.-C., BOYER, P., DUVILLARD, P., CHIRIC, E., and RIOU, G. (1985). Characterization of a Human Ovarian Adenocarcinoma Line, IGROV1, in Tissue Culture and in Nude Mice. Cancer Res **45**, 4970-4979.

BERGELSON, J.M., CUNNINGHAM, J.A., DROGUETT, G., KURT-JONES, E.A., KRITHIVAS, A., HONG, J.S., HORWITZ, M.S., CROWELL, R.L., and FINBERG, R.W. (1997). Isolation of a Common Receptor for Coxsackie B Viruses and Adenoviruses 2 and 5. In *Science*. *pp*. 1320-1323.

BERRIDGE, G., CHALK, R., D'AVANZO, N., DONG, L., DOYLE, D., KIM, J.I., XIA, X., BURGESS-BROWN, N., DERISO, A., CARPENTER, E.P., and GILEADI, O. (2011). High-performance liquid chromatography separation and intact mass analysis of detergent-solubilized integral membrane proteins. Anal. Biochem. **410**, 272-280.

BISCHOFF, J.R., KIRN, D.H., WILLIAMS, A., HEISE, C., SHARON, H., MUNA, M., NG, L., NYE, J.A., SAMPSON-JOHANNES, A., FATTAEY, A., and MCCORMICK, F. (1996). An Adenovirus Mutant That Replicates Selectively in p53-Deficient Human Tumor Cells. Science **274**, 373-376.

BJØRGE, L., HAKULINEN, J., VINTERMYR, O.K., JARVA, H., JENSEN, T.S., IVERSEN, O.E., and MERI, S. (2005). Ascitic complement system in ovarian cancer. British Journal of Cancer **92**, 895-905.

BJØRGE, L., HAKULINEN, J., WAHLSTRÖM, T., MATRE, R., and MERI, S. (1997). Complement-regulatory proteins in ovarian malignancies. International Journal of Cancer **70**, 14-25.

BLANCHE, F., MONEGIER, B., FAUCHER, D., DUCHESNE, M., AUDHUY, F., BARBOT, A., BOUVIER, S., DAUDE, G., DUBOIS, H., GUILLEMIN, T., and MATON, L. (2001). Polypeptide composition of an adenovirus type 5 used in cancer gene therapy. Journal of Chromatography A **921**, 39-48.

BOTTINI, C., MIOTTI, S., FIORUCCI, S., FACHERIS, P., MÉNARD, S., and COLNAGHI, M.I. (1993). Polarization of the α6β4 integrin in ovarian carcinomas. International Journal of Cancer **54**, 261-267.

BRÜNING, A., KÖHLER, T., QUIST, S., WANG-GOHRKE, S., MOEBUS, V.J., KREIENBERG, R., and RUNNEBAUM, I.B. (2001). Adenoviral Transduction Efficiency of Ovarian Cancer Cells Can Be Limited by Loss of Integrin β3 Subunit Expression and Increased by Reconstitution of Integrin aVβ3. Human gene therapy **12**, 391-399.

BULLER, R.E., RUNNEBAUM, I.B., KARLAN, B.Y., HOROWITZ, J.A., SHAHIN, M., BUEKERS, T., PETRAUSKAS, S., KREIENBERG, R., SLAMON, D., and PEGRAM, M. (2002a). A phase I/II trial of rAd/p53 (SCH 58500) gene replacement in recurrent ovarian cancer. Cancer gene therapy **9**, 553-566.

BULLER, R.E., SHAHIN, M.S., HOROWITZ, J.A., RUNNEBAUM, I.B., MAHAVNI, V., PETRAUSKAS, S., KREIENBERG, R., KARLAN, B., SLAMON, D., and PEGRAM, M. (2002b). Long term follow-up of patients with recurrent ovarian cancer after Ad p53 gene replacement with SCH 58500. Cancer gene therapy **9**, 567-572.

BURGER, R.A. (2011). Overview of anti-angiogenic agents in development for ovarian cancer. Gynecologic Oncology **121**, 230-238.

BUTTITTA, F., MARCHETTI, A., GADDUCCI, A., PELLEGRINI, S., MORGANTI, M., CARNICELLI, V., COSIO, S., GAGETTI, O., GENAZZANI, A.R., and BEVILACQUA, G. (1997). P53 alterations are predictive of chemoresistance and aggressiveness in ovarian carcinomas: A molecular and immunohistochemical study. British Journal of Cancer **75**, 230-235.

CAHILL, R.A., and REDMOND, H.P. (2008). Cytokine orchestration in post-operative peritoneal adhesion formation. World Journal of Gastroenterology **14**, 4861-4866.

CAILHIER, J.F., PARTOLINA, M., VUTHOORI, S., WU, S., KO, K., WATSON, S., SAVILL, J., HUGHES, J., and LANG, R.A. (2005). Conditional Macrophage Ablation Demonstrates That Resident Macrophages Initiate Acute Peritoneal Inflammation. J Immunol **174**, 2336-2342.

CARLISLE, R.C., DI, Y., CERNY, A.M., SONNEN, A.F.P., SIM, R.B., GREEN, N.K., SUBR, V., ULBRICH, K., GILBERT, R.J.C., FISHER, K.D., FINBERG, R.W., and SEYMOUR, L.W. (2009). Human erythrocytes bind and inactivate type 5 adenovirus by presenting Coxsackie virus-adenovirus receptor and complement receptor 1. Blood **113**, 1909-1918.

CASH, J.L., HART, R., RUSS, A., DIXON, J.P.C., COLLEDGE, W.H., DORAN, J., HENDRICK, A.G., CARLTON, M.B.L., and GREAVES, D.R. (2008). Synthetic chemerin-derived peptides suppress inflammation through ChemR23. J. Exp. Med. **205**, 767-775.

CASSEL, W.A., and GARRETT, R.E. (1965). Newcastle disease virus as an antineoplastic agent. Cancer **18**, 863-868.

CHEONG, Y.C., LAIRD, S.M., LI, T.C., SHELTON, J.B., LEDGER, W.L., and COOKE, I.D. (2001). Peritoneal healing and adhesion formation/reformation. In *Human Reproduction Update*. *pp*. 556-566.

CRUK. (accessed 6 June 2011). Ovarian cancer survival statistics. http://info.cancerresearchuk.org/cancerstats/types/ovary/survival/.

DINGLI, D., PENG, K.-W., HARVEY, M.E., GREIPP, P.R., O'CONNOR, M.K., CATTANEO, R., MORRIS, J.C., and RUSSELL, S.J. (2004). Image-guided radiovirotherapy for multiple myeloma using a recombinant measles virus expressing the thyroidal sodium iodide symporter. Blood **103**, 1641-1646.

EISENHAUER, E.A., and VERMORKEN, J.B. (1998). The taxoids. Comparative clinical pharmacology and therapeutic potential. Drugs **55**, 5-30.

ENGLER, H., MACHEMER, T.R., SCHLUEP, T., WEN, S.-F., QUIJANO, E., WILLS, K.N., HARPER, A.E., MANEVAL, D.C., and CONROY, S.E. (2003). Development of a Formulation that Enhances Gene Expression and Efficacy following Intraperitoneal Administration in Rabbits and Mice. Mol Ther **7**, 558-564.

FENDER, P., BOUSSAID, A., MEZIN, P., and CHROBOCZEK, J. (2005). Synthesis, cellular localization, and quantification of penton-dodecahedron in serotype 3 adenovirus-infected cells. Virology **340**, 167-173.

FIELDS, B.N., KNIPE, D.M., and HOWLEY, P.M. (2007). *Fields virology*. (Wolters Kluwer Health/Lippincott Williams & Wilkins, Philadelphia).

FISHELSON, Z., DONIN, N., ZELL, S., SCHULTZ, S., and KIRSCHFINK, M. (2003). Obstacles to cancer immunotherapy: expression of membrane complement regulatory proteins (mCRPs) in tumors. Molecular Immunology **40**, 109-123.

FISHER, K.D., and SEYMOUR, L.W. (2010). HPMA copolymers for masking and retargeting of therapeutic viruses. Advanced Drug Delivery Reviews **62**, 240-245.

FISHER, K.D., STALLWOOD, Y., GREEN, N.K., ULBRICH, K., MAUTNER, V., and SEYMOUR, L.W. (2001). Polymer-coated adenovirus permits efficient retargeting and evades neutralising antibodies. Gene Ther **8**, 341-348.

FLAK, M.B., CONNELL, C.M., CHELALA, C., ARCHIBALD, K., SALAKO, M.A., PIRLO, K.J., LOCKLEY, M., WHEATLEY, S.P., BALKWILL, F.R., and MCNEISH, I.A. (2010). P21 promotes oncolytic adenoviral activity in ovarian cancer and is a potential biomarker. Molecular Cancer **9**.

FLEISCHLI, C., SIRENA, D., LESAGE, G., HAVENGA, M.J.E., CATTANEO, R., GREBER, U.F., and HEMMI, S. (2007). Species B adenovirus serotypes 3, 7, 11 and 35 share similar binding sites on the membrane cofactor protein CD46 receptor. The Journal of general virology **88**, 2925-2934.

FOGH, J. (1975). Human tumour cells in vitro. Plenum Press, 115-159.

FRISCH, S.M., and MYMRYK, J.S. (2002). Adenovirus-5 E1A: paradox and paradigm. Nat Rev Mol Cell Biol **3**, 441-452.

GAGGAR, A., SHAYAKHMETOV, D.M., and LIEBER, A. (2003). CD46 is a cellular receptor for group B adenoviruses. Nat Med **9**, 1408-1412.

GALANIS, E., HARTMANN, L.C., CLIBY, W.A., LONG, H.J., PEETHAMBARAM, P.P., BARRETTE, B.A., KAUR, J.S., HALUSKA, P.J., ADERCA, I., ZOLLMAN, P.J., SLOAN, J.A., KEENEY, G., ATHERTON, P.J., PODRATZ, K.C., DOWDY, S.C., STANHOPE, C.R., WILSON, T.O., FEDERSPIEL, M.J., PENG, K.-W., and RUSSELL, S.J. (2010). Phase I Trial of Intraperitoneal Administration of an Oncolytic Measles Virus Strain Engineered to Express Carcinoembryonic Antigen for Recurrent Ovarian Cancer. Cancer Research **70**, 875-882.

GANLY, I., KIRN, D., ECKHARDT, S.G., RODRIGUEZ, G.I., SOUTAR, D.S., OTTO, R., ROBERTSON, A.G., PARK, O., GULLEY, M.L., HEISE, C., VON HOFF, D.D., and KAYE, S.B. (2000). A Phase I study of Onyx-015, an E1B attenuated adenovirus, administered intratumorally to patients with recurrent head and neck cancer. Clinical Cancer Research **6**, 798-806.

GARBER, K. (2006). China Approves World's First Oncolytic Virus Therapy For Cancer Treatment. J. Natl. Cancer Inst. **98**, 298-300.

GIARD, D.J., AARONSON, S.A., and TODARO, G.J. (1973). In vitro cultivation of human tumors: establishment of cell lines derived from a series of solid tumors. Journal of the National Cancer Institute **51**, 1417-1423.

GO, R.S., and ADJEI, A.A. (1999). Review of the comparative pharmacology and clinical activity of cisplatin and carboplatin. Journal of Clinical Oncology **17**, 409-422.

GONÇALVES, M.A.F.V., and DE VRIES, A.A.F. (2006). Adenovirus: from foe to friend. Reviews in Medical Virology **16**, 167-186.

GREBER, U.F., SUOMALAINEN, M., STIDWILL, R.P., BOUCKE, K., EBERSOLD, M.W., and HELENIUS, A. (1997). The role of the nuclear pore complex in adenovirus DNA entry. Embo J **16**, 5998-6007.

GREBER, U.F., WILLETTS, M., WEBSTER, P., and HELENIUS, A. (1993). Stepwise dismantling of adenovirus 2 during entry into cells. Cell **75**, 477-486.

GREEN, N.K., HERBERT, C.W., HALE, S.J., HALE, A.B., MAUTNER, V., HARKINS, R., HERMISTON, T., ULBRICH, K., FISHER, K.D., and SEYMOUR, L.W. (2004). Extended plasma circulation time and decreased toxicity of polymer-coated adenovirus. Gene Therapy **11**, 1256-1263.

GREEN, N.K., MORRISON, J., HALE, S., BRIGGS, S.S., STEVENSON, M., SUBR, V., ULBRICH, K., CHANDLER, L., MAUTNER, V., SEYMOUR, L.W., and FISHER, K.D. (2008). Retargeting polymer-coated adenovirus to the FGF receptor allows productive infection and mediates efficacy in a peritoneal model of human ovarian cancer. The Journal of Gene Medicine **10**, 280-289.

GURNANI, M., LIPARI, P., DELL, J., SHI, B., and NIELSEN, L.L. (1999). Adenovirus-mediated p53 gene therapy has greater efficacy when combined with chemotherapy against human head and neck, ovarian, prostate, and breast cancer. Cancer Chemotherapy and Pharmacology **44**, 143-151.

HALL, K., BLAIR ZAJDEL, M.E., and BLAIR, G.E. (2009). Defining the role of CD46, CD80 and CD86 in mediating adenovirus type 3 fiber interactions with host cells. Virology **392**, 222-229.

HAMILTON, T.C., YOUNG, R.C., LOUIE, K.G., BEHRENS, B.C., MCKOY, W.M., GROTZINGER, K.R., and OZOLS, R.F. (1984). Characterization of a Xenograft Model of Human Ovarian Carcinoma Which Produces Ascites and Intraabdominal Carcinomatosis in Mice. Cancer Res **44**, 5286-5290.

HANEY, A.F. (2000). Identification of macrophages at the site of peritoneal injury: evidence supporting a direct role for peritoneal macrophages in healing injured peritoneum. Fertility and Sterility **73**, 988-995.

HARTKOPF, A.D., FEHM, T., WALLWIENER, D., and LAUER, U. (2011). Oncolytic virotherapy of gynecologic malignancies. Gynecologic Oncology **120**, 302-310.

HASENBURG, A., TONG, X.W., FISCHER, P.D.D.C., ROJAS-MARTINEZ, A., NYBERG-HOFFMAN, C., KAPLAN, A.L., KAUFMAN, R.H., RAMZY, I., AGUILAR-CORDOVA, E., and KIEBACK, D.G. (2001). Adenovirus-Mediated Thymidine Kinase Gene Therapy in Combination with Topotecan for Patients with Recurrent Ovarian Cancer: 2.5-Year Follow-Up. Gynecologic Oncology **83**, 549-554.

HASENBURG, A., TONG, X.W., ROJAS-MARTINEZ, A., NYBERG-HOFFMAN, C., KIEBACK, C.C., KAPLAN, A., KAUFMAN, R.H., RAMZY, I., AGUILAR-CORDOVA, E., and KIEBACK, D.G. (2000). Thymidine kinase gene therapy with concomitant topotecan chemotherapy for recurrent ovarian cancer. Cancer gene therapy **7**, 839-844.

HEIM, A., EBNET, C., HARSTE, G., and PRING-ÅKERBLOM, P. (2003). Rapid and quantitative detection of human adenovirus DNA by real-time PCR. Journal of Medical Virology **70**, 228-239.

HEISE, C., GANLY, I., KIM, Y.T., SAMPSON-JOHANNES, A., BROWN, R., and KIRN, D. (2000). Efficacy of a replication-selective adenovirus against ovarian carcinomatosis is dependent on tumor burden, viral replication and p53 status. Gene Therapy **7**, 1925-1929.

HEISE, C., SAMPSON-JOHANNES, A., WILLIAMS, A., MCCORMICK, F., VON HOFF, D.D., and KIRN, D.H. (1997). ONYX-015, an E1B gene-attenuated adenovirus, causes tumor-specific cytolysis and antitumoral efficacy that can be augmented by standard chemotherapeutic agents. Nat Med **3**, 639-645.

HENNESSY, B.T., COLEMAN, R.L., and MARKMAN, M. (2009). Ovarian cancer. The Lancet **374**, 1371-1382.

HERMISTON, T. (2006). A demand for next-generation oncolytic adenoviruses. Curr Opin Mol Ther **8**, 322-330.

HERNANDEZ-ALCOCEBA, R., PIHALJA, M., QIAN, D., and CLARKE, M.F. (2002). New oncolytic adenoviruses with hypoxia- and estrogen receptor-regulated replication. Human gene therapy **13**, 1737-1750.

HOLTERMAN, L., VOGELS, R., VAN DER VLUGT, R., SIEUWERTS, M., GRIMBERGEN, J., KASPERS, J., GEELEN, E., VAN DER HELM, E., LEMCKERT, A., GILLISSEN, G., VERHAAGH, S., CUSTERS, J., ZUIJDGEEST, D., BERKHOUT, B., BAKKER, M., QUAX, P., GOUDSMIT, J., and HAVENGA, M. (2004). Novel Replication-Incompetent Vector Derived from Adenovirus Type 11 (Ad11) for Vaccination and Gene Therapy: Low Seroprevalence and Non-Cross-Reactivity with Ad5. In *J. Virol. pp*. 13207-13215.

HONG, S.S., HABIB, N.A., FRANQUEVILLE, L., JENSEN, S., and BOULANGER, P.A. (2003). Identification of Adenovirus (Ad) Penton Base Neutralizing Epitopes by Use of Sera

from Patients Who Had Received Conditionally Replicative Ad (Addl1520) for Treatment of Liver Tumors. J. Virol. **77**, 10366-10375.

ICON AND AGO, T.C. (2003). Paclitaxel plus platinum-based chemotherapy versus conventional platinum-based chemotherapy in women with relapsed ovarian cancer: the ICON4/AGO-OVAR-2.2 trial. The Lancet **361**, 2099-2106.

JONSSON, M.I., LENMAN, A.E., FRANGSMYR, L., NYBERG, C., ABDULLAHI, M., and ARNBERG, N. (2009). Coagulation Factors IX and X Enhance Binding and Infection of Adenovirus Types 5 and 31 in Human Epithelial Cells. J. Virol. **83**, 3816-3825.

KELLY, E., and RUSSELL, S.J. (2007). History of Oncolytic Viruses: Genesis to Genetic Engineering. Mol Ther **15**, 651-659.

KIM, J.H., OH, J.Y., PARK, B.H., LEE, D.E., KIM, J.S., PARK, H.E., ROH, M.S., JE, J.E., YOON, J.H., THORNE, S.H., KIRN, D., and HWANG, T.H. (2006). Systemic Armed Oncolytic and Immunologic Therapy for Cancer with JX-594, a Targeted Poxvirus Expressing GM-CSF. Mol Ther **14**, 361-370.

KIMBALL, K., NUMNUM, T., ROCCONI, R., and ALVAREZ, R. (2006). Gene therapy for ovarian cancer. Current Oncology Reports **8**, 441-447.

KIMBALL, K.J., PREUSS, M.A., BARNES, M.N., WANG, M., SIEGAL, G.P., WAN, W., KUO, H., SADDEKNI, S., STOCKARD, C.R., GRIZZLE, W.E., HARRIS, R.D., AURIGEMMA, R., CURIEL, D.T., and ALVAREZ, R.D. (2010). A Phase I Study of a Tropism-Modified Conditionally Replicative Adenovirus for Recurrent Malignant Gynecologic Diseases. Clinical Cancer Research **16**, 5277-5287.

KNUDSEN, E., IVERSEN, P.O., VAN ROOIJEN, N., and BENESTAD, H.B. (2002). Macrophage-dependent regulation of neutrophil mobilization and chemotaxis during development of sterile peritonitis in the rat. European journal of haematology **69**, 284-296.

KOSKI, A., KANGASNIEMI, L., ESCUTENAIRE, S., PESONEN, S., CERULLO, V., DIACONU, I., NOKISALMI, P., RAKI, M., RAJECKI, M., GUSE, K., RANKI, T., OKSANEN, M., HOLM, S.-L., HAAVISTO, E., KARIOJA-KALLIO, A., LAASONEN, L., PARTANEN, K., UGOLINI, M., HELMINEN, A., KARLI, E., HANNUKSELA, P., PESONEN, S., JOENSUU, T., KANERVA, A., and HEMMINKI, A. (2010). Treatment of Cancer Patients With a Serotype 5/3 Chimeric Oncolytic Adenovirus Expressing GMCSF. Mol Ther **18**, 1874-1884.

KRISTENSEN, G., PERREN, T., QIAN, W., PFISTERER, J., LEDERMANN, J. A., JOLY, F., CAREY, M. S., BEALE, P. J., CERVANTES, A., OZA, A. M. (2011). Result of interim analysis of overall survival in the GCIG ICON7 phase III randomized trial of bevacizumab in women with newly diagnosed ovarian cancer. J Clin Oncol **29**.

KUBICKA, U., OLSZEWSKI, W.L., TARNOWSKI, W., BIELECKI, K., ZIÓŁKOWSKA, A., and WIERZBICKI, Z. (1996). Normal Human Immune Peritoneal Cells: Subpopulations and Functional Characteristics. Scandinavian Journal of Immunology **44**, 157-163.

KUHN, I., HARDEN, P., BAUZON, M., CHARTIER, C., NYE, J., THORNE, S., REID, T., NI, S., LIEBER, A., FISHER, K., SEYMOUR, L., RUBANYI, G.M., HARKINS, R.N., and HERMISTON, T.W. (2008). Directed evolution generates a novel oncolytic virus for the treatment of colon cancer. PLoS ONE **3**.

KUMAR, S., MAHDI, H., BRYANT, C., SHAH, J.P., GARG, G., and MUNKARAH, A. (2010). Clinical trials and progress with paclitaxel in ovarian cancer. In *International Journal of Women's Health*. *pp*. 411-427.

LEOPOLD, P.L., and CRYSTAL, R.G. (2007). Intracellular trafficking of adenovirus: Many means to many ends. Advanced Drug Delivery Reviews **59**, 810-821.

LEOPOLD, P.L., and PFISTER, K.K. (2006). Viral Strategies for Intracellular Trafficking: Motors and Microtubules. Traffic **7**, 516-523.

LICHTENSTEIN, D.L., TOTH, K., DORONIN, K., TOLLEFSON, A.E., and WOLD, W.S.M. (2004). Functions and mechanisms of action of the adenovirus E3 proteins. International Reviews of Immunology **23**, 75-111.

LISZEWSKI, M.K., POST, T.W., and ATKINSON, J.P. (1991). Membrane Cofactor Protein (MCP or CD46): Newest Member of the Regulators of Complement Activation Gene Cluster. Annual Review of Immunology **9**, 431-455.

LIU, A.Y. (2000). Differential Expression of Cell Surface Molecules in Prostate Cancer Cells. Cancer Research **60**, 3429-3434.

LIU, B.L., ROBINSON, M., HAN, Z.Q., BRANSTON, R.H., ENGLISH, C., REAY, P., MCGRATH, Y., THOMAS, S.K., THORNTON, M., BULLOCK, P., LOVE, C.A., and COFFIN, R.S. (2002). ICP34.5 deleted herpes simplex virus with enhanced oncolytic, immune stimulating, and anti-tumour properties. Gene Ther **10**, 292-303.

LIU, H.L., and CHEN, J. (2009). Oncolytic virus as an agent for the treatment of malignant ascites. Cancer Biotherapy and Radiopharmaceuticals **24**, 99-101.

LYLE, C., and MCCORMICK, F. (2010). Integrin αvβ5 is a primary receptor for adenovirus in CAR-negative cells. Virology Journal **7**.

MANTIA-SMALDONE, G.M., EDWARDS, R.P., and VLAD, A.M. (2010). Targeted treatment of recurrent platinum-resistant ovarian cancer: Current and emerging therapies. In *Cancer Management and Research*. *pp*. 25-38.

MEI, Y.-F., SKOG, J., LINDMAN, K., and WADELL, G. (2003). Comparative analysis of the genome organization of human adenovirus 11, a member of the human adenovirus species B, and the commonly used human adenovirus 5 vector, a member of species C. In *Journal of General Virology*. *pp*. 2061-2071.

MEIER, O., and GREBER, U.F. (2004). Adenovirus endocytosis. The Journal of Gene Medicine **6**, S152-S163.

MENON, U., GENTRY-MAHARAJ, A., HALLETT, R., RYAN, A., BURNELL, M., SHARMA, A., LEWIS, S., DAVIES, S., PHILPOTT, S., LOPES, A., GODFREY, K., ORAM, D., HEROD, J., WILLIAMSON, K., SEIF, M.W., SCOTT, I., MOULD, T., WOOLAS, R., MURDOCH, J., DOBBS, S., AMSO, N.N., LEESON, S., CRUICKSHANK, D., MCGUIRE, A., CAMPBELL, S., FALLOWFIELD, L., SINGH, N., DAWNAY, A., SKATES, S.J., PARMAR, M., and JACOBS, I. (2009). Sensitivity and specificity of multimodal and ultrasound screening for ovarian cancer, and stage distribution of detected cancers: results of the prevalence screen of the UK Collaborative Trial of Ovarian Cancer Screening (UKCTOCS). The lancet oncology **10**, 327-340.

METZGER-FILHO, O., MOULIN, C., and D'HONDT, V. (2010). First-line systemic treatment of ovarian cancer: A critical review of available evidence and expectations for future directions. Current Opinion in Oncology **22**, 513-520.

MIYAZAWA, N., LEOPOLD, P.L., HACKETT, N.R., FERRIS, B., WORGALL, S., FALCK-PEDERSEN, E., and CRYSTAL, R.G. (1999). Fiber Swap between Adenovirus Subgroups B and C Alters Intracellular Trafficking of Adenovirus Gene Transfer Vectors. In *J. Virol. pp*. 6056-6065.

MORRISON, J., BRIGGS, S.S., GREEN, N., FISHER, K., SUBR, V., ULBRICH, K., KEHOE, S., and SEYMOUR, L.W. (2008). Virotherapy of ovarian cancer with polymer-cloaked adenovirus retargeted to the epidermal growth factor receptor. Mol Ther **16**, 244-251.

MORRISON, J., BRIGGS, S.S., GREEN, N.K., THOMA, C., FISHER, K.D., KEHOE, S., and SEYMOUR, L.W. (2009). Cetuximab retargeting of adenovirus via the epidermal growth factor receptor for treatment of intraperitoneal ovarian cancer. Human gene therapy **20**, 239-251.

MURAKAMI, P., and MCCAMAN, M.T. (1999). Quantitation of Adenovirus DNA and Virus Particles with the PicoGreen Fluorescent Dye. Anal. Biochem. **274**, 283-288.

MURUVE, D.A., BARNES, M.J., STILLMAN, I.E., and LIBERMANN, T.A. (1999). Adenoviral gene therapy leads to rapid induction of multiple chemokines and acute neutrophil-dependent hepatic injury in vivo. Human gene therapy **10**, 965-976.

MUTSAERS, S.E. (2002). Mesothelial cells: Their structure, function and role in serosal repair. In *Respirology*. *pp*. 171-191.

NEWMAN, W., and SOUTHAM, C.M. (1954). Virus treatment in advanced cancer. A pathological study of fifty-seven cases. Cancer **7**, 106-118.

NIELSEN, L.L., GURNANI, M., SYED, J., DELL, J., HARTMAN, B., CARTWRIGHT, M., and JOHNSON, R.C. (1998). Recombinant E1-deleted adenovirus-mediated gene therapy for cancer: Efficacy studies with p53 tumor suppressor gene and liver histology in tumor xenograft models. Human gene therapy **9**, 681-694.

NWANEGBO, E., VARDAS, E., GAO, W., WHITTLE, H., SUN, H., ROWE, D., ROBBINS, P.D., and GAMBOTTO, A. (2004). Prevalence of Neutralizing Antibodies to Adenoviral Serotypes 5 and 35 in the Adult Populations of The Gambia, South Africa, and the United States. In *Clinical and Diagnostic Laboratory Immunology*. *pp*. 351-357.

OLIVER, C.J., SHORTRIDGE, K.F., and BELYAVIN, G. (1976). Diffusion coefficient and molecular weight of type 5 adenovirus by photon correlation spectroscopy. Biochimica et Biophysica Acta **437**, 589-598.

OTHMAN, M., LABELLE, A., MAZZETTI, I., ELBATARNY, H.S., and LILLICRAP, D. (2007). Adenovirus-induced thrombocytopenia: the role of von Willebrand factor and P-selectin in mediating accelerated platelet clearance. Blood **109**, 2832-2839.

PAPPIN, D.J.C., HOJRUP, P., and BLEASBY, A.J. (1993). Rapid identification of proteins by peptide-mass fingerprinting. Current biology : CB **3**, 327-332.

PARATO, K.A., SENGER, D., FORSYTH, P.A.J., and BELL, J.C. (2005). Recent progress in the battle between oncolytic viruses and tumours. Nat Rev Cancer **5**, 965-976.

PENG, K.-W., FACTEAU, S., WEGMAN, T., O'KANE, D., and RUSSELL, S.J. (2002a). Non-invasive in vivo monitoring of trackable viruses expressing soluble marker peptides. Nat Med **8**, 527-531.

PENG, K.W., TENEYCK, C.J., GALANIS, E., KALLI, K.R., HARTMANN, L.C., and RUSSELL, S.J. (2002b). Intraperitoneal therapy of ovarian cancer using an engineered measles virus. Cancer Research **62**, 4656-4662.

PIPIYA, T., SAUTHOFF, H., HUANG, Y.Q., CHANG, B., CHENG, J., HEITNER, S., CHEN, S., ROM, W.N., and HAY, J.G. (2005). Hypoxia reduces adenoviral replication in cancer cells by downregulation of viral protein expression. Gene Ther **12**, 911-917.

PRUITT, K.D., TATUSOVA, T., KLIMKE, W., and MAGLOTT, D.R. (2009). NCBI Reference Sequences: current status, policy and new initiatives. Nucleic Acids Res **37**, D32-36.

RAKI, M., HAKKARAINEN, T., BAUERSCHMITZ, G.J., SARKIOJA, M., DESMOND, R.A., KANERVA, A., and HEMMINKI, A. (2007). Utility of TK//GCV in the context of highly effective oncolysis mediated by a serotype 3 receptor targeted oncolytic adenovirus. Gene Ther **14**, 1380-1388.

RAPER, S.E., CHIRMULE, N., LEE, F.S., WIVEL, N.A., BAGG, A., GAO, G.-P., WILSON, J.M., and BATSHAW, M.L. (2003). Fatal systemic inflammatory response syndrome in a ornithine transcarbamylase deficient patient following adenoviral gene transfer. Molecular Genetics and Metabolism **80**, 148-158.

ROBERTS, M.S., LORENCE, R.M., GROENE, W.S., and BAMAT, M.K. (2006). Naturally oncolytic viruses. Curr Opin Mol Ther **8**, 314-321.

RUSSELL, S.J., and PENG, K.W. (2009). Measles virus for cancer therapy. In *Current Topics in Microbiology and Immunology*. *pp*. 213-241.

RUSSELL, W.C. (2009). Adenoviruses: update on structure and function. The Journal of general virology **90**, 1-20.

RUX, J.J., and BURNETT, R.M. (2004). Adenovirus Structure. Human gene therapy **15**, 1167-1176.

SANDBERG, L., PAPAREDDY, P., SILVER, J., BERGH, A., and MEI, Y.-F. (2009). Replication-Competent Ad11p Vector (RCAd11p) Efficiently Transduces and Replicates in Hormone-Refractory Metastatic Prostate Cancer Cells. Human gene therapy **20**, 361-373.

SANDERCOCK, J., PARMAR, M.K.B., TORRI, V., and QIAN, W. (2002). First-line treatment for advanced ovarian cancer: Paclitaxel, platinum and the evidence. British Journal of Cancer **87**, 815-824.

SAPHIRE, A.C.S., GUAN, T., SCHIRMER, E.C., NEMEROW, G.R., and GERACE, L. (2000). Nuclear Import of Adenovirus DNA in Vitro Involves the Nuclear Protein Import Pathway and hsc70. J. Biol. Chem. **275**, 4298-4304.

SCHNELL, M.A., ZHANG, Y., TAZELAAR, J., GAO, G.P., YU, Q.C., QIAN, R., CHEN, S.J., VARNAVSKI, A.N., LECLAIR, C., RAPER, S.E., and WILSON, J.M. (2001). Activation of innate immunity in nonhuman primates following intraportal administration of adenoviral vectors. Mol Ther **3**, 708-722.

SEGERMAN, A., ATKINSON, J.P., MARTTILA, M., DENNERQUIST, V., WADELL, G., and ARNBERG, N. (2003). Adenovirus Type 11 Uses CD46 as a Cellular Receptor. In *J. Virol. pp*. 9183-9191.

SHASHKOVA, E.V., MAY, S.M., and BARRY, M.A. (2009). Characterization of human adenovirus serotypes 5, 6, 11, and 35 as anticancer agents. Virology **394**, 311-320.

SHAYAKHMETOV, D.M., EBERLY, A.M., LI, Z.-Y., and LIEBER, A. (2005). Deletion of Penton RGD Motifs Affects the Efficiency of both the Internalization and the Endosome Escape of Viral Particles Containing Adenovirus Serotype 5 or 35 Fiber Knobs. J. Virol. **79**, 1053-1061.

SHEN, B.H., BAUZON, M., and HERMISTON, T.W. (2006). The effect of hypoxia on the uptake, replication and lytic potential of group B adenovirus type 3 (Ad3) and type 11p (Ad11p). Gene Ther **13**, 986-990.

SHEN, B.H., and HERMISTON, T.W. (2005). Effect of hypoxia on Ad5 infection, transgene expression and replication. Gene Ther **12**, 902-910.

SIGNAS, C., AKUSJARVI, G., and PETTERSSON, U. (1985). Adenovirus 3 fiber polypeptide gene: implications for the structure of the fiber protein. J. Virol. **53**, 672-678.

SINGER, V.L., JONES, L.J., YUE, S.T., and HAUGLAND, R.P. (1997). Characterization of PicoGreen reagent and development of a fluorescence-based solution assay for double-stranded DNA quantitation. Anal. Biochem. **249**, 228-238.

SIRENA, D., LILIENFELD, B., EISENHUT, M., KALIN, S., BOUCKE, K., BEERLI, R.R., VOGT, L., RUEDL, C., BACHMANN, M.F., GREBER, U.F., and HEMMI, S. (2004). The Human Membrane Cofactor CD46 Is a Receptor for Species B Adenovirus Serotype 3. In *J. Virol. pp*. 4454-4462.

SMITH, J.G., CASSANY, A., GERACE, L., RALSTON, R., and NEMEROW, G.R. (2008). Neutralizing Antibody Blocks Adenovirus Infection by Arresting Microtubule-Dependent Cytoplasmic Transport. J. Virol. **82**, 6492-6500.

SMITH, R.R., HUEBNER, R.J., ROWE, W.P., SCHATTEN, W.E., and THOMAS, L.B. (1956). Studies on the use of viruses in the treatment of carcinoma of the cervix. Cancer **9**, 1211-1218.

STALLWOOD, Y., FISHER, K.D., GALLIMORE, P.H., and MAUTNER, V. (2000). Neutralisation of adenovirus infectivity by ascitic fluid from ovarian cancer patients. Gene Therapy **7**, 637-643.

STONE, D., FURTHMANN, A., SANDIG, V., and LIEBER, A. (2003). The complete nucleotide sequence, genome organization, and origin of human adenovirus type 11. Virology **309**, 152-165.

STONE, D., LIU, Y., LI, Z.Y., TUVE, S., STRAUSS, R., and LIEBER, A. (2007). Comparison of Adenoviruses From Species B, C, E, and F After Intravenous Delivery. Mol Ther.

STONE, D., NI, S., LI, Z.-Y., GAGGAR, A., DIPAOLO, N., FENG, Q., SANDIG, V., and LIEBER, A. (2005). Development and Assessment of Human Adenovirus Type 11 as a Gene Transfer Vector. In *J. Virol. pp*. 5090-5104.

SUBR, V., KOSTKA, L., SELBY-MILIC, T., FISHER, K., ULBRICH, K., SEYMOUR, L.W., and CARLISLE, R.C. (2009). Coating of adenovirus type 5 with polymers containing quaternary amines prevents binding to blood components. Journal of Controlled Release **135**, 152-158.

SULAIMAN, H., DAWSON, L., LAURENT, G.J., BELLINGAN, G.J., and HERRICK, S.E. (2002). Role of plasminogen activators in peritoneal adhesion formation. In *Biochem. Soc. Trans. pp*. 126-131.

SUMIDA, S.M., TRUITT, D.M., LEMCKERT, A.A.C., VOGELS, R., CUSTERS, J.H.H.V., ADDO, M.M., LOCKMAN, S., PETER, T., PEYERL, F.W., KISHKO, M.G., JACKSON, S.S., GORGONE, D.A., LIFTON, M.A., ESSEX, M., WALKER, B.D., GOUDSMIT, J., HAVENGA, M.J.E., and BAROUCH, D.H. (2005). Neutralizing Antibodies to Adenovirus Serotype 5 Vaccine Vectors Are Directed Primarily against the Adenovirus Hexon Protein. In *The Journal of Immunology*. *pp*. 7179-7185.

SUZUKI, K., ALEMANY, R.N., YAMAMOTO, M., and CURIEL, D.T. (2002). The Presence of the Adenovirus E3 Region Improves the Oncolytic Potency of Conditionally Replicative Adenoviruses. Clinical Cancer Research **8**, 3348-3359.

TAIT, D.L., OBERMILLER, P.S., HATMAKER, A.R., REDLIN-FRAZIER, S., and HOLT, J.T. (1999). Ovarian Cancer BRCA1 Gene Therapy: Phase I and II Trial Differences in Immune Response and Vector Stability. Clinical Cancer Research **5**, 1708-1714.

THOMAS, C.E., EHRHARDT, A., and KAY, M.A. (2003). Progress and problems with the use of viral vectors for gene therapy. Nat Rev Genet **4**, 346-358.

THORNER, A.R., VOGELS, R., KASPERS, J., WEVERLING, G.J., HOLTERMAN, L., LEMCKERT, A.A.C., DILRAJ, A., MCNALLY, L.M., JEENA, P.M., JEPSEN, S., ABBINK, P., NANDA, A., SWANSON, P.E., BATES, A.T., O'BRIEN, K.L., HAVENGA, M.J.E., GOUDSMIT, J., and BAROUCH, D.H. (2006). Age Dependence of Adenovirus-Specific Neutralizing Antibody Titers in Individuals from Sub-Saharan Africa. J. Clin. Microbiol. **44**, 3781-3783.

TOLLEFSON, A.E., SCARIA, A., HERMISTON, T.W., RYERSE, J.S., WOLD, L.J., and WOLD, W.S. (1996). The adenovirus death protein (E3-11.6K) is required at very late stages of infection for efficient cell lysis and release of adenovirus from infected cells. J. Virol. **70**, 2296-2306.

TOTH, K., DHAR, D., and WOLD, W.S.M. (2010). Oncolytic (replication-competent) adenoviruses as anticancer agents. Expert Opinion on Biological Therapy **10**, 353-368.

TUVE, S., WANG, H., JACOBS, J.D., YUMUL, R.C., SMITH, D.F., and LIEBER, A. (2008). Role of Cellular Heparan Sulfate Proteoglycans in Infection of Human Adenovirus Serotype 3 and 35. PLoS Pathogens **4**, e1000189.

TUVE, S., WANG, H., WARE, C., LIU, Y., GAGGAR, A., BERNT, K., SHAYAKHMETOV, D., LI, Z., STRAUSS, R., STONE, D., and LIEBER, A. (2006). A New Group B Adenovirus Receptor Is Expressed at High Levels on Human Stem and Tumor Cells. In *J. Virol. pp*. 12109-12120.

VANDERKWAAK, T.J., WANG, M., GÓMEZ-NAVARRO, J., RANCOURT, C., DMITRIEV, I., KRASNYKH, V., BARNES, M., SIEGAL, G.P., ALVAREZ, R., and CURIEL, D.T. (1999). An Advanced Generation of Adenoviral Vectors Selectively Enhances Gene Transfer for Ovarian Cancer Gene Therapy Approaches. Gynecologic Oncology **74**, 227-234.

VASEY, P.A., SHULMAN, L.N., CAMPOS, S., DAVIS, J., GORE, M., JOHNSTON, S., KIRN, D.H., O'NEILL, V., SIDDIQUI, N., SEIDEN, M.V., and KAYE, S.B. (2002). Phase I trial of intraperitoneal injection of the E1B-55-kd-gene-deleted adenovirus ONYX-015 (dl1520) given on days 1 through 5 every 3 weeks in patients with recurrent/refractory epithelial ovarian cancer. Journal of Clinical Oncology **20**, 1562-1569.

VERGOTE, I., AMANT, F., AMEYE, L., and TIMMERMAN, D. (2009). Screening for ovarian carcinoma: not quite there yet. The lancet oncology **10**, 308-309.

VERGOTE, I., TROPÉ, C.G., AMANT, F., KRISTENSEN, G.B., EHLEN, T., JOHNSON, N., VERHEIJEN, R.H.M., VAN DER BURG, M.E.L., LACAVE, A.J., PANICI, P.B., KENTER, G.G., CASADO, A., MENDIOLA, C., COENS, C., VERLEYE, L., STUART, G.C.E., PECORELLI, S., and REED, N.S. (2010). Neoadjuvant Chemotherapy or Primary Surgery in Stage IIIC or IV Ovarian Cancer. New England Journal of Medicine **363**, 943-953.

VOGELS, R., ZUIJDGEEST, D., VAN RIJNSOEVER, R., HARTKOORN, E., DAMEN, I., DE BETHUNE, M.-P., KOSTENSE, S., PENDERS, G., HELMUS, N., KOUDSTAAL, W., CECCHINI, M., WETTERWALD, A., SPRANGERS, M., LEMCKERT, A., OPHORST, O., KOEL, B., VAN MEERENDONK, M., QUAX, P., PANITTI, L., GRIMBERGEN, J., BOUT, A., GOUDSMIT, J., and HAVENGA, M. (2003). Replication-Deficient Human Adenovirus Type 35 Vectors for Gene Transfer and Vaccination: Efficient Human Cell Infection and Bypass of Preexisting Adenovirus Immunity. In *Journal of Virology*. *pp*. 8263-8271.

WADDINGTON, S.N., MCVEY, J.H., BHELLA, D., PARKER, A.L., BARKER, K., ATODA, H., PINK, R., BUCKLEY, S.M.K., GREIG, J.A., DENBY, L., CUSTERS, J., MORITA, T., FRANCISCHETTI, I.M.B., MONTEIRO, R.Q., BAROUCH, D.H., VAN ROOIJEN, N.,

NAPOLI, C., HAVENGA, M.J.E., NICKLIN, S.A., and BAKER, A.H. (2008). Adenovirus Serotype 5 Hexon Mediates Liver Gene Transfer. Cell **132**, 397-409.

WADELL, G., HAMMARSKJÖLD, M.-L., WINBERG, G., VARSANYI, T.M., and SUNDELL, G. (1980). GENETIC VARIABILITY OF ADENOVIRUSES*. Annals of the New York Academy of Sciences **354**, 16-42.

WAGNER, E.K., HEWLETT, M. J., BLOOM D. C., CAMERINI D. (2008). *Basic Virology*. (Blackwell Publishing Ltd).

WANG, H., LI, Z.-Y., LIU, Y., PERSSON, J., BEYER, I., MOLLER, T., KOYUNCU, D., DRESCHER, M.R., STRAUSS, R., ZHANG, X.-B., WAHL, J.K., URBAN, N., DRESCHER, C., HEMMINKI, A., FENDER, P., and LIEBER, A. (2011). Desmoglein 2 is a receptor for adenovirus serotypes 3, 7, 11 and 14. Nat Med **17**, 96-104.

WANG, X., and BERGELSON, J.M. (1999). Coxsackievirus and Adenovirus Receptor Cytoplasmic and Transmembrane Domains Are Not Essential for Coxsackievirus and Adenovirus Infection. J. Virol. **73**, 2559-2562.

WANG, Y., GANGESWARAN, R., ZHAO, X., WANG, P., TYSOME, J., BHAKTA, V., YUAN, M., CHIKKANNA-GOWDA, C.P., JIANG, G., GAO, D., CAO, F., FRANCIS, J., YU, J., LIU, K., YANG, H., ZHANG, Y., ZANG, W., CHELALA, C., DONG, Z., and LEMOINE, N. (2009). CEACAM6 attenuates adenovirus infection by antagonizing viral trafficking in cancer cells. J. Clin. Invest. **119**, 1604-1615.

WICKHAM, T.J., MATHIAS, P., CHERESH, D.A., and NEMEROW, G.R. (1993). Integrins [alpha]v[beta]3 and [alpha]v[beta]5 promote adenovirus internalization but not virus attachment. Cell **73**, 309-319.

WIETHOFF, C.M., WODRICH, H., GERACE, L., and NEMEROW, G.R. (2005). Adenovirus Protein VI Mediates Membrane Disruption following Capsid Disassembly. J. Virol. **79**, 1992-2000.

WILLS, K.N., MANEVAL, D.C., MENZEL, P., HARRIS, M.P., SUTJIPTO, S., VAILLANCOURT, M.-T., HUANG, W.-M., JOHNSON, D.E., ANDERSON, S.C., WEN, S.F., BOOKSTEIN, R., SHEPARD, H.M., and GREGORY, R.J. (1994). Development and Characterization of Recombinant Adenoviruses Encoding Human p53 for Gene Therapy of Cancer. Human gene therapy **5**, 1079-1088.

WOHLFART, C. (1988). Neutralization of adenoviruses: kinetics, stoichiometry, and mechanisms. J. Virol. **62**, 2321-2328.

WOLF, J.K., BODURKA, D.C., GANO, J.B., DEAVERS, M., RAMONDETTA, L., RAMIREZ, P.T., LEVENBACK, C., and GERSHENSON, D.M. (2004). A phase I study of Adp53 (INGN 201; ADVEXIN) for patients with platinum- and paclitaxel-resistant epithelial ovarian cancer. Gynecologic Oncology **94**, 442-448.

WONGANAN, P., and CROYLE, M.A. (2010). PEGylated Adenoviruses: From Mice to Monkeys. Viruses **2**, 468-502.

YANNOUTSOS, N., IJZERMANS, J.N., HARKES, C., BONTHUIS, F., ZHOU, C.Y., WHITE, D., MARQUET, R.L., and GROSVELD, F. (1996). A membrane cofactor protein transgenic mouse model for the study of discordant xenograft rejection. Genes to Cells **1**, 409-419.

YOU, Z., FISCHER, D.C., TONG, X., HASENBURG, A., AGUILAR-CORDOVA, E., and KIEBACK, D.G. (2001). Coxsackievirus-adenovirus receptor expression in ovarian cancer cell lines is associated with increased adenovirus transduction efficiency and transgene expression. Cancer gene therapy **8**, 168-175.

ZAISS, A.-K., LIU, Q., BOWEN, G.P., WONG, N.C.W., BARTLETT, J.S., and MURUVE, D.A. (2002). Differential Activation of Innate Immune Responses by Adenovirus and Adeno-Associated Virus Vectors. In *J. Virol. pp*. 4580-4590.

ZAISS, A.K., MACHADO, H.B., and HERSCHMAN, H.R. (2009). The influence of innate and pre-existing immunity on adenovirus therapy. Journal of Cellular Biochemistry **108**, 778-790.

ZEIMET, A.G., and MARTH, C. (2003). Why did p53 gene therapy fail in ovarian cancer? The lancet oncology **4**, 415-422.

ZEIMET, A.G., MULLER-HOLZNER, E., SCHULER, A., HARTUNG, G., BERGER, J., HERMANN, M., WIDSCHWENDTER, M., BERGELSON, J.M., and MARTH, C. (2002). Determination of molecules regulating gene delivery using adenoviral vectors in ovarian carcinomas. Gene Ther **9**, 1093-1100.

ZHANG, Y., CHIRMULE, N., GAO, G.P., QIAN, R., CROYLE, M., JOSHI, B., TAZELAAR, J., and WILSON, J.M. (2001). Acute cytokine response to systemic adenoviral vectors in mice is mediated by dendritic cells and macrophages. Mol Ther **3**, 697-707.